Cellulose acetate / plasticizer systems : structure, morphology and dynamics

Congyu Bao

N° d'ordre 49-2015 Année 2015

THESE DE L'UNIVERSITE DE LYON

Délivrée par

L'UNIVERSITE CLAUDE BERNARD LYON 1

ECOLE DOCTORALE MATERIAUX

DIPLOME DE DOCTORAT
(Arrêté du 7 août 2006)

Soutenue publiquement le 28 avril 2015 par

Cong Yu BAO

CELLULOSE ACETATE/PLASTICIZER SYSTEMS: STRUCTURE, MORPHOLOGY AND DYNAMICS

Devant la commission d'examen

M. Christian CARROT	Rapporteur
M. Laurent DAVID	
M. Laurent HEUX	Rapporteur
M. Didier LONG	Directeur de thèse
Mme. Valérie MIRI	
M. Yoshiyuki NISHIO	
M. Armin STEIN	
M. Caroll VERGELATI	Encadrant industriel


SOLVAY


cnrs

ACKNOWLEDGEMENT

First, I would like to thank my PhD supervisor Dr. Didier LONG and my industrial advisor Dr. Caroll VERGELATI. Their advices and trust were one of the most important keys of my success.

I would like to give the second acknowledgement to Acetow GmbH of Solvay group. Their rich experience on the research of cellulose acetate was a big help for my study, since this was the first time that cellulose acetate had been studied in my laboratory. Special thanks to Dr. Armin STEIN, for his kindness and useful advices.

Another acknowledgement is dedicated to my colleagues in LPMA/APMD department of Solvay group. Paul, Jean-Yves, Florence, Pierre-Yves, Alexandra, Sandrine, Olivier, Alexandre, Leo and etc. all helped me a lot during the last three years. Your expertise in polymer science allowed me to discover this interesting field in details.

Of course, in our lab, the non-permanent staff is a dynamic group with many scientific discussions and much fun. I had a wonderful three-year experience in Lyon thanks to them.

Here, another special thanks to the XRD team in the campus of Doua and the SANS D11 team in ILL Grenoble, France. They all contributed to the analytical characterization of my samples and their expertise was priceless for our final interpretations.

Finally, I would like to thank my parents for all what they did for me during these years.

TABLE OF CONTENTS

LIST OF FIGURES

LIST OF TABLES

CHAPTER 1

INTRODUCTION AND OBJECTIVES OF THIS RESEARCH

Nowadays, polymers play an important role in our daily life. They have wide applications such as automobile parts, textiles, plastics, etc. Most of polymers widely used in industry are petroleum-based synthetic polymers (e.g. nylon, polyester) because of their low production cost and excellent applicative properties. However, petroleum is not a renewable resource and as predicted by Hubbert peak theory, we must take care of the remaining petroleum reserves because there are less and less resources every day. Various approaches have been proposed in order to resolve this problem, one of which is the return of natural polymers.

Natural polymers, such as natural rubber or polysaccharides, are renewable resources. They have been introduced in industry long before synthetic ones. However, in the second half of the 20th century, the worldwide oil exploration changed everything. Natural polymers have been largely replaced by petroleum-based synthetic polymers.

1.1 – From cellulose to its derivatives

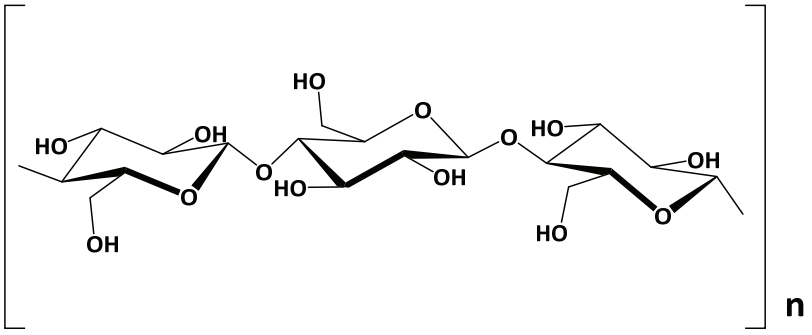

Figure 1: Chemical structure of cellulose

Cellulose is the world's most abundant renewable material, about 7.5 x 10^{10} tons of production per year. There are two primary sources of cellulose on earth for its industrial development: wood pulp and cotton linters (short fibers not used to spin yarns). Their typical compositions are illustrated in Table 1 and 2.

Component	Softwood,%	Hardwood,%
Cellulose	40 - 45	38 - 49
Hemicellulose	25 - 30	30 - 35
Lignin	25 - 30	20 - 25
Total extractives	2 - 5	3 - 7

Table 1: Average chemical composition of the main constituents in the cell wall of a typical softwood and hardwood (Kadla and Dai 2007)

	Percent of dry weight	
Component	Typical	Range
Cellulose	94.0	88.0 - 96.0
Protein	1.3	1.1 - 1.9
Pectic Substances	1.2	0.7 - 1.2
Ash	1.2	0.7 - 1.6
Wax	0.6	0.4 - 1.0
Total Sugars	0.3	
Pigment	Trace	
Others	1.4	

Table 2: Composition of typical cotton fibers (Wakelyn 2007)

Cellulose is a polysaccharide consisting of β-1,4 glycosidic linkages of anhydroglucose units (Figure 1). Hydrogen bonds (H-bonds) can be easily formed within and between cellulosic chains, as illustrated in Figure 2. Cellulose is insoluble in water and in most of organic solvents, but it is soluble in certain ionic liquids (*French et al. 2007*). The insolubility in water is often referred to as strong intermolecular hydrogen bonding between cellulose molecules. Cellulose itself is difficult to be used in industry, but its derivatives are much easier to handle.

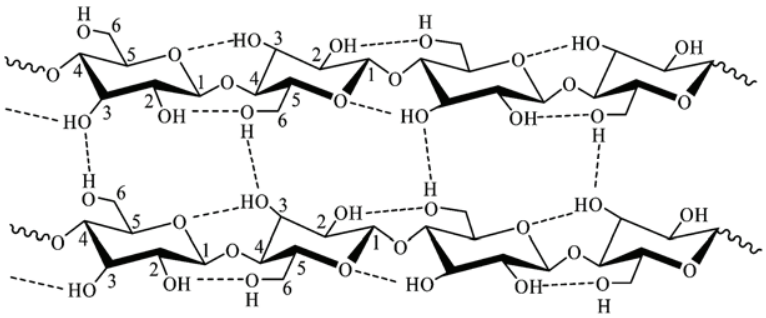

Figure 2: The schematic structure of cellulose and the numbering of carbon atoms constituting its repeat unit showing the hydrogen bonds (dashed) within and between cellulosic chains (Lu et al. 2014)

All cellulose derivatives are based on the substitution of hydroxyl groups of cellulose by other functional groups. Thus, a definition term Degree of substitution needs to be introduced here: The degree of substitution (DS) of a polymer is the (average) number of substituent groups attached per base unit (in the case of condensation polymers) or per monomeric unit (in the case of addition polymers). The term has been used mainly in cellulose chemistry where each anhydroglucose (β-glucopyranose) unit has three reactive (hydroxyl) groups; degrees of substitution may therefore range from zero (cellulose itself) to three (fully substituted cellulose). In the case of cellulose acetate, DS is the average number of acetyl groups attached per anhydroglucose unit (from *Encyclopedia of Polymer Science and Technology*). In total, eight possible anhydroglucose units (AGU) of cellulose acetate are listed below (Figure 3):

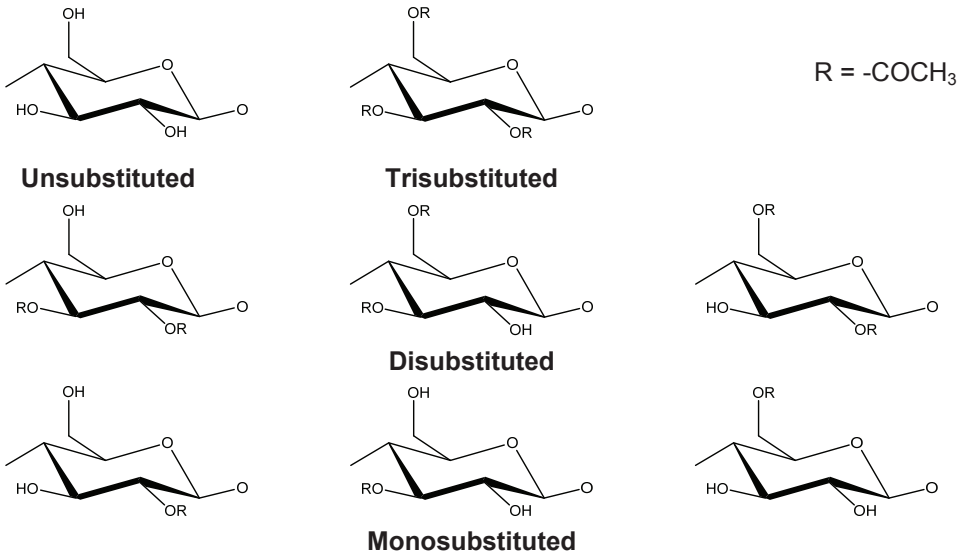

Figure 3: eight possible anhydroglucose units of cellulose acetate – unsubstituted, partially substituted and fully substituted anhydroglucose units (R = -$COCH_3$)

The present work is focused on one of the most common cellulose derivatives in industry: cellulose acetate. Cellulose acetate (CA) is an environmentally friendly product from manufacturing to degradation processes. Its raw material is cellulose, the most abundant renewable source from the nature. Its industrial manufacturing is a continuous process with recovery of acetic acid and self-production of acetic anhydride. Relatively little chemical waste remains after the manufacturing process. Some of CA-fabricated products (e.g. packaging, films) have been approved for food or cosmetics use. Finally, bio-degradation of CA-fabricated products is totally possible via various methods. Cellulose acetate is also a transparent, glossy, non-flammable and tough polymer with good dimensional stability and high resistance against heat and chemicals. Nowadays, fully substituted cellulose triacetate (CTA) and partially substituted cellulose diacetate (CDA, DS = 2.5) are the most commercialized cellulose acetate in the market.

1.2 – History of cellulose acetate

Cellulose acetate was historically discovered by Paul Schützenberger in 1865, by reacting cellulose with acetic anhydride. Cellulose triacetate was industrialized (first patents in 1894, *Rustemeyer 2004*) much earlier than acetone-soluble cellulose diacetate (discovered by George Miles in 1904). CTA could be applied as photographic film, artificial silk or hornlike plastic materials. But the major commercial breakthrough was the application of cellulose diacetate as a textile fiber. The success of cellulose acetate fiber lasted until 1960's when cheaper petroleum-based synthetic fibers (such as nylon and polyester) entered textile market. The chronicle of cellulose acetate's industrial applications is summarized in Figure 4. Apart from the applications mentioned above, filter tow for cigarettes, polarizer protection film and other environmentally friendly plastics should also be noted.

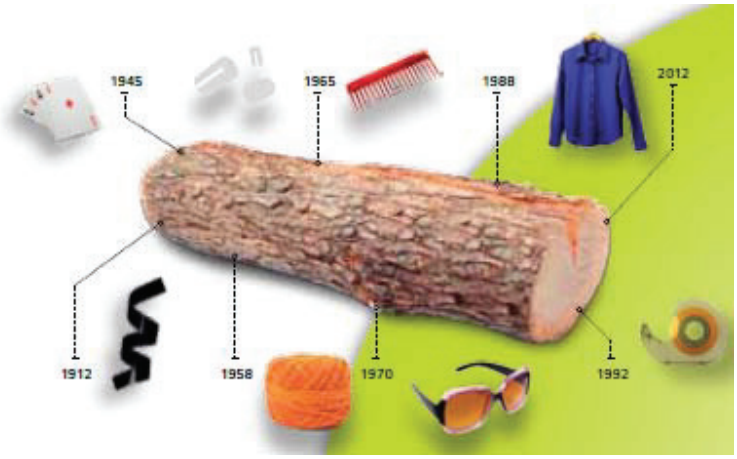

Figure 4: The chronicle of cellulose acetate's industrial applications over 100 years (from Ocalio® brochure)

Another potential market of cellulose acetate is filter tow for cigarettes. A linear and constant growth has been observed in the CA filter tow market since 1960s. It is currently the biggest market of cellulose acetate in industry. Some of the major players in this market are Celanese Corporation, Eastman Chemical Company, Daicel Corporation, Solvay Acetow GmbH and Mitsubishi Rayon Co.

1.3 – Evolution of cellulose acetate market

World consumption of cellulose acetate is mainly in four different markets: filter tow for cigarettes, textile fibers, polarizer protection film in liquid crystal displays (LCD) and coatings, plastics and membranes. The following Table 3 and Figure 5 present the estimated 2011-2016 evolution of world consumption of cellulose acetate flakes (from *CEH Marketing Research Report of Cellulose Acetate Flake, April 2012*):

World Consumption of Cellulose Acetate Flake

	2011		2016		Average Annual Growth Rate, 2011-2016 (percent)
	Thousands of Metric Tons	Percent of Total	Thousands of Metric Tons	Percent of Total	
Cigarette Filter Tow	672.0	82.1	755.0	81.6	2.4
Textile Fibers	56.0	6.8	61.0	6.6	1.7
Coatings, Plastics and Films	48.9	6.0	47.8	5.2	–0.5
Liquid Crystal Displays	42.0	5.1	61.0	6.6	7.7
Total	818.9	100%	924.8	100%	2.5%

SOURCE: CEH estimates.

Table 3: Estimated 2011-2016 evolution of world consumption of cellulose acetate flake (from CEH Marketing Research Report of Cellulose Acetate Flake, April 2012)

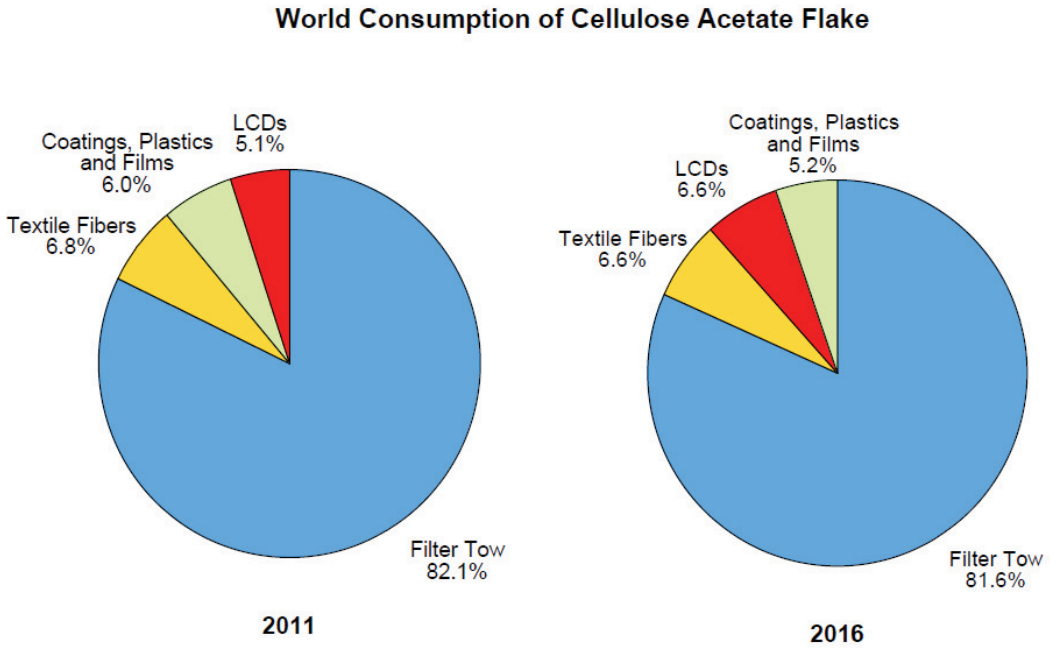

Figure 5: Estimated 2011-2016 evolution of world consumption of cellulose acetate flake (from CEH Marketing Research Report of Cellulose Acetate Flake, April 2012)

According to this marketing research report, polarizer protection film in LCD will be the CA market which has the most important growth in the period of 2011-2016 (+ 7.7%). Other applications, such as filter tow for cigarettes and textile fibers, will be the constant growing markets for cellulose acetate. The main target of cellulose acetate market is now towards high-value market rather than commodity market.

1.4 – Industrial manufacturing

In industry, cellulose acetate is produced via the acetylation of cellulose. Three industrial processes have been mainly applied in the cellulose acetate manufacturing history.

- The acetic acid process
- The methylene chloride process
- The heterogeneous process

The Methylene Chloride Process was developed by Bayer, which replaces acetic acid of the Acetic Acid Process with methylene chloride. The solvent allows “reflux” cooling to remove the heat of acetylation and is a better solvent for cellulose triacetate than acetic acid. However, high investment and low productivity are the drawbacks of this method. With improvements of product quality issued from the Acetic Acid Process, the Methylene Chloride Process has been abandoned since 2003.

The Heterogeneous Process is based on a non-solvent instead of acetic acid or methylene chloride. It is dedicated to the production of cellulose triacetate flakes. The non-solvent can be of petroleum ether or toluene type. It results cellulose triacetate flakes in a fibrous state. The process has been abandoned in the late 1990’s.

Here, we will focus on the acetic acid process which is the most widely used method for the production of commercial cellulose acetate. In the acetic acid process, two major stages are involved: the acetylation of cellulose and the hydrolysis of cellulose triacetate. Therefore, the following raw materials are required for the industrial production of cellulose acetate:

- Wood pulp/cotton linter (cellulose source)
- Acetic acid (solvent)
- Acetic anhydride (reagent)
- Sulfuric acid (catalyst).

1.4.1 – Activation of wood pulp

Wood pulp is the most common cellulose source used for the cellulose acetate manufacturing industry. The commercial products are usually available in sheets. In order to achieve the best performance of cellulose acetylation, the commercial wood pulp sheets need to be firstly activated.

The activation (pre-treatment) stage consists in three steps:

- Mechanical disintegration
- Swelling in acetic acid
- Sulphuric acid addition

The result of the activation stage is a homogeneous accessibility of cellulose hydroxyl groups for the reagent during the next acetylation stage.

1.4.2 – Acetylation stage

Acetylation of cellulose is considered as a kind of esterification: the hydroxyl groups of cellulose can be substituted by acetyl groups. In the literature, the following equations are widely accepted as the general acetylation mechanism:

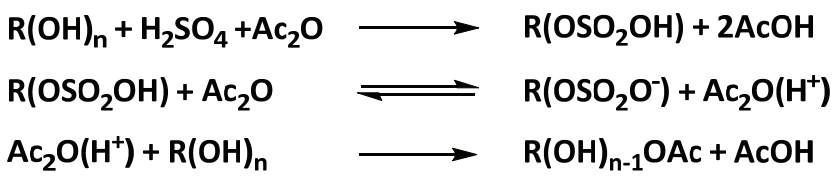

Figure 6: The general acetylation mechanism of cellulose acetate

In industry, the acetylation stage is usually in a continuous process (as shown in Figure 8).

1.4.3. – Hydrolysis stage

The hydrolysis of cellulose triacetate is mainly performed under acidic conditions in industrial process. Water or dilute acetic acid is needed to start this hydrolysis process:

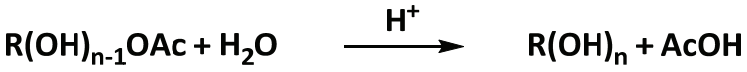

Figure 7: Hydrolysis of cellulose triacetate

Finally, the hydrolysis will be stopped when the desired degree of substitution of cellulose acetate is reached.

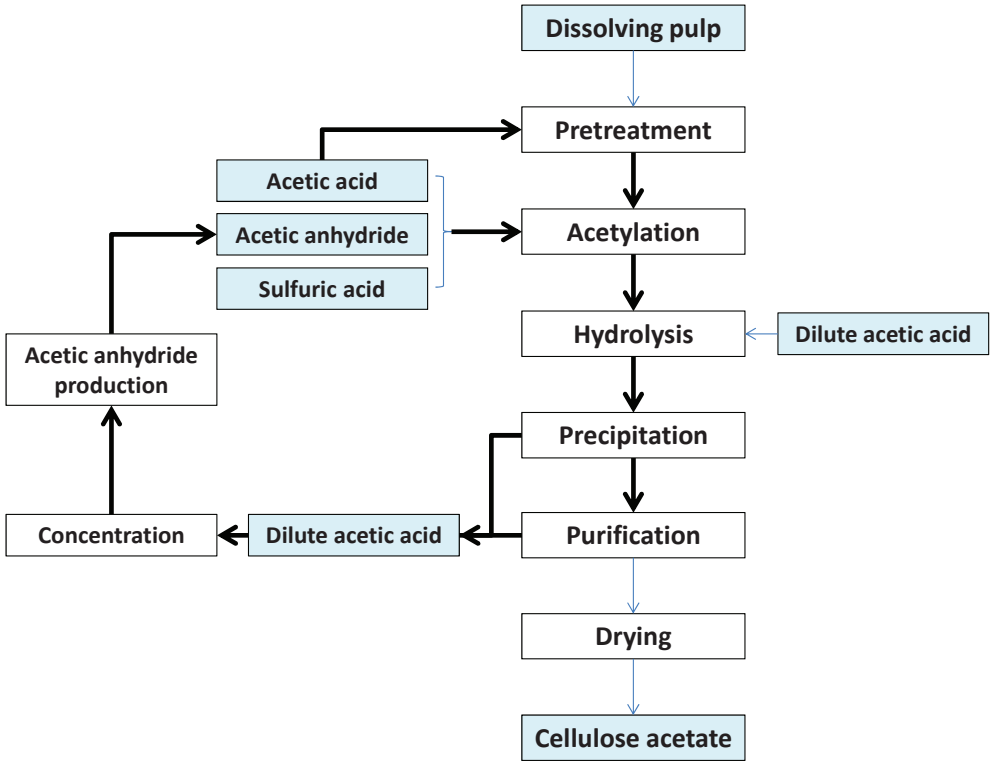

Figure 8: Simplified outline of industrial manufacturing process of cellulose acetate (Rustemeyer 2004).

1.4.4 – Final treatments

Once desired cellulose acetate is formed in solution, it needs to be precipitated, washed and dried. At the same time, a part of acetic acid can be recovered and recycled for further use in the continuous process. In some cases, recovered acetic acid is sufficient enough to be used for the self-production of acetic anhydride (as illustrated in Figure 8).

1.5 – General properties of unplasticized cellulose acetate

1.5.1 – Solubility of cellulose acetate in organic solvents

The solubility of cellulose acetate depends on the average degree of substitution (DS). Figure 9 outlines the solubility of commercial cellulose acetate in various organic solvents. Here, “degree of substitution” of cellulose acetate is replaced by another term: “acetic acid, %”. The conversion of DS in acetyl and acetic acid content is calculated according to Equation 1 and listed in Table 4. Formic acid and solvent mixture of methylene chloride / methanol (9:1) are able to dissolve all commercial cellulose acetates. Acetone is a good solvent for cellulose diacetate (DS 2.0 – 2.7).

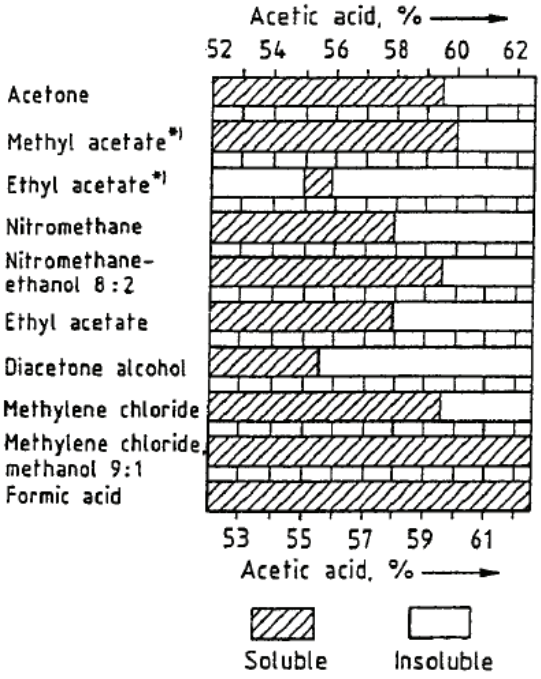

Figure 9: Solubility of commercial cellulose acetate in various organic solvents (Cellulose Ester of Ullmann's encyclopedia of industrial chemistry)

$$DS = \frac{162 \times \%_{Acetyl}}{(43 \times 100) - [(43 - 1) \times \%_{Acetyl}]}$$

Equation (1)

Where:

- 162 = molar weight of cellulose monomer
- 43 = molar weight of acetyl group
- $\%_{Acetyl}$ = acetyl content (wt.%)

Compound	DS	Acetyl Content	Acetic Acid Content
Cellulose	0	0.0%	0.0%
Cellulose Monoacetate	1	21.1%	29.4%
Cellulose Diacetate (CDA)	2	34.9%	48.8%
Cellulose Triacetate (CTA)	3	44.8%	62.5%

Table 4: Relationship of cellulose acetate's DS to acetyl content and combined acetic acid

1.5.2 – Thermal properties of cellulose acetate

Thermal properties of cellulose acetate were resumed by *Kamide and Saito 1985* in Figure 10.

The dependence of glass transition temperature (T_g) on the degree of substitution of cellulose acetate is generally described by Equation 2:

$$T_g(K) = 523 - 20.3\,DS$$

Equation (2)

In Figure 10, the crosspoint between T_g and decomposition temperature (T_d) is found at DS ~1.7, which means from this point, T_g of cellulose acetate is measurable by conventional characterization techniques. Another crosspoint is found at DS ~2.5 between melting temperature T_m and T_d. According to *Kamide and Saito 1985*, the limited range of DS ~2.5 is the only cellulose acetate whose T_m is lower than T_d. This is why DS 2.5 is the most suitable DS to be transformed through melt processing techniques and is always found among the commercial cellulose acetate grades. Its typical DSC thermogram is shown in Figure 11.

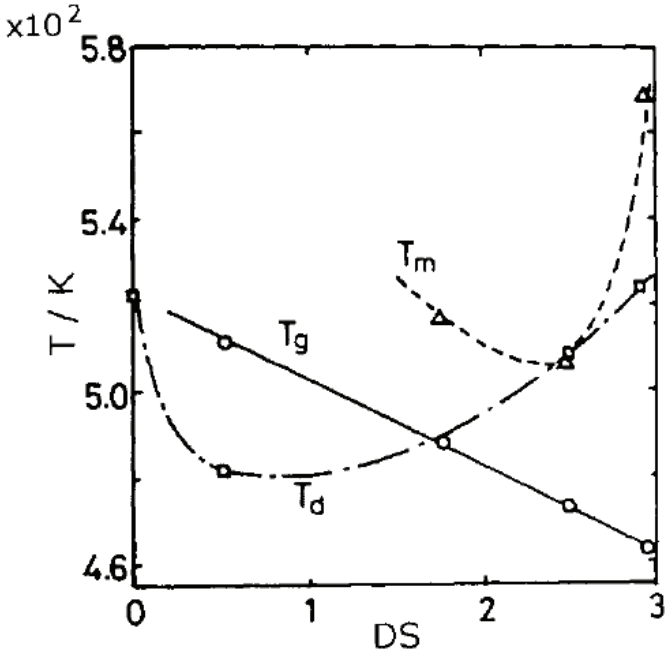

Figure 10: Dependence of glass transition temperature T_g, melting temperature T_m and decomposition temperature T_d on the average degree of substitution of cellulose acetate (Kamide and Saito 1985).

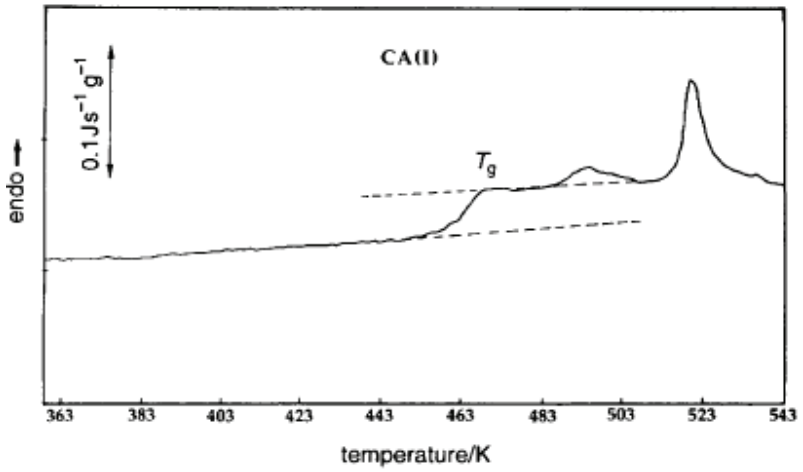

Figure 11: Typical DSC thermogram of unplasticized cellulose acetate powder (DS 2.5, McBrierty et al. 1996)

The glass transition temperature of DS 2.5 was identified at 190°C, along with polymer melting peaks at higher temperatures. The decomposition of cellulose acetate may occur at the same temperature range (*McBrierty et al. 1996*).

1.5.3 – Dynamic properties of cellulose acetate

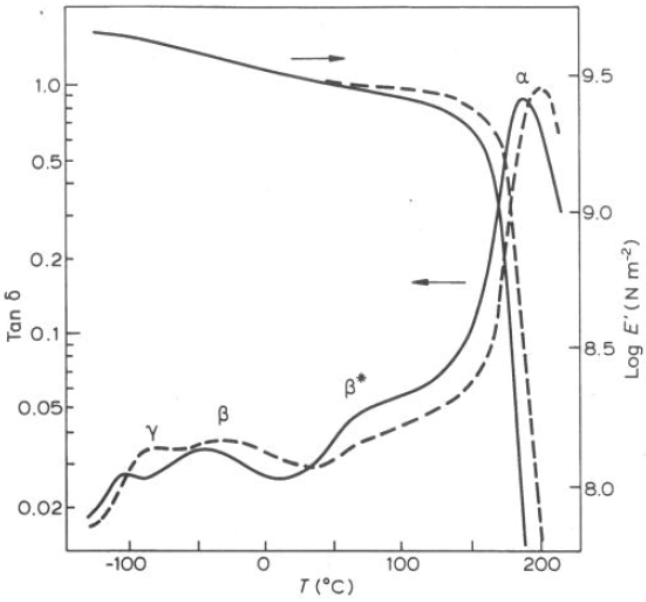

Figure 12: DMTA spectra of cellulose acetate at frequencies (–) 0.3 Hz and (--) 30 Hz (Scandola et al. 1985a)

Dynamic properties of cellulose acetate are generally evaluated by Dynamic Thermal Mechanical Analysis (DMTA) and Broadband Dielectric Spectroscopy (BDS). Literature researches were focused on cellulose acetate DS 2.5 (Figure 12 and 13). Mechanical and dielectric relaxations were identified.

Primary α-relaxation of cellulose acetate (DS 2.5) was determined at ~200°C (at frequency 3 Hz). The shoulder β* was believed to be related to the loss of water. Two secondary relaxations of cellulose acetate (denoted as β- and γ-relaxations) were found in the sub-glass region (*Scandola et al. 1985a*).

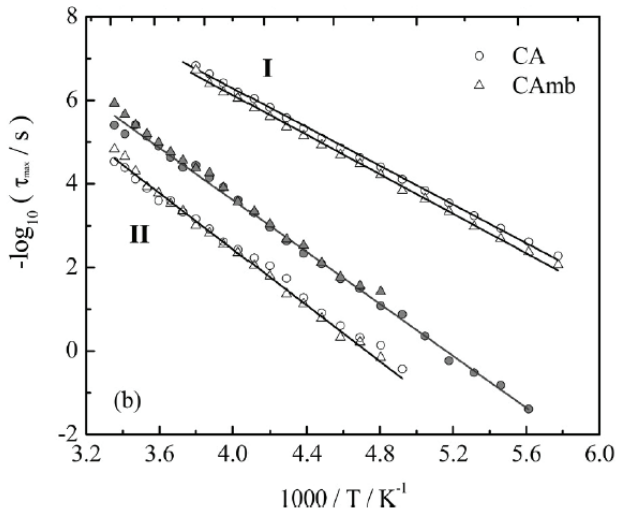

Figure 13: Temperature dependence of relaxation times of cellulose acetate (I: γ-relaxation and II: β-relaxation). (Sousa et al. 2010)

Dielectric studies of cellulose acetate (DS 2.5) have been reported in the literature along with those of polysaccharides (*Seymour et al. 1979, McBrierty et al. 1996, Einfeldt et al. 2001, Jafarpour et al. 2007, Kaminski et al. 2009, Sousa et al. 2010, Kusumi et al. 2011, Roig et al. 2011*). β- and γ-relaxations of cellulose acetate were identified but their molecular origins remain undetermined. The terminal α-relaxation of cellulose acetate was not as well documented as secondary relaxations due to conductivity interferences.

1.5.4 – Structural properties of cellulose acetate

The majority of structural studies of cellulose acetate are focused on cellulose triacetate (CTA). CTA is a semi-crystalline and has two polymorphs: CTA I and CTA II, the latter has been thoroughly analyzed by *Roche et al. 1978*. Little information is available for other amorphous cellulose acetates in the literature.

The International Centre for Diffraction Data (ICDD) has launched a project in order to collect the Powder Diffraction Files (PDF) for the study of polymorphism and crystallinity in cellulosics.
Fawcett et al. 2013 publish a resumed technical article containing diffractograms of cellulose acetate. An X-ray diffraction example of commercial cellulose acetate (DS 2.5) is shown in Figure 14. Three crystalline transitions are identified in a mainly amorphous background signal. Their weak intensities are issued from a low degree of crystallinity in the unplasticized cellulose diacetate.

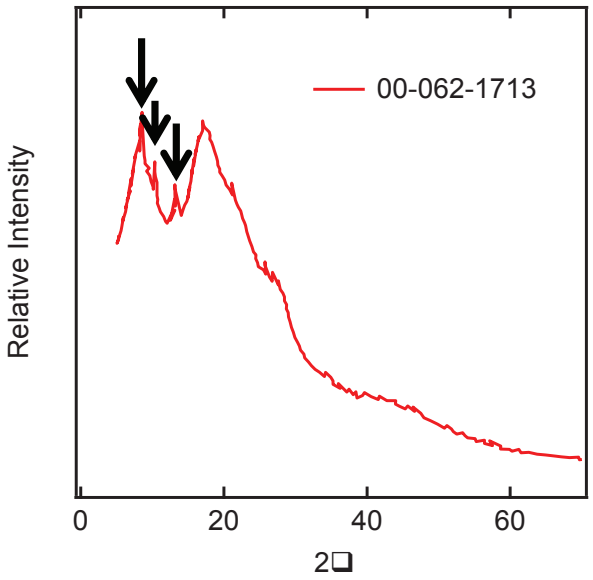

Figure 14: Diffractogram of cellulose diacetate (DS 2.5) from PDF N° 00-062-1713 (Fawcett et al. 2013). Arrows point out the crystalline transitions.

1.5.5 – Miscibility behavior of cellulose acetate

The work of *Dyer et al. 2013* on the blends of cellulose acetates (with different DS) is one of the neutron scattering studies of cellulose acetate available in the literature. The blend miscibility was proven to depend on the difference in degree of substitution (ΔDS) of cellulose acetate blend. However, the study covers a very limited range of correlation length and thus is incomplete. Other interesting work is done by *Kulkarni 1994a, b*.

1.6 – Plasticizers of cellulose acetate

Cellulose acetate has its own weakness: it needs to be plasticized for being industrially processed from the melt because its melting temperature is too close to its decomposition temperature. A plasticizer is an additive that is mixed with a polymer in order to make it more flexible, durable, and processable by

lowering transition temperature of the macromolecule. Literature bibliographic research of plasticized cellulose acetates is summarized in Table 5.

Literature Reference	Cellulose Acetate (DS)	Plasticizer
Buchanan, Dorschel et al. 1996	Blends of DS 2.49 (Eastman CA398-30) and DS 2.06 (Hydrolysis of DS 2.49)	Poly(ethylene glycol) (PEG 400)
Buchanan, Pearcy et al. 1997	DS 2.49 (Eastman CA398-30)	Poly(ethylene succinate)
Buchanan, Buchanan et al. 2003	DS 2.47 (Eastman product)	Arabinoxylan acetate
Nishio, Matsuda et al. 1997	DS 2.9 (acetylation of unmodified cellulose)	Poly(ε-caprolactone)
Miyashita, Suzuki et al. 2002 Ohno, Yoshizawa et al. 2005	DS 1.80, 2.18, 2.33, 2.48, 2.70, and 2.95 (Daicel products)	Poly(vinyl acetate) (PVAc), Poly(N-vinyl pyrrolidone) (PVP), Poly(N-vinyl pyrrolidone-co-vinyl acetate) [P(VP-co-VAc)]
Ohno and Nishio 2007a Ohno and Nishio 2007b	DS 1.80, 2.18, 2.33, 2.48, 2.70, and 2.95 (Daicel products)	Poly(vinyl acetate) (PVAc), Poly(N-vinyl pyrrolidone) (PVP), Poly(N-vinyl pyrrolidone-co-vinyl acetate) [P(VP-co-VAc)] Poly(methyl methacrylate) (PMMA) Poly(N-vinylpyrrolidone-co-methyl methacrylate) [P(VP-co-MMA)]
Higeshiro, Teramoto et al. 2009	DS 2.45 (Daicel product)	Poly(vinyl pyrrolidone-co-vinyl acetate)-graftpoly(ε-caprolactone) (PVPVAc-g-PCL)
Unohara, Teramoto et al. 2011	DS 2.15 (Daicel product)	Cellulose diacetate-graft-poly(L-lactide) (CDA-g-PLLA) Poly(vinyl acetate-co-vinyl alcohol)-graft-PLLA [P(VAc-co-VOH)-g-PLLA]
Aoki, Teramoto et al. 2011	DS 2.28 (Daicel product)	Poly(methyl methacrylate) (PMMA) CA-MA (mercaptoacetic acid)
Yoshitake, Suzuki et al. 2013	DS 1.80, 2.18, 2.48, 2.70, and 2.95 (Daicel products)	Poly(acryloyl morpholine) (PACMO)
Shashidhara, Guruprasad et al. 2002	Combined acetic acid = 53.5–55.5% w/w	Nylon 6
Cerqueira, Valente et al. 2009	DS 2.60 and 2.88	Polyaniline
Gaibler, Rochefort et al. 2004	DS 2.49 (Eastman CA398-30)	Polyvinyl phenol
Zhou, Zhang et al. 2003	Combined acetic acid, 54.5–56.0 wt%	Castor oil-based polyurethane
Choi, Lim et al. 2005	Eastman product	30% Triethyl citrate (TEC) Natural fibres

Warth, Mulhaupt et al. 1996	DS 2.5 (Acetow GmbH)	Lactones Hydroxyfunctional plasticizers Organosolv lignin, cellulose, starch, and chitin
Shaikh, Pandare et al. 2009	DS 2.6 to 3 (from bagasse cellulose)	Residual hemicellulose
Gutiérrez, De Paoli et al. 2012	Tenite Acetate 105 Cellulose acetate (38.7% acetyl degree) Eastman products	Dioctyl phthalate Glycerol triacetate Triethyl citrate Curauá fibers
Quintana, Persenaire et al. 2013	DS 2.5 (British American Tobacco)	Triacetin Tripropionin Triethyl citrate Tributyl citrate Tributyl 2-acetyl citrate Poly(ethylene glycol) 200
Mohanty, Wibowo et al. 2003 Park, Misra et al. 2004	DS 2.5 Eastman product	Triethyl citrate (TEC)
Meier, Kanis et al. 2004	CA with ca. 40% of acetyl content	Poly(caprolactone triol)
McBrierty, Keely et al. 1996	DS 2.5	Diethyl phthalate

Table 5: Summary of bibliographic references on additives able to plasticize cellulose acetates.

Plasticizers are incorporated in the amorphous parts of polymers while the structure and size of any crystalline part remains unaffected. Plasticizers are expected to reduce the modulus, tensile strength, hardness, density, melt viscosity, glass transition temperature, electrostatic chargeability, and volume resistivity of a polymer, while at the same time increasing its flexibility, elongation at break, toughness, dielectric constant, and power factor (Definition in "*Encyclopedia of Polymer Science and Technology*"). Plasticizers are usually low molecular weight (M_W) chemicals, which specifically interact with polymers and spread them apart in order to increase free volume in one system. Thus, plasticizers reduce polymer-polymer bonding and provide more molecular mobility for the macromolecules.

An ideal plasticizer should be highly compatible with polymers, stable in any kind of temperature environments, sufficiently lubricating over a wide temperature range, insensitive to radiations, leaching and migration resistant, inexpensive and should respect health and safety regulations. The current market offers numerous choices of plasticizers with a range of attributes that can be selected for specific applications to meet critical material requirements.

Plasticizers can be divided into two categories: internal plasticizers and external plasticizers. External plasticizers are not attached to polymer chains by covalent bonds and can therefore be lost by evaporation, migration or extraction. On the other hand, internal plasticizers are inherently part of the plastic and remain part of the product. Sometimes binary or even ternary plasticizer blends can be used to improve certain performance properties and/or to lower cost.

The most commonly used plasticizers worldwide are esters of phthalic acid. Phthalate esters were initially found to be no harmful to human beings and therefore have been used in various products such as children's toys and medical plastics where they may come in close contact with the human body. However in 2013, one of the most widely used phthalate plasticizer - di-(2-ethylhexyl) phthalate (DEHP), has been officially classified by the International Agency for Research on Cancer (IARC) to be possibly carcinogenic to humans (group 2B).

1.7 – Objectives of the current research work

The current research work is partially financed by Solvay group, who holds the Acetow GmbH, the third biggest supplier of cellulose acetate in the world. Cellulose acetate, as other natural polymers, has regained attention for various industrial applications due to its biodegradability and renewability. Cellulose acetate has been survived against petro-based synthetic polymers in industry thanks to the filter tow market for cigarettes in the late 20th century. Nowadays, the global market tends to assure a sustainable development which encourages the return of renewable materials.

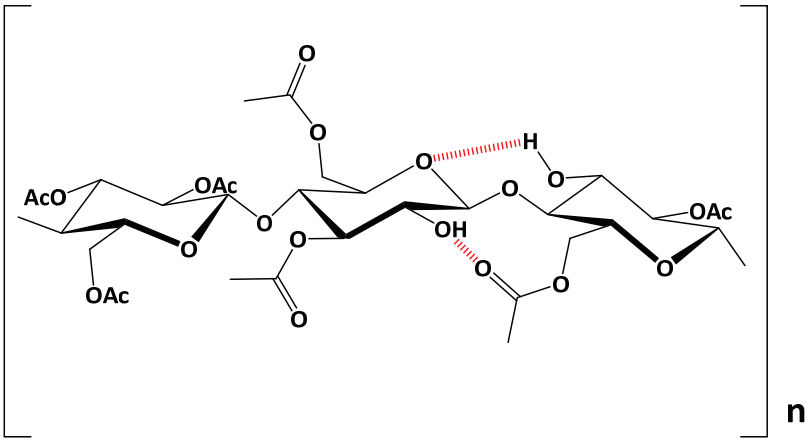

Figure 15: Chemical structure of cellulose acetate (DS 2.45, commercial grade) with possible intra H-bonding

Cellulose acetate is a derivative of cellulose, the most abundant organic polymer on Earth. It has an important polar interaction network consisting of hydrogen bonding and dipole-dipole interactions, which is believed to have significant influence on its ultimate properties (Figure 15). Dynamic relaxations of cellulose acetate are supposed to be dependent on polar interactions, especially for segmental motions (i.e. α-relaxation). It will be interesting to figure out how the strength and the density of polar interaction network marks its influence on polymer relaxations. This kind of polymers with specific interactions is rarely documented in the literature and it will be interesting to extend our investigations (theoretical and experimental researches) on it.

To do so, the first step is to modulate the strength and the density of polar interaction network with three parameters:

- **Degree of substitution (DS)**

The strength and the density of hydrogen bond network is strongly dependent on the amount of hydroxyl groups, which is defined by the degree of substitution. On the other hand, the strength and the density of dipolar interaction network is strongly related to the amount of acetyl side groups, which is also defined by the degree of substitution. Thus, three different DS will be under investigation in the present work:

- DS 2.45, the commercial grade of cellulose acetate
- DS 1.83 and DS 2.08, issued from pilot production

The chosen DS are required to accomplish the following conditions: possibility to dissolve in an organic solvent or solvent mixture, accessibility to their T_g (DS range of 1.7 ~ 3) and resulted samples suitable for characterizations.

- **Typology of plasticizers**

Plasticizers are able to modulate the polar interaction network by proposing different kinds of polymer-plasticizer interactions. Under the present work, traditional plasticizers of cellulose acetate are preferred. In this context, triacetin (TA) and diethyl phthalate (DEP) are selected as the plasticizers of cellulose acetate (Figure 16). Interactions between TA and cellulose acetate are supposed to be dissimilar with those between DEP and cellulose acetate.

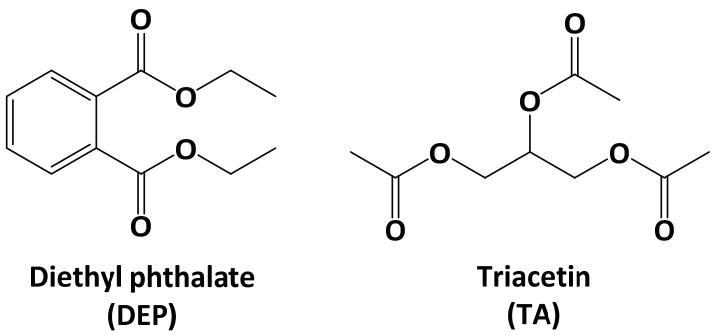

Figure 16: Chemical structure of plasticizers – diethyl phthalate and triacetin

Triacetin is a common plasticizer of cellulose acetate and an eco-friendly one. It has been less applied in industrial processes than DEP but is proven as an efficient CA plasticizer. With increasing demand of environmental protections and “green” polymers, TA is now considered as a potential candidate to replace the phthalate plasticizers.

Diethyl phthalate has been one of the most common plasticizers of cellulose acetate until the end of the 20th century. Due to some toxicity/security issues, its industrial use will be sharply reduced in the next future and replaced by eco-friendly plasticizers. For our study, DEP is considered as the reference plasticizer of the phthalate family.

- **Plasticizer content**

The third and last modulation factor is the plasticizer content, which is expected to vary from 0 to 50%, weight fraction. Considering the unprocessability of the unplasticized cellulose acetate in industrial processing, solvent casting method will be applied for sample preparation in this reasearch work.

The second step of the study is the characterization, which includes thermal (Modulated Differential Scanning Calorimetry, MDSC), thermo-mechanical (Dynamic Mechanical Thermal Analysis, DMTA), dielectric (Broadband Dielectric Spectroscopy, BDS), structural (Wide-Angle X-Ray Scattering, WAXS) and neutron scattering (Small-Angle Neutron Scattering, SANS) measurements.

Therefore, to resume the objectives of our work, it is important to:

- Confirm the plasticization effect of DEP and TA on cellulose acetate
- Identify and understand the miscibility behavior between the plasticizer and the polymer
- Study the influence of the polar interaction network (in terms of density and strength) on these behaviors
- Establish the link between the structure of plasticized CA systems and their dynamic properties as well as their relaxation mechanisms

Thus, this report is organized as follows: experimental conditions are presented in Chapter 2, some detailed information is listed in Appendix I and II.

In Chapter 3, we focus on the miscibility study between plasticizers and cellulose acetate by interpreting the thermal, thermo-mechanical and neutron scattering results. Chapter 4 is dedicated to the structural study by XRD technique. In Chapter 5, we focus on the dynamical properties of plasticized CA systems: identification of relaxation processes either by mechanical or by dielectric analysis, interpretations of their molecular origins/relaxation mechanisms. Each of these three chapters is completed with a global comparison and well-resumed conclusion with all available results.

A more complete discussion assembling all experimental results is made in the Chapter 6, in order to propose and to justify credible interpretations on the important behaviors observed in plasticized CDAs. General conclusions and perspectives can be finally found in Chapter 7.

CHAPTER 2

EXPERIMENTAL SECTION

2.1 – Materials

2.1.1 – Cellulose acetate and its solubility in organic solvents

Cellulose acetate flakes (CA) were kindly supplied by Solvay Acetow GmbH with three different degrees of substitution (DS 1.83, DS 2.08 and DS 2.45). They were used as raw materials of plasticized CA systems. The solubility of cellulose acetate in various organic solvents has been previously discussed. "Solvent Casting" method requires a solvent or a solvent mixture which fits the following conditions:

- Good solubility of cellulose acetate in this solvent
- Optimized volatility (for slow evaporation)
- No toxicity (according to our laboratory's policy regarding solvent manipulations)

Cellulose acetate with DS 2.45

Cellulose acetate with DS 2.45 is the commercial product for cigarette filter tow. It is chosen as the reference system of this work. Acetone is chosen as its organic solvent.

Cellulose acetate with DS 1.83

Cellulose acetate samples of DS 1.83 are obtained from a 'pilot-scale' level and cannot be considered as commercial products.

DS 1.83 is an interesting degree of substitution to study with non-negligible amounts of hydroxyl groups, for the evolution of the polar interaction network of the corresponding CA matrix. Acetone cannot totally dissolve the original flakes of DS 1.83 alone at room temperature. Small amount of water is needed to complete the dissolution step. The solvent mixture is acetone/water (95/5, v/v) in volume fraction for the first dissolution. After that, a second dissolution of treated DS 1.83 is performed in acetone with success.

Cellulose acetate with DS 2.08

DS 2.08 is an unusual but interesting degree of substitution for our investigations as little information is found in the literature, concerning its specific behavior. Surprisingly DS 2.08 is not at all dissolved by acetone at room temperature while DS 1.83 can be partially dissolved by acetone. Acetone/water is a good solvent mixture for DS 2.08 but the resulted film is not suitable for further characterizations.

Ethyl acetate, methyl formate, methanol, isopropanol, chloroform and dichloromethane were also tested without success. Finally, we succeeded with a mixture of acetone/methanol (75/25, v/v). Thus, organic solvents or solvent mixtures applied in this work are:

- DS 1.83 – acetone/water (95/5, v/v), then second dissolution in acetone
- DS 2.08 – acetone/methanol (75/25, v/v)
- DS 2.45 – acetone

2.1.2 – Plasticizers of cellulose acetate

Triacetin

Triacetin (TA), also called glycerin triacetate, is one of the most common plasticizers of cellulose acetate. It is also an eco-friendly plasticizer. Triacetin and cellulose acetate share same side functional groups: acetyl groups. Table 6 shows the properties and characteristics of triacetin.

Diethyl phthalate

Diethyl phthalate (DEP) belongs to the family of phthalates which is often used as plasticizer for a wide range of polymer systems (notably PVC). DEP differs from TA in that there is an aromatic ring in its chemical structure. Table 6 shows the properties and characteristics of DEP. Unfortunately, the phthalate family may have some toxicity issues so that they have been less and less used as plasticizers in industry.

	Triacetin	Diethyl Phthalate
Chemical Structure	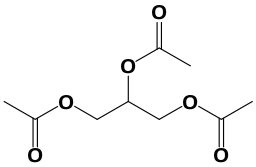	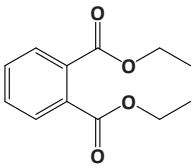
CAS Number	102-76-1	84-66-2
Formula	$C_9H_{14}O_6$	$C_{12}H_{14}O_4$
Molecular Weight	218 $g.mol^{-1}$	222 $g.mol^{-1}$
Density	1.16 $g.cm^{-3}$ at 25°C	1.12 $g.cm^{-3}$ at 20°C
Appearance	Oily liquid	Oily liquid

Table 6: Properties and characteristics of triacetin and diethyl phthalate

2.2 – Preparation of cellulose acetate films through Solvent Casting method

Solvent casting is the only preparation method at the laboratory scale to produce both plasticized and unplasticized cellulose acetate films. It is a common film-making method used in the literature.

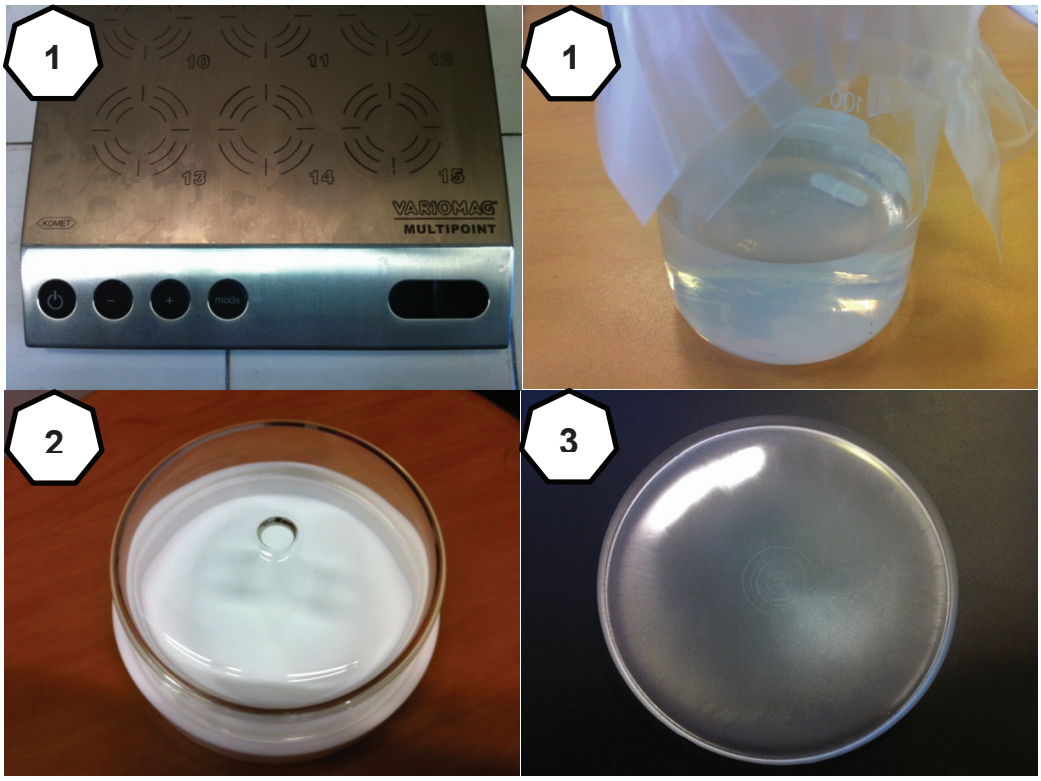

Figure 17: Photographs of solvent casting method (step 1 to 3, respectively).

1) Plasticized cellulose acetate solution

Cellulose acetate and plasticizer mixtures in the desired weight proportions were dissolved in the corresponded solvent (mixtures) at a concentration of 10%. Plasticizer content in the plasticized cellulose acetate systems varied from 0 to 50% in weight fraction. The solutions were stirred for at least 24 h at room temperature and then poured into a Teflon tray.

2) Solvent evaporation

Films were made by slow solvent evaporation at room temperature and stored in a desiccator until analysis. Slow solvent evaporation prevents films from surface damaging and air bubbles.
Acetone is the solvent for the evaporation process because of its volatile nature. Teflon tray is specially designed for slow solvent evaporation and for film removal process.

3) Characteristics of plasticized CA films

Finally, plasticized CA films are measured as 10 cm in diameter and 300-400 mm thickness (as shown in Figure 17). They are relatively transparent and have a good mechanical resistance. The shape and dimension of plasticized CA films are totally suitable for further characterizations.

Karl Fischer titration method

Trace amounts of water were quantified by Karl Fischer titration method at 160 °C. It helps us to improve further experimental conditions and to have a glance at the influence of water on our films.

NMR spectroscopy used for the determination of plasticizer content

NMR samples were prepared using acetone-d6. Tetramethylsilane (TMS) was used as internal standard for each sample. ^{1}H NMR spectra were measured over the range of 0 - 15 ppm with a Bruker 300 MHz instrument (Karlsruhe, Germany). From the obtained spectra, the exact plasticizer content was determined using pyrrole as the reference. Standard deviation is estimated at ± 1~2%, weight fraction.

2.3 – Miscibility study of cellulose acetate

2.3.1 – Modulated Differential Scanning Calorimetry (MDSC)

Figure 11 (see Chapter 1) is a typical thermogram of cellulose acetate obtained by the traditional Differential Scanning Calorimetry (DSC). The step decrease of the heat flow which is related to the glass transition seems to be superimposed with other transitions and is not easy to be determined. To resolve this problem, it was decided to use the modulated DSC (MDSC) instead of the traditional one.

Modulated DSC calorimetry has been commercialized at the end 1990's and has been proven as an efficient tool to analyze complex transitions. It is an improved version of the traditional DSC which provides significant advantages over the latter one: separation of complex transitions, increased sensitivity for detection of weak transitions and, most importantly, measurement of heat flow and heat capacity in a single experiment (Figure 18).

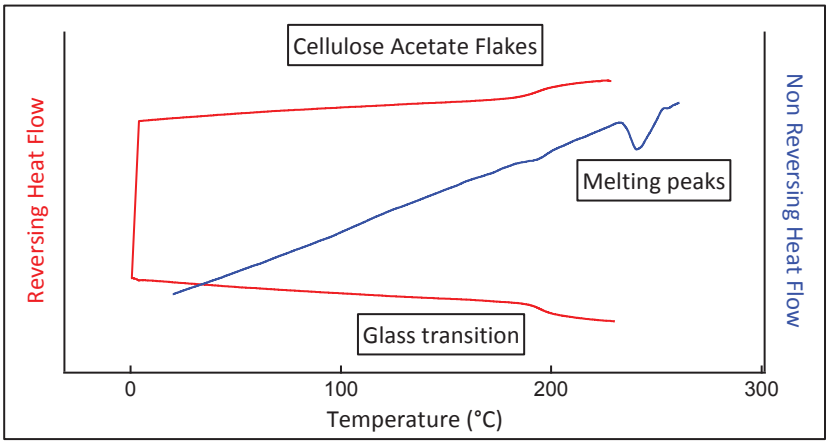

Figure 18: Our DSC thermogram of unplasticized secondary cellulose acetate flakes. Heating rate 5°C.min^{-1}. Data collected by MDSC.

Modulated DSC differs from traditional DSC in that it applies two simultaneous heating rates to the sample (Figure 19). The linear heating rate provides the same information as traditional DSC (i.e. total heat flow rate), while the modulated sinusoidal heating rate is used to calculate the fraction of the total heat flow rate that corresponds to a changing heating rate. This fraction is called reversing heat flow which is dependent on heat capacity (or changes in heat capacity). The remaining fraction of the total heat flow is then called non-reversing heat flow, which is a time-dependent or kinetic component. Complex transitions can then be separated according to this principle: Heat flow = reversing heat flow (heat capacity dependent) + non-reversing heat flow (kinetic/time dependent).

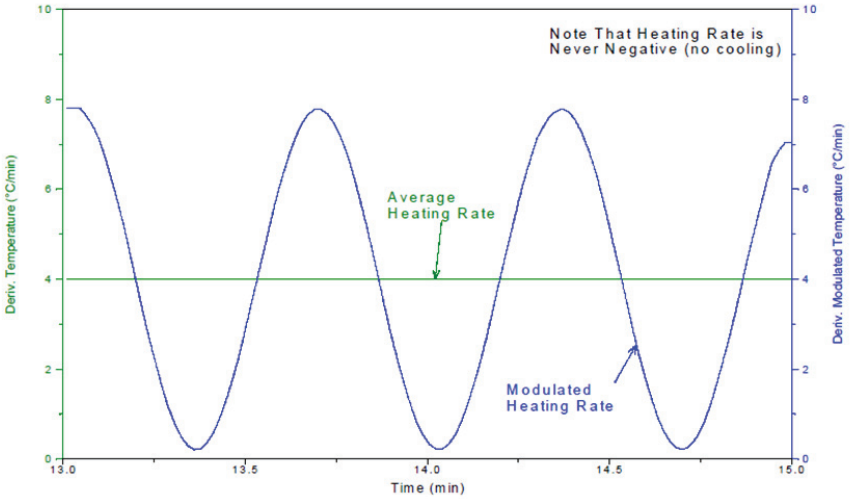

Figure 19: Principles of modulated DSC

In this work, the most important transition to be studied is the glass-to-rubber transition of plasticized cellulose acetates, which should be found in the reversing heat flow. Other thermal transitions, such as decomposition or cristallization process, can be found in the non-reversing heat flow.

MDSC measurements were performed by using a Q2000 differential scanning calorimeter (TA Instruments, United States) equipped with a liquid N_2 cooling device. Indium was used for temperature and heat flow calibration. Sapphire was used to calibrate the MDSC reversing heat capacity signal. For each measurement, 5 - 10 mg of material was sealed into a Tzero aluminum pan and placed in the autosampler. Samples were preconditioned at 70 °C for 15 min to eliminate any residual solvent. Thermograms were recorded during heating at a scanning rate of 5 °C/min. Modulation was performed every 40 s at ± 2 °C. Glass transition temperatures were determined from the second scan in order to discard the influence of thermal history.

Determination of phase compositions

In case of phase separations, the MDSC can also help us to calculate phase compositions and their volume fraction by comparing theoretical and experimental T_g values and the heat capacity step ΔCp. Theoretical T_g values were predicted from the Couchman-Karasz equation (*Couchman & Karasz, 1978*), an empirical law which assumes no specific interactions between the two components of the blend:

$$T_g = \frac{w_1 \times \Delta Cp_1 \times T_{g1} + w_2 \times \Delta Cp_2 \times T_{g2}}{w_1 \times \Delta Cp_1 + w_2 \times \Delta Cp_2}$$

Equation (3)

Where

- T_{g1} is the glass transition temperature of the pure polymer
- T_{g2} that of plasticizer
- w_1 and w_2 the weight fraction of each component
- ΔC_{p1} and ΔC_{p2} the increment of heat capacity

Phase composition was also calculated from the above equation by using its corresponded experimental T_g value. Thus, the resulted w_1 and w_2 are the weight fractions of each component in this phase domain. The volume fractions of each phase domain in a plasticized CDA system were determined by the heat capacity step ΔC_p.

$$\%_{\varphi} = \frac{\Delta C_{pi}}{\Delta C_{pc}} \times 100\%$$

Equation (4)

Where

- ΔC_{pi} is the heat capacity step of a phase domain
- ΔC_{pc} is the heat capacity step of a pure component

When the phase domain is rich in cellulose acetate, then ΔC_{pc} should be that of unplasticized CA system. On the other hand, when the phase domain is rich in plasticizer, then ΔC_{pc} should be that of pure plasticizer. The MDSC results and related calculations will help us establish a first view on the miscibility behavior of plasticized cellulose acetate systems.

2.3.2 – Dynamic Mechanical Thermal Analysis (DMTA)

Dynamic Mechanical Analyzer (DMA) works by applying a sinusoidal deformation to a sample of known geometry. The sample will deform under a controlled stress or strain according to instruments. Then DMA measures stiffness and damping which are generally reported as modulus and tan δ. The modulus can be divided into two parts: the storage modulus (E') and the loss modulus (E") because of the sinusoidal deformation:

$$\sigma(t) = \gamma_0[E' \sin \omega t + E'' \cos \omega t]$$

Equation (5)

Storage modulus (E') is a measure of the elastic response of a material (stored energy) while loss modulus (E") is a measure of the viscous response of a material which is associated to dissipation of energy. The ratio between the loss and the storage moduli is called the loss angle or tan δ, which is the out-of-phasing angle between stress and strain, and which represents the energy proportion dissipated as heat by the polymer in a sample. Figure 12 (see Chapter 1) is a general example of the modulus plot of cellulose acetate against temperature. The glass transition is characterized as a large drop (a decade or more) in the storage modulus when log E' is plotted against a linear temperature scale. A peak can be seen in E" and tan δ signals at the same time. Secondary transitions could also be detected but with much less intensity.

A Rheometrics Scientific Analyzer RSA II was used to perform DMTA measurements. Samples were cut into rectangular films having the following dimensions: length of 26.5 mm, width of 4.5 mm and thickness of 0.3 mm. Strain limit was fixed at 0.02 %. Thus the mechanical response of all samples will be found in the linear regime. Curves were recorded at frequencies 1 Hz during heating from ~-100 °C at a scanning rate of 2 °C/min.

Theoretical T_αs for polymer-plasticizer blends can be predicted by the Fox equation (*Fox, 1956*), another empirical law which assumes no specific interactions between the two components of the blend.

$$\frac{1}{T_g} = \frac{w_1}{T_{g1}} + \frac{w_2}{T_{g2}}$$

Equation (6)

Where

- T_{g1} is the glass transition temperature of the pure polymer
- T_{g2} that of plasticizer
- w_1 and w_2 the weight fraction of each component

2.3.3 – Small-Angle Neutron Scattering (SANS)

Small-Angle Neutron Scattering (SANS) is a well-established characterization method for microstructure investigations in various materials, such as macromolecules, colloids, porous systems or proteins, etc. Furthermore, it can reveal inhomogeneity from the near atomic scale (~0.5 nm) to the near micron scale (~1 000 nm). Consequently, SANS is considered as a powerful tool to characterize the miscibility behavior of plasticized cellulose acetates.

The SANS experiments were performed on the D11 beamline at Institut Laue Langevin (ILL, Grenoble, France), using a neutron wavelength of 6 Å (λ).The instrument layout of D11 is shown in Figure 20. A polychromatic neutron beam comes from the vertical cold source of the ILL high flux reactor and is monochromated by a velocity selector. The neutrons are then collimated by a series of moveable glass guides in order to control their divergence, size and intensity.

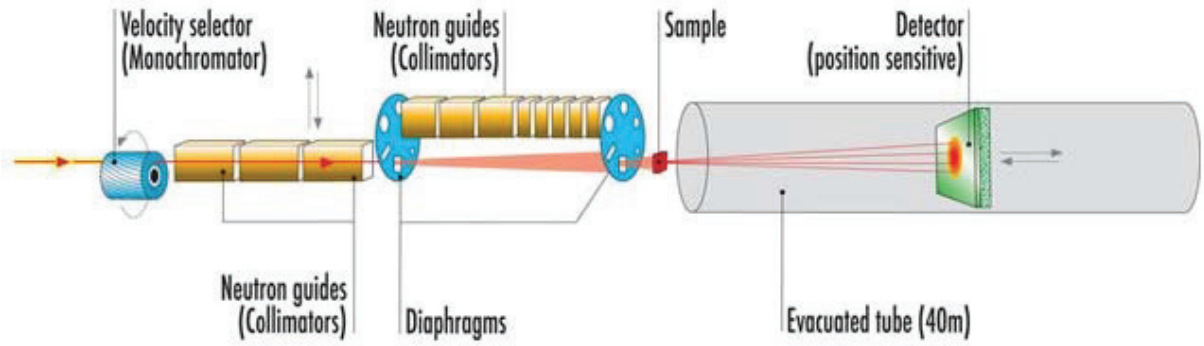

Figure 20: Instrument layout of D11 (Institut Laue Langevin, Grenoble, France)

When the neutron beam is directed at a sample, some of the incident radiation is transmitted by the sample, some is absorbed and some is scattered. Neutrons scattered from the sample are detected on a multi-position detector which may be placed at any distance between 1.2 and 39 meters from the sample position, giving a total accessible momentum transfer (q) range of 3.10^{-4} to 1 $Å^{-1}$. Three detector distances were applied in our study: 1, 8 and 28 m to cover a q range of 2.15 * 10^{-3} – 0.5 $Å^{-1}$. Complete characteristics of D11 instrument are listed in Appendix I.

Definitions of Small-Angle Neutron Scattering

One of the most important definitions in SANS is the scattering cross section, which is a measure of how strongly neutrons will be scattered from the nucleus. The total scattering cross section (σ_s, cm^2) is defined as:

$$\sigma_s = \frac{total\ number\ of\ neutrons\ scattered\ by\ second}{\Phi}$$

Equation (7)

Where Φ is the number of incident neutrons per unit area per second.

The differential cross section is defined as:

$$\frac{d\sigma}{d\Omega} = \frac{number\ of\ neutrons\ scattered\ per\ second\ into\ d\Omega\ in\ direction\ \theta,\phi}{\Phi d\Omega}$$

Equation (8)

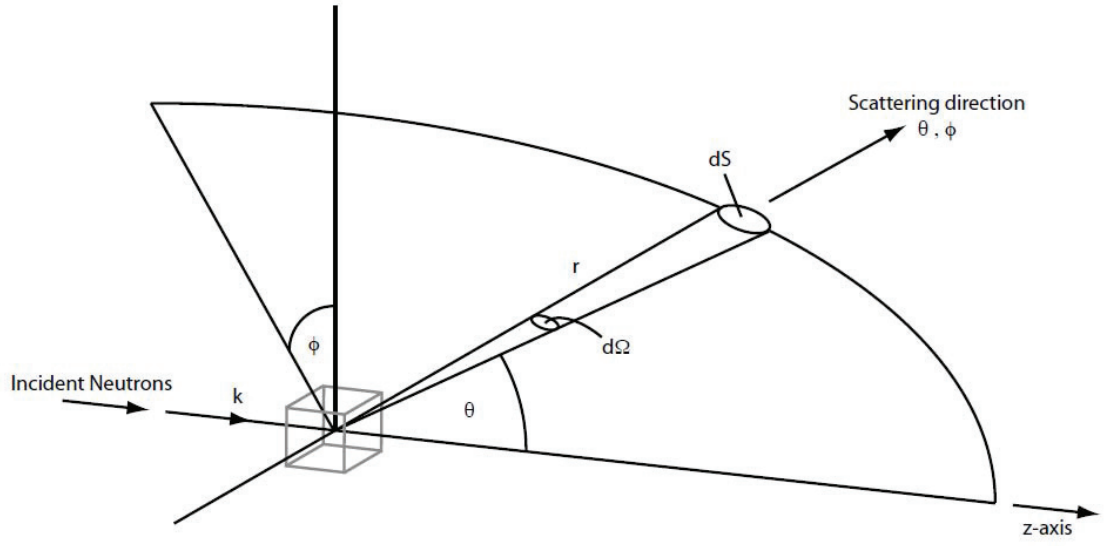

Figure 21: The geometry of a scattering experiment

It can also be expressed as:

$$I(q) = \frac{d\sigma}{d\Omega}(per\ unit\ volume) = N(\Delta\rho)^2 V^2 P(q) S(q)$$

Equation (9)

Where

I(q):	Scattering intensity (cm^{-1})
q	Scattering vector ($Å^{-1}$)
N:	Number of scattering objects per unit volume (cm^{-3}), ≈ φ/ξ^3 according to Figure (φ is volume fraction of scattering objects in the sample)
$\Delta\rho$:	Scattering length density contrast (cm^{-2})
V:	Volume of scattering objects (cm^3), ≈ ξ^3 according to Figure
P(q):	Normalized form factor, which represents the interference of neutron scattered from different parts of the same object (dimensionless)
S(q):	Normalized structure factor, which represents the interference of neutrons scattered from different objects (dimensionless)

Figure 22 shows scattering objects with a correlation length ξ in a SANS sample which can be expressed by the Equation 9. Later in Chapter 3.3, the Debye-Bueche Equation is based on the Equation 9.

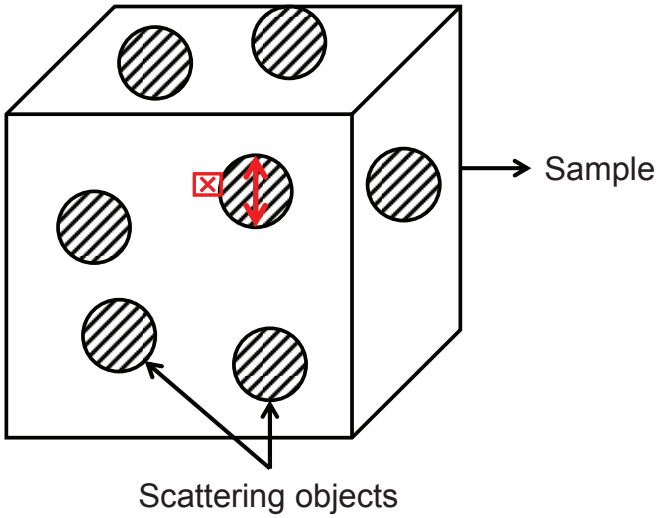

Figure 22: Illustration of scattering objects (with a correlation length ξ) in a SANS sample.

Scattering vector *q* is defined as:

$$q = \frac{4\pi}{\lambda}\sin\left(\frac{\theta}{2}\right)$$

Equation (10)

Where

- λ: neutron wavelength (Å)
- θ: scattering angle between the incident beam and the scattered beam

A quantity called scattering length density is defined as follows:

$$\rho = \frac{\sum_i^n b_i}{\overline{V}}$$

Equation (11)

Or

$$\rho = \left(\sum n_i \times b_i\right) \times \frac{d \times N_A}{M_w}$$

Equation (12)

Where

- ρ: coherent scattering length density of a material
- n_i: number of an isotope in a monomer
- b_i: coherent scattering length of an isotope
- $\overline{V}$: the volume containing the n atoms
- d: density of a material ($g.cm^{-3}$)
- N_A: Avogadro constant (mol^{-1})
- M_w: molar mass of a monomer ($g.mol^{-1}$)

Thus, the scattering length density contrast between two phases is defined as:

$$\Delta\rho = \rho_1 - \rho_2$$

Equation (13)

Where

- ρ_1 and ρ_2 are the scattering length densities of the phase 1 and phase 2, respectively.

NIST Centre for Neutron Research (NCNR) provides a summary table of neutron scattering lengths and cross sections with the complete list of elements and isotopes (*Sears 1992*).

Table 7 is the summary of theoretical coherent scattering length densities of all samples. Neutrons are elastically scattered either by nuclear scattering (through interaction with the nucleus) or by magnetic scattering (through interaction of unpaired electrons with the magnetic moment of the neutron). Neutron scattering lengths vary randomly with atomic number. It also varies between isotopes of the same element. The most useful example is hydrogen and deuterium: ^{1}H is one of the rare isotopes whose coherent neutron scattering length density is negative. Thus the scattering length of a molecule can be varied by replacing hydrogen with deuterium. This technique is called “contrast variation” or “deuterium labelling” and is one of the key advantages of neutron scattering over X-rays and light (Figure 23).

	ρ (cm^{-2})
DS 1.83	1.73E+10
DS 2.08	1.76E+10
DS 2.45	1.79E+10
DEP	1.54E+10
DEP d_{14}	5.56E+10
TA	1.35E+10
TA d_9	4.17E+10

Table 7: Summary of theoretical coherent scattering length densities of cellulose acetates and plasticizers. DEP d_{14} and TA d_9 are the deuterated plasticizers.

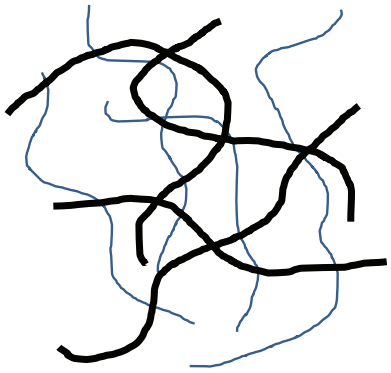

Figure 23: Schematic representation for a mixture of deuterated and non-deuterated polymers (bold lines represent the deuterated part of polymer blend).

Incoherent neutron scattering intensity

Neutron scattering is characterized by coherent and incoherent contributions to scattering. In our SANS experiments, we are interested in the coherent contributions. The incoherent part of neutron scattering needs to be calculated and to be separated from the coherent part (Equation 14).

$$I_{incoherent} = \frac{d \times N_A \times n_H \times xs_H}{M_w \times 4\pi}$$

Equation (14)

Where

- d: density of a material ($g.cm^{-3}$)
- N_A: Avogadro constant (mol^{-1})
- M_w: molar mass of a monomer ($g.mol^{-1}$)
- n_H: number of ^1H in a monomer
- xs_H: incoherent scattering cross section of ^1H (10^{-24} cm^2)

According to NIST Centre for Neutron Research (NCNR), the incoherent scattering cross section of ^1H is $80.27*10^{-24}$ cm^2. Other isotopes' incoherent scattering cross sections are negligible compared to ^1H's value. Incoherent neutron scattering is *q* (the scattering vector) independent. Table 8 is the summary of incoherent scattering results of all samples.

	SANS Sample	Incoherent (cm^{-1})	Plateau Value (cm^{-1})	Differences
Triacetin d_9	DS 2.45 + 10% TA	0.26	0.43	0.17
	DS 2.45 + 20% TA	0.25	0.42	0.17
	DS 2.45 + 40% TA	0.21	0.38	0.17
	DS 1.83 + 10% TA	0.27	0.50	0.23
	DS 1.83 + 20% TA	0.25	0.39	0.14
	DS 1.83 + 40% TA	0.21	0.39	0.18
	DS 2.08 + 10% TA	0.27	0.40	0.13
	DS 2.08 + 20% TA	0.25	0.49	0.24
	DS 2.08 + 40% TA	0.21	0.42	0.21
Triacetin	DS 2.45 + 10% TA	0.28	0.52	0.24
	DS 2.45 + 20% TA	0.28	0.50	0.22
	DS 1.83 + 10% TA	0.29	0.53	0.24
	DS 2.08 + 10% TA	0.29	0.53	0.24
Diethyl Phthalate d_{14}	DS 2.45 + 45% DEP	0.16	0.36	0.20
	DS 2.45 + 30% DEP	0.20	0.43	0.23
	DS 2.45 + 20% DEP	0.23	0.46	0.23
	DS 2.45 + 10% DEP	0.25	0.50	0.25
Diethyl Phthalate	DS 2.45 + 30% DEP	0.28	0.47	0.19
	DS 2.45 + 20% DEP	0.28	0.49	0.21
	DS 1.83 + 30% DEP	0.29	0.47	0.18
	DS 2.08 + 20% DEP	0.28	0.49	0.21

Table 8: Summary of incoherent scattering results of all samples (deuterated and protonated samples)

2.4 – Structural study of cellulose acetate

2.4.1 – Degree of crystallinity by calorimetry

The crystallinity degree of cellulose acetate is estimated by the ratio between the melting enthalpy of the material under study (ΔH_m) and the respective value for the totally crystalline material (ΔH^0_m):

$$\chi_c(\%) = \frac{\Delta H_m}{\Delta H_m^0} \times 100$$

Equation (15)

Where ΔH^0_m = 58.8 J/g as proposed by *Cerqueira et al. 2006*.

2.4.2 – X-ray diffraction

Wide-angle X-ray scattering (WAXS) is used to gather structural information of cellulose acetate systems in the present work. This technique is based on the Bragg's Law of diffraction which describes the condition for a reflected X-Ray beam to constructively interfere with an incident beam:

$$n\lambda = 2d \sin\theta$$

Equation (16)

Where

- n: an integer
- λ: the wavelength of incident X-ray beam
- θ: the angle of incident X-ray beam
- d: distance between crystalline layers

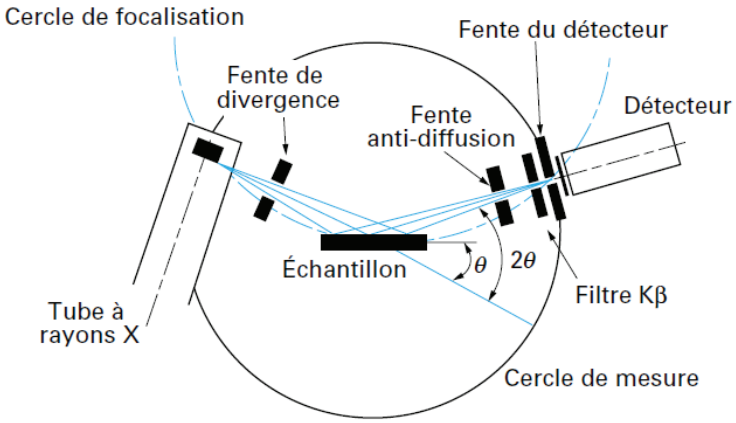

Figure 24:Scheme of X-ray diffractometer (from Technique de l'Ingénieur p1080)

WAXS differs from small-angle X-ray scattering (SAXS) because its scattering angles 2 θ is larger than 5°. The experimental setup is the following: an X-Ray beam is sent to the sample at a given incident angle, the beam penetrates in the sample and it is reflected. A detector placed behind the sample detects the reflected beams and their scattered intensity as shown schematically on Figure 24. Finally, the resulted X-ray diffractogram is the plot of scattered intensity against the scattering angle 2 θ. Due to major amorphous nature of cellulose acetate, WAXS diffractograms are expected with little crystalline peaks. Nevertheless, useful structural information can be gathered by X-ray patterns.

X-ray diffractograms were measured on a Bruker D8 Advance diffractometer (Bruker, Germany) by refraction method using nickel-filtered CuKα radiation (λ = 1.5406 Å) operated in the ω-2 θ scanning mode between 1 and 90° (2 θ).

2.5 – Dynamic properties of cellulose acetate

2.5.1 – Broadband Dielectric Spectroscopy (BDS)

Broadband dielectric spectroscopy (BDS) is our characterization technique for studying dynamic properties of plasticized CDA systems. Analogous to a sinusoidal deformation in DMTA measurement, an electric field is applied to a dielectric material. By measuring dynamics of polarization of a material, one can obtain information regarding its molecular motion. BDS is a powerful technique because it covers a large frequency range and temperature range in a single experiment. However, only materials with sufficiently high polarisability are suitable for this characterization technique. BDS measurements were carried out in the frequency range of 0.06 - 10^7 Hz by means of an Alpha-N analyzer from Novocontrol GmbH (Hundsangen, Germany). Isothermal frequency scans were performed from - 130°C up to 200°C in steps of 4°C/scan. Temperature was controlled to better than 0.1 K with a Novocontrol Quatro cryosystem. Parallel gold-plated electrodes with a diameter of 20 mm were used. The sample thickness was 0.3 - 0.4 mm.

Data analysis

In order to analyze dielectric relaxation processes, several model functions have been proposed in the literature. Debye relaxation is the dielectric relaxation response of an ideal, non-interacting population of dipoles to an alternating external electric field:

$$\varepsilon^*(\omega) = \varepsilon_\infty + \frac{\Delta\varepsilon}{1 + i\omega\tau_D}$$

Equation (17)

Where

- $\Delta\varepsilon = \varepsilon_s - \varepsilon_\infty$ is the dielectric strength (the difference between the real permittivity values at the low and high frequency limits)
- τ_D is the Debye relaxation time

Debye-like relaxation behavior is rarely observed. Usually dielectric peaks are much broader than Debye-like ones. The broadening of dielectric functions could be described by Cole-Cole equation (*Cole & Cole, 1941, 1942*):

$$\varepsilon^*(\omega) = \varepsilon_\infty + \frac{\Delta\varepsilon}{1 + (i\omega\tau_{CC})^\alpha}$$

Equation (18)

Where α is the symmetrical broadening factor of dielectric function with $0 < \alpha \leq 1$. Debye model is actually a simplified version of Cole-Cole equation if $\alpha = 1$. Cole-Cole equation is frequently used as the model function of data analysis of secondary relaxation processes.

The commercial software "WinFit" was used to fit the isothermal dielectric relaxation data by using a sum of the model function introduced by Havriliak and Negami (*Havriliak & Negami, 1967*):

$$\varepsilon^*(\omega) = \varepsilon_\infty + \sum_j \frac{\Delta\varepsilon_j}{\left[1 + \left(i\omega\tau_j\right)^{\alpha_{HNj}}\right]^{\beta_{HNj}}}$$

Equation (19)

Where

- $\Delta\varepsilon = \varepsilon_s - \varepsilon_\infty$ is the dielectric strength (the difference between the real permittivity values at the low and high frequency limits)
- $\tau \approx (2\pi f_{max})^{-1}$ is the characteristic relaxation time
- α_{HN} and β_{HN} are the shape parameters ($0 < \alpha_{HN} < 1$, $0 < \alpha_{HN} \cdot \beta_{HN} < 1$)
- j is the number of relaxation processes

Cole-Cole equation is also a simplified version of Havriliak-Negami equation if $\beta = 1$.

CHAPTER 3

MISCIBILITY BEHAVIOR OF CELLULOSE ACETATE - PLASTICIZER BLENDS

In Chapter 3, miscibility behavior of plasticized cellulose acetate is studied through the exploration of three characterization techniques: Modulated Differential Scanning Calorimetry (MDSC), Dynamic Mechanical Thermal Analysis (DMTA) and Small-Angle Neutron Scattering (SANS). The first two are conventional techniques used for materials science while SANS is able to provide information about structure and dynamics of polymers on a length scale of 5 ~ 1000 Å, which is not an accessible range for MDSC and DMTA. The objective of the study is to understand miscibility behavior between cellulose acetate and its plasticizers from a macroscopic and a microscopic point of view.

3.1 – Miscibility behavior of plasticized cellulose acetate: a MDSC study

First, it would be better to introduce the criteria of “miscibility” before any discussion or interpretation. The miscibility term is commonly estimated by the determination of the glass transition temperature(s) of the binary system. From a thermodynamic perspective, polymer blends may be miscible, partially miscible, or immiscible. A miscible blend will exhibit a single glass transition between the T_g values of both components with a sharpness of the transition similar to that of the components. Broadening of glass transitions is a criterion of heterogeneous dispersion of components in the blend. With cases of limited miscibility (partial miscibility), two separate transitions between those of the constituents may result, depicting a component-1 rich phase and a component-2 rich phase. T_g values of separated phases are between those of pure components. A fully immiscible polymer blend will result the finding of T_g‘s of component 1 and component 2.

Cellulose acetates with three different degrees of substitution (DS 1.83, DS 2.08 and DS 2.45) plasticized by triacetin and diethyl phthalate are discussed here. The plasticizer content varies from 0% to 50% weight fraction, by steps of 10%. Cellulose acetates with specific plasticizer percents may be produced and analyzed if necessary. In this chapter, representative samples are analyzed in details. In case of partial miscibility (i.e. phase separation), plasticized cellulose acetate is considered as a two-phase system: cellulose acetate-rich phase (CDA-rich phase) and plasticizer-rich phase. As a reminder, glass transition temperatures are determined from the second heating scan in order to discard the influence of thermal history.
Thermal analysis is able to provide important details on the behavior of plasticized cellulose acetates:

- Identification of glass transition and ability for phase separation.
- Miscibility diagram of cellulose acetate and its plasticizers.
- Calculation of phase compositions according to empirical Couchman-Karasz equation.
- Determination of volume fractions of each phase in case of phase separation.

3.1.1 – Cellulose acetate (DS 2.45) plasticized by triacetin and diethyl phthalate

The first series of plasticized cellulose acetate to be analyzed is DS 2.45 plasticized by triacetin (TA, Figure 25). DS 2.45 is the commercial grade of cellulose acetate and is considered as our reference system. TA is reported as an efficient plasticizer of cellulose acetate or related derivatives (*Fordyce and Meyer 1940; Suvorova et al. 1995, Fringant et al. 1998*).

Triacetin is an eco-friendly plasticizer but has a low molecular weight (218 $g.mol^{-1}$). Cellulose acetate with DS 2.45 is a high-molecular-weight polymer ($M_w \approx 65\,000$ $g.mol^{-1}$). The polymer and the plasticizer are not miscible in all proportions. Acetyl groups of triacetin are supposed to interact with cellulose acetate through dipolar interactions and hydrogen bondings (H-bonds). The influence of these polar interactions on glass transition is unknown. Prediction of glass transition temperatures in a binary blend is generally described by a few empirical equations, such as Couchman-Karasz Equation or Fox Equation (*Fox 1956, Couchman and Karasz 1978*). These empirical models are based on the assumption of a perfect binary system in which the two constituents never interact with each other. As a result, deviations of experimental results from the empirical model are expected for our plasticized cellulose acetate series. T_g's prediction will be based on the Couchman-Karasz Equation for thermal analysis, as others did in their studies (*Fringant et al. 1998*). Glass transition can be identified either by a smooth step in the 'reversing heat flow' curve or by a peak in the 'derivative reversing heat capacity' curve. The glass transition signal of cellulose acetate is broad and not intense because of heterogeneous distribution of 8 possible anhydroglucose units of cellulose acetate.

Three plasticizer contents are selected to illustrate miscibility behavior of TA-plasticized DS 2.45 series (Figure 25):

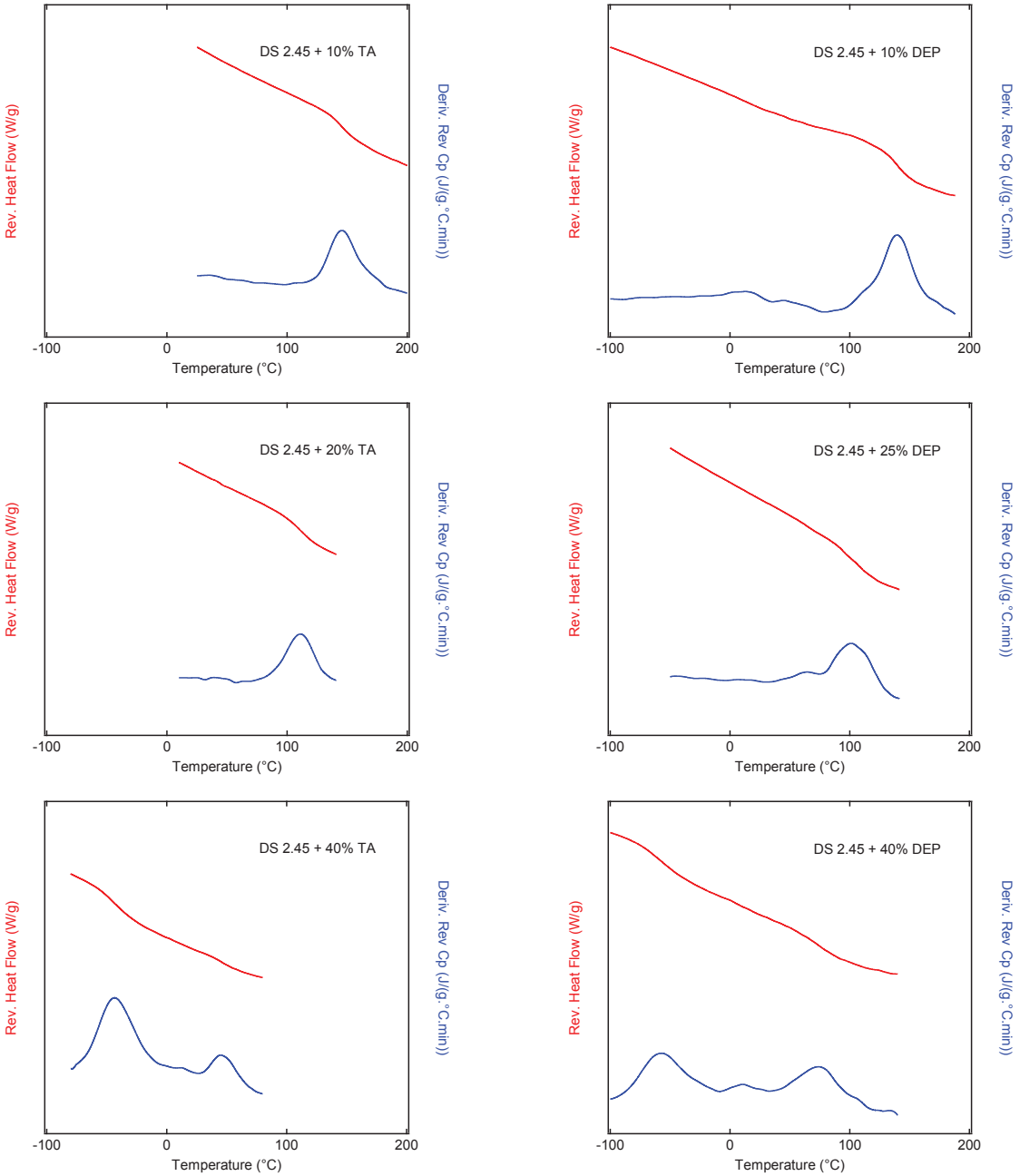

Figure 25: Left - MDSC thermograms of DS 2.45 + TA and Right - MDSC thermograms of DS 2.45 + DEP. Red lines: heat flow with glass transition steps. Blue lines: derivative heat capacity with glass transition peaks.

- 10% TA, which is a low plasticized composition, represents a totally miscible system. One glass transition is identified.
- 20% TA, which is considered as a threshold limit of phase separation, represents the beginning of partial miscibility between cellulose acetate and triacetin. A second T_g is merely observed.
- 40% TA, which is highly plasticized, represents a partially miscible system. Two glass transitions are found: one for CDA-rich phase and another for TA-rich phase.

The evolution of glass transition temperatures of TA-plasticized DS 2.45 series is plotted in Figure 26, as well as its miscibility diagram as a function of plasticizer content.

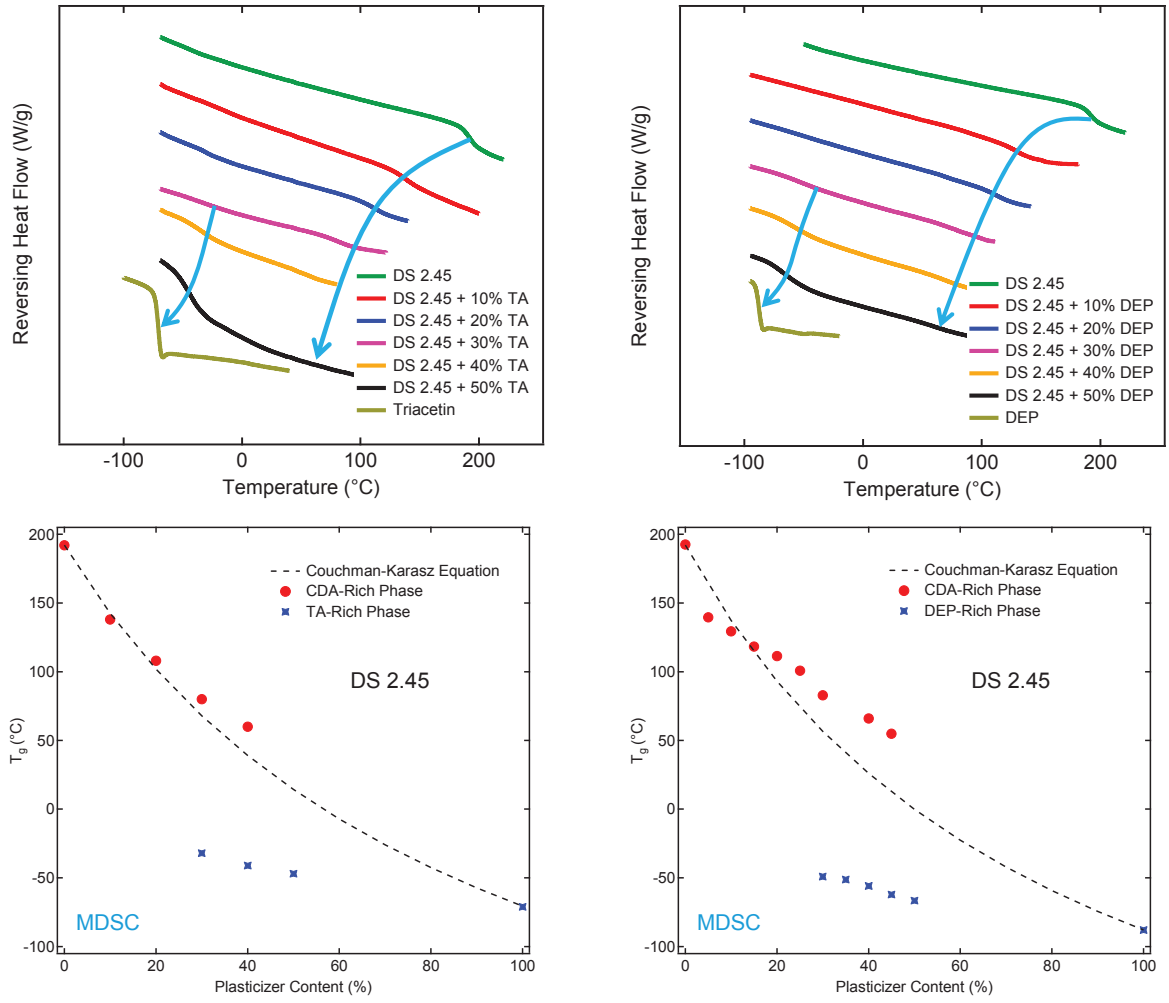

Figure 26: Top - MDSC thermograms of plasticized DS 2.45 series, arrows indicate glass transition temperatures. Bottom - Miscibility diagrams of plasticized DS 2.45 series, Couchman-Karasz Equation is considered as the theoretical prediction of T_g's.

General observations are listed below:

- The plasticization effect of triacetin on cellulose acetate is efficient because of the important decrease of T_g's. Broadening of glass transitions with increasing plasticizer content is observed and is attributed to the heterogeneity of the system.
- Partial miscibility threshold limit of TA-plasticized DS 2.45 series is established ~20% TA. From this point, two glass transitions are identified in thermal analysis: T_g of CDA-rich phase and T_g of TA-rich phase. Both of them are composition-dependent and are between the T_g values of pure polymer and plasticizer.
- Deviations of experimental T_g's from the Couchman-Karasz prediction are observed as expected. This is supposed to be due to the presence of dipolar interactions and H-bonds created between the polymer and the plasticizer.

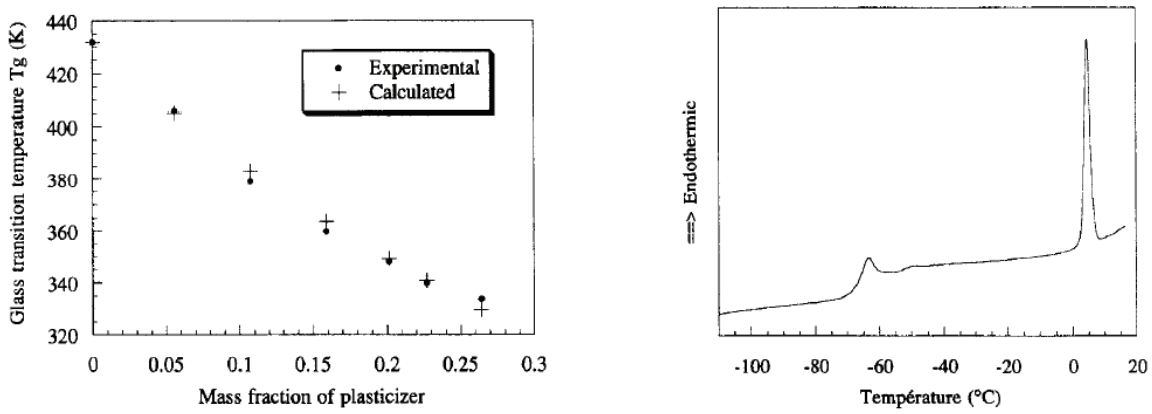

Figure 27: Left - Evolution of T_g's of starch acetate with the amount of plasticizer and comparison with the theoretical curve. Right - Thermogram of triacetin after rapid quenching at 110°C. Scanning rate 15°C/min (Fringant et al. 1998).

Determination of phase composition is based on the measured T_g's and the Couchman-Karasz law. Volume fractions of respective phases are estimated by ΔCp (increment of heat capacity). Details of calculation are listed in Chapter 2. *Fringant et al. 1998* is the reference article of plasticization effect of triacetin: the external plasticization of starch acetate by triacetin was examined by the Couchman-Karasz equation, one of the empirical calculations of T_g's of polymer-diluent system. In Figure 27, a good agreement was observed between the model and the experimental data, demonstrating that triacetin is a good plasticizer over a wide range of composition and it is efficient in producing starch acetate plastics with a low T_g. The heat capacity increment at glass transition temperature (ΔCp) of each component was known in thermal analysis:

- ΔC_p of starch acetate = 0.23 $J.g^{-1}.K^{-1}$
- ΔC_p of triacetin = 0.50 $J.g^{-1}.K^{-1}$

These values are considered as the literature reference for our study of TA-plasticized cellulose acetates. ΔCp of cellulose acetate and of triacetin resulted from our MDSC analysis are:

- ΔC_p of cellulose acetate (DS 2.45) = 0.27 $J.g^{-1}.K^{-1}$
- ΔC_p of triacetin = 0.57 $J.g^{-1}.K^{-1}$

TA-plasticized CDA	T_g^{ck} (°C)	T_g^{CDA} (°C)	T_g^{TA} (°C)	CDA-rich phase		TA-rich phase	
				% CDA	% TA	% CDA	% TA
Unplasticized DS 2.45	192	192	N/A	100	0	N/A	N/A
DS 2.45 + 10% TA	143	142	N/A	90.0	10.0	N/A	N/A
DS 2.45 + 20% TA	102	109	N/A	82.0	18.0	Merely observed	
DS 2.45 + 30% TA	68	82	-35	75.0	25.0	24.0	76.0
DS 2.45 + 40% TA	39	60	-40	68.0	32.0	21.0	79.0
DS 2.45 + 50% TA	14	N/A	-47	N/A	N/A	17.0	83.0
Triacetin	-70	N/A	-70	N/A	N/A	0	100
DEP-plasticized CDA	**T_g^{ck} (°C)**	**T_g^{CDA} (°C)**	**T_g^{DEP} (°C)**	**CDA-rich phase**		**DEP-rich phase**	
				% CDA	**% DEP**	**% CDA**	**% DEP**
Unplasticized DS 2.45	192	192	N/A	100	0	N/A	N/A
DS 2.45 + 10% DEP	137	141	N/A	90.0	10.0	N/A	N/A
DS 2.45 + 20% DEP	93	113	N/A	85.0	15.0	N/A	N/A
DS 2.45 + 30% DEP	57	84	-49	78.0	22.0	26.0	74.0
DS 2.45 + 40% DEP	26	69	-58	74.0	26.0	20.0	80.0
DS 2.45 + 50% DEP	0	65	-68	72.0	28.0	14.0	86.0
Diethyl Phthalate	-88	N/A	-88	N/A	N/A	0	100

Table 9: Phase compositions of DS 2.45 + TA issued from glass transition temperatures. T_g^{ck} (°C): Couchman-Karasz prediction; T_g^{CDA} (°C): glass transition temperature of CDA-rich phase; T_g^{TA} (°C): glass transition temperature of TA-rich phase

Table 9 summarizes phase compositions of DS 2.45 + TA series. It has to be mentioned that the composition of a phase domain is estimated from the Couchman-Karasz empirical model. Non-negligible standard deviations (± 3% plasticizer content) need to be taken into account due to the broadness of glass transitions of plasticized DS 2.45 series and the use of the empirical equation.

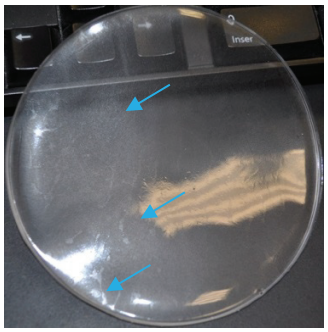

Figure 28: Photograph of highly plasticized cellulose acetate with triacetin. Arrows point out the exudation of the plasticizer.

According to our experimental protocol, plasticizer content in cellulose acetates never exceeds 50%, weight fraction. Plasticizer exudation is visible to the naked eye from 50% TA (Figure 28). No interest is justified to continue raising the plasticizer content.

The second series to be analyzed is DS 2.45 plasticized by diethyl phthalate (DEP, Figure 25). DEP is a historically common plasticizer of cellulose acetate along with other phthalate esters (*Fordyce and Meyer 1940, Seymour et al. 1979, Scandola and Ceccorulli 1985b and Keely et al. 1995*). Its chemical structure is different from triacetin's: DEP consists of an aromatic ring with two carboxylic acid ethyl esters in 'ortho' positions (Figure 29). The study of DEP-plasticized DS 2.45 series is an opportunity for us to understand the influence of plasticizer's chemical structure on the behavior of cellulose acetate. DEP may have the same ability as triacetin to interact with cellulose acetate through dipolar interactions and H-bonds because of the carboxylic acid ethyl ester side groups. It is also susceptible to interact with cellulose acetate in a different way due to the presence of the aromatic ring. Three plasticizer contents are selected to illustrate various miscibility behaviors:

- 10% DEP, represents a totally miscible system. One glass transition is identified.
- 25% DEP, is considered as the threshold limit of phase separation.
- 40% DEP, represents a partially miscible system. Two glass transitions are found.

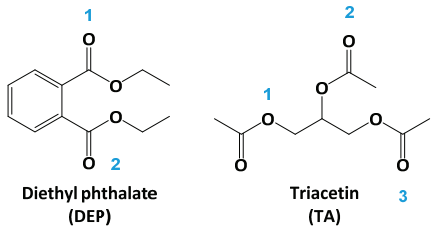

Figure 29: Available sites to interact with cellulose acetate through dipolar interactions for DEP and TA.

According to the results of Figure 25, 26 and Table 9, important observations about DEP-plasticized DS 2.45 series are listed below (ΔC_p of DEP = 0.60 $J.g^{-1}.K^{-1}$):

- The plasticization effect of diethyl phthalate on cellulose acetate is efficient because of the important decrease of T_g's. Broadening of glass transitions with increasing plasticizer content is observed and is attributed to the heterogeneity of the system. Nevertheless, the decrement of T_g's (ΔT_g) is more significant for triacetin-plasticized DS 2.45 series than the DEP series. The plasticization effect of triacetin on cellulose acetate is more powerful than that of DEP.

- Partial miscibility threshold limit of DEP-plasticized DS 2.45 series is estimated ~25% DEP. From this point, two glass transitions are identified in thermal analysis: T_g of CDA-rich phase and T_g of DEP-rich phase. Both of them are composition-dependent and are between the T_g values of pure polymer and plasticizer. Compared to the miscibility behavior of TA-plasticized DS 2.45 series, DS 2.45 + DEP series maintains a wider miscibility range than the TA series.

- Deviations of experimental T_g's from the Couchman-Karasz prediction are also observed. This is supposed to be due to the presence of specific interactions created between the polymer and the plasticizer. This point will be recalled in the next chapters.

3.1.2 – Cellulose acetate (DS 2.08) plasticized by triacetin and diethyl phthalate

Cellulose acetate with DS 2.08 is one of the 'pilot-scale' flakes provided from our supplier. *Kamide and Saito 1985* predicted its glass transition temperature at ~207°C. *Buchanan et al. 1996* studied a cellulose acetate blend of DS 2.06 and DS 2.49. Their unplasticized DS 2.06 is completely amorphous and its T_g is found at 209°C. According to our thermal analysis, the T_g of the unplasticized DS 2.08 is measured at 201°C.

Three plasticizer contents are selected to illustrate its miscibility behavior (Figure 30): the same percent as those of DS 2.45 series. Figure 31 and Table 10 summarize the MDSC results of TA-plasticized DS 2.08 series. The T_g of the unplasticized DS 2.08 is 9°C higher than the T_g of the unplasticized DS 2.45. As expected, the glass transition signal is broad due to the heterogeneity of the system. According to the Couchman-Karasz Equation, plasticized DS 2.08 series should have a higher T_g value than the plasticized DS 2.45 series.

The plasticization effect of triacetin on cellulose acetate with DS 2.08 is efficient because of the important decrease of T_g's. Broadening of glass transitions with increasing plasticizer content, partial miscibility threshold limit and deviations of experimental T_g's from the Couchman-Karasz prediction are all similar to the behavior of TA-plasticized DS 2.45 series.

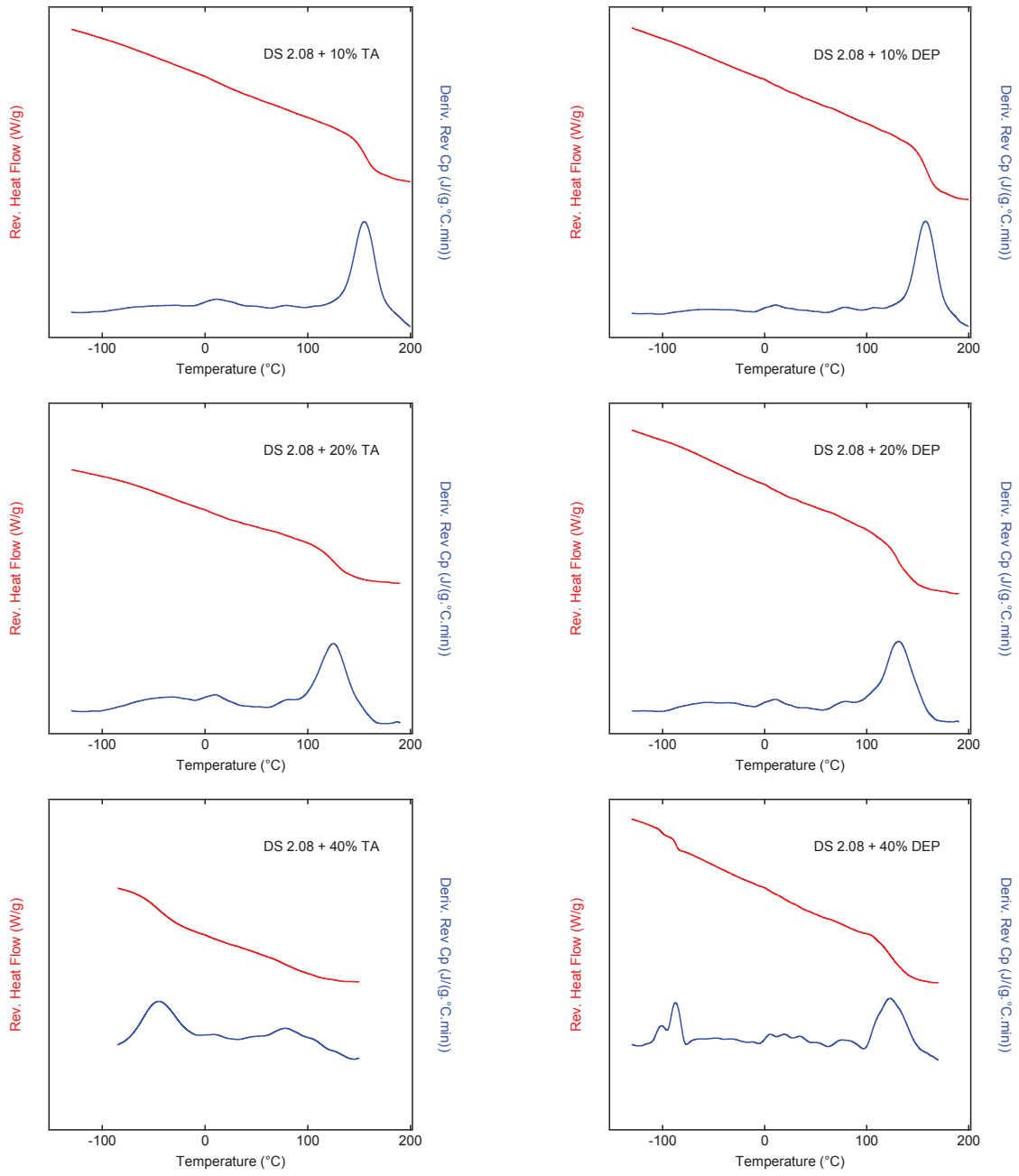

Figure 30: Left - MDSC thermograms of DS 2.08 + TA and Right - MDSC thermograms of DS 2.08 + DEP. Red lines: heat flow with glass transition steps. Blue lines: derivative heat capacity with glass transition peaks.

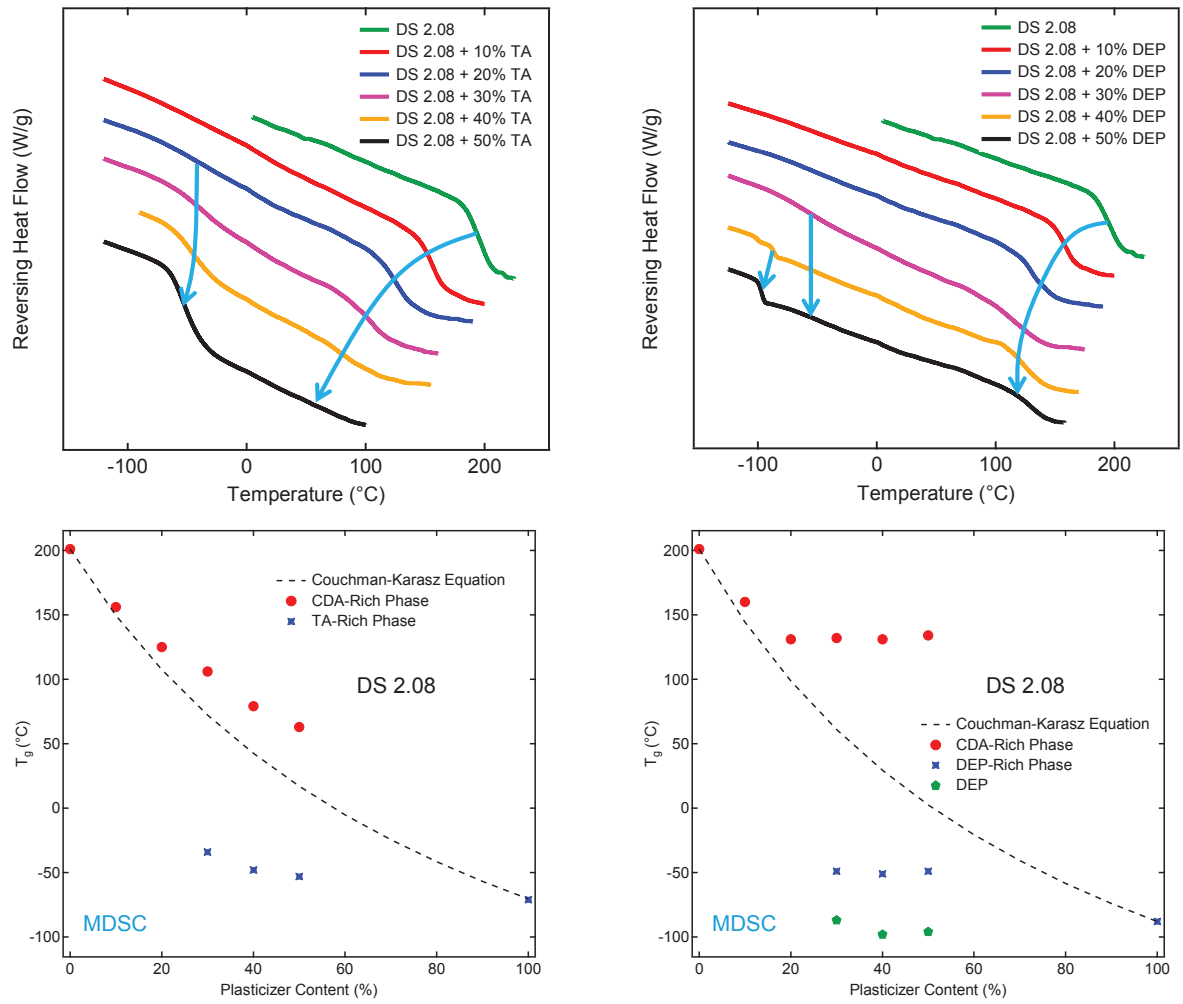

Figure 31: Top - MDSC thermograms of plasticized DS 2.08 series, arrows indicate glass transition temperatures. Bottom - Miscibility diagrams of plasticized DS 2.08 series, Couchman-Karasz Equation is considered as the theoretical prediction of T_g's.

The plasticization effect of diethyl phthalate on cellulose acetate with DS 2.08 is not as efficient as on cellulose acetate with DS 2.45 (Figure 30, 31 and Table 10), although the partial miscibility threshold limit is still estimated at ~25% DEP. A third glass transition temperature is identified around - 90°C when the DEP content exceeds 30% weight fraction. This third T_g is supposed to be related to a ~100% DEP phase domain because the T_g of pure DEP liquid is - 88°C (from internal work not reported in this study). This makes the highly plasticized DS 2.08 + DEP series a three-phase system: CDA-rich phase, DEP-rich phase and DEP phase. Furthermore, in the event where the third transition is identified, compositions of CDA-rich phase and DEP-rich phase do not evolve anymore.

TA-plasticized CDA	T_g^{ck} (°C)	T_g^{CDA} (°C)	T_g^{TA} (°C)	CDA-rich phase		TA-rich phase	
				% CDA	% TA	% CDA	% TA
Unplasticized DS 2.08	201	201	N/A	100	0	N/A	N/A
DS 2.08 + 10% TA	150	156	N/A	91.5	8.5	N/A	N/A
DS 2.08 + 20% TA	107	125	N/A	84.5	15.5	Merely observed	
DS 2.08 + 30% TA	72	101	-39	78.5	21.5	21.5	78.5
DS 2.08 + 40% TA	43	74	-46	70.5	29.5	17.0	83.0
DS 2.08 + 50% TA	17	N/A	-54	N/A	N/A	12.0	88.0
Triacetin	-70	N/A	-70	N/A	N/A	0	100

DEP-plasticized CDA	T_g^{ck} (°C)	T_g^{CDA} (°C)	T_g^{DEP1} (°C)	T_g^{DEP2} (°C)	T_g^{DEP3} (°C)	CDA-rich phase		DEP-rich phase	
						% CDA	% DEP	% CDA	% DEP
Unplasticized DS 2.08	201	201	N/A	N/A	N/A	100	0	N/A	N/A
DS 2.08 + 10% DEP	144	160	N/A	N/A	N/A	93.0	7.0	N/A	N/A
DS 2.08 + 20% DEP	99	134	N/A	N/A	N/A	88.0	12.0	N/A	N/A
DS 2.08 + 30% DEP	61	132	-49	-87	N/A	87.5	12.5	25.0	75.0
DS 2.08 + 40% DEP	29	131	-49	-87	-100	87.5	12.5	25.0	75.0
DS 2.08 + 50% DEP	2	134	-49	N/A	-97	88.0	12.0	25.0	75.0
Diethyl Phthalate	-88	N/A	-88	N/A	N/A	N/A	N/A	0	100

Table 10: Phase compositions of DS 2.08 + TA issued from glass transition temperatures. T_g^{ck} (°C): Couchman-Karasz prediction; T_g^{CDA} (°C): glass transition temperature of CDA-rich phase; T_g^{TA} (°C): glass transition temperature of TA-rich phase.

In Table 10, one can see that 12.5% DEP is the highest plasticizer content which efficiently plasticizes DS 2.08 (% DEP in CDA-rich phase). Thus, the lowest T_g of DEP-plasticized DS 2.08 is observed at ~130°C. It is important to understand the mechanism of the formation of the third thermal transition in DEP-plasticized DS 2.08. Our hypothesis is that the third transition corresponds to cavities partially filled with plasticizer molecules.

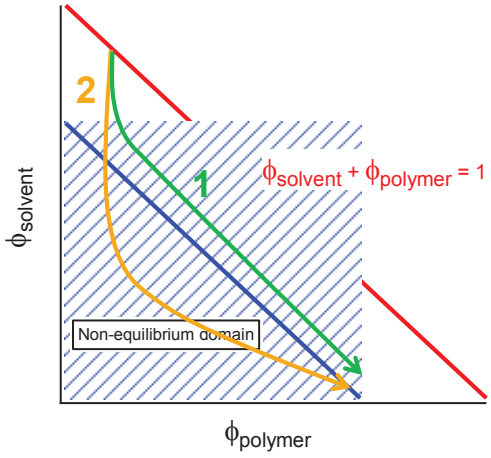

Figure 32: Scheme of the formation of cavities (trajectory N°2, yellow curve). No cavities formed through trajectory N°1 (green curve).

The mechanisms which lead to the formation of cavities are illustrated in Figure 32. Let us consider a CDA film with solvent. Initially, before evaporation takes place, the density may be normalized by 1, corresponding to a dense system. Then, evaporation takes place. The trajectories in the (Φ_p, Φ_s) space are illustrated in the same figure. If the evaporation process is slow enough, the trajectory never enters the unstable domain: the total density remains sufficiently high for the system to be in the stable state (trajectory N°1, green curve). If the evaporation process is fast as compared to the film contraction process, then the trajectory may enters the unstable domain (shaded area in Figure 32, trajectory N°2, yellow trajectory).

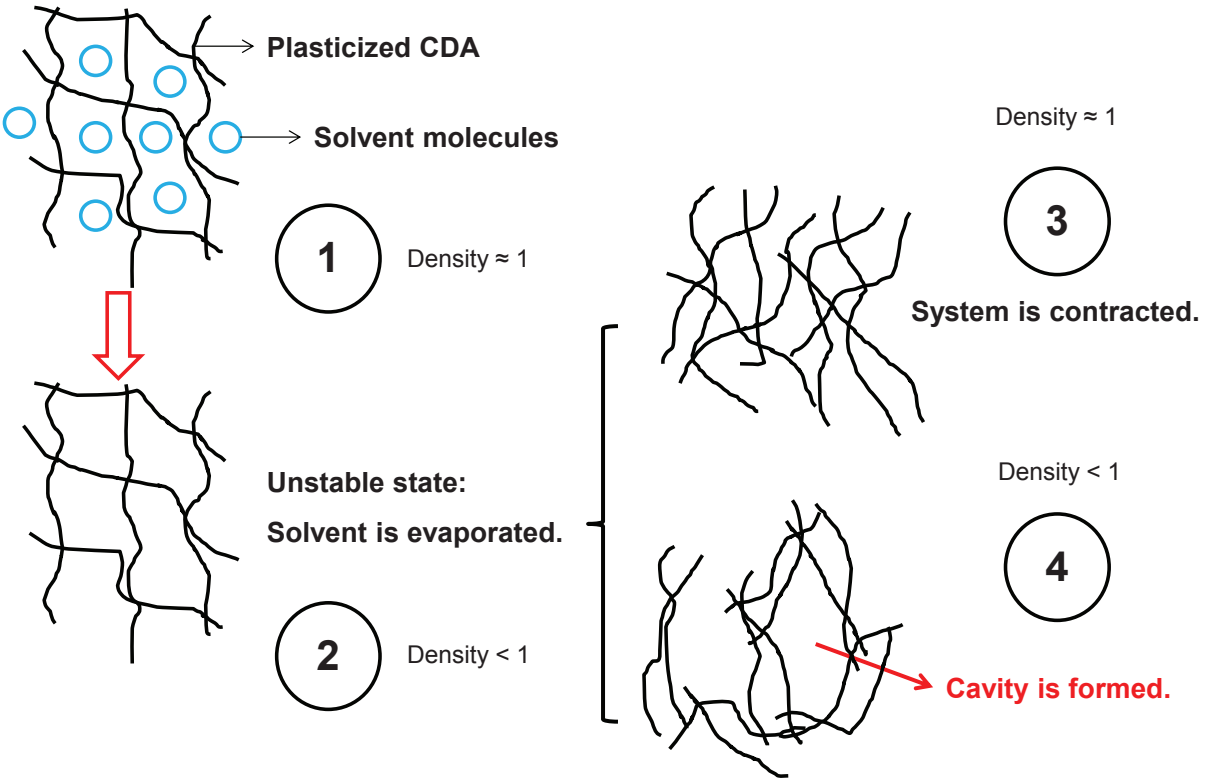

Figure 33: Different steps from solvent evaporation to formation of cavities (Trajectory N°2 in Figure 32).

Thus, during the solvent evaporation, two different situations may occur:

- Case 1 represents a solvent evaporation step without creating cavities. Its solvent evaporation speed is slow enough to avoid the unstable domain: the film contraction is fast enough for the total density to remain sufficiently high. This situation is favored when the plasticized polymer film has a low T_g.

- Case 2 if the solvent evaporation speed is fast as compared to film contraction, the total density decreases sufficiently for the trajectory to enter the unstable domain. This situation is favored when the plasticized film has a high T_g.

These effects are possible because solvent diffusion and mechanical contraction are two different mechanisms: solvent diffusion is controlled by fast path in the material, whereas film contraction is controlled by the alpha-relaxation process. The latter is controlled by the slowest part of the relaxation spectrum of the material as measured in dielectric spectroscopy or in mechanical spectroscopy (e.g. *Long & Lequeux 2001, Merabia et al. 2004, Julien, PhD thesis, Lyon 2014*).

The formation of cavities is illustrated in Figure 33: in the first step, solvent has diffused out of the sample. Empty regions appear before contraction takes place (Step 2 in Figure 33). If the sample has had time to partially contract, it may still remain in the stable region of the phase space (trajectory N°1, Figure 32). In this case, contraction will continue, without formation of cavities (Step 3 in Figure 33). If the sample has not contracted sufficiently during the solvent evaporation stage, the sample may enter the unstable domain (trajectory N°2). Then, cavities may appear (Step 4 in Figure 33).

Note that the size and volume fraction of the cavities should depend on the glass transition temperature (T_g) of the plasticized CDA. When the T_g is low enough, contraction takes place rapidly, and no cavities may appear. For a higher T_g, contraction may be too slow for preventing cavities. On the other hand, mechanical relaxation may be sufficiently quick for building large cavities in the sample. If the T_g is even higher, the cavity formation process may stop when the cavities are still relatively small.

3.1.3 – Cellulose acetate (DS 1.83) plasticized by triacetin and diethyl phthalate

The third and last cellulose acetate to be analyzed is DS 1.83, whose hydroxyl side groups should be the most abundant among the three DS. *Kamide and Saito 1985* predicted its glass transition temperature at ~212°C. *Ohno and Nishio 2007a* used DS 1.80 (supplied from Daicel Chemical Industries, Ltd.) for their miscibility study of cellulose acetate blends. The T_g of DS 1.80 was then reported as 203°C, compared to a T_g value of 204°C which is measured by thermal analysis for our DS 1.83 grade. MDSC thermograms of cellulose acetate with DS 1.83 plasticized by triacetin and diethyl phthalate are shown in Figure 34 and 35.

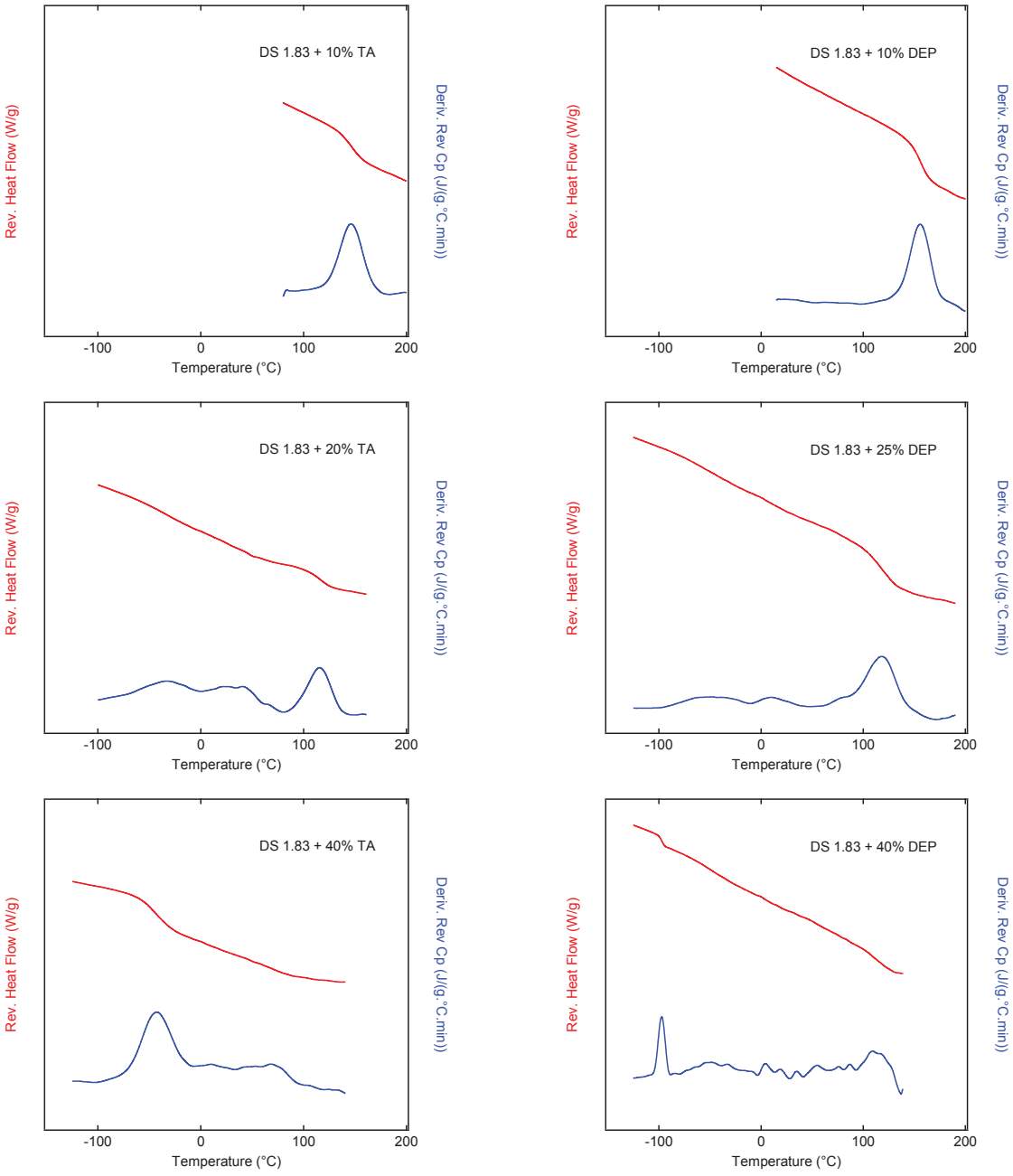

Figure 34: Left - MDSC thermograms of DS 1.83 + TA and Right - MDSC thermograms of DS 1.83 + DEP. Red lines: heat flow with glass transition steps. Blue lines: derivative heat capacity with glass transition peaks.

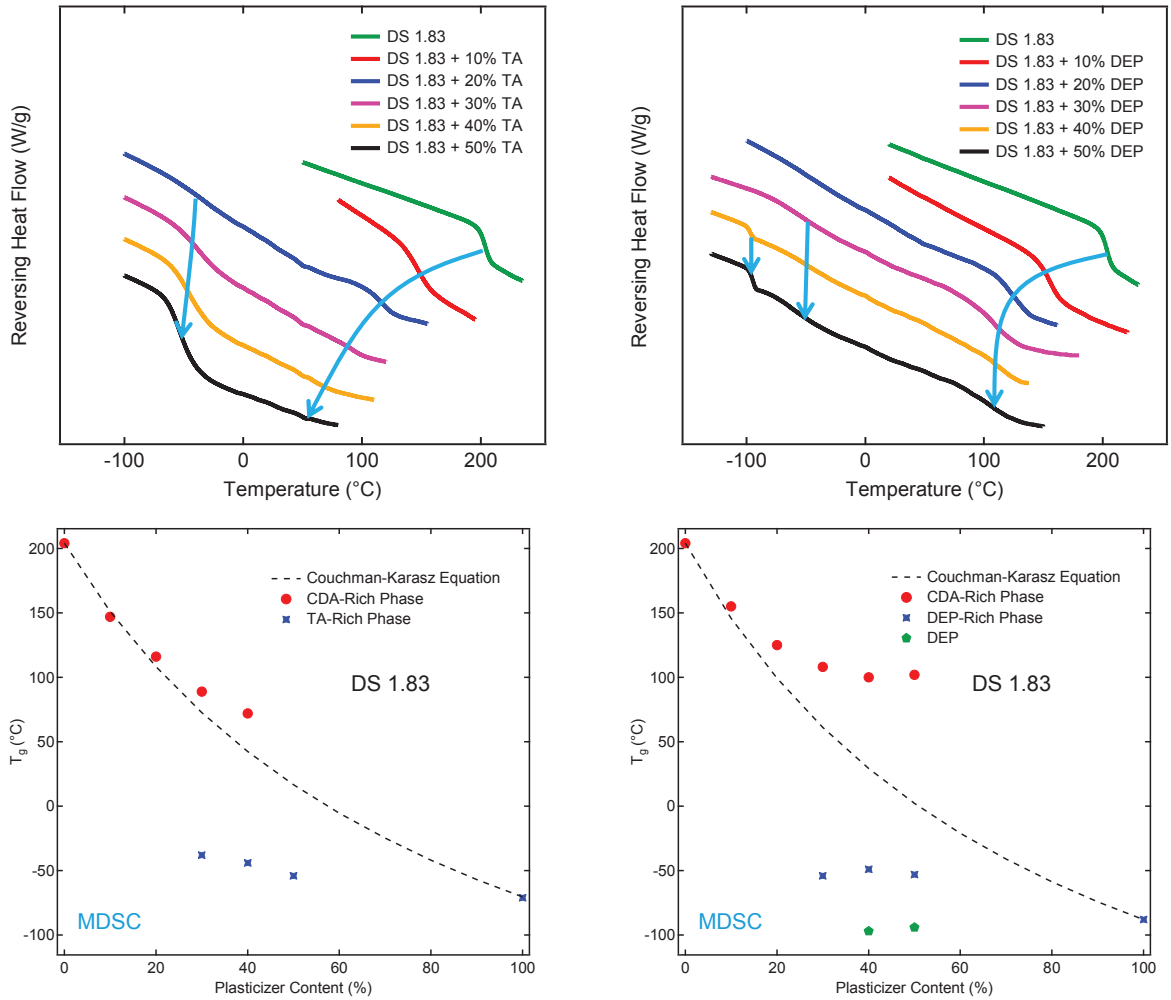

Figure 35: Top - MDSC thermograms of plasticized DS 1.83 series, arrows indicate glass transition temperatures. Bottom - Miscibility diagrams of plasticized DS 1.83 series, Couchman-Karasz Equation is considered as the theoretical prediction of T_g's.

The plasticization effect of triacetin on cellulose acetate with DS 1.83 is efficient as shown by the important decrease of T_g's. The miscibility behavior between DS 1.83 and triacetin is almost the same as the behavior of two other TA-plasticized cellulose acetates. It is interesting to notice that at the same triacetin content, the T_g of DS 1.83 series is always lower than the T_g of DS 2.08 series. As a reminder, the T_g of the unplasticized DS 1.83 is 3°C higher than that of the unplasticized DS 2.08 (Equation 2). Thus, the decrement of T_g's (ΔT_g) is more important in DS 1.83 series until the plasticized content reaches 40% weight fraction.

TA-plasticized CDA	T_g^{ck} (°C)	T_g^{CDA} (°C)	T_g^{TA} (°C)	CDA-rich phase		TA-rich phase	
				% CDA	% TA	% CDA	% TA
Unplasticized DS 1.83	204	204	N/A	100	0	N/A	N/A
DS 1.83 + 10% TA	151	147	N/A	89.0	11.0	N/A	N/A
DS 1.83 + 20% TA	108	116	N/A	82.0	18.0	Merely observed	
DS 1.83 + 30% TA	73	89	-38	75.0	25.0	22.0	78.0
DS 1.83 + 40% TA	42	73	-44	70.0	30.0	18.5	81.5
DS 1.83 + 50% TA	17	N/A	-54	N/A	N/A	12.0	88.0
Triacetin	-70	N/A	-70	N/A	N/A	0	100

DEP-plasticized CDA	T_g^{ck} (°C)	T_g^{CDA} (°C)	T_g^{DEP1} (°C)	T_g^{DEP2} (°C)	CDA-rich phase		DEP-rich phase	
					% CDA	% DEP	% CDA	% DEP
Unplasticized DS 1.83	204	204	N/A	N/A	100	0	N/A	N/A
DS 1.83 + 10% DEP	146	155	N/A	N/A	92.0	8.0	N/A	N/A
DS 1.83 + 20% DEP	99	125	N/A	N/A	86.0	14.0	N/A	N/A
DS 1.83 + 30% DEP	61	108	-54	N/A	82.0	18.0	23.0	77.0
DS 1.83 + 40% DEP	29	100	-49	-97	80.0	20.0	25.5	74.5
DS 1.83 + 50% DEP	2	102	-53	-94	80.5	19.5	23.5	76.5
Diethyl Phthalate	-88	N/A	-88	N/A	N/A	N/A	0	100

Table 11: Phase compositions of DS 1.83 + TA issued from glass transition temperatures. T_g^{ck} (°C): Couchman-Karasz prediction; T_g^{CDA} (°C): glass transition temperature of CDA-rich phase; T_g^{TA} (°C): glass transition temperature of TA-rich phase.

With regard to DEP-plasticized DS 1.83 series, the miscibility behavior is much like that of DS 2.08 series (Table 11). Meanwhile, the exceptions are made for the two following points:

- The third T_g is observed when the DEP content exceeds 40% weight fraction, instead of 30% in DS 2.08. This is regarded as a result of less worse miscibility between DS 1.83 and DEP.

- The plasticization of diethyl phthalate on DS 1.83 is more efficient, according to the obtained T_g's values and the decrement of T_g's (ΔT_g). The minimum T_g of DEP-plasticized DS 1.83 is ~100°C, instead of 130°C for DS 2.08 series.

3.1.4 – Conclusions of the MDSC study on the miscibility behavior of plasticized cellulose acetate

Modulated DSC study of plasticized cellulose acetates leads us to understand the miscibility behavior between the polymer and its plasticizers. The plasticization of triacetin is efficient on cellulose acetates with three different degrees of substitution (DS 1.83, DS 2.08 and DS 2.45). The partial miscibility threshold limit is established at ~ 20% TA for all three systems. Thus, TA-plasticized cellulose acetate is considered as a two-phase system after the phase separation: CDA-rich phase and TA-rich phase. Deviations of experimental T_g's from the Couchman-Karasz prediction are observed, probably due to the presence of dipolar interactions and H-bonds created between the polymer and the plasticizer.

The plasticization effect of diethyl phthalate on cellulose acetate is different from one DS to another. However, the partial miscibility threshold limit is estimated at ~ 25% DEP for all three systems. A third T_g is identified when DS 1.83 and DS 2.08 series are highly plasticized, which results a three-phase system: CDA-rich phase, DEP-rich phase and pure DEP phase. We propose that the appearance of the third T_g is due to the presence of cavities filled with plasticizer molecules.

Among the three DS, the reference degree of substitution – DS 2.45 presents the best miscibility behavior with triacetin and diethyl phthalate. On the contrary, DS 1.83 and DS 2.08 undergo certain degree of immiscibility with DEP at high plasticizer content. And since then, the plasticization of DEP becomes less efficient. The influence of molecular structure of cellulose acetate and plasticizers on the miscibility behavior and the formation of cavities proposed above will be discussed again in next chapters with other characterization techniques.

3.2 – Miscibility behavior of plasticized cellulose acetate: a DMTA study

The second conventional characterization of cellulose acetate is Dynamic Thermal Mechanical Analysis (DMTA). It provides information about the α-relaxations of plasticized cellulose acetate, instead of T_g's from thermal analysis. In fact, α-relaxation corresponds to the onset of segmental motion of a polymer, which is the molecular origin of glass transition. Therefore, the respective temperature of α-relaxation (T_α) can be regarded as a kind of glass transition temperature. T_α must be presented along with its respective frequency. Simultaneously, secondary relaxations, which are originated from localized motions of the polymer, can also be detected by DMTA.

In Chapter 3.2, α-relaxations and secondary relaxations of plasticized cellulose acetate are identified. T_α's is compared to the theoretical T_g's obtained from empirical Fox Equation (Equation 6). Miscibility behavior of plasticized cellulose acetate is then studied and a comparison with results obtained from MDSC experiment is also expected. Finally, preliminary details of relaxation behavior are discussed. They will be fully interpreted in Chapter 5 along with dielectric results.

3.2.1 – Cellulose acetate (DS 2.45) plasticized by triacetin and diethyl phthalate

In Figure 36, the storage modulus (E') and the damping factor (tan δ) of plasticized cellulose acetate with DS 2.45 are plotted versus the temperature at frequency 1 Hz. Determination of T_α is based on the tan δ curve. The T_α of unplasticized DS 2.45 is measured at 212°C. *Scandola and Ceccorulli 1985a* studied a cellulose acetate with DS 2.4 by thermal mechanical analysis and its T_α was reported at 197°C and at frequency 3 Hz. The effect of plasticizers on the dynamic mechanical spectrum of cellulose acetate with DS 2.45 is summarized in the same figure. It can be observed that the α-relaxation of DS 2.45 series is shifted to lower temperatures with increasing plasticizer content, such as the decrease of T_g's observed from thermal analysis. In the meantime, the drop of modulus E' which corresponds to the main transition undergoes the same shift towards lower temperatures with increasing plasticizer content.

A secondary relaxation (denoted as β-relaxation) is identified in the plasticized DS 2.45 series. β-relaxation is a well-known secondary relaxation of cellulose acetate but its molecular origin is still not clearly interpreted. As the amount of plasticizer increases, β-relaxation is shifted to lower temperatures, and its magnitude is increased. This temperature shift is the same as the T_g's of plasticizer-rich phase in MDSC analysis, which leads us to believe that the related tan δ peak is an overlapping contribution between the β-relaxation and the α'-relaxation of plasticizer-rich phase. Partial miscibility threshold limits of plasticized DS 2.45 series are confirmed by thermo-mechanical analysis at ~20% TA and ~25% DEP.

Both α- and α'-relaxations are composition-dependent and are between the T_α values of the polymer and the plasticizer.

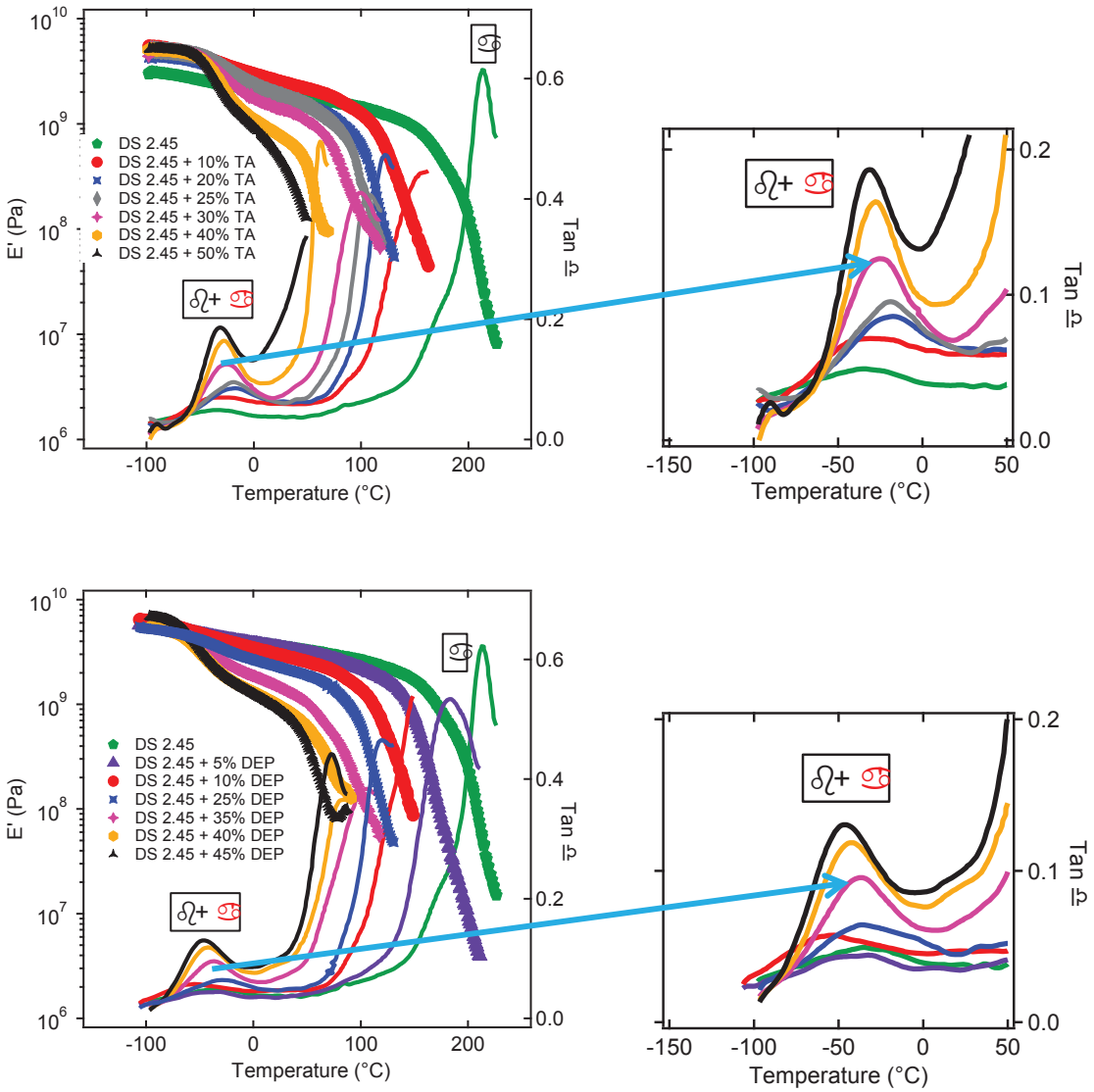

Figure 36: Left - DMTA spectra of plasticized cellulose acetate with DS 2.45 at frequency 1 Hz (only E' and tan δ are represented). Plasticizer content varies from 0 to 50% in weight fraction. Right - Zoom of tan δ plot against temperature at sub-glass temperature range.

Miscibility diagrams of plasticized DS 2.45 series are presented in Figure 37, as a function of plasticizer content. The empirical Fox Equation is used for calculations of theoretical T_g's. As mentioned in Chapter 2, this equation assumes no specific interactions between the two components of the blend. Therefore, deviations of experimental T_α's from the Fox prediction are observed as expected.

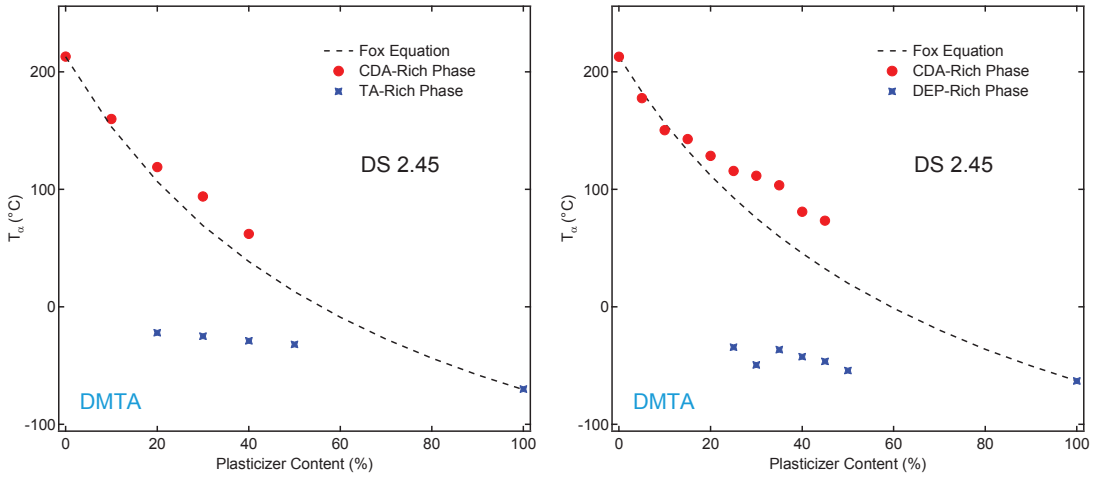

Figure 37: Left - Miscibility diagrams of TA-plasticized DS 2.45 series, Right - Miscibility diagrams of DEP-plasticized DS 2.45 series, Fox Equation is considered as the theoretical prediction of T_g's.

3.2.2 – Cellulose acetate (DS 2.08) plasticized by triacetin and diethyl phthalate

Dynamic mechanical spectrum of plasticized DS 2.08 series is plotted in Figure 39, where the modulus E' and the damping factor tan δ as a function of temperature are shown. DS 2.08 + TA series is similar to DS 2.45 + TA series, such as the decrease of T_α's with increasing plasticizer content, the overlapping of β-relaxation and α'-relaxation and the partial miscibility threshold limit at ~20% TA. However, deviations of T_α's from the Fox prediction are more important than those found in DS 2.45 + TA series (Figure 38).

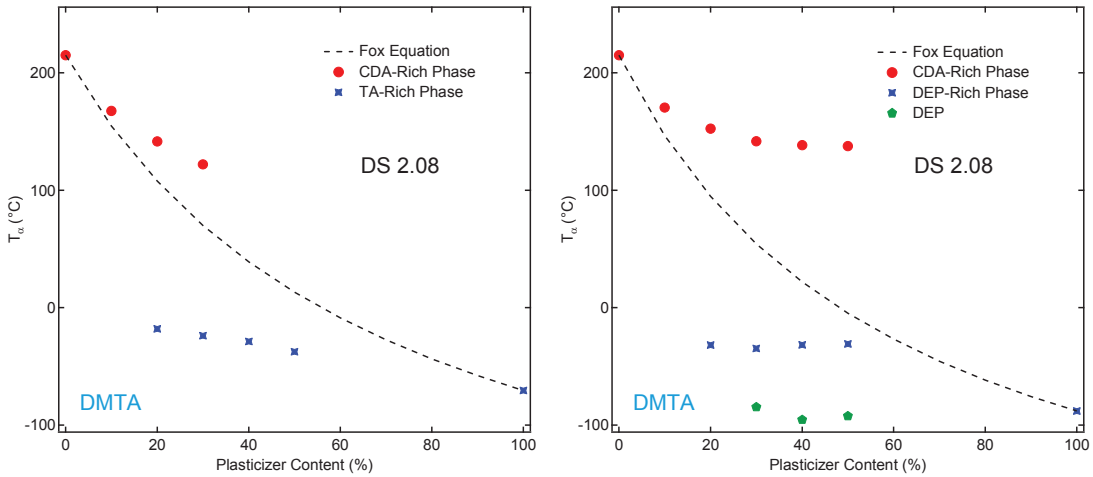

Figure 38: Left - Miscibility diagrams of TA-plasticized DS 2.08 series, Right - Miscibility diagrams of DEP-plasticized DS 2.08 series, Fox Equation is considered as the theoretical prediction of T_g's.

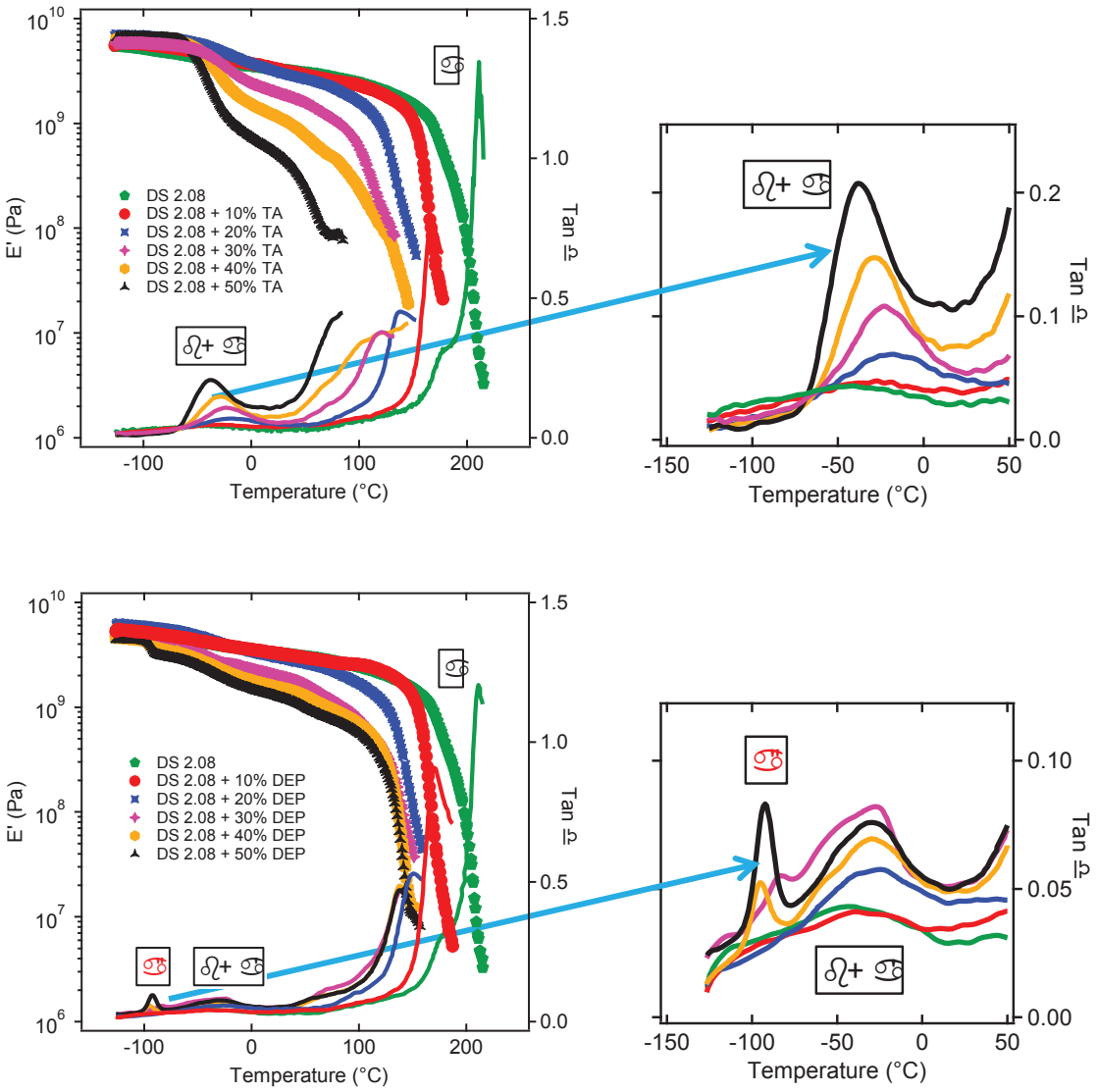

Figure 39: Left - DMTA spectra of plasticized cellulose acetate with DS 2.08 at frequency 1 Hz (only E' and tan δ are represented). Plasticizer content varies from 0 to 50% in weight fraction. Right - Zoom of tan δ plot against temperature at sub-glass temperature range.

DS 2.08 + DEP series does not follow the pattern of DS 2.45 + DEP series. In highly plasticized DS 2.08, a third α-type relaxation is found at the same temperature range as the α-relaxation of DEP. Considering the MDSC results, this relaxation is denoted as α"-relaxation and is attributed to the α-relaxation of DEP. The behavior of the overlapping peak (of β-relaxation and α'-relaxation) is also similar to thermal analysis: compositions of the two relaxations do not evolve anymore with the presence of α"-relaxation (Figure 38).

3.3.3 – Cellulose acetate (DS 1.83) plasticized by triacetin and diethyl phthalate

Miscibility behavior of plasticized DS 1.83 series is much like that of plasticized DS 2.08 series (Figure 40 and 41). Again, T_α's decrease efficiently when triacetin content increases. Deviations of T_α's from the Fox Equation are less important than those observed in TA-plasticized DS 2.08 series. Partial miscibility limits are the same as other plasticized DS series. α"-relaxation of DEP phase is detected from 40% DEP. All results are consistent with MDSC findings.

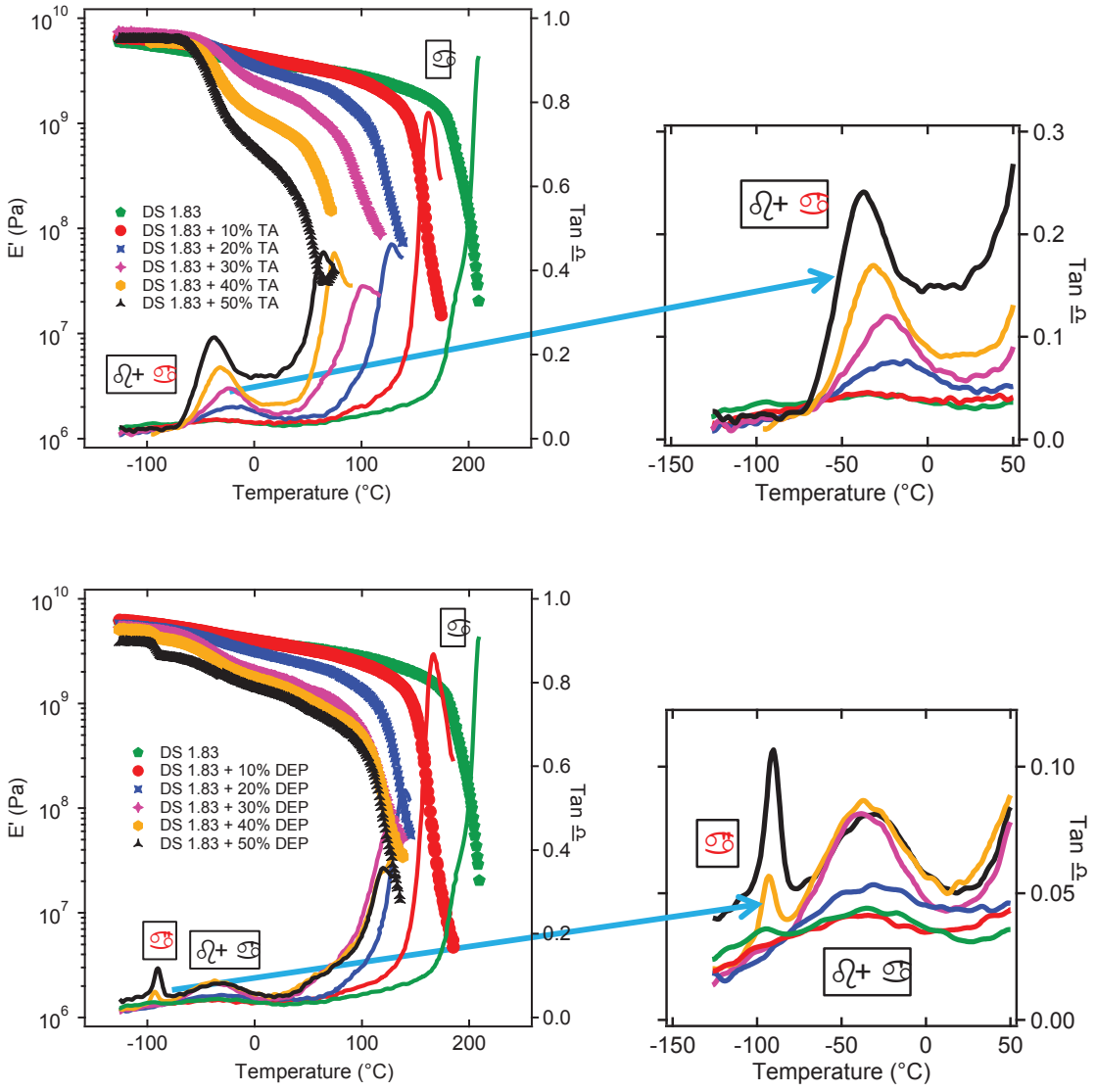

Figure 40: Left - DMTA spectra of plasticized cellulose acetate with DS 1.83 at frequency 1 Hz (only E' and tan δ are represented). Plasticizer content varies from 0 to 50% in weight fraction. Right - Zoom of tan δ plot against temperature at sub-glass temperature range.

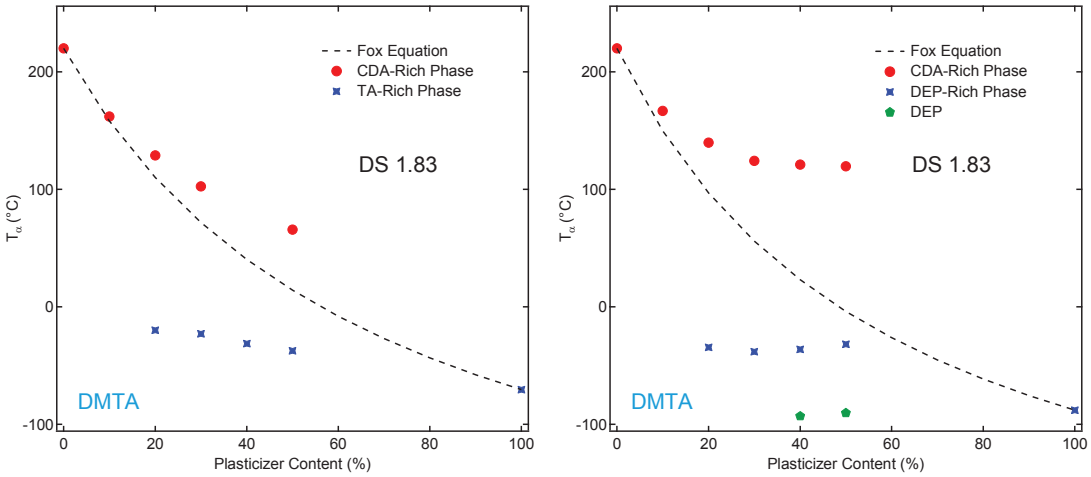

Figure 41: Left - Miscibility diagrams of TA-plasticized DS 1.83 series, Right - Miscibility diagrams of DEP-plasticized DS 1.83 series, Fox Equation is considered as the theoretical prediction of T_g's.

3.2.4 – Conclusions of the DMTA study on the miscibility behavior of plasticized cellulose acetate

Thermo-mechanical analysis confirms the conclusions obtained from MDSC analysis on the miscibility behavior of plasticized cellulose acetate. Three main relaxations (α-, α'- and α"-relaxations) are identified and related to the three T_g's of thermal analysis. Miscibility diagrams established from DMTA results are the same as those obtained from MDSC results.

3.2.5 – Access to thermo-mechanical transitions of plasticized cellulose acetate

Useful equations

Thermo-mechanical transitions of polymers are described by different types of behavioral laws, which we would like to re-introduce prior to the analysis of specific transitions of plasticized cellulose acetates:

- Arrhenius Equation

Secondary transitions are generally described by the Arrhenius Equation:

$$\tau(T) = \tau_0 exp\left(\frac{E_a}{k_B T}\right)$$

Equation (20)

Where

- E_a: activation energy representing the energy barrier for molecular rearrangement ($kJ.mol^{-1}$)
- τ_0: relaxation time at infinite temperature (s)
- k_B: Boltzmann's constant ($m^{2.}kg.s^{-2}.K^{-1}$)
- T: temperature (K)

- Williams-Landel-Ferry (WLF) Equation

The temperature-frequency relationship of primary α-transitions can be described by Williams–Landel–Ferry (WLF) equation:

$$\log(f_T) - \log(f_{T_r}) = \frac{C_1(T - T_r)}{C_2 + T - T_r}$$

Equation (21)

Where

- Index r: reference temperature or frequency
- C_1: constant related to free volume fraction at reference temperature
- C_2: constant corresponds to thermal expansion of the free volume

- Vogel-Fulcher-Tammann (VFT) Equation

Another representation for the temperature-frequency relationship of primary α-transitions is called Vogel-Fulcher-Tammann (VFT) equation (*Vogel, 1921, Fulcher, 1925, Tammann & Hesse, 1926*). WLF and VFT equations are mathematically equivalent.

$$\tau = \tau_0 \, exp \frac{A}{T - T_0}$$

Equation (22)

Where:

- T_0: Vogel temperature (K)
- τ: relaxation time which is related to frequencies (s)
- A: constant

With the above equation, one can calculate the resulted activation energy of dynamic transitions. All transitions are generally plotted together in the literature to form a relaxation map, in which the logarithm of relaxation time is plotted as a function of 1000/T, where T is the absolute temperature.

It is useful to compare results obtained by different characterization techniques at various temperature and frequency range, such as DMTA or BDS measurements.

- Identification of simple or cooperative motions in secondary transitions

During our study on secondary transitions of cellulose acetate, the Eyring theory (*Eyring 1936*) and the framework of Starkweather (*Starkweather 1988*) catch special attention. Several research groups which are specialized in cellulose and its derivatives quoted and used their work for data analysis of secondary relaxations.

$$f = \frac{kT}{2\pi h}\, exp\, \frac{-\Delta G^*}{RT}$$

Equation (23)

$$\Delta G^* = \Delta H_a - T\Delta S_a$$

Equation (24)

Then we can obtain:

$$\ln \frac{f}{T} = \ln \frac{k}{2\pi h} + \frac{\Delta S_a}{R} - \frac{\Delta H_a}{RT}$$

Equation (25)

Where:

- k: Boltzmann Constant ($m^2.kg.s^{-2}.K^{-1}$)
- h: Planck Constant ($m^2.kg.s^{-1}$)
- R: Gas Constant ($J.K^{-1}.mol^{-1}$)
- f: Motional Frequency (Hz)
- T: Temperature (K)
- ΔG^*: Transition Gibbs Energy ($J.mol^{-1}$)
- ΔH_a: Activation Enthalpy (J)
- ΔS_a: Activation Entropy ($J.K^{-1}$)

According to the framework of Starkweather, transitions fall into two categories:

- Simple transitions, characterized by low values of the activation entropy (0-30 $J.K^{-1}.mol^{-1}$) and associated with motions of small chemical sequences

- Complex transitions, characterized by high values of the activation entropy (80 $J.K^{-1}.mol^{-1}$ or more) and corresponding to cooperative motions of neighboring groups

Literature results of thermo-mechanical transitions of plasticized cellulose acetate

Four thermo-mechanical transitions were identified for cellulose derivatives in the literature and denoted α, β*, β and γ from higher to lower temperatures. Meanwhile, different interpretations were reported concerning the two secondary relaxations (β- and γ-relaxations).

γ-relaxation

It was reported in the literature that γ-relaxation depends on amounts of water trace in cellulose acetate samples. If CDA is sufficiently dried, γ-relaxation should be invisible in mechanical and dielectric measurements. If not, then γ-relaxation is related to amounts of water trace: intensity of γ-relaxation decreases and characteristic temperature of γ-relaxation increases when less water trace is present in the system. In recently years, scientists made similar experimental observations on γ-relaxation: activation energy of 32-52 $kJ.mol^{-1}$ and relatively negligible entropy contribution. However, molecular origin of γ-relaxation has not been very well defined. Here are two interesting interpretations:

Scandola and Ceccorulli 1985a considered γ-relaxation as a result of water-associated primary hydroxyl group of cellulose acetate. They found similar activation energy values and relaxation temperatures at same frequency between γ-relaxation and $–CH_2OH$ relaxation of cellulose (ΔE_a = 54 $kJ.mol^{-1}$ at -86°C and frequency 3 Hz). However, in our point of view, the amount of unsubstituted primary hydroxyl groups in DS 2.45 is not large enough to explain γ-relaxation of cellulose acetate. There is on average one remaining unsubstituted hydroxyl group per two anhydroglucose units for DS 2.45. The ratio of acetyl groups versus hydroxyl groups is already 5 to 1. Furthermore, among hydroxyl groups, only one third may be primary hydroxyl groups (three possible positions: C2, C3 and C6). The ratio of acetyl groups versus methylol groups is actually 15 to 1. This interpretation is thus considered unjustified.

McBrierty et al. 1996 studied cellulose acetate samples plasticized by diethyl phthalate. They proposed several possibilities to explain γ-relaxation: the onset of mobility of tightly bound water, the onset of mobility of loosely bound water and the glass transition of DEP molecules. The last proposition is not justified since γ-relaxation already exists in unplasticized CDA sample. That leaves us two possibilities related to mobility of water molecules. If γ-relaxation is due to mobility of water, then it should be a primary relaxation process which is fitted with WLF or VFT law. According to our experimental results, γ-relaxation is a secondary relaxation process which follows Arrhenius behavior (details in dielectric analysis). Other interpretations of γ-relaxation are based on the dynamic study of broadband dielectric spectroscopy. The related literature review will be discussed in Chapter 5.

β-relaxation

Scandola and Ceccorulli 1985b also discussed the molecular origin of β-relaxation of DEP-plasticized cellulose acetate. They observed that at high plasticizer content, the participation of DEP molecules in the motion responsible for the β-relaxation is clearly suggested. But how DEP molecules are involved in the molecular motion of β-relaxation? The authors proposed that a polymer-diluent interaction was formed and then yielded a change in bulkiness of the relaxing units when DEP content became efficient, which led to a modification of pre-existing secondary β-relaxation. *Seymour et al. 1979* shared the same point of view.

McBrierty et al. 1996 identified three principal sub-peaks in the broad peak of β-relaxation. They confirmed that β-relaxation was complex and should be related to cooperative motions involving side groups and main cellulosic rings. Again, further information will be provided in Chapter 5 along with literature review of dielectric results of dynamic transitions.

Preliminary interpretations of our experimental results

The first thing to be noted about our experimental results is that γ-relaxation has not been found in any plasticized cellulose acetate through our DMTA analysis. Since drying procedure is done prior to analysis, the sample is considered as sufficiently dried to remove the γ-relaxation.

β-relaxation is found at the same temperature range as α'-relaxation. The resulted overlapping peak in the tan δ curve makes the interpretation more difficult than expected. β-relaxation is recognized as a result of cooperative motions, but no further details can be revealed by DMTA measurement. It is not certain that if the participation of plasticizer molecules may change the nature of the secondary relaxation. Combination of thermo-mechanical and dielectric results may help us find the right answer.

β^*-shoulder is located from 50 to 150°C and is centered at 100°C and frequency 1 Hz. Considering this specific temperature value, it is not surprising that the shoulder is interpreted as evaporation of water trace from samples. Such a conclusion is also obtained by other authors such as *Scandola and Ceccorulli 1985a*. DMTA spectra are compared to MDSC thermograms in the same temperature range: a loss peak in the non-reversible heating flow is identified from MDSC measurement in the first heating scan if the sample has no drying procedure prior to analysis (Appendix III).

In conclusion, thanks to the first results obtained by DMTA analysis, relaxation behavior and molecular motions of dynamic transitions will be thoroughly studied in Chapter 5.

3.3 – Miscibility mechanisms: a Small-Angle Neutron Scattering study

Small-Angle Neutron Scattering (SANS) is aimed at understanding miscibility mechanisms of plasticized cellulose acetate. We expect to observe miscibility behaviors such as phase separation, cavitation (filled with plasticizer molecules) and fluctuations of concentration, etc. In the present study, plasticizers Triacetin (TA) and Diethyl Phthalate (DEP) are deuterated. Deuterium labelling is the most common method used for identification of phase separation in SANS experiment. ^{1}H is the only element/isotope whose coherent scattering length density is negative. Due to commercial availability, triacetin d_9 and diethyl phthalate d_{14} are used as the deuterated plasticizers. Thanks to the deuterium labelling, the important scattering length density contrasts between CDA-rich phase and plasticizer-rich phase can be observed and are regarded as a result of phase separation.

In this chapter, the following contents are discussed:

- First, on the basis of MDSC and DMTA characterizations, conclusions and hypotheses about the miscibility behavior of plasticized cellulose acetate are reviewed. Their corresponded SANS responses are discussed.
- Second, the SANS result is fitted and analyzed according to the above hypotheses. Every possibility is studied and justified.
- Third, after the first SANS measurement, conclusions and perspectives are announced.

3.3.1 – Miscibility behaviors being susceptible to be detected in SANS

Phase separation

It is proven that phase separation occurs in the plasticized cellulose acetates and results a two-phase system: CDA-rich phase and plasticizer-rich phase (Figure 42). In neutron scattering analysis, phase separated systems with well-defined (narrow) interfaces between two phases are analyzed by the Debye-Bueche Equation (*Debye and Bueche 1949, Debye et al. 1957*):

$$I(q) = \frac{I_0}{(1 + \xi^2 q^2)^2}$$

Equation (26)

Where

- I_0: the extrapolated scattering intensity of each blend at q = 0 (cm^{-1})
- ξ: correlation length (nm)
- q: scattering vector ($Å^{-1}$)

And I_0 is defined as:

$$I_0 = 8\pi\xi^3(\Delta\rho)^2\varphi_1\varphi_2$$

Equation (27)

Where

- φ_i: volume fractions of each phase domain in the blend (dimensionless)
- $\Delta\rho$: coherent scattering length density contrast (cm^{-2})

Equation 9 of Chapter 2 is equivalent to Equation 26. In Figure 22, the correlation length of scattering objects is denoted ξ, which means that its volume (V in Equation 9) is ~ ξ^3. The number of scattering objects per unit volume (N in Equation 9) corresponds to φ / ξ^3, as φ is the volume fraction of scattering objects in the sample. Other terms in Equation 26 come from the normalized form factor P(q) and structure factor S(q).

Thus, we obtain for large q the Porod law $I \approx q^{-4}$. The resulted scattering pattern is displayed in Figure 43, plotted as absolute scattering intensity I(q) as a function of scattering vector q. The hump at $q \approx 0.01$ $Å^{-1}$ is the result of phase separation in a polymer blend.

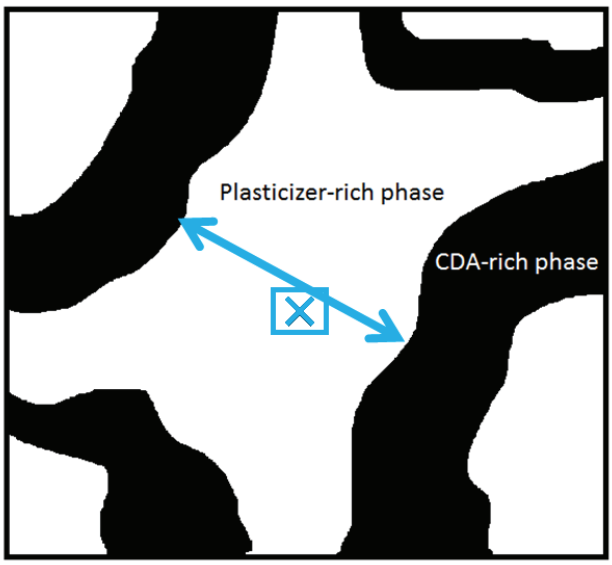

Figure 42: Phase separation in the plasticized cellulose acetates. ξ: correlation length

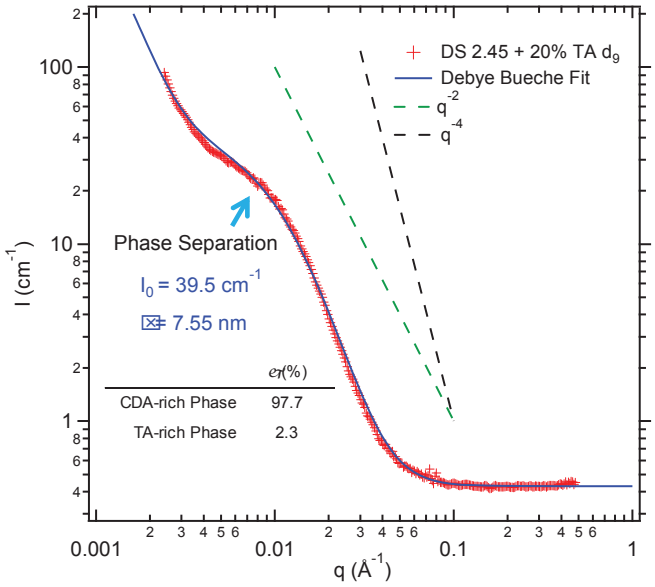

Figure 43: A typical neutron scattering pattern of phase separation of polymer blends.

According to the Debye-Bueche Equation, the scattering intensity of phase separation I(q) is dependent on three variables and their influences are shown in Figure 44:

- the contrast ($\Delta\rho$: cm^{-2}) of scattering length densities of separated phases
- the length scale (ξ: nm) of separated phases
- and the volume fractions (φ) of separated phases

Deuterium labelling is mandatory to enhance the contrast of scattering length densities of separated phases. The scattering length densities of deuterated plasticizers can be easily distinguished from those of cellulose acetates and protonated plasticizers (Table 7 in Chapter 2). Consequently, the I(q) of phase separation between cellulose acetate and deuterated plasticizer will be far more intense than the intensity of phase separation between cellulose acetate and protonated plasticizer ($I(q) \propto \Delta\rho^2$). The larger the contrast $\Delta\rho$, the higher the scattering intensity I(q).

The length scale (ξ) of separated phases is an important key to locate their SANS signals or conversely analyzing SANS signals allow to determine or estimate length scales. Since phase separation has been observed in the conventional techniques, ξ_{min} should be at least ~5 nm. In Chapter 3.1, it has been noted that plasticizer exudation is visible to the naked eye from 50% plasticizer content, i.e. ξ_{max} should be in the µm scale. If this is the case, the related hump may be in the inaccessible q range, as shown in Figure 44.

At the moment, the influence of plasticizer content on the length scale (ξ) of separated phases remains unknown. As mentioned above, the scattering intensity I(*q*) is dependent on the length scale (ξ) of separated phases according to the equation below:

$$I(q) = \frac{8\pi\xi^3(\Delta\rho)^2\varphi_1\varphi_2}{(1+\xi^2q^2)^2}$$

Equation (28)

The scattering intensity I(*q*) is dependent on the correlation length ξ such as:

- When $q \to 0$, the scattering intensity I(*q*) is proportional to ξ^3.
- When $q \to \infty$, the scattering intensity I(*q*) is proportional to ξ^{-1}.

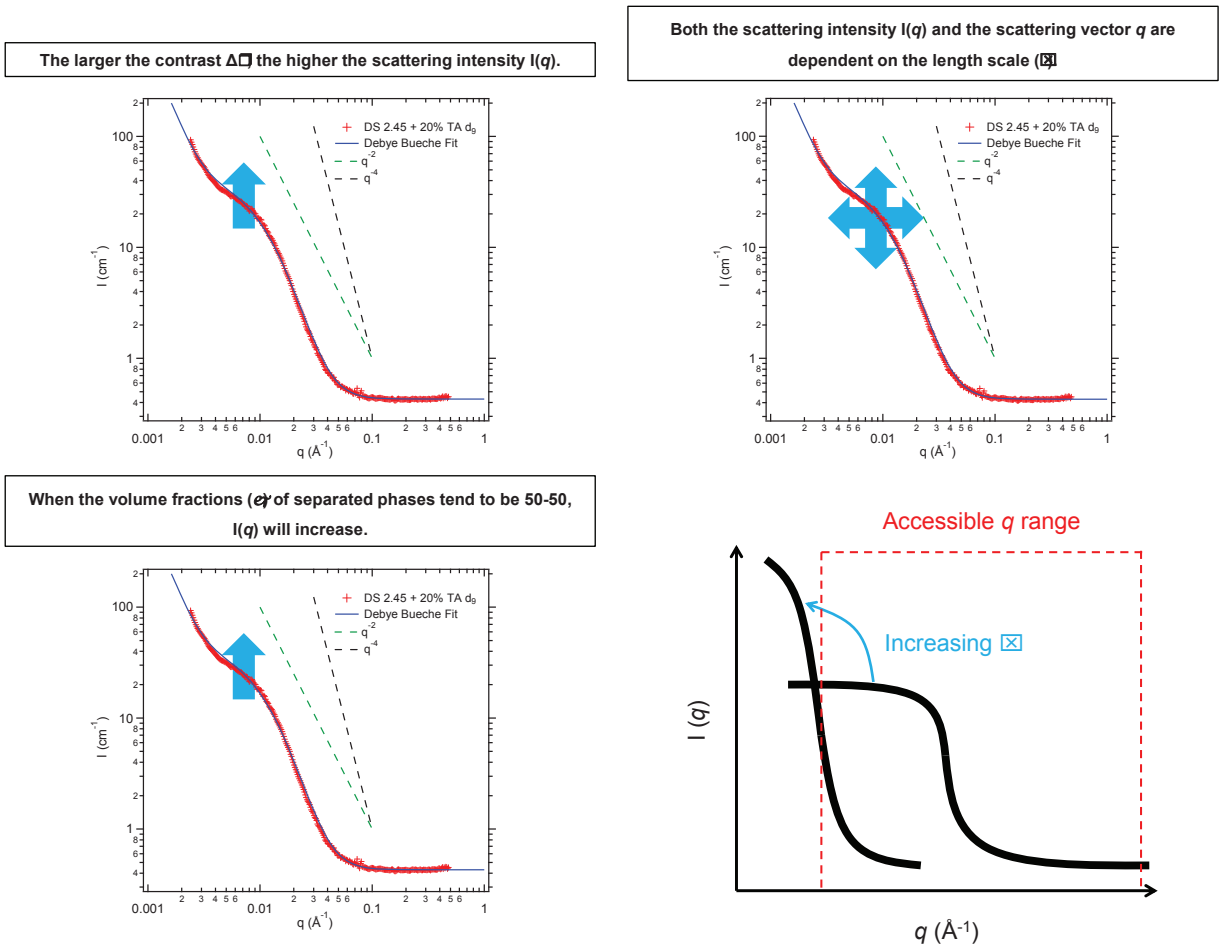

Figure 44: Four different neutron scattering patterns of phase separation in TA-plasticized cellulose acetate (DS 2.45). Bold arrows indicate the possible movements of SANS curve; thin arrow indicates the position of the hump which should be related to phase separation on the μm scale.

Last but not least, volume fractions (φ) of separated phases should be strongly related to plasticizer content of cellulose acetate systems. Consistent results are required between conventional techniques and SANS analysis. When the volume fractions (φ) of separated phases tend to be 50-50, I(q) will increase ($I(q) \propto (1-\varphi).\varphi$).

Cavities partially filled with plasticizer molecules

In Chapter 3.1, a third transition has been identified in highly DEP-plasticized DS 1.83 and DS 2.08 series. We assume that this is due to the presence of cavities partially filled with plasticizer molecules (Figure 45). Indeed, voids may be created inside the film during solvent evaporation and cavities may be filled by certain amounts of plasticizer molecules. The formation of cavities during the solvent evaporation step of "solvent casting" method is one of our main hypotheses in the present study. A question is then asked: is it possible to find cavities in other plasticized cellulose acetates? Cavities have not been observed in the conventional techniques for TA-plasticized cellulose acetates or DS 2.45 + DEP series. Either no cavities exist in these systems, or cavities are empty or their volume fraction is negligible or the size of cavities is too small to be detected in MDSC and DMTA measurements. However, since SANS is a powerful tool for micro-structure investigations of materials, the presence of cavities may be revealed.

Cavities partially filled with plasticizer molecules can be regarded as a sort of phase separation: one phase corresponds to the cavities and another one corresponds to plasticized cellulose acetate. Thus, it should be analyzed by the Debye-Bueche Equation and the corresponding scattering intensity I(q) is dependent on three variables:

- the contrast ($\Delta\rho$) of scattering length densities of separated phases

The contrast between cavities and plasticized cellulose acetate is dependent on the unknown amounts of plasticizers filling into cavities, because the cavity phase domain is composed of voids and plasticizers. The plasticizer filling ratio ($\Phi_{plasticizer}$) may be calculated if both protonated and deuterated samples are tested in SANS analysis. The scattering intensity I(q) is proportional to $\Delta\rho^2$, which means their respective ratio between protonated and deuterated samples should be consistent with each other.

- the length scale (ξ) of separated phases (i.e. the size of cavities)
- and the volume fractions (φ) of separated phases (i.e. the volume fraction of cavities)

As previously mentioned, cavities have not been observed in the conventional techniques for plasticized DS 2.45 series. If neutron scattering study reveals the presence of cavities, two interpretations are then possible: either the size of cavities is too small to be detected or their volume fraction is negligible in the conventional techniques.

If cavities are partially filled with plasticizer molecules, then the size of cavity phase domain should be large enough to contain these low-molecular-weight molecules. That means it should be above the detection limit of MDSC analysis. As a result, the negligible volume fraction of cavities should be the reason why cavities have not been observed in the conventional techniques for plasticized DS 2.45 series.

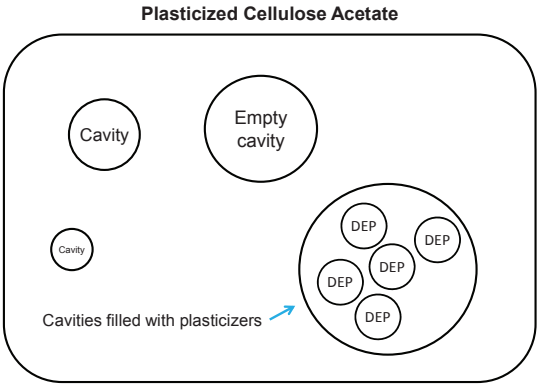

Figure 45: Empty cavities and cavities partially filled with plasticizer molecules (example of diethyl phthalate) in the plasticized cellulose acetates.

Cavities without plasticizers

Since it is not possible to control the mechanism of formation of cavities, the presence of empty cavities cannot be excluded. Their contrast of scattering length densities ($\Delta\rho$) is easy to calculate because ρ of cavities is equal to 0. Empty cavities can be unambiguously observed in protonated plasticized cellulose acetates.

Concentration fluctuations of the studied system

One of the most common miscibility behavior observed in neutron scattering study is the concentration fluctuations of the studied system. Unlike the previous possibilities, it should be analyzed by a q^{-2} power law. The length scale (ξ) of concentration fluctuations remains to be determined experimentally.
Modified Ornstein-Zernike Equation (*Ornstein and Zernike 1914*) is applied for describing concentration fluctuations of a system:

$$I(q) = \frac{I_0}{1 + \xi^2 q^2}$$

Equation (29)

Molecular liquids of plasticizers

Deuterated plasticizers are used to creat “Contrast Variation” in order to observe miscibility behavior of plasticized cellulose acetate. At a near-molecular scale, the plasticized cellulose acetate background is considered as homogeneous and has zero contrast. Plasticizer molecules are randomly arranged and with the presence of important amounts of plasticizers, the effect of molecular liquids may be observed in SANS analysis: the correlation length between two molecules is experimentally observed to be ~1 nm (Figure 46 and 47). It is also considered as a sort of phase separation, which should be analyzed by the Debye-Bueche Equation. The effect of molecular liquids of protonated plasticizers will not be identified because its contrast is negligible in the studied system.

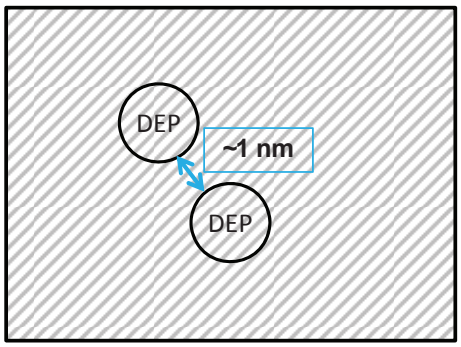

Figure 46: Molecular liquids of deuterated plasticizers (example of diethyl phthalate) in the plasticized CDA.

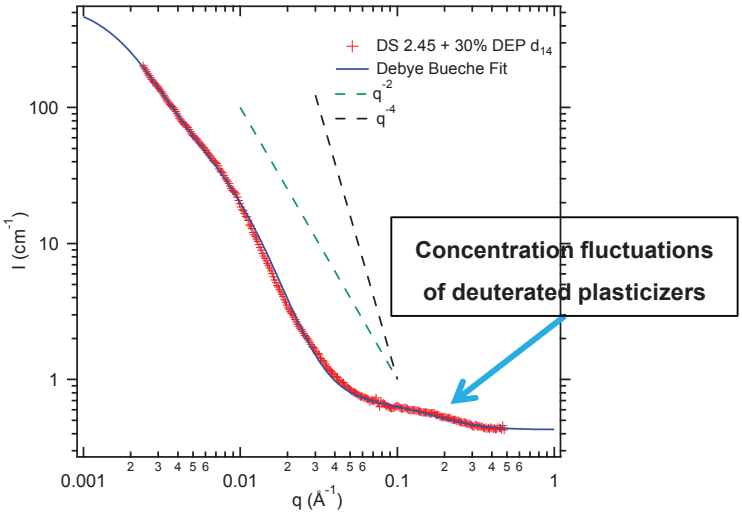

Figure 47: SANS pattern of concentration fluctuations of deuterated plasticizers (example of diethyl phthalate).

Concentration fluctuations of main cellulosic chain

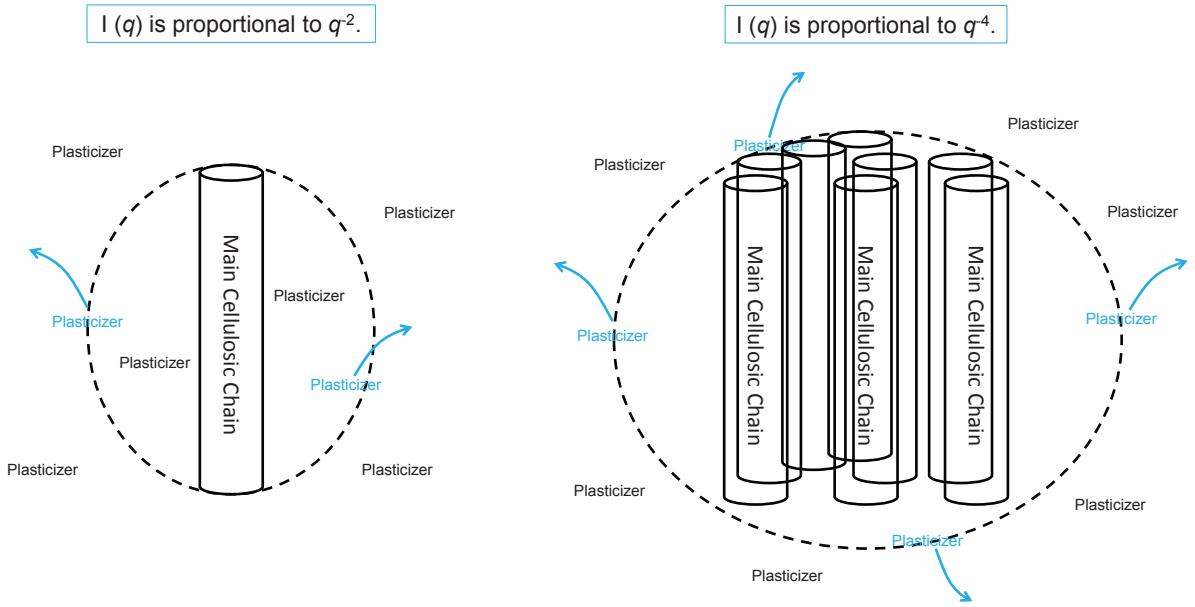

Figure 48: Left – Small concentration fluctuations of main cellulosic chain. Right – Important concentration fluctuations of main cellulosic chain.

In fact, cellulose acetate can be regarded as a semi-flexible polymer: it has a large persistence length. In this context, there may be a specific concentration fluctuation which is related to the main cellulosic chain: plasticizers are expelled from a localized cellulose acetate-rich domain (e.g. a bundle of cellulosic chains) and then dispersed in another localized domain because of the main chain behavior (Figure 48). The resulted contrast is directly related to the degree of plasticizer expulsion:

- If the main chains of plasticized cellulose acetate are isolated from each other (Figure 48 left), the degree of plasticizer expulsion will be low, which results certain concentration fluctuations in a localized area (there is locally an excess of cellulose acetate with respect to the average concentration in a region whose size is comparable to the persistence length of the polymer, see *Lodge & McLeish 2000*). It should be analyzed by the modified Ornstein-Zernike Equation.

- If a bundle of cellulosic chains are gathered together, the degree of plasticizer expulsion will be high enough to produce strong concentration fluctuations, which results in a phase separation-like effect (regions with very few plasticizer molecules and other ones with very few polymers, Figure 48 right). It should be analyzed by the Debye-Bueche Equation.

More importantly, the correlation length of the above assumption should be comparable to the persistent length of the sample system (Figure 49). As indicated in the literature (*Kamide 2005*), the persistent length of cellulose acetate is about 10 nm (20 repetition units of 0.5 nm length scales).

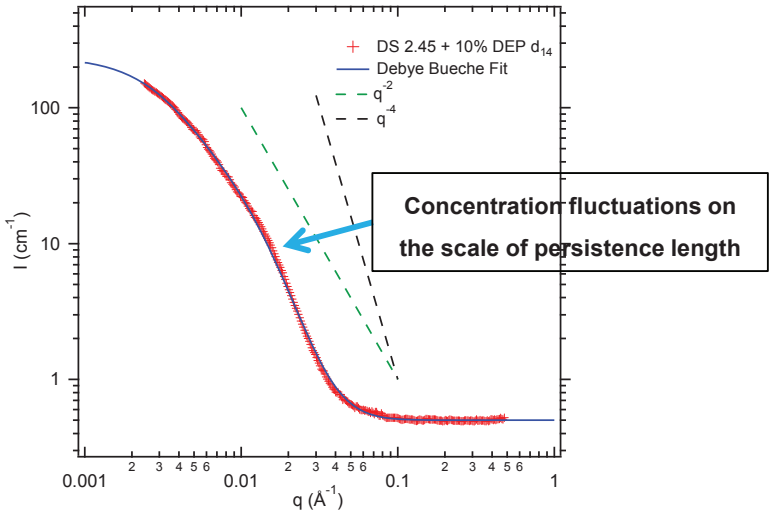

Figure 49: SANS pattern of concentration fluctuations on the scale of persistence length (example of diethyl phthalate).

Interferences at the surfaces of plasticized cellulose acetate films

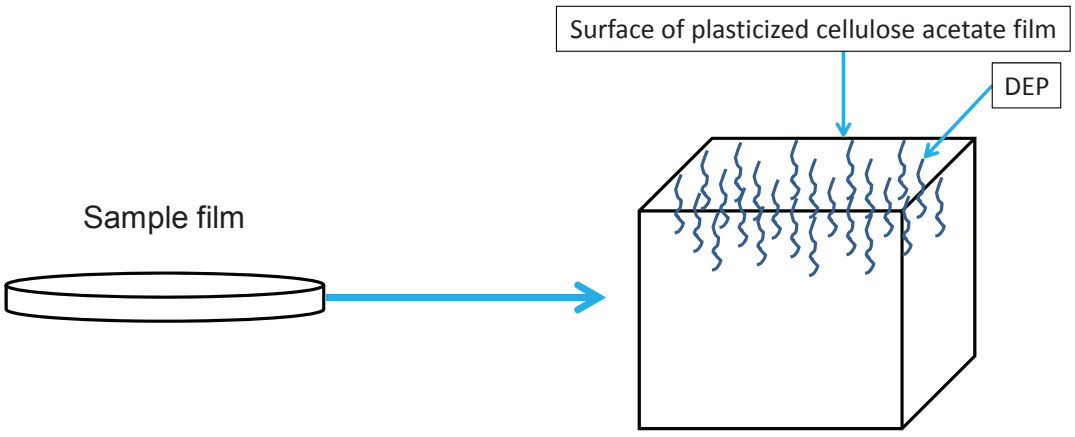

Figure 50: Illustrations of superficial interferences of plasticized cellulose acetate films

The last situation which may be detected in neutron scattering analysis is due to potential effects at the surfaces of plasticized cellulose acetate films. One such situation is segregation of plasticizers on the surface (Figure 50). On the other hand, due to the "solvent casting" method, it is possible to have surface irregularity (roughness) in our samples. Of course, this kind of irregularity is limited by thickness of the surface area. It should not exceed 1% of film thickness, which is not significant as compared to the whole sample. Consequently, the resulted SANS signal may be confused with that of cavities partially filled with plasticizers because the contrast ($\Delta\rho$)of scattering length densities are similar.

3.3.2 – Interpretation of SANS results

The coherent scattering length density of a phase domain ($\rho_{phase\ domain}$) in the plasticized cellulose acetate is calculated as:

$$\rho_{phase\ domain} = \Phi_{CDA}\rho_{CDA} + (1 - \Phi_{CDA})\rho_{Plasticizer}$$

Equation (30)

Where

- Φ_{CDA}: cellulose acetate content in one phase domain
- ρ_{CDA}: coherent scattering length density of cellulose acetate
- $\rho_{Plasticizer}$: coherent scattering length density of plasticizer

Nevertheless, the following situations must be taken into account:

a) If the plasticized cellulose acetate is a miscible system, $\rho_{phase\ domain}$ will be $\rho_{plasticized\ cellulose\ acetate}$.
b) If the plasticized cellulose acetate is a partially miscible system, $\rho_{phase\ domain}$ will be either $\rho_{CDA\text{-}rich\ phase}$ or $\rho_{plasticizer\text{-}rich\ phase}$. Phase compositions are determined according to thermal results (Tables in Chapter 3.1).
c) If the plasticized cellulose acetate is a three-phase system, $\rho_{phase\ domain}$ will be one of the following possibilities: $\rho_{CDA\text{-}rich\ phase}$, $\rho_{plasticizer\text{-}rich\ phase}$ or $\rho_{cavities}$. The last one is supposed to be related to the cavity phase domain: either with empty cavities ($\rho_{cavities}$ = 0) or with cavities partially filled with plasticizers ($\rho_{cavities} = \Phi_{Plasticizer}\ \rho_{Plasticizer}$). $\Phi_{Plasticizer}$ is the plasticizer filling ratio in cavities.

Table 12 is the summary of coherent scattering length densities of different phase domains in the plasticized cellulose acetate.

Plasticizer	Sample	$\Phi_{Plasticized\ CDA}$ (cm^{-2})	$\Phi_{CDA\text{-}rich\ phase}$ (cm^{-2})	$\Phi_{Plasticizer\text{-}rich\ phase}$ (cm^{-2})
Triacetin d_9	DS 1.83 + 10% TA d_9	2.00E+10		
	DS 1.83 + 20% TA d_9		2.17E+10	3.51E+10
	DS 1.83 + 40% TA d_9		2.46E+10	3.72E+10
	DS 2.08 + 10% TA d_9	1.97E+10		
	DS 2.08 + 20% TA d_9		2.13E+10	3.52E+10
	DS 2.08 + 40% TA d_9		2.47E+10	3.76E+10
	DS 2.45 + 10% TA d_9	2.03E+10		
	DS 2.45 + 20% TA d_9		2.22E+10	3.53E+10
	DS 2.45 + 40% TA d_9		2.55E+10	3.67E+10
Triacetin	DS 1.83 + 10% TA	1.69E+10		
	DS 2.08 + 10% TA	1.73E+10		
	DS 2.45 + 10% TA	1.74E+10		
	DS 2.45 + 20% TA		1.71E+10	1.47E+10
Diethyl Phthalate d_{14}	DS 2.45 + 10% DEP d_{14}	2.16E+10		
	DS 2.45 + 20% DEP d_{14}	2.35E+10		4.35E+10
	DS 2.45 + 30% DEP d_{14}		2.62E+10	4.58E+10
	DS 2.45 + 45% DEP d_{14}		2.81E+10	4.92E+10
Diethyl Phthalate	DS 1.83 + 30% DEP		1.69E+10	1.58E+10
	DS 2.08 + 20% DEP	1.73E+10		1.59E+10
	DS 2.45 + 20% DEP	1.75E+10		1.62E+10
	DS 2.45 + 30% DEP		1.73E+10	1.60E+10

Table 12: Summary of coherent neutron scattering length densities calculated based on thermal analysis.

3.3.2.1 – Analysis of the curves of DS 2.45 + DEP series

The first series to be analyzed is cellulose acetate with DS 2.45 plasticized by deuterated DEP or TA (Figure 51). Arrows indicate fitting contributions corresponding to specific correlation lengths:

- Black arrow indicates a fitting contribution corresponding to a large correlation length (ξ), which is found out of the experimental range. We propose that this fitting contribution is related to phase separation.
- Red arrow indicates a fitting contribution corresponding to a large correlation length (ξ), which is in the experimental range. Cavities are attributed to this contribution.
- Green arrow indicates a fitting contribution corresponding to an intermediate correlation length (ξ), which is proposed as a result of concentration fluctuations due to the main cellulosic chains. Its correlation length is equivalent to the persistence length of cellulose acetate.
- Blue arrow indicates a fitting contribution corresponding to a small correlation length (ξ). We propose that this contribution corresponds to concentration fluctuations of plasticizer molecules.

Some exceptions are found in the SANS experiment and they are all noted and discussed in this chapter.

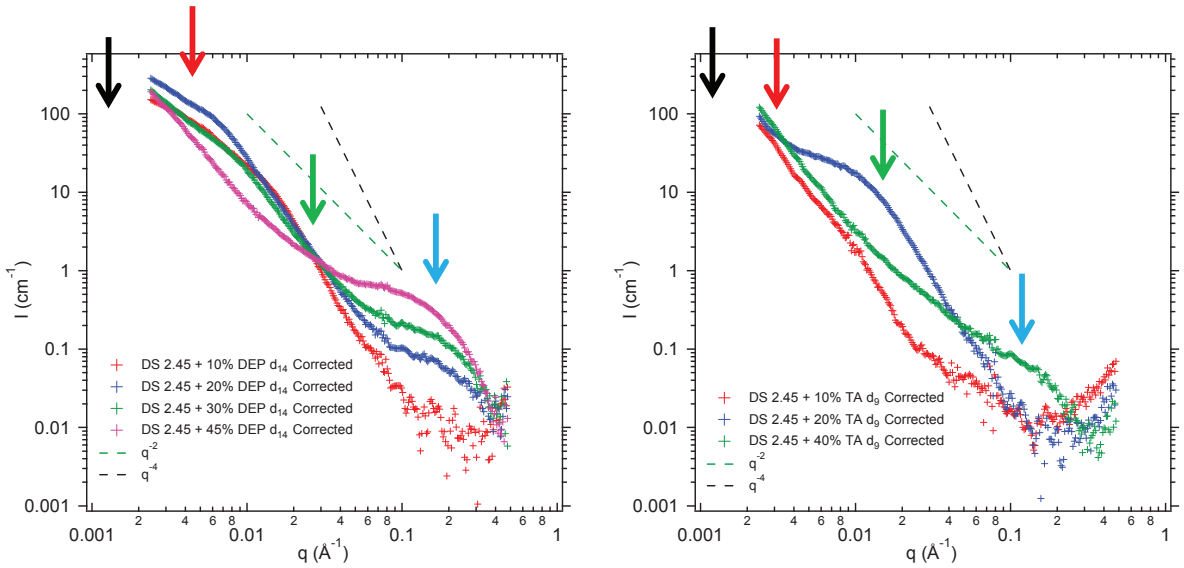

Figure 51: SANS curve of cellulose acetates plasticized by deuterated triacetin and diethyl phthalate. Here the incoherent scattering has been subtracted.

DS 2.45 + 10% DEP d_{14} is fit by two separated Debye-Bueche distributions, whose parameters are listed in Figure 52. The hump corresponding to ξ = 24.1 nm is supposed to originate from cavities (as explained in the next sample). Unfortunately, since the data of corresponded protonated DS 2.45 + 10% DEP is missing, the plasticizer filling ratio in cavities remains unknown. The hump corresponding to ξ = 8.2 nm is believed to be related to concentration fluctuations near the persistence length scale (as explained in the next sample). Phase separation is not detectable here because DS 2.45 + 10% DEP is a miscible system.

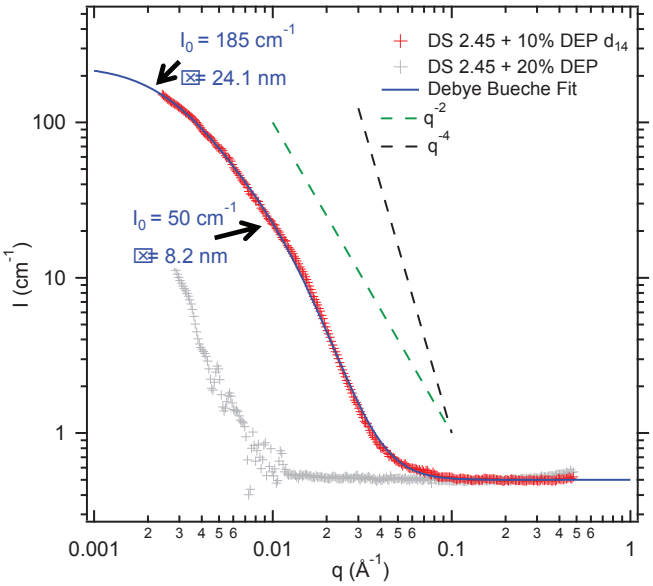

Figure 52: SANS curve of DS 2.45 + 10% DEP d_{14}, fit by two Debye-Bueche distributions. The curve of DS 2.45 + 20% DEP is shown for comparison.

I_0	ξ	$(\Delta\rho)^2$	$\varphi_1\varphi_2$	φ_1	φ_2
(cm^{-1})	(cm)	(cm^{-4})			
50	8.20E-07	1.42E+19	2.54E-01	0.5	0.5

	ρ	% CDA	% DEP	% Phase
Phase 1	1.98E+10	95	5	50
Phase 2	2.35E+10	85	15	50

Table 13: Details of calculation for concentration fluctuations near the persistence length scale of DS 2.45 + 10% DEP d_{14}. $(\Delta\rho)^2$ is obtained from the ρ values in phase 1 and 2. φ_1 and φ_2 are the volume fractions of each phase. % CDA and % DEP denote composition in each phase.

DS 2.45 + 20% DEP d_{14} is fit by four Debye-Bueche distributions and is compared to the same protonated sample in Figure 53. The interpretation of the four distributions is given by orders (from large to small ξ values) and the obtained results are shown in Table 14.

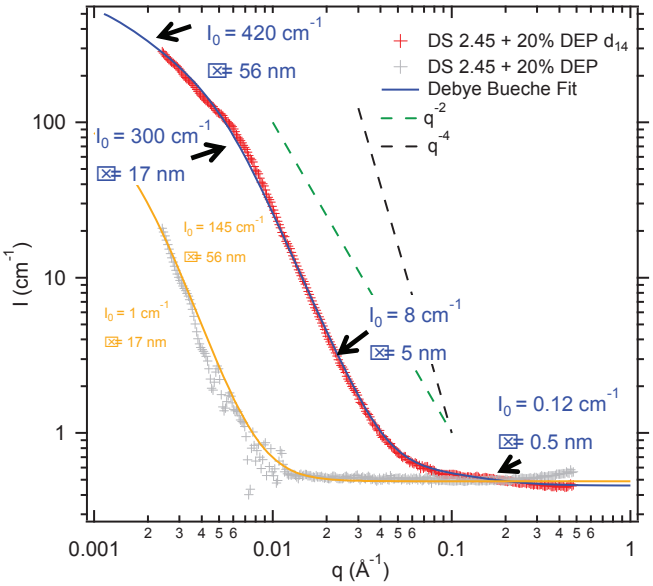

Figure 53: SANS curve of DS 2.45 + 20% DEP d_{14}, fit by four Debye-Bueche distributions and is compared to its protonated sample.

1. The hump corresponding to ξ = 56 nm is attributed to cavities partially filled with DEP molecules. Other possibilities are ruled out by considering the ratio between the signals of the systems with deuterated and protonated plasticizers:

   - If phase separation is the origin of this part of the signal, then according to the Debye-Bueche Equation, we should have (with (Δρ) values given by the phase compositions estimated from DSC results):

$$\frac{I_0^{deuterated}}{I_0^{protonated}} \approx \frac{(\Delta\rho)^2_{deuterated}}{(\Delta\rho)^2_{protonated}} \approx 222$$

     Which does not agree with our experimental ratio:

$$\frac{I_0^{deuterated}}{I_0^{protonated}} = \frac{420}{145} = 2.90$$

Thus, the distribution corresponding to ξ = 56 nm could not be due to phase separation.

- If empty cavities are the origin of this part of signal, then the calculation is:

$$\frac{I_0^{deuterated}}{I_0^{protonated}} \approx \frac{(\Delta\rho)^2_{deuterated}}{(\Delta\rho)^2_{protonated}} = \frac{5.54 * 10^{20}}{3.06 * 10^{20}} = 1.81$$

Which is again not in agreement with our experimental ratio (2.90).

- If cavities fully filled with plasticizers are the origin of this part of signal, then we should have:

$$\frac{I_0^{deuterated}}{I_0^{protonated}} \approx \frac{(\Delta\rho)^2_{deuterated}}{(\Delta\rho)^2_{protonated}} = \frac{1.03 * 10^{21}}{4.61 * 10^{18}} = 222$$

The value is too large compared to our experimental ratio (2.90).

Consequently, the presence of cavities partially filled with DEP molecules is considered as a potential explanation of the data. Cavities may appear since we do not completely control the solvent evaporation step in the solvent casting method. The respective threshold limits of the $(\Delta\rho)^2$ ratio correspond to empty cavities (1.81, 0% plasticizer filling ratio) and cavities fully filled with plasticizers (222, 100% plasticizer filling ratio). Thus, an intermediate plasticizer filling ratio ($\Phi_{plasticizer}$) is required to complete the calculation:

We know that experimentally:

$$\frac{I_0^{deuterated}}{I_0^{protonated}} = \frac{420}{145} = 2.90$$

Thus, we should have:

$$\frac{(\Delta\rho)^2_{deuterated}}{(\Delta\rho)^2_{protonated}} = 2.90$$

Since $(\Delta\rho)^2 = \left(\rho_{plasticized\ CDA} - \rho_{DEP} \times \Phi_{DEP}\right)^2$, we can deduce that the average plasticizer filling ratio in the cavities is 65.3%:

$$\frac{(\Delta\rho)^2_{deuterated}}{(\Delta\rho)^2_{protonated}} = \frac{\left(\rho_{plasticized\ CDA} - \rho_{DEP} \times 65.3\%\right)^2_{deuterated}}{\left(\rho_{plasticized\ CDA} - \rho_{DEP} \times 65.3\%\right)^2_{protonated}} = \frac{1.62 \times 10^{20}}{5.59 \times 10^{19}} = 2.91$$

However, the volume fraction of cavities deduced from the intensity of the signal only represents 0.059% of the total plasticized cellulose acetate (Table 14). This is why this phenomenon is not detected by conventional characterization techniques.

I_0	☒	$(\Delta\rho)^2$	$e_1 e_2$	e_1	e_2
(cm^{-1})	(cm)	(cm^{-4})			
420	5.60E-06	1.62E+20	5.86E-04	0.99941	0.00059
	ρ	% CDA	% DEP	% Phase	
Phase 1	2.35E+10	85	15	99.941	
Phase 2	3.63E+10	0	65.3	0.059	

I_0	☒	$(\Delta\rho)^2$	$e_1 e_2$	e_1	e_2
(cm^{-1})	(cm)	(cm^{-4})			
300	1.70E-06	3.99E+20	6.09E-03	0.9939	0.0061
	ρ	% CDA	% DEP	% Phase	
Phase 1	2.35E+10	85	15	99.39	
Phase 2	4.35E+10	32	68	0.61	

I_0	☒	$(\Delta\rho)^2$	$e_1 e_2$	e_1	e_2
(cm^{-1})	(cm)	(cm^{-4})			
8	5.00E-07	1.03E+19	2.48E-01	0.5	0.5
	ρ	% CDA	% DEP	% Phase	
Phase 1	2.37E+10	84.5	15.5	50	
Phase 2	2.69E+10	76	24	50	

Table 14: Details of calculation for the different contributions in DS 2.45 + 20% DEP d_{14} (cavities partially filled with plasticizers, phase separation and concentration fluctuations near the persistence length scale, respectively).

2. The hump corresponding to ξ = 17 nm is attributed to phase separation. This interpretation relies on the comparison with the results of other techniques (mostly DSC). According to the Debye-Bueche Equation, I_0 is proportional to $(\Delta\rho)^2$. Thus, we can deduce that:

$$\frac{I_0^{deuterated}}{I_0^{protonated}} \approx \frac{(\Delta\rho)^2_{deuterated}}{(\Delta\rho)^2_{protonated}}$$

The other variables in the equation (ξ and φ) are the same between protonated and deuterated samples. In this case, we have experimentally:

$$\frac{I_0^{deuterated}}{I_0^{protonated}} = \frac{300}{1} = 300$$

And the density contrasts due to phase separation are:

$$\frac{(\Delta\rho)^2_{deuterated}}{(\Delta\rho)^2_{protonated}} = \frac{3.99 * 10^{20}}{1.79 * 10^{18}} \approx 222$$

The obtained result is consistent with our interpretation. In this case, the volume fraction of phase separation finally represents 0.61% of the total plasticized CDA, thus it is not detected in the conventional characterization techniques. This is consistent with the fact that this sample is close to the limit of phase separation as observed by DSC.

3. The hump corresponding to ξ = 5 nm is attributed to concentration fluctuations due to the main cellulosic chains, which are usually found in the persistence length scale. Here, the distribution is analyzed by the Debye-Bueche Equation (a q^{-4} law), i.e. an large number of main cellulosic chains are gathered together which results a strong degree of plasticizer expulsion in the localized area and thus create large concentration fluctuations. This phenomenon requires being in a cellulose acetate-rich phase. Finally, the resulted concentration fluctuations are calculated as ± 4.25% of DEP content (Table 14).

4. The last hump corresponding to ξ = 0.5 nm is supposed to be due to concentration fluctuations of plasticizer molecules, due to the small ξ values. No other assumption works in this correlation length scale.

DS 2.45 + 30% DEP d_{14} is fit by three Debye-Bueche distributions and is compared to the same protonated sample in Figure 54.

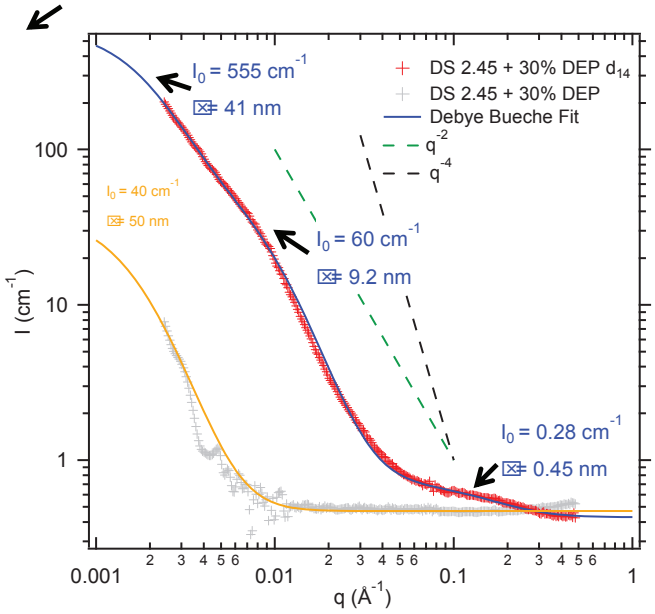

Figure 54: SANS curve of DS 2.45 + 30% DEP d_{14}, fit by three Debye-Bueche distributions and comparison to the same protonated sample.

1. The hump corresponding to ξ = 41 nm is considered as the result of cavities partially filled with DEP molecules. The reasoning is the same as that of DS 2.45 + 20% DEP. Here, the plasticizer filling ratio is found at 84.8% DEP content (Table 15). Its volume fraction remains as small as 0.154%.

2. The hump corresponding to ξ = 9.2 nm is believed to be concentration fluctuations due to the main cellulosic chains. It is analyzed by the Debye-Bueche equation, i.e. the phenomenon stays in a cellulose acetate-rich phase. As a result, the fluctuation amplitude is found at ± 4.75% of DEP content.

3. The hump corresponding to ξ = 0.45 nm is attributed to fluctuations of plasticizer molecules, due to the small ξ values.

4. According to our MDSC analysis, DS 2.45 + 30% DEP is a two-phase system: CDA-rich phase and DEP-rich phase. Phase separation is the miscibility behavior that we are looking for and it should in principle be detected in SANS curves. However, none of the three distributions works for phase separation assumption. Thus, the only remaining possibility is that phase separation occurs in a larger ξ value, which is out of the accessible *q* range (the black arrow in the left in Figure 49). That means its respective ξ value approaches to the μm-scale and should not have impacts on the accessible SANS curve. In Figure 55, a possible distribution of phase separation is presented. Here, ξ is set at 200 nm, which is the smallest correlation length possible to the situation. As shown in the same figure, this Debye-Bueche fit has zero impact on the experimental curve. Other fits with larger ξ values are also available but is less and less credible because the ξ value must hold a reasonable threshold limit.

I_0	☒	$(\Delta\rho)^2$	e_1e_2	e_1	e_2
(cm^{-1})	(cm)	(cm^{-4})			
555	4.10E-06	2.07E+20	1.53E-03	0.99846	0.00154
	ρ	% CDA	% DEP	% Phase	
Phase 1	3.27E+10	Phase separation		99.846	
Phase 2	4.71E+10	0	84.8	0.154	

I_0	☒	$(\Delta\rho)^2$	e_1e_2	e_1	e_2
(cm^{-1})	(cm)	(cm^{-4})			
60	9.20E-07	1.28E+19	2.39E-01	0.5	0.5
	ρ	% CDA	% DEP	% Phase	
Phase 1	2.47E+10	82	18	50	
Phase 2	2.82E+10	72.5	27.5	50	

Table 15: Details of calculation for the different distributions of DS 2.45 + 30% DEP d_{14} (cavities partially filled with plasticizers and concentration fluctuations near the persistence length scale, respectively).

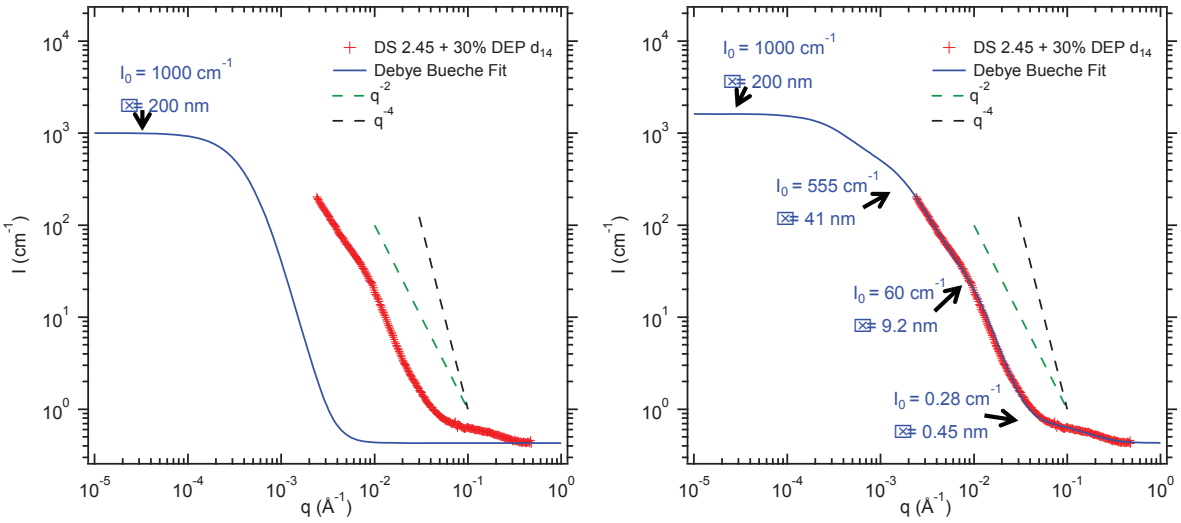

Figure 55: Illustration of the distribution due to phase separation in DS 2.45 + 30% DEP d_{14}, it is clear that this distribution has no influence on the experimental SANS curve.

DS 2.45 + 45% DEP d_{14} is fit by four Debye-Bueche distributions in Figure 56.

1. The hump corresponding to ξ = 36.7 nm is considered as the result of cavities. But the lack of related protonated SANS result keeps us away from determining the plasticizer filling ratio in cavities.

2. The hump corresponding to ξ = 11 nm is attributed to concentration fluctuations due to the main cellulosic chains. It is worth to point out that in DS 2.45 + 45% DEP d_{14}, the distribution is analyzed by a q^{-2} law. That means the respective degree of plasticizer expulsion induced by the main cellulosic chains is low and it happens in the plasticizer-rich phase. The conclusion makes sense because DS 2.45 + 45% DEP d_{14} is already dominated by the plasticizer-rich phase (MDSC results).

3. The hump corresponding to ξ = 0.44 nm is attributed to fluctuations of plasticizer molecules due to the small ξ values.

4. Again, the distribution of phase separation is supposed to be located out of the accessible *q* range.

According to the Debye-Bueche Equation (Equation 26 - 28), I_0 of large-scale phase separation can be estimated under certain conditions:

- $\Delta\rho^2$ and φ are known from thermal analysis, according to the T_g's and ΔC_p of separated phases. Compositions of each phase are calculated based on the Couchman-Karasz fit with incertitude.

- The correlation length ξ need to be large enough that the Debye-Bueche distribution of phase separation has no impact on the accessible SANS curve.

Because of the incertitude due to the Couchman-Karasz fit, non-negligible deviations are found when ξ is estimated for phase separation case. The minimum value of ξ is obtained ~10 µm. That means when the incertitude is taken into account, ~10 µm is the minimum acceptable value to complete the above conditions.

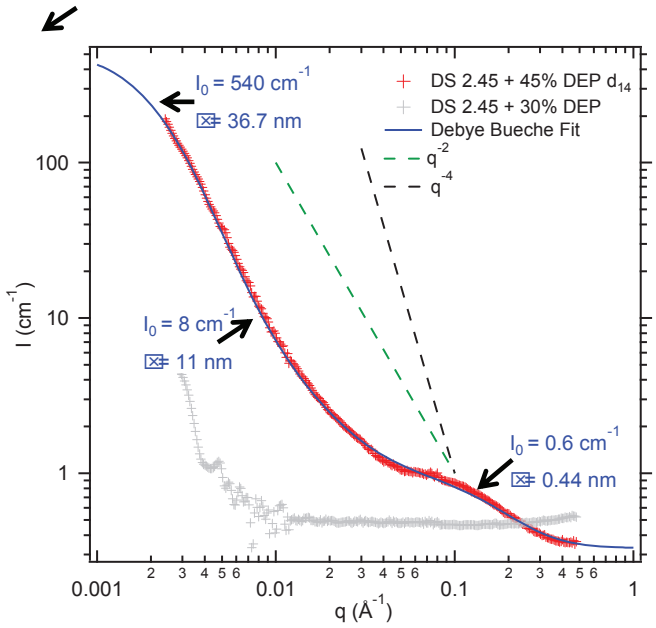

Figure 56: SANS curve of DS 2.45 + 45% DEP d_{14}, fit by three Debye-Bueche distributions.

I_0	☒	$(\Delta\rho)^2$	$\phi_1\phi_2$	ϕ_1	ϕ_2
(cm^{-1})	(cm)	(cm^{-4})			
8	1.10E-06	9.60E+17	2.49E-01	0.5	0.5

	ρ	% CDA	% DEP	% Phase
Phase 1	4.86E+10	18.6	81.4	50
Phase 2	4.95E+10	16	84	50

Table 16: Details of calculation for concentration fluctuations near the persistence length scale of DS 2.45 + 45% DEP d_{14}.

3.3.2.2 – Analysis of the curves of DS 2.45 + TA series

DS 2.45 + 10% TA d_9 is fit by two Debye-Bueche distributions and is compared to its protonated sample in Figure 57. Since it is a miscible system, the humps corresponding to ξ = 60 nm and ξ = 12.8 nm are attributed to cavities partially filled with plasticizers and concentration fluctuations due to the main cellulosic chains, respectively. The related calculations are listed in Table 17.

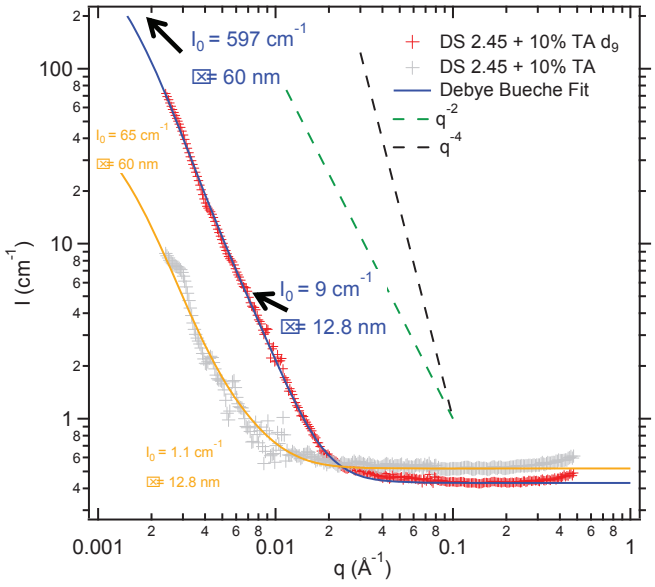

Figure 57: SANS curve of DS 2.45 + 10% TA d_9, fit by two Debye-Bueche distributions and is compared to its protonated sample.

I_0	ξ	$(\Delta\rho)^2$	$e_1 e_2'$	e_1'	e_2'
(cm^{-1})	(cm)	(cm^{-4})			
597	6.00E-06	2.78E+20	3.96E-04	0.9996	0.0004

	ρ	% CDA	% TA	% Phase
Phase 1	2.03E+10	90	10	99.96
Phase 2	3.69E+10	0	88.5	0.04

I_0	☒	$(\Delta\rho)^2$	$\phi_1\phi_2$	ϕ_1	ϕ_2
(cm^{-1})	(cm)	(cm^{-4})			
9	1.28E-06	6.96E+17	2.45E-01	0.5	0.5

	ρ	% CDA	% TA	% Phase
Phase 1	1.98E+10	92	8	50
Phase 2	2.06E+10	88.5	11.5	50

Table 17: Details of calculation for the different distributions of DS 2.45 + 10% TA d_9 (cavities partially filled with plasticizers and concentration fluctuations near the persistence length scale, respectively).

DS 2.45 + 20% TA d_9 is fit by two Debye-Bueche distributions and is compared to its protonated sample in Figure 58. The hump corresponding to ξ = 95 nm is clearly due to cavities partially filled with plasticizers and its related plasticizer filling ratio is 79.5%.

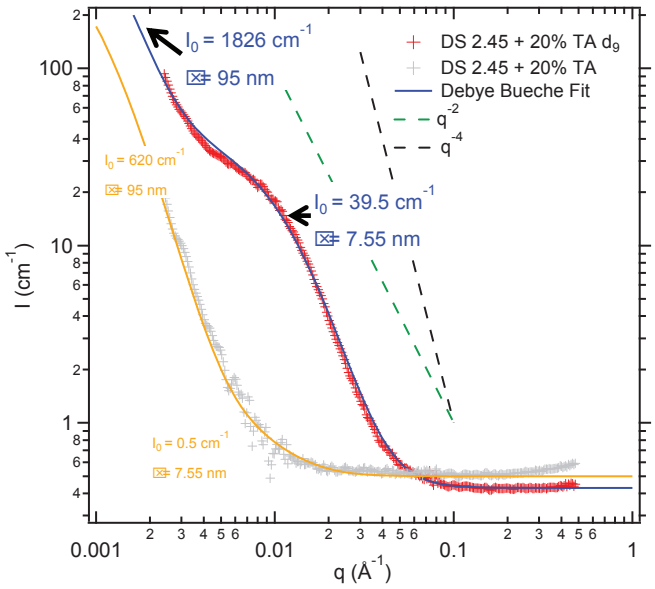

Figure 58: SANS curve of DS 2.45 + 20% TA d_9, fit by two Debye-Bueche distributions and is compared to its protonated sample.

Regarding the second hump corresponding to ξ = 7.55 nm, two possibilities may explain the situation:

- DS 2.45 + 20% TA is close to the partial miscibility threshold limit between the polymer and the plasticizer. Thus, phase separation can be observed in the SANS curve. The resulted correlation length, the ratio of density contrast between protonated and deuterated samples and the calculated volume fractions of two separated phases are all reasonable values.

- Second possibility is concentration fluctuations due to the main cellulosic chains, which should be found in every system. The correlation length (ξ = 7.55 nm) is close to the persistence length of cellulose acetate.

Consequently, it is difficult to say if the hump corresponding to ξ = 7.55 nm is due to a single behavior or two different ones. The calculations are shown in Table 18.

I_0	☒	$(\Delta\rho)^2$	e_1e_2	e_1	e_2
(cm^{-1})	(cm)	(cm^{-4})			
1826	9.50E-06	1.21E+20	7.00E-04	0.9993	0.0007

	ρ	% CDA	% TA	% Phase
Phase 1	2.22E+10	82	18	99.93
Phase 2	3.32E+10	0	79.5	0.07

I_0	☒	$(\Delta\rho)^2$	e_1e_2	e_1	e_2
(cm^{-1})	(cm)	(cm^{-4})			
39.5	7.55E-07	1.72E+20	2.12E-02	0.978	0.022

	ρ	% CDA	% TA	% Phase
Phase 1	2.22E+10	82	18	97.8
Phase 2	3.53E+10	27	73	2.2

Table 18: Details of calculation for the different distributions of DS 2.45 + 20% TA d_9 (cavities partially filled with plasticizers and phase separation, respectively).

DS 2.45 + 40% TA d_9 is fit by four Debye-Bueche distributions in Figure 59.

1. The hump corresponding to ξ = 40.5 nm is considered as the result of cavities. But the lack of related protonated SANS result keeps us away from determining the plasticizer filling ratio in cavities.

2. The hump corresponding to ξ = 8 nm is attributed to concentration fluctuations due to the main cellulosic chains. It is important to note that the distribution is analyzed by a q^{-2} law, which means this is standard concentration fluctuations in the plasticizer-rich phase. The calculation is listed in Table 19.

3. The hump corresponding to ξ = 0.7 nm is attributed to fluctuations of plasticizer molecules due to the small ξ values.

4. Again, the distribution of phase separation is supposed to be located out of the accessible *q* range.

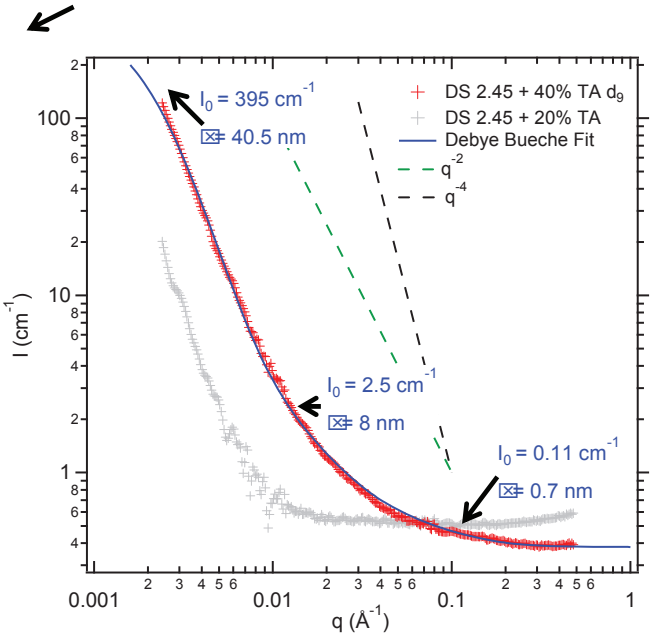

Figure 59: SANS curve of DS 2.45 + 40% TA d_9, fit by four Debye-Bueche distributions.

I_0	☒	$(\Delta\rho)^2$	e_1e_2	e_1	e_2
(cm^{-1})	(cm)	(cm^{-4})			
2.5	8.00E-07	7.78E+17	2.50E-01	0.5	0.5

	ρ	% CDA	% TA	% Phase
Phase 1	3.63E+10	22.7	77.3	50
Phase 2	3.72E+10	19	81	50

Table 19: Details of calculation for concentration fluctuations near the persistence length scale of DS 2.45 + 40% TA d_9.

3.3.2.3 – Interpretation on DS 2.08 + TA series

DS 2.08 + 10% TA d_9 is fit by three Debye-Bueche distributions and is compared to its protonated sample in Figure 60. It is a miscible system so that the humps corresponding to ξ = 70 nm and ξ = 4.5 nm are attributed to cavities partially filled with plasticizers and concentration fluctuations due to the main cellulosic chains, respectively. The related calculations are listed in Table 20.

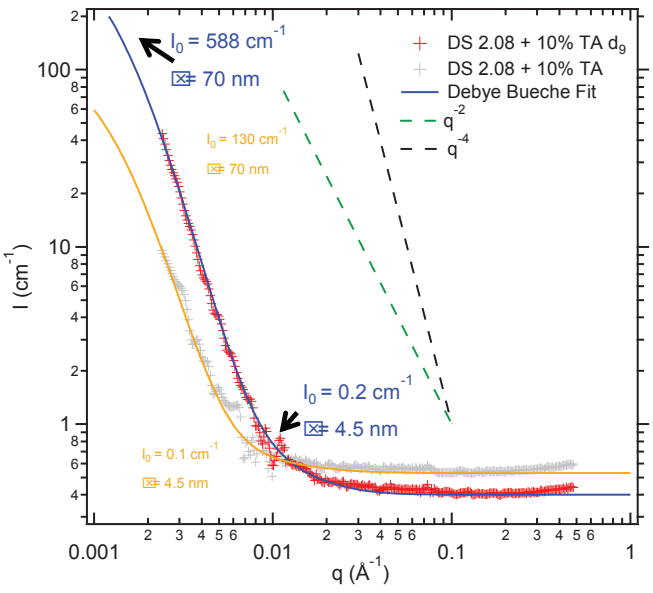

Figure 60: SANS curve of DS 2.08 + 10% TA d_9, fit by two Debye-Bueche distributions and is compared to its protonated sample.

I_0	☒	$(\Delta\rho)^2$	$e_1 e_2$	e_1	e_2
(cm^{-1})	(cm)	(cm^{-4})			
588	7.00E-06	1.88E+20	3.62E-04	0.99963	0.00037
	ρ	% CDA	% TA	% Phase	
Phase 1	1.97E+10	91.5	8.5	99.963	
Phase 2	3.34E+10	0	80	0.037	
I_0	☒	$(\Delta\rho)^2$	$e_1 e_2$	e_1	e_2
(cm^{-1})	(cm)	(cm^{-4})			
0.2	4.50E-07	3.50E+17	2.49E-01	0.5	0.5
	ρ	% CDA	% TA	% Phase	
Phase 1	2.00E+10	92.45	7.55	50	
Phase 2	1.94E+10	90	10	50	

Table 20: Details of calculation for the different distributions of DS 2.08 + 10% TA d_9 (cavities partially filled with plasticizers and calculation for concentration fluctuations near the persistence length scale, respectively).

DS 2.08 + 20% TA d_9 is fit by three Debye-Bueche distributions in Figure 61. According to previous analysis, the humps corresponding to ξ = 56.1 nm, ξ = 7 nm and ξ = 4.5 nm are considered as a result of: cavities, phase separation and concentration fluctuations due to the main cellulosic chains, respectively. The plasticizer filling ratio in cavities remains unknown because of the lack of the protonated result. Phase separation may be observed since the miscibility threshold limit is ~ 20% TA. The related calculations are listed in Table 21.

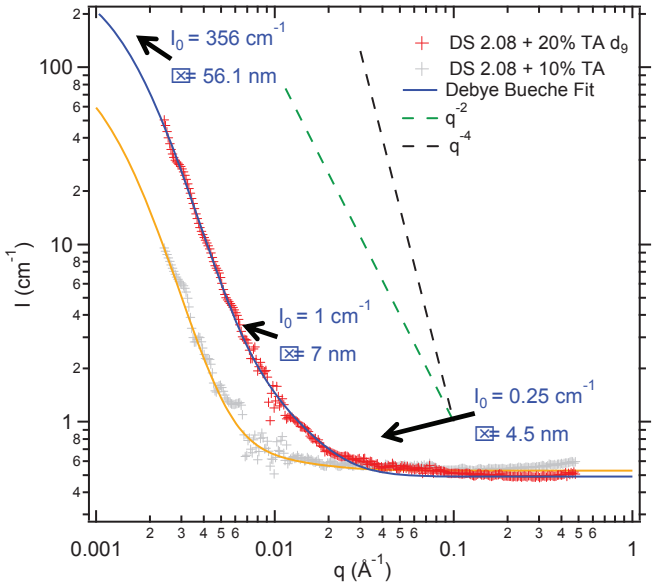

Figure 61: SANS curve of DS 2.08 + 20% TA d_9, fit by three Debye-Bueche distributions.

I_0	ξ	$(\Delta\rho)^2$	$\varepsilon_1\varepsilon_2$	ε_1	ε_2
(cm^{-1})	(cm)	(cm^{-4})			
1	7.00E-07	1.92E+20	6.03E-04	0.99939	0.00061
	ρ	% CDA	% TA	% Phase	
Phase 1	2.13E+10	84.5	15.5	99.939	
Phase 2	3.52E+10	27	73	0.061	
I_0	ξ	$(\Delta\rho)^2$	$\varepsilon_1\varepsilon_2$	ε_1	ε_2
(cm^{-1})	(cm)	(cm^{-4})			
0.25	4.50E-07	4.40E+17	2.48E-01	0.5	0.5
	ρ	% CDA	% TA	% Phase	
Phase 1	2.10E+10	85.75	14.25	50	
Phase 2	2.17E+10	83	17	50	

Table 21: Details of calculation for the different distributions of DS 2.08 + 20% TA d_9 (phase separation and calculation for concentration fluctuations near the persistence length scale, respectively).

DS 2.08 + 40% TA d_9 is fit by three Debye-Bueche distributions in Figure 62.

1. The hump corresponding to ξ = 55 nm is considered as the result of cavities. But the lack of related protonated SANS result keeps us away from determining the plasticizer filling ratio in cavities.

2. The hump corresponding to ξ = 12 nm is attributed to concentration fluctuations due to the main cellulosic chains. It is important to note that the distribution is analyzed by a q^{-2} law, which means this is standard concentration fluctuations in the plasticizer-rich phase. The calculation is listed in Table 22.

3. The hump corresponding to ξ = 0.85 nm is attributed to fluctuations of plasticizer molecules due to the small ξ values.

4. Again, the distribution of phase separation is supposed to be located out of the accessible *q* range.

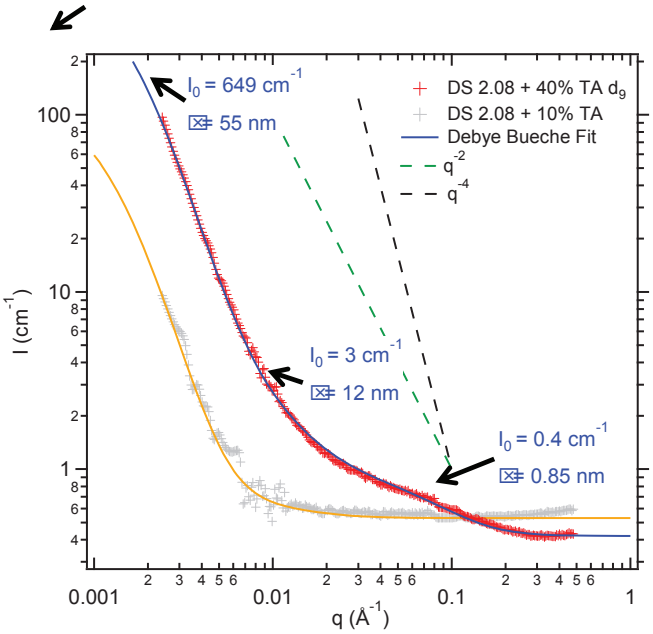

Figure 62: SANS curve of DS 2.08 + 40% TA d_9, fit by three Debye-Bueche distributions.

I_0	☒	$(\Delta\rho)^2$	e_1e_2	e_1	e_2
(cm^{-1})	(cm)	(cm^{-4})			
3	1.20E-06	2.82E+17	2.45E-01	0.5	0.5

	ρ	% CDA	% TA	% Phase
Phase 1	3.74E+10	18	82	50
Phase 2	3.79E+10	15.8	84.2	50

Table 22: Details of calculation for the distributions of DS 2.08 + 40% TA d_9 (calculation for concentration fluctuations near the persistence length scale).

3.3.2.4 – Interpretation on DS 1.83 + TA series

DS 1.83 + 10% TA d_9 is fit by two Debye-Bueche distributions in Figure 63. Its distributions and related fit are much like DS 2.08 + 10% TA d_9.

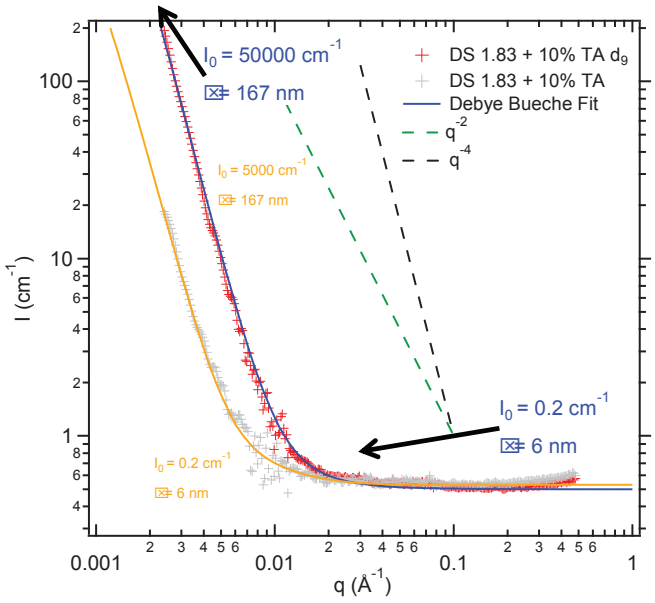

Figure 63: SANS curve of DS 1.83 + 10% TA d_9, fit by two Debye-Bueche distributions and comparison to its protonated sample.

I_0	☒	$(\Delta\rho)^2$	e_1e_2'	e_1'	e_2'
(cm^{-1})	(cm)	(cm^{-4})			
50000	1.67E-05	2.66E+20	1.61E-03	0.99838	0.00162

	ρ	% CDA	% TA	% Phase
Phase 1	2.00E+10	89	11	99.838
Phase 2	3.63E+10	0	87	0.162

I_0	☒	$(\Delta\rho)^2$	e_1e_2'	e_1'	e_2'
(cm^{-1})	(cm)	(cm^{-4})			
0.2	6.00E-07	1.47E+17	2.51E-01	0.5	0.5

	ρ	% CDA	% TA	% Phase
Phase 1	1.97E+10	90	10	50
Phase 2	2.01E+10	88.43	11.57	50

Table 23: Details of calculation for the different distributions of DS 1.83 + 10% TA d_9 (cavities partially filled with plasticizers and calculation for concentration fluctuations near the persistence length scale, respectively).

DS 1.83 + 20% TA d_9 is fit by three Debye-Bueche distributions in Figure 64.

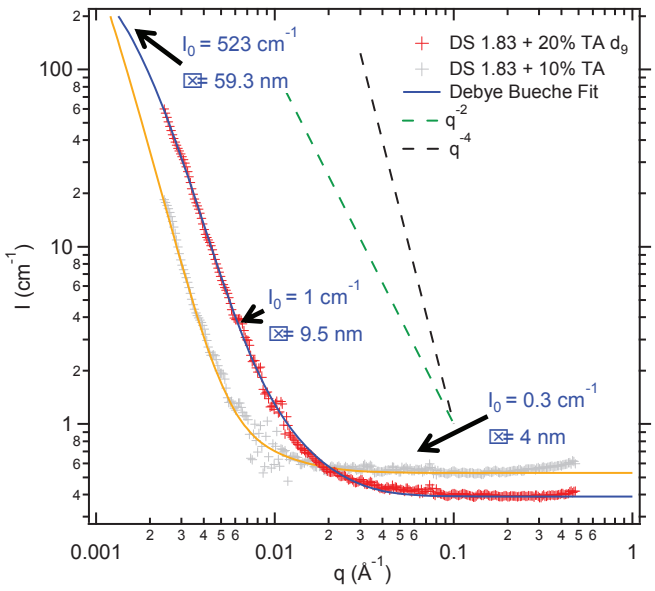

Figure 64: SANS curve of DS 1.83 + 20% TA d_9, fit by three Debye-Bueche distributions.

DS 1.83 + 40% TA d_9 is fit by three Debye-Bueche distributions in Figure 65. Its distributions and related fit are much like DS 2.08 + 40% TA d_9.

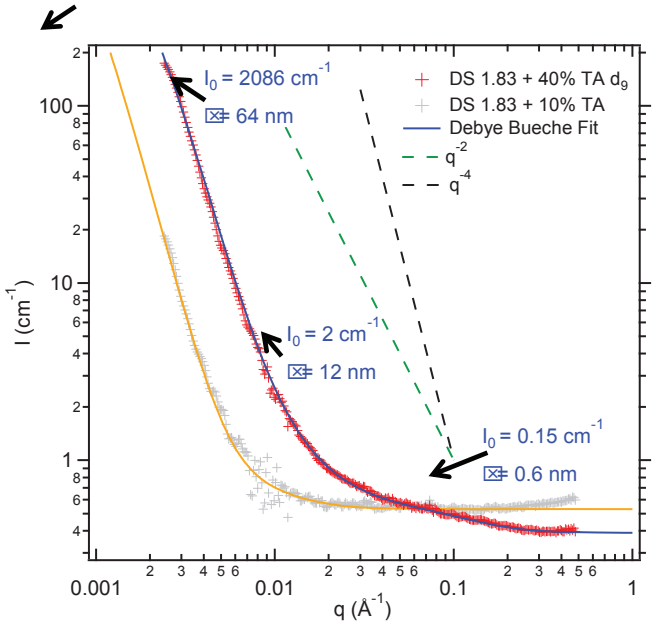

Figure 65: SANS curve of DS 1.83 + 40% TA d_9, fit by three Debye-Bueche distributions.

I_0	ξ	$(\Delta\rho)^2$	$e_1 e_2$	e_1	e_2
(cm^{-1})	(cm)	(cm^{-4})			
2	1.20E-06	1.83E+17	2.52E-01	0.5	0.5

	ρ	% CDA	% TA	% Phase
Phase 1	3.69E+10	19.75	80.25	50
Phase 2	3.73E+10	18	82	50

Table 24: Details of calculation for the different distributions of DS 1.83 + 40% TA d_9 (calculation for concentration fluctuations near the persistence length scale).

Conclusions

Neutron scattering technique has been used to gain insight into miscibility behavior of plasticized CDA. Our analysis is concentrated on plasticized DS 2.45 series from which we are able to propose the first interpretations (Table 25):

At q ≈ 0.1 Å^{-1} **(small ☒values)** High plasticizer content	Options are limited due to restricted ☒values. It is attributed to deuterated plasticizer molecules. The amplitude of the contribution is consistent with this hypothesis.
At q ≈ 0.01 Å^{-1} **(medium ☒values)**	☒is related to persistence length of cellulose acetate (≈ 10 nm). In this characteristic size domain, CDA is in excess which means fluctuations of concentration. The phenomenon is actually similar to phase separation. At high plasticizer content, slope is q^{-2}.
At q ≈ 0.01 Å^{-1} **(medium ☒values)** Phase separation limit	Phase separation phenomenon Only applicable for 20% TA and 20% DEP samples
At q ≈ 0.003 Å^{-1} **(large ☒values)**	Cavities partially filled with or without deuterated plasticizers Plasticizer filling ratio can be calculated if data from protonated systems are available.
At q < 0.003 Å^{-1} **(very large ☒values)** High plasticizer content	Phase separation phenomenon No precise data can be obtained since we do not have enough information from SANS curves, the corresponding signal being out of the experimental range.

Table 25: Resume of neutron scattering analysis

It is feasible to work with Ultra-Small Angle Neutron Scattering (USANS) with $q \sim 10^{-4}$ Å^{-1}. The measurement will be extremely interesting because we may have a chance to see phase separation at µm scale. Otherwise, it is also important to complete neutron scattering analysis of other DS in the standard q range. Another interesting technique to be considered is Light Scattering (LS). It can also provide information on the µm scale.

CHAPTER 4

STRUCTURAL PROPERTIES OF PLASTICIZED CELLULOSE ACETATE

Cellulose acetate is an amorphous polymer with the exception of cellulose triacetate (CTA, DS = 3), which is a semi-crystalline polymer. Detailed X-Ray Diffraction (XRD) research of cellulose triacetate was reported in the literature (*Boy et al. 1967, Roche et al. 1978, Fawcett et al. 2013*). Few amorphous cellulose acetate data is available for structural analysis. In the scope of the present work, XRD study is carried out to achieve the following goals:

- Occurring of crystallinity (to confirm the one revealed by thermal analysis).
- Structural analysis of unplasticized cellulose acetate.
- Influence of plasticizer on structural properties of cellulose acetate with various degrees of substitution.

Structure analysis of cellulose acetate is based on results from X-ray diffraction method. Result description is referred to available conformational knowledge of cellulose acetate, such as interaction lengths and angles, chain arrangements or molecular orientations. Useful information is listed below:

- Cellulose acetate with DS 1.75 – 2.5 (produced by deacetylation of cellulose triacetate) exhibits partially crystalline structures (*Kamide and Saito 1985*). The related powder X-ray patterns suggest the crystal form of secondary cellulose acetate coming from CTA II, such as Figure 68.
- The crystalline domains of cellulose acetate with DS 2.5 consist of parts of neighboring chains containing sequences made of several trisubstituted anhydroglucose units (AGU).
- The segmental length of cellulose acetate is known as 19 anhydroglucose units on the average for DS 2.5 (*Kamide, 2005*). The length scale of one AGU unit is ~0.5 nm, which results the persistence length (l_p) of ~10 nm for DS 2.5.

- It should be pointed out that cellulose acetate with low DS does not show crystalline order, which requires three-dimensional periodicity. Meanwhile, two-dimensional orientation correlation (such as liquid crystal) is proven to be present.

4.1 – Degree of crystallinity of cellulose acetate

Contrary to the MDSC measurement which allows us to calculate the degree of crystallinity for certain plasticized CDAs, the XRD technique fails to give such a quantitative analysis because of limited experimental conditions and data. No background reference (i.e. diffractogram of a totally amorphous cellulose acetate) is available for peak deconvolution.

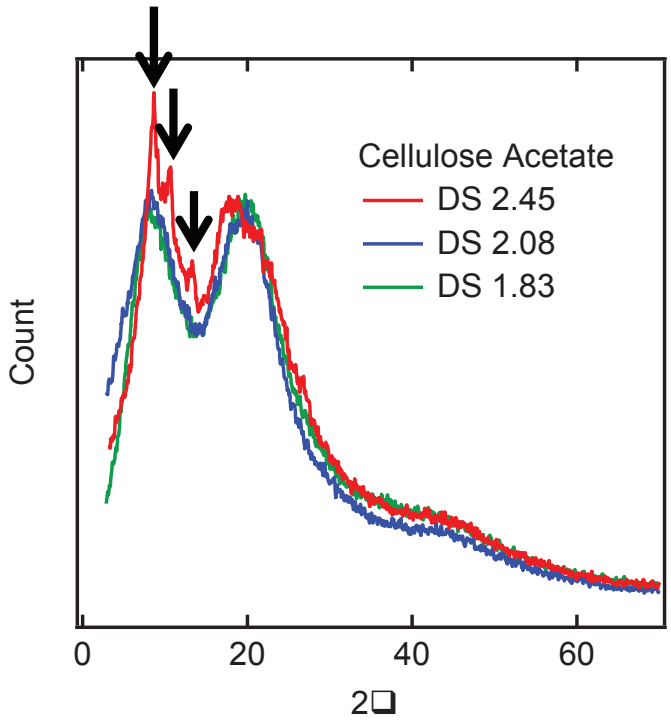

Figure 66: X-ray diffractogram of cellulose acetates (DS 1.83, DS 2.08 and DS 2.45). Relative intensities are normalized according to the second amorphous peak at $2\theta = 20°$.

Degree of crystallinity (χ_c) is 9 ~ 16% for the unplasticized cellulose acetate (DS 2.45), according to the thermal analysis (Chapter 3.1). Three transitions which represent crystalline phase are identified in DS 2.45 (Figure 66). Their intensities are so weak that they cover only ~10% of the total diffractogram area. This observation means that disorder prevails among polymer chains. As shown in the same figure, cellulose acetates with DS 1.83 and DS 2.08 are totally amorphous, as no specific transitions can be clearly identified for both of them.

XRD result of cellulose acetates is predictable: hydrolysis of cellulose triacetate is the second step of acetylation process. The process is heterogeneous: i.e. the substitution of acetyl side groups is not controlled. Eight possible anhydroglucose units may be found in the same cellulose acetate (see Figure 3 in Chapter 1). For example, the average number of acetyl groups per anhydroglucose unit is 2.45 for cellulose acetate (DS 2.45). In fact, DS 2.45 is composed of at least 50% of CTA monomer. Due to important amount of CTA monomer, micro-crystalline systems may be formed, which results in a certain degree of crystallinity. DS 1.83 and DS 2.08 are composed of less CTA monomer, which results a 100% amorphous state.

4.2 – Structural analysis of unplasticized cellulose acetate

The International Centre for Diffraction Data (ICDD) gathers a collection of XRD results of cellulose and its derivatives (*Fawcett et al. 2013*). However, related analysis and interpretation are still limited. Our objective is to realize a preliminary structural analysis of cellulose acetate in amorphous state. ICDD data will be served as useful reference. *Bocahut et al. 2014* propose amorphous models of cellulose acetate and molecular dynamics simulation is able to calculate its characteristic length scales, regarded as a theoretical reference.

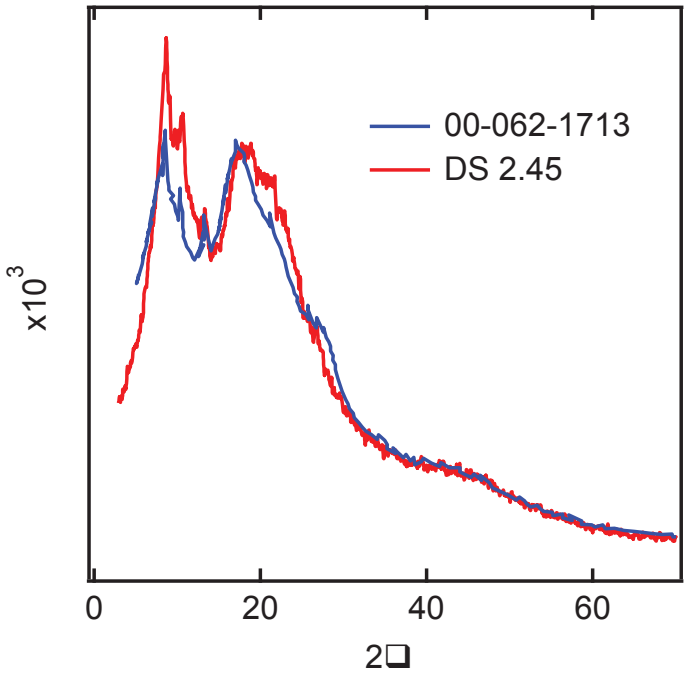

Figure 67: Reference: ICDD Powder Diffraction File N° 00-062-1713 of cellulose acetate (pharmaceutical reference standard) against our experimental DS 2.45. Relative intensities are normalized according to the second amorphous peak at 2θ = 20°.

ICDD Powder Diffraction File (PDF) N° 00-062-1713 is the X-ray diffractogram of commercial cellulose acetate (DS 2.5, United States Pharmacopeia grade). Its relative intensity is normalized with that of unplasticized DS 2.45 according to the second amorphous hump at 2θ = 20° (Figure 67).

Transitions which represent crystalline phase at d-spacing distances: d = 6.7, 8.4 and 10.4 Å are identified using literature data of the crystalline phase of cellulose triacetate (CTA II) as reference. Amorphous phase is the one that manifests no long-range intermolecular order. But short-range inter- or intra-molecular order may exist which leads to weak X-ray scattering intensity and broad background signal. Three amorphous humps are noted (Figure 68):

1) Hump at 2θ ≈ 10° should be originated from short-range intermolecular order of amorphous phase. Its d-spacing distance (9 ~ 10 Å) is the characteristic distance of two neighboring cellulosic chains.
2) Hump at 2θ ≈ 20° should be related to intramolecular order of amorphous phase. Its d-spacing distance (4 ~ 5.5 Å) is the characteristic distance of two neighboring anhydroglucose units.
3) Hump at 2θ ≈ 40° corresponds to a d-spacing distance of 2 ~ 3 Å. It is supposed to be related to short-range intramolecular order, i.e. hydrogen bonding.

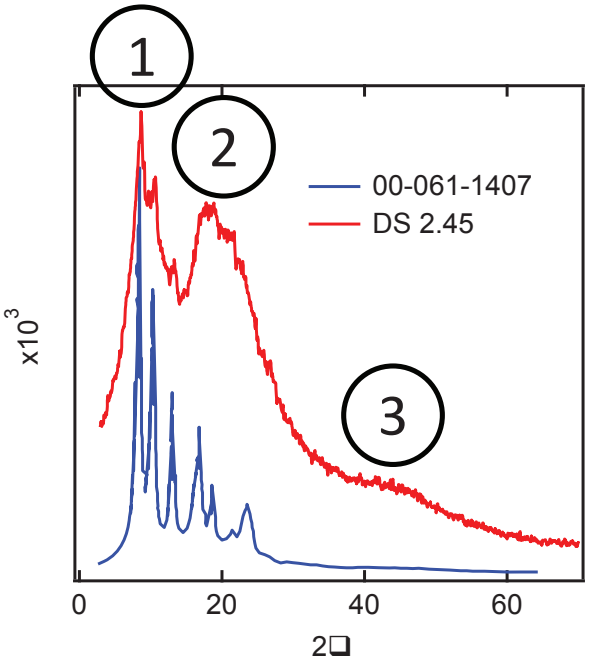

Material	a (Å)	b (Å)	c (Å)
CTA II	11.53	24.69	10.54
Space Group	♋	♌	♑
$P2_12_12_1$	90°	90°	90°

2❑	d (Å)	h	k	l
8.449	10.46	1	1	0
10.449	8.46	2	1	0
13.184	6.71	3	1	0

Figure 68: X-ray diffractogram of cellulose acetate (DS 2.45) compared to the reference: ICDD Powder Diffraction File N° 00-061-1407 of cellulose triacetate (polymorph CTA II). Right: calculations of crystalline transitions and related Miller indices.

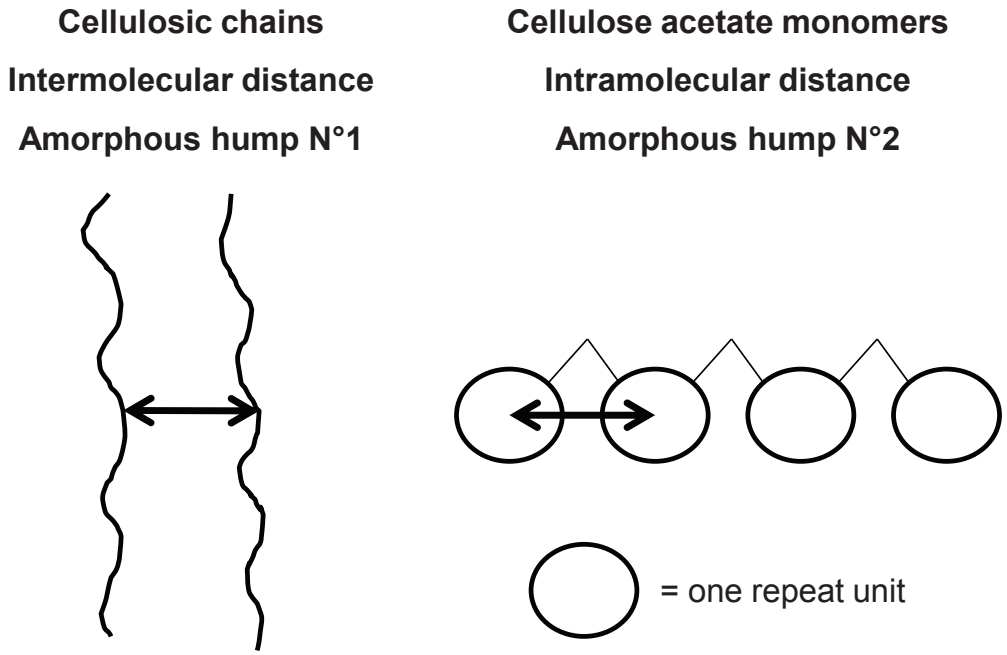

Figure 69: Illustrations of inter- (Left) and intra (Right)-molecular distances of cellulose acetate.

An X-ray diffractogram example of cellulose triacetate (polymorph CTA II, Powder Diffraction File N° 00-061-1407) is recorded in ICDD database (Figure 68). Crystalline transitions of cellulose acetate (DS 2.45) are identified on the basis of this reference. CTA II is a well-established polymorph of cellulose triacetate. Unit cell proposed by *Roche et al. 1978* is commonly accepted and applied as the reference. As a result, crystal structure of DS 2.45 can now be calculated, including its Miller indices (Table in Figure 68). Considering the original weak intensities observed in CTA II, extra crystalline transitions should not be excluded from our DS 2.45 sample because some of them could probably be hindered under strong amorphous background signal.

4.3 – Influence of plasticizer on structural properties of amorphous cellulose acetate

Plasticization of cellulose acetate (DS 2.45) takes place and its crystalline phase disappears with increasing plasticizer content (Figure 70). Micro-crystalline blocks of cellulose triacetate are supposed to be the origin of this crystalline phase and are probably located at random in an amorphous background in DS 2.45. When plasticizer interacts with the polymer chains, the CTA blocks are more or less affected even disrupted.

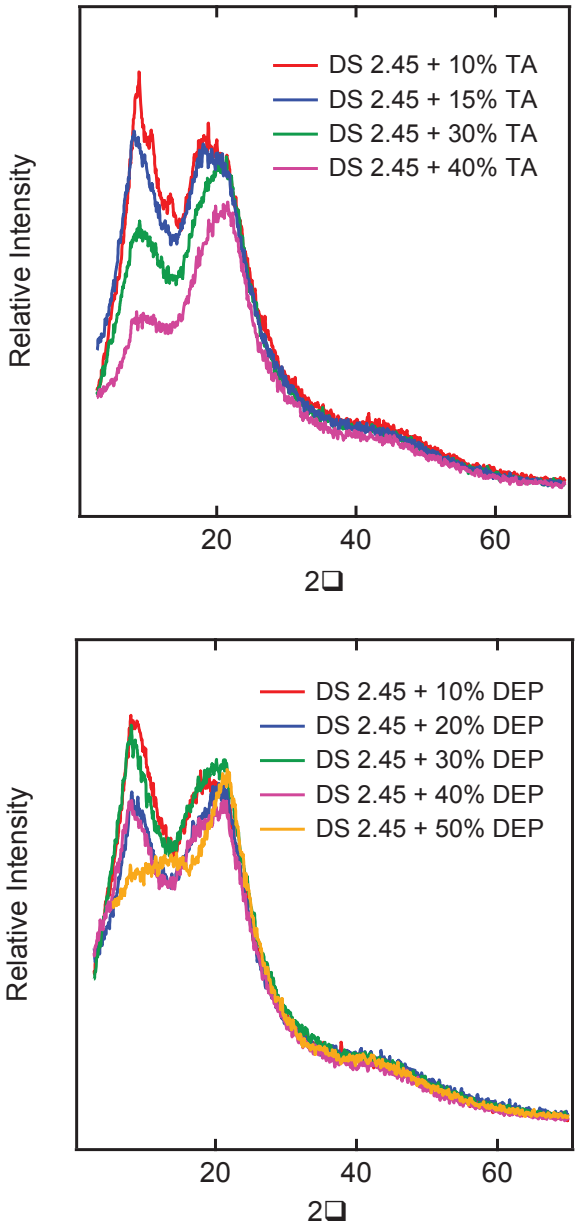

Figure 70: X-ray diffractogram of plasticized DS 2.45 series .Top: Influence of TA on structure properties of cellulose acetate. Bottom: Influence of DEP on structure properties of cellulose acetate.

The size and the number of micro-crystalline blocks are the reasons why plasticizer is able to “dissolve” the crystalline phase. These nm-scale blocks are much easier to disrupt than a complete crystalline system. Crystalline peaks of TA-plasticized DS 2.45 are reduced progressively and disappeared, which illustrates the influence of plasticizer on the crystalline phase of cellulose acetate.

The first amorphous hump at $2\theta \approx 10°$ is supposed to be originated from an intermolecular order, i.e. the characteristic distance of two neighboring cellulosic chains. It is the most affected amorphous hump by the plasticization effect: the role of plasticizer is to break the inter-molecular H-bonds of cellulose acetate and to interact itself with cellulose acetate. Thus, the intermolecular distance between the chains that compose the plasticized system must have been changed and become heterogeneous. This explains why the relative intensity of the hump decreases with increasing plasticizer content.

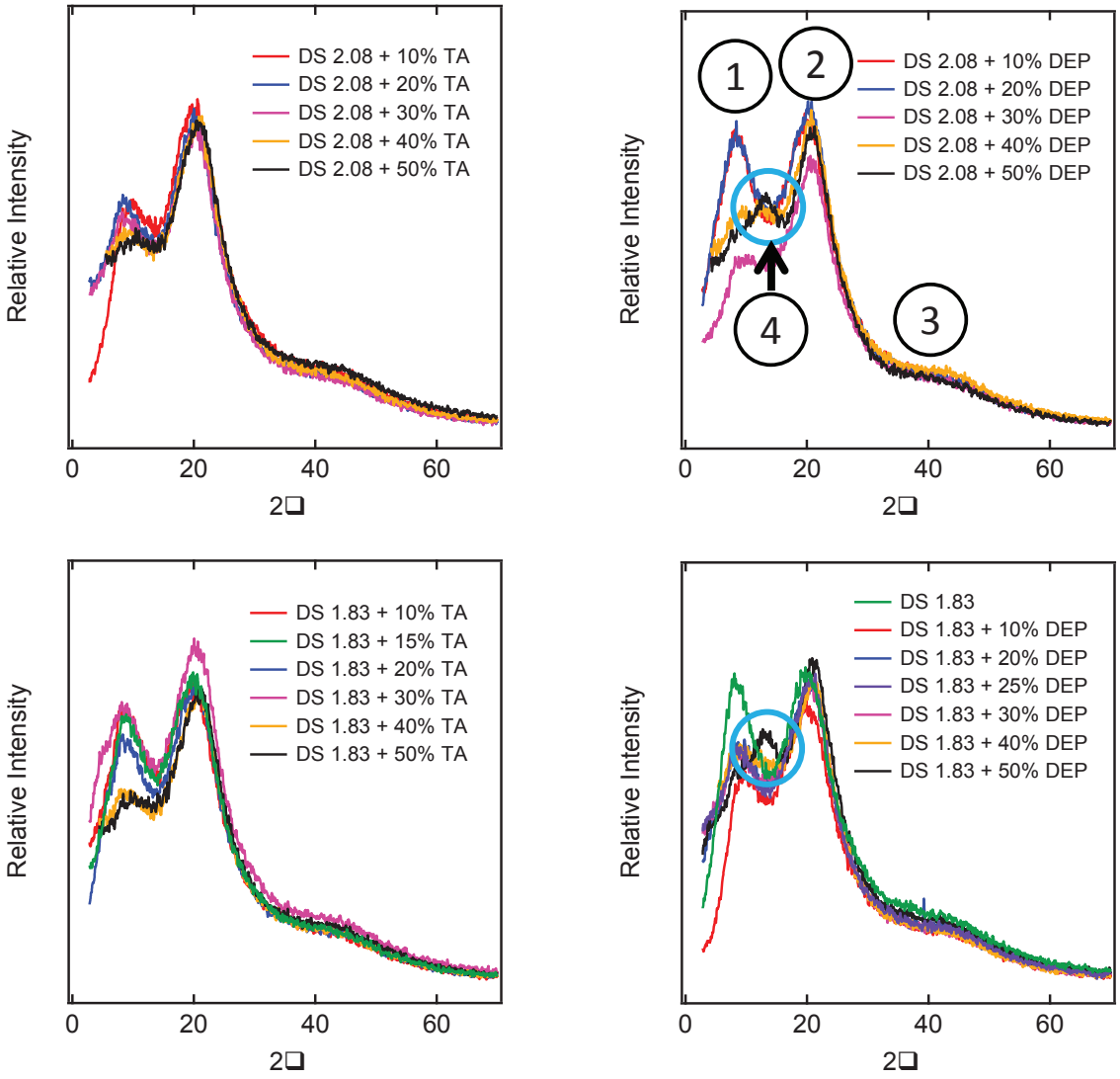

Figure 71: Top - X-ray diffractogram of plasticized DS 2.08 series. Blue circle indicates the hump related to cavities partially filled with plasticizer molecules. Bottom - X-ray diffractogram of plasticized DS 1.83 series. Four amorphous humps are numerated as indicated in the report.

It is not yet clear why the influence of plasticizer is different on the diffractograms of the 3 DS: as one can be seen in Figure 70 and 71, the amplitude of relative intensities of 3 DS series with increasing plasticizer contents is at random. Nevertheless, highly plasticized cellulose acetates have weaker relative intensities at the first amorphous hump ($2\theta \approx 10°$) than the ones with low plasticizer contents. And it is true for all XRD analysis. This observation is supposed to be related to the fact that more and more plasticizer molecules enter into cellulose acetate's system with increasing plasticizer content. Their presence can create disorder of the polymer chains and thus mask the regular periodicity of cellulose acetate.

Another important point is the discovery of a fourth amorphous hump at $2\theta \approx 13°$ at high DEP plasticizer content in DS 1.83 and DS 2.08. Its related interpretation is based on results from thermal and thermo-mechanical measurements. The position of this fourth amorphous hump is coincident with the interpretation of the third T_g observed by the MDSC analysis, which we assigned to the main transition of pure DEP. Theoretical calculations (performed as follows) can reinforce such an interpretation: the fourth amorphous hump is found at $2\theta \approx 13°$, which corresponds to a characteristic length of 6.7 Å. Knowing the physical properties of DEP (molecular weight = 222 $g.mol^{-1}$ and density = 1.12 $g.cm^{-3}$), we can deduce: its molecular volume = $222/(1.12*N_A) = 330*10^{-24}$ cm^3 (if each molecule is considered as a cube). Upon this assumption, theoretical distance between two neighboring DEP molecules is $(\text{molecular volume})^{1/3} \approx 6{,}9$ Å. It is therefore a good match between theoretical and experimental values. In conclusion, the fourth hump could be attributed to the characteristic order of DEP molecules due to the existence of cavities.

The second and third amorphous humps are barely affected by the presence of plasticizer. It is a reasonable consequence for intramolecular order (i.e. the second hump) because plasticizer cannot change the structural nature of cellulose acetate. However, since the third hump is assumed to be related to H-bonds, no interpretation is yet available about its apparently constant position with different plasticizer contents: as both TA and DEP are known to be able to change dramatically the H-bonding polymer network and have an effect on its corresponding hump, its interpretation needs to be challenged.

4.4 – Conclusions

XRD study investigates on the structural properties of plasticized cellulose acetates. The influence of DS, of plasticizers and of plasticizer content is shown in the chapter. An analysis is realized on the different crystalline transitions and amorphous humps of plasticized CDAs. A fourth amorphous hump is attributed to the DEP molecules, which is equivalent to the identification of the third T_g in MDSC measurement. The next step of the structural study of plasticized CDAs should be the study of possible orientation preference in the polymer by using X-Ray transmission mode or other characterizations and its influence on the optical properties of the plasticized CDAs.

CHAPTER 5

DYNAMIC PROPERTIES OF PLASTICIZED CELLULOSE ACETATE

Chapter 5 is dedicated to the study of dynamic properties of plasticized cellulose acetate. In Chapter 3.2, a preliminary study of dynamic transitions is done using thermo-mechanical results at frequency 1 Hz. As a reminder, four transitions are identified and denoted α, β^*, β and γ from higher to lower temperatures. In this chapter, results from Broadband Dielectric Spectroscopy (BDS) are added to thermo-mechanical results in order to achieve reliable interpretations on dynamic behavior and molecular motions of each transition. Note that a summary of the relaxations observed through BDS experiments is given in a specific table at the end of the chapter (Table 29). Prior to analysis, a survey of the literature is proposed.

BDS can be used to investigate molecular motions in a wide range of frequencies, when dipoles are coupled to the applied electric field. Rotations of acetyl side groups and hydroxyl groups are the first two possibilities. Rotations of glucosidic linkage (Φ and Ψ angles) between AGU units can be the third proposition. Other internal motions include: chair-boat interconversion of the pyranose ring (the interconversion passes through different intermediate geometries of the pyranose ring, which is called as "Puckering Effect".), vibrations of cellulose acetate chain (several AGU units involved, exemplifying a possible local chain motion), etc. In Figure 72, the above molecular motions are represented in simplified schemes.

According to characteristics of different transitions, the above molecular motions are discussed and analyzed one after another in following sub-chapters. Same list of molecular motions is applicable for dynamic mechanical measurements. It may be possible that the molecular response during mechanical or dielectric solicitation is different: relaxation may be observed in one experiment but not in another because the amplitude of the response to the solicitation is too small.

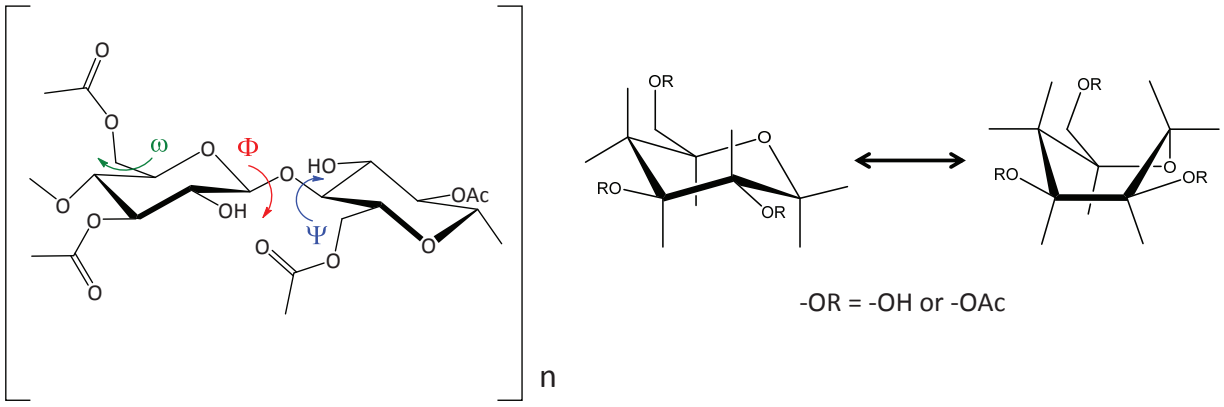

Figure 72: Left - Representation of rotation of acetyl side groups (ω) and rotations of O-glucosidic linkage (Φ and Ψ) in cellulose acetate chain conformation. Right - Simplified representation of chair-boat interconversion of the pyranose ring.

5.1 – Literature review: dielectric studies of cellulose acetate or related polymers

Dielectric studies on different polysaccharides were reported in the literature, but mainly for secondary relaxations (*Seymour et al. 1979, Doyle & Pethrick, 1992, McBrierty et al. 1996, Einfeldt et al. 2001, Jafarpour et al. 2007, Kaminski 2012, Kaminski et al. 2008 and 2009, Laredo et al. 2009, Montès et al. 1997 and 1998, Sousa et al. 2010, Kusumi et al. 2011, Roig et al. 2011*). Low frequency studies on cellulose acetates are difficult because of conductivity. Most of these dielectric studies however have been focused on cellulose and its derivatives, and only few results have been reported about dielectric properties of plasticized cellulose acetate systems. *Seymour et al. 1979* focused on phthalate plasticizers such as dioctyl phthalate and diphenyl phthalate. *McBrierty et al. 1996* studied the dynamics of cellulose acetate with 26% diethyl phthalate.

The dielectric constant of cellulose acetate (CDA) has been found to be comprised between 4 and 6 (*Rustemeyer, 2004*), depending on the applied frequency. The dielectric constants of dibutyl phthalate (6.4) and dimethyl phthalate (8.5) have been reported (*Maryott, 1951, Aminabhavi et al. 1993*), which should provide a lower and upper bound for that of diethyl phthalate. And the dielectric constant of triacetin varies between 6 and 10, according to *Ikada and Watanabe 1974* (other information available in *Chen and Wang 2012*). Therefore, both the polymer and the plasticizers should answer to dielectric measurement. Table 26 summarizes propositions of molecular origins of β- and γ-relaxations of cellulose acetate or related polysaccharides by different authors. The review about possible molecular motion of γ-relaxation can be found in Chapter 3.2. Molecular origin of γ-relaxation should be one of the following propositions: rotations of acetyl side groups, rotations of remaining hydroxyl groups and molecular motions of water, etc.

Authors	Saccharide	Molecular origins of the slower secondary relaxation process (denoted as β relaxation)	Molecular origins of the faster secondary relaxation process (denoted as γ relaxation)
K. Kaminski et al. 2009	Polysaccharides	β relaxation process is closely connected to the motion of the monomeric units via glycosidic linkage, a kind of local main chain motion, and can be identified with the JG relaxation of the polysaccharides that has strong connection to the structural α-relaxation.	This process has intramolecular character and is related to the motion within the monomeric unit building the polysaccharide
R. W. Seymour et al. 1979	Cellulose esters	Motion of the anhydroglucose ring	
V. J. McBrierty et al. 1996	Cellulose acetate	Involving coorperative motionof the polar side groups and the sugar rings in the main chain	The glass transition of tightly bound water
M. Scandola et al. 1985	Cellulose acetate	Local motions of the main chain (glucopyranose rings)	Water associated with the unesterified methylol groups of cellulose acetate is responsible of the relaxation
M. Sousa et al. 2010	Cellulose acetate	Associated with side-group rotations but strongly correlated with the cyclic unit motion	A join effect of the cyclic unit motion and the polar groups that reorientate coupled to it A very limited length scale A low entropic contribution
J. Einfeldt et al. 2001	Cellulose acetate	Motion of a monomeric unit	2 Side group motions (2,3-O-Ac and 6-O-Ac)
H. Montès et al. 1997	Cellulose	β relaxation has considerable activation entropy, and it is associated to localized motion of the main chain; in addition, they showed that four glycosidic bonds are involved in the local chain motion but cautioned that the actual number can be smaller because ΔE_2 was obtained without taking into account the intermolecular effect in the computer simulation	γ relaxation does not involve a significant entropic contribution and originates from the rotation of the methylol group in the anhydroglucose unit
F. Roig et al. 2011	Cellulose	The mobility of cellulose backbone	The molecular mobility of the side groups of glycosidic rings Water acts as an anti-plasticizer
J. B. Gonzalez-Campos et al. 2009	Chitosan	Related to side group motions by means of the glucosidic linkage	

Table 26: Summary of the molecular origins proposed by different authors for the secondary relaxations of cellulose acetate/polysaccharides (Kaminski et al. 2009)

Contrary to γ-relaxation, β-relaxation is much less affected by the presence of water. According to the summary made by *Sousa et al. 2010*, the activation energy of β-relaxation should be found between 76 and 85 kJ.mol^{-1}. In the literature, β-relaxation process is always related to motions of anhydroglucose rings. However, several possibilities were discussed during the last decades.

- In the case of cellulose, *Montès et al. 1997* concluded that β-relaxation should be associated with approximately four glycosidic linkages of the main chain, a result of computer simulation. Their computer simulations of amorphous cellulose show that the rotation of glucose rings around a single β-(1-4) glycosidic linkage has an energetic barrier in the order of 20 kJ.mol^{-1}. When comparing this result to the measured activation energy of the β-relaxation (≈ 85 kJ.mol^{-1}), they estimated that four glycosidic bonds are involved in the local chain motion but cautioned that the actual number can be smaller because the energetic barrier was calculated without taking into account the intermolecular effect in the computer simulation.

- *Kaminski et al. 2009* propose that the β-relaxation has a strong connection to the structural primary relaxation. Other authors (*Einfeldt et al. 2001, Sousa et al. 2010*) mentioned the extreme short pre-exponential factor of the β-relaxation. They were convinced that the molecular origin of the β-relaxation involved cooperative motions of the polar side groups and the sugar rings in the main chain. This proposal is based on the Eyring theory and the work of Starkweather 1988. Details of theory could be found in Chapter 3.2. The authors consider that the very large pre-exponential factor of the Arrhenius equation is the result of some entropic contributions, which are related to some cooperativity of an orientational motion within dipolar groups. As in cellulose acetate system, the possible cooperativity between two different molecular motions was quite limited. In general, this cooperative effect was attributed to the cooperative motion of the polar side groups and the sugar rings in the main chain.

α-relaxation of cellulose acetate is difficult to be measured by dielectric experiments. *McBrierty et al. 1996* and *Kusumi et al. 2011* are one of the few authors who reported the α-relaxation of plasticized cellulose acetate (Figure 73). *McBrierty et al. 1996* described the α-relaxation behavior of unplasticized and plasticized cellulose acetate with 26% DEP content. *Kusumi et al. 2011* studied the α-relaxation behavior of poly (ε-caprolactone)-grafted cellulose acetate. The above articles are the only references in which α-relaxation results are available.

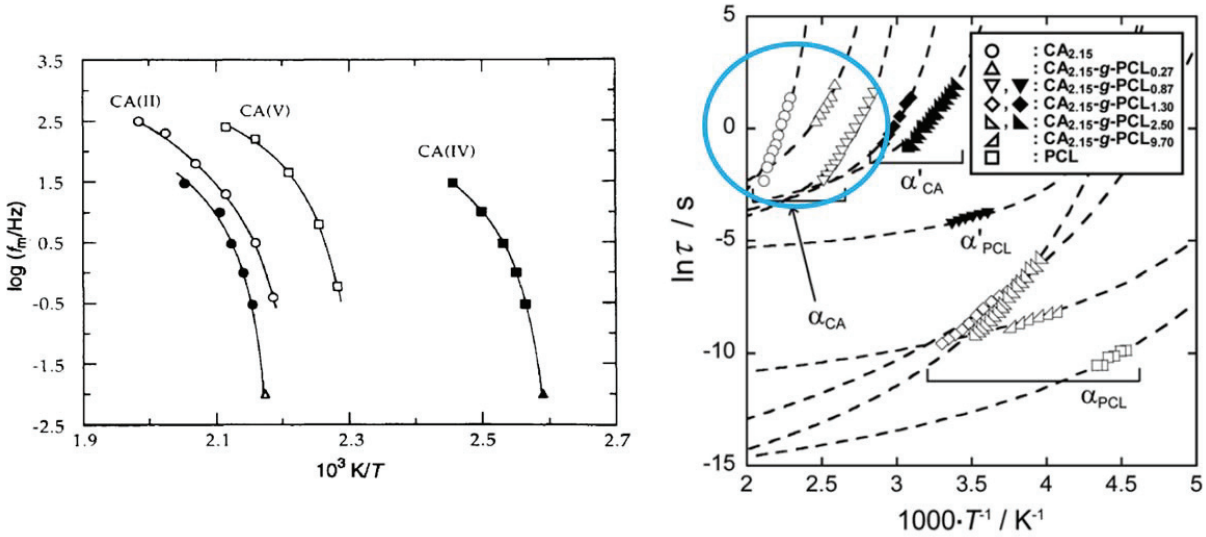

Figure 73: Left - α-relaxation behavior of unplasticized and plasticized cellulose acetates (from McBrierty et al. 1996). Right - α-relaxation behavior of unplasticized and plasticized cellulose acetates (from Kusumi et al. 2011).

5.2 – Identification and interpretations of dynamic relaxations

5.2.1 – General feature of dielectric results of plasticized cellulose acetate

In Figure 74, dielectric results of plasticized cellulose acetate are illustrated with 3D representations. We have identified three secondary transitions and three primary α-transitions in dielectric spectra (from lower to higher temperatures):

- **γ'-relaxation**: low-temperature secondary transition, only occurring for DEP-plasticized systems, supposed to be the secondary relaxation of DEP molecules
- **γ-relaxation**: "simple" secondary transition, supposed to be rotations of acetyl side groups of cellulose acetate
- **α"-relaxation**: glass transition of DEP phase (only available in highly plasticized DS 1.83 and DS 2.08)
- **β-relaxation**: complex secondary transition of plasticized cellulose acetate
- **α'-relaxation**: glass transition of plasticizer-rich phase after phase separation
- **α-relaxation**: main glass transition of plasticized cellulose acetate or glass transition of CDA-rich phase after phase separation

Note that γ-and γ'-relaxations are not observed in thermo-mechanical analysis. In this subchapter, interpretations of dynamic relaxations are discussed in the same order as that presented above.

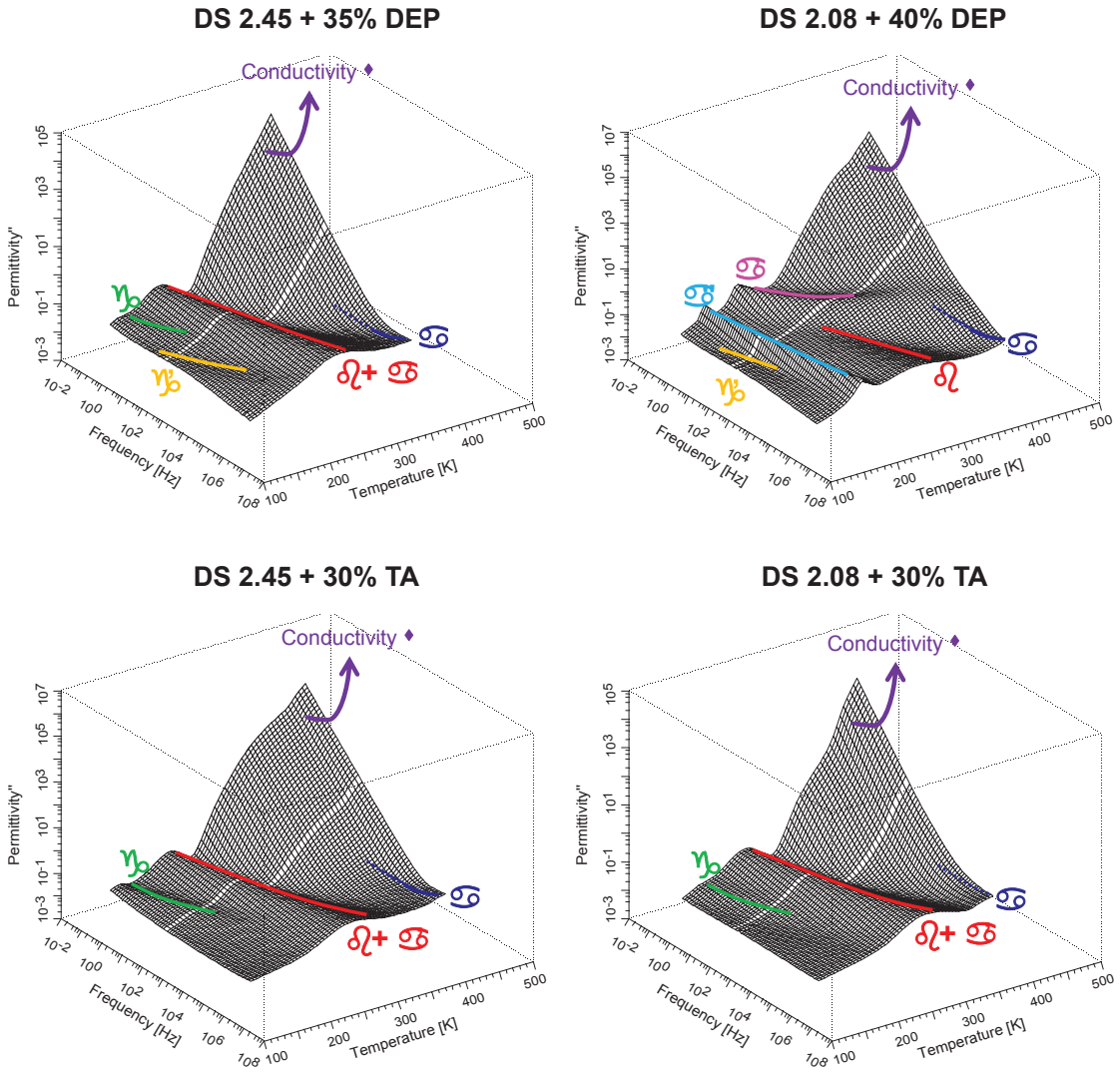

Figure 74: Top - 3D representation of dielectric spectra of DEP-plasticized cellulose acetate with DS 2.08 and DS 2.45. Bottom - 3D representation of dielectric spectra of TA-plasticized cellulose acetate with DS 2.08 and DS 2.45. Plasticized DS 1.83 series are similar to the plasticized DS 2.08 series.

5.2.2 – α''-relaxation and γ'-relaxation

As concluded in Chapter 3, the major discovery of DEP-plasticized DS 1.83 and DS 2.08 series is the third glass transition related to DEP molecules. It is also observed in BDS measurement and is denoted α''-relaxation (Figure 75 left). With the presence of α''-relaxation in highly plasticized DS 1.83 and DS 2.08, γ-relaxation is masked.

The relaxation behavior of α"-relaxation is compared to that of α-relaxation of pure DEP liquid (*Pawlus et al. 2003*) in Figure 76. As shown in the figure, α"-relaxation of three different CDA samples are plotted together. In the accessible temperature/frequency range, the relaxation behavior of α"-relaxation is much like that of α-relaxation of pure DEP. Minor difference is considered as a result of environmental background effect (e.g. influence of plasticized cellulose acetate backbone). Consequently, α"-relaxation is confirmed as the glass transition of DEP molecules by three different characterizations (MDSC, DMTA and BDS).

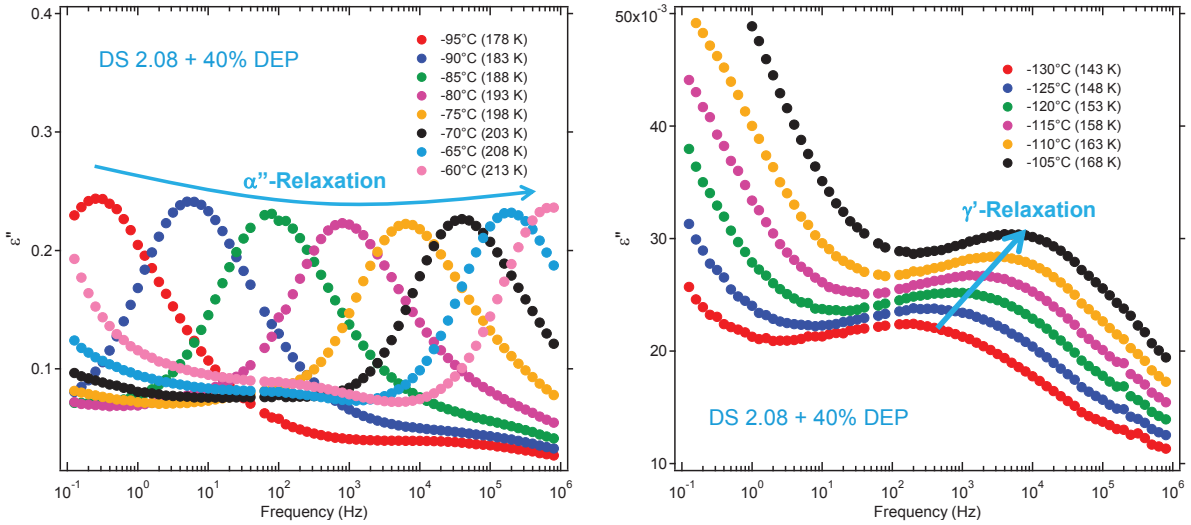

Figure 75: Left - Frequency dependence of the imaginary part of the complex dielectric permittivity (ε") from 178 to 213 K in steps of 5 K, for α"-relaxation of DS 2.08 + 40% DEP. Right - Frequency dependence of the imaginary part of the complex dielectric permittivity (ε") from 143 to 168 K in steps of 5 K, for γ'-relaxation of DS 2.08 + 40% DEP.

γ'-relaxation is a secondary transition only detected in DEP-plasticized cellulose acetates (Figure 75 right). To the best of our knowledge, no related literature record is found in analogous systems. It is for sure a DEP-dependent transition. In Figure 76, the relaxation behavior of γ'-relaxation is compared to that of β-relaxation of pure DEP liquid (*Pawlus et al. 2003*). Strong similarity is found between our experimental results and the literature data. Furthermore, the activation energy (E_a) and pre-exponential factor (log τ_0) calculated from the Arrhenius Equation are also consistent with the literature data (Table 27). *Hensel-Bielowka et al. 2004* determined the mean activation energy of β-relaxation of DEP as 3395 K, which is equal to 28.20 kJ.mol^{-1} (see Appendix IV for calculation). Thus, γ'-relaxation is believed to be the secondary relaxation of DEP molecules.

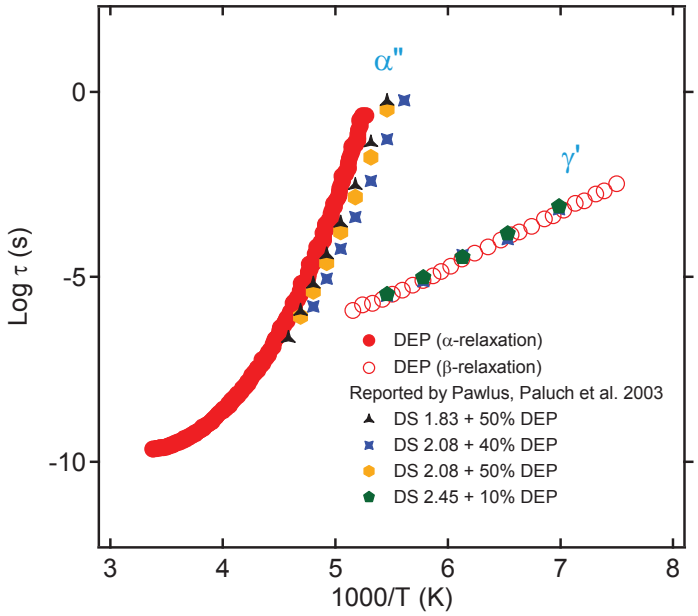

Figure 76: Evolution of α"-relaxation and γ'-relaxation with increasing DEP content in plasticized cellulose acetate. Comparison with literature results of pure DEP liquid from Pawlus et al. 2003.

5.2.3 – β-relaxation and γ-relaxation

Frequency dependence of the imaginary part of the complex dielectric permittivity (ε") for β-relaxation and γ-relaxation is shown in Figure 77. The two secondary transitions have been one of the unsolved topics in cellulosic study for a long time.

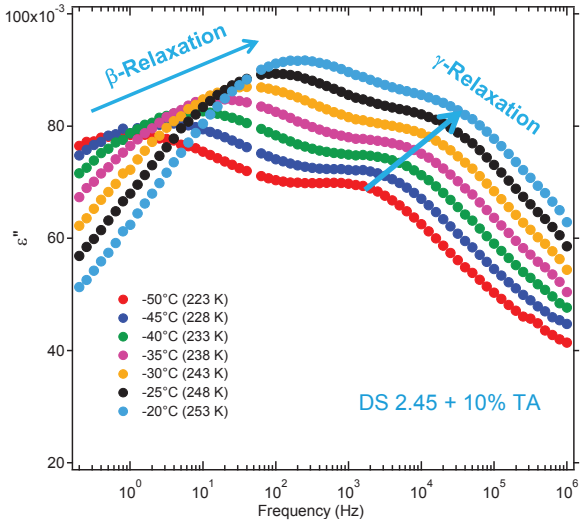

Figure 77: Frequency dependence of the imaginary part of the complex dielectric permittivity (ε") from 223 to 253 K in steps of 5 K, for β-relaxation and γ-relaxation of DS 2.45 + 10% TA.

	♌		♑		♑'	
	E_a (kJ/mol)	Log f_0	E_a (kJ/mol)	Log f_0	E_a (kJ/mol)	Log f_0
DS 1.83 + 10% TA	81	-19.4	50	-16.2		
DS 1.83 + 20% TA	118	-26.7	61	-18.8		
DS 1.83 + 30% TA	144	-32.1				
DS 1.83 + 40% TA	158	-36.1				
DS 1.83 + 50% TA	163	-38.5				
DS 1.83 + 10% DEP	79	-19.1	55	-17.0	25	-12.4
DS 1.83 + 20% DEP	88	-21.9	53	-16.6	31	-14.2
DS 1.83 + 25% DEP	100	-24.5			28	-13.5
DS 1.83 + 30% DEP	117	-28.7			30	-14.0
DS 1.83 + 40% DEP					28	-13.6
DS 1.83 + 50% DEP						
DS 2.08 + 10% TA	101	-23.0	53	-16.2		
DS 2.08 + 20% TA	120	-26.9	54	-16.8		
DS 2.08 + 30% TA	132	-29.5				
DS 2.08 + 40% TA	158	-36.0				
DS 2.08 + 50% TA	156	-37.2				
DS 2.08 + 10% DEP	94	-21.9	56	-16.5	31	-14.3
DS 2.08 + 20% DEP	115	-27.0	56	-17.6	33	-14.8
DS 2.08 + 30% DEP	80	-21.0			30	-13.9
DS 2.08 + 40% DEP	86	-22.3			29	-13.9
DS 2.08 + 50% DEP	73	-19.8			29	-13.9
DS 2.45 + 10% TA	77	-18.7	49	-16.1		
DS 2.45 + 20% TA	89	-21.1	40	-14.1		
DS 2.45 + 25% TA	124	-29.5				
DS 2.45 + 40% TA	144	-32.9				
DS 2.45 + 50% TA						
DS 2.45 + 10% DEP	80	-19.5	50	-16.6	32	-14.3
DS 2.45 + 15% DEP	92	-22.0	47	-19.5	30	-14.0
DS 2.45 + 25% DEP	95	-23.6			29	-13.8
DS 2.45 + 35% DEP	120	-29.4			28	-13.6
DS 2.45 + 45% DEP	130	-32.9				

Table 27: Arrhenius fitting parameters of secondary transitions of plasticized cellulose acetate.

Experimental results of γ-relaxation obtained by different authors in the literature are consistent: the resulted activation energy (E_a) and pre-exponential factor (log τ_0) from the Arrhenius fit are always coherent and remain in the same order of magnitude (*Sousa et al. 2010*). However, there is no accepted interpretation for the molecular motions responsible for the γ-relaxation. Since limited publications are found concerning dynamic relaxations of cellulose acetate, we also take into account experimental data and interpretations on polysaccharides to ensure the integrity of our own discussions. The review of *Kaminski et al. 2009* (Table 26) is then regarded as the ultimate reference about identification of the origins of secondary relaxations in polysaccharides.

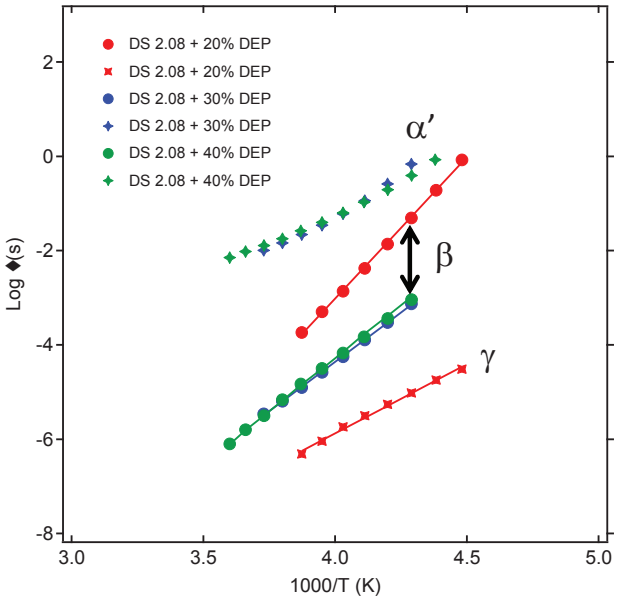

Figure 78: Relaxation map of secondary transitions of plasticized cellulose acetate.

Main characteristics of γ-relaxation are listed as below:

- γ-relaxation can be described by the Arrhenius law.
- Its activation energy is 40 - 52 kJ.mol^{-1} with relatively negligible entropy contribution. γ-relaxation has an intramolecular character.
- Thus, it is considered as a “simple transition”, regarding the definitions in Chapter 3.2.
- γ-relaxation is strongly correlated with β-relaxation. However, it seems to be independent of the structure of plasticizers.

Activation energies and pre-exponential factors of γ-relaxation calculated from our experimental dielectric study are listed in Table 27. After the phase separation, the overlapping peak of β-relaxation and α'-relaxation becomes much more intense than the peak of γ-relaxation. Due to this important intensity difference, the fit obtained from "WinFit" software is no more creditable because various possibilities of fit exist. This is the reason why the Arrhenius fitting parameters of γ-relaxation are only available for CDAs with low plasticizer contents (Table 27). The results are in good agreement with literature reports.

One of the most common propositions for γ-relaxation is molecular motions of side groups. There are two kinds of side groups in cellulose acetate: hydroxyl groups and acetyl groups. Relaxation time (τ_{OH}) of hydroxyl groups should be very fast because the molecular size is relatively small. Quantities of hydroxyl groups are limited in cellulose acetate (DS 2.45), which should be taken into account when interpreting molecular motions of γ-relaxation. Relaxation time (τ_{acetyl}) of acetyl groups should be fast but troubled by steric effect of CDA's backbone. Quantities of acetyl side groups are sufficient enough to be responsible for a secondary transition. Both hydroxyl groups and acetyl groups can interact with water. In the absence of water trace in CDA system, γ-relaxation approaches β-relaxation which means that these two secondary transitions should be tightly related to each other.

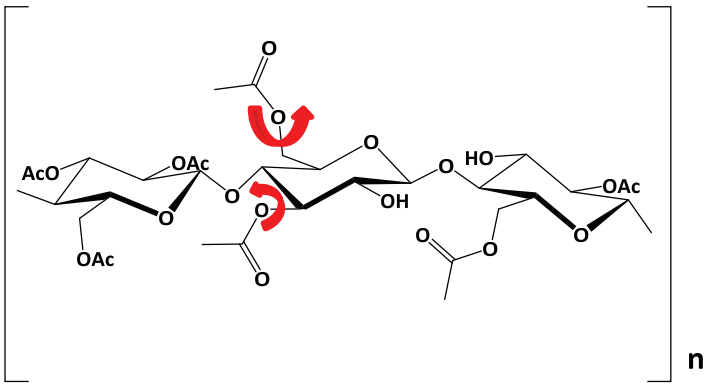

Figure 79: Rotation of acetyl side groups of cellulose acetate, one the most common propositions for the molecular motion of γ-relaxation.

By gathering all available information about the γ-relaxation, our proposition for its molecular origin is the rotation of acetyl side groups of cellulose acetate (Figure 79). This is because:

- The rotation of acetyl side groups is a localized molecular motion with limited access to interact with other motions. It fits the fact that γ-relaxation is a secondary transition with negligible entropy contribution.
- It can be impacted by the presence of water trace, by creating H-bonds with water molecules.

- As introduced in the previous paragraph, the magnitude of γ-relaxation time is consistent with that required for the rotation of acetyl side groups.
- Acetyl side groups are attached to the cellulose acetate main chains, which results in a certain limitation of the degree of rotation. That means the rotation of acetyl side groups is dependent on the cellulose acetate main chains. Consequently, the obtained activation energy is higher than that of the free acetyl side groups (without strains from the neighboring groups). Its pre-exponential factor should be modified, too. The dependence of the rotation on the cellulose acetate main chains is a result of slightly cooperative motion, which results a slightly unphysical pre-exponential factor (Table 27).

β-relaxation of plasticized cellulose acetate is widely recognized as a secondary transition. Meanwhile, its characteristics are not as typical as other sub-glass transitions. General characteristics of β–relaxation are described as follows: it has considerable activation entropy contribution which means the related molecular origin should be a cooperative motion; it also has considerable activation energy which is significant compared to standard secondary transition values. β–relaxation may have strong connection to the primary α–relaxation, especially at high frequency and high temperature range. The most common proposition about the molecular origin of β–relaxation is a kind of local main chain motion.

The activation energy (E_a) of β-relaxation of cellulose acetate is found between 76 and 85 kJ.mol^{-1} in the literature (*Sousa et al. 2010*). E_a's of DS 1.83 and DS 2.45 series are found in the same range. DS 2.08 requires more energy than the other two DS series (Table 27). All samples have a pre-exponential factor of β-relaxation which is faster than the Debye time and thus is unphysical. This is regarded as a result of cooperative motions. Cooperative motion may be present in cellulose acetate but must include the main cellulosic chain. That means β-relaxation includes motions of cellulosic chain. As already mentioned, cellulose acetate is semi-flexible due to the rigidity of its main chain. It is reported that it needs 20 repetition units to make a 360° turn-over (which is the persistence length) (*Kamide 2005*). α-relaxation is due to the segmental motion of cellulose acetate which is mainly motions of cellulosic chain. This assures certain degrees of connection between α- and β- relaxations. We may suppose the molecular origin of β-relaxation is the localized motion of cellulosic chain, e.g. small movements of 3 or 4 repetition units which does not require as much energy as segmental motion. This is the assumption that we are working with. However, we are not sure if β-relaxation could be called as Johari-Goldstein β-relaxation which is considered as the precursor of the segmental motion (see Appendix V). Supplementary data is needed to make further conclusions.

If the molecular origin of the β-relaxation is the localized motion of cellulosic chain, then the nature of the molecular origin of the β-relaxation is actually the same as the α-relaxation. Consequently, the influence of plasticizers on the α-relaxation means that such an influence should also be observed on the β-relaxation. The β-relaxation of plasticized CDA includes the participation of the plasticizer. However, no idea has been fixed about the nature of this participation. Only *Seymour et al. 1979* and *Scandola and Ceccorulli 1985b* discussed the point in the literature, there is no other information available.

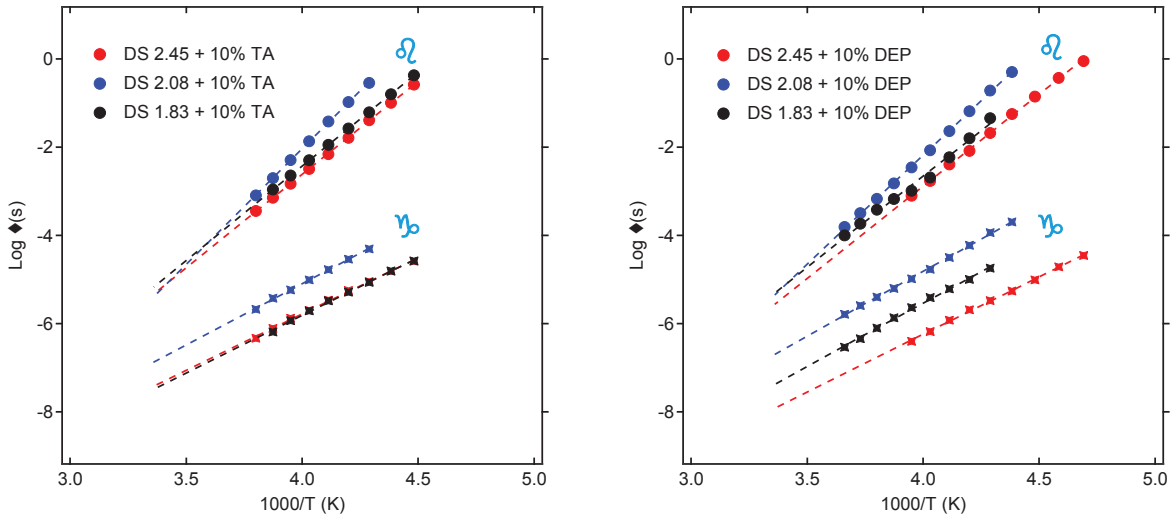

Figure 80: Left - Comparison of the relaxation map of 3 DS plasticized by 10% TA. Right - Comparison of the relaxation map of 3 DS plasticized by 10% DEP.

The influence of DS on the β-relaxation is analyzed as follows:

- At low plasticizer content (i.e. 10% TA or DEP), DS 2.08 series has the highest activation energies (15 to 20 kJ.mol^{-1} higher than the two other series, Figure 80).
- For TA-plasticized CDAs, the activation energies of the β-relaxation become more and more important with increasing plasticizer content. DS 2.45 series has the lowest activation energies. The increase of the activation energies is caused by the overlapping peak after the phase separation: the contribution of the α'-relaxation intensifies the energy required for the relaxation.
- For DEP-plasticized CDAs, it is difficult to analyze the influence of DS on the β-relaxation.

The influence of the plasticizer on the β-relaxation is also a topic to be studied:

- At low plasticizer content and similar miscibility conditions, TA-plasticized and DEP-plasticized CDAs have the same order of the activation energies.
- When phase separation occurs, the activation energies of the β-relaxation become more and more important as explained in the previous paragraph.

- Fortunately, after the apparition of the α"-relaxation, the overlapping peak becomes separable and the activation energy of the β-relaxation can be calculated alone (for example, the DS 2.08 + DEP series). It is found at the order of 80 kJ.mol^{-1}.

As known in the literature, it is difficult to decrypt the molecular origin of β–relaxation only with experimental data. The next step is to combine already available information with results from dynamic molecular simulations and to propose a creditable assumption.

5.2.4 – α'-relaxation

We propose that α'-relaxation corresponds to segmental motions of plasticizer-rich phase. It is thus equivalent to the second T_g identified in MDSC analysis. As shown in Chapter 3.2, α'-relaxation is overlapped with β-relaxation in thermo-mechanical analysis. Dielectric measurement brings more details on α'-relaxation because a new transition is found in highly plasticized DS 1.83 and DS 2.08 series.

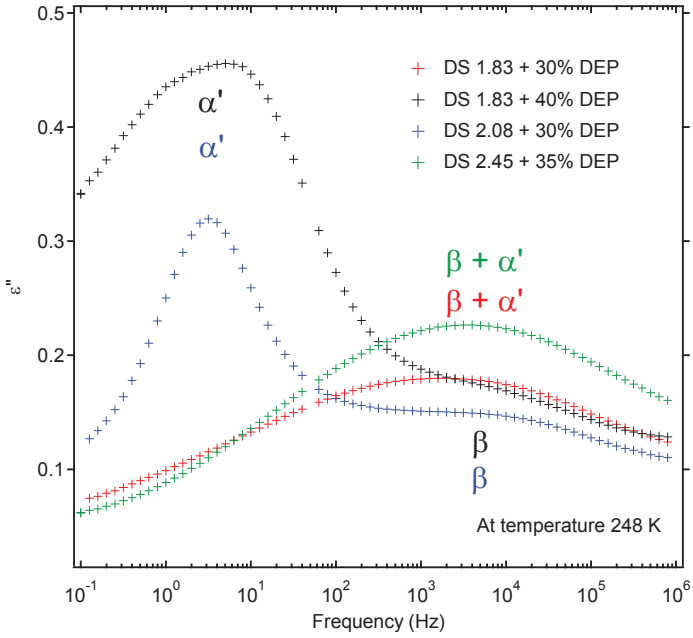

Figure 81: Dielectric spectra of DEP-plasticized cellulose acetate at temperature 248 K (or -25°C).

In Figure 81, DS 2.45 + 35% DEP and DS 1.83 + 30% DEP are both two-phase systems: CDA-rich phase and DEP-rich phase. Their dielectric spectra at -25°C are the overlapping peak of α'-relaxation and β-relaxation, the same as DMTA analysis. On the other hand, DS 1.83 + 40% DEP and DS 2.08 + 30% DEP are both three-phase systems: CDA-rich phase, DEP-rich phase and DEP phase.

Their dielectric spectra at -25°C indicate two different transitions: the first one is similar to the overlapping peak and the second one is at lower frequencies and much more intense. The latter is then considered as separated α'-relaxation of plasticizer-rich phase. This is because:

- According to MDSC analysis, in a three-phase system, composition of DEP-rich phase does not evolve anymore. It means that the α'-relaxation of the three-phase system is higher in temperature or lower in frequency as compared to a two-phase system at similar plasticizer amount.

- The behavior of the transition follows the VFT equation (Figure 82), which is characteristic of the primary transitions.

- It should also be remarked that the relaxation behavior of the overlapping peak of DS 2.45 + 35% DEP and DS 1.83 + 30% DEP is situated between those of the separated α'-relaxation and β-relaxation of DS 2.08 + 30% DEP (Figure 82). It looks like the relaxation behaviors of the separated α'-relaxation and β-relaxation of DS 2.08 + 30% DEP are the deconvolution results of the relaxation behavior of the overlapping peak, which is consistent with our assumptions.

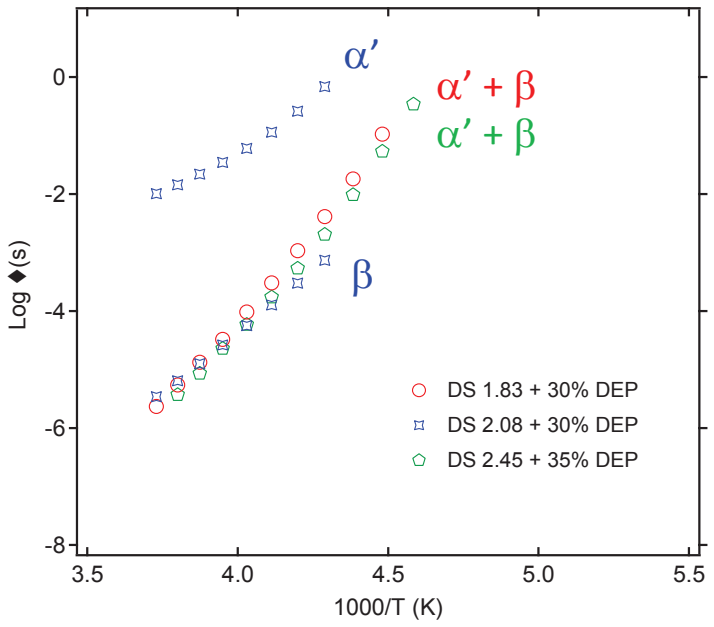

Figure 82: The related relaxation map of α'- and β-relaxations of DEP-plasticized CDA.

5.2.5 – α-relaxation

α-relaxation is the most important transition of plasticized cellulose acetate. Here, we analyze the results of its relaxation map revealed by the three DS's. α-relaxation is related either to motions of cellulose acetate (in a fully miscible system) or to motions of CDA-rich phase (in a partially miscible system). As previously mentioned, it is difficult to study the primary α-relaxation of unplasticized cellulose acetate due to thermal degradation. However, plasticized cellulose acetates, such as DEP-plasticized systems have a lower glass transition temperature which may allow for studying the α-relaxation process by dielectric spectroscopy in a large frequency range. It is not our purpose to display every α–relaxation process. The idea is to point out the evolution of α-relaxation with different DS and plasticizers. We focus on DEP-plasticized CDAs.

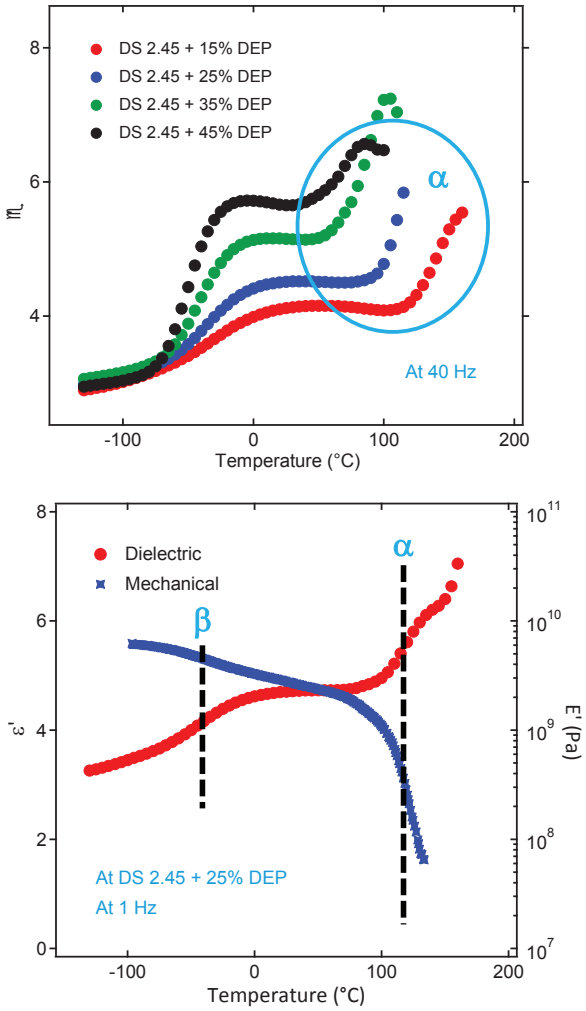

Figure 83: Top - Illustration of α-relaxation of plasticized cellulose acetate with DS 2.45 series at 40 Hz. Bottom- The comparison of the dielectric result with thermo-mechanical result at 1 Hz for DS 2.45 + 25% DEP.

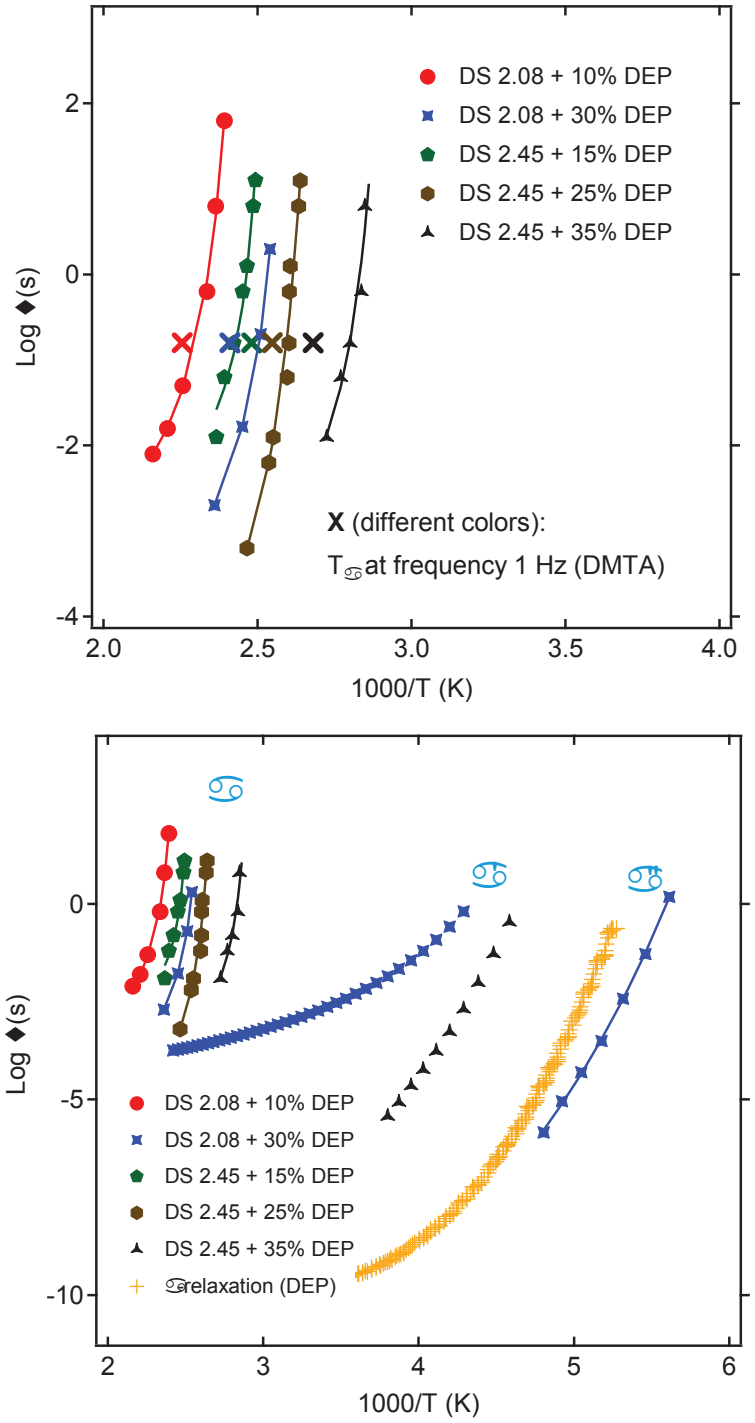

Figure 84: Top - Relaxation map of α–relaxation processes (represented by DEP-plasticized cellulose acetates with DS 2.08 and DS 2.45). Bottom - General feature of the relaxation map of plasticized CDA including three primary transitions.

Note that the characteristic dielectric relaxation time is obtained with the complex permittivity plot against temperature, which has relatively large error bars (Figure 83). The mechanical relaxation time is determined with the E" plot versus temperature at frequency 1 Hz, in order to have equivalence with the complex permittivity. Taking into account all error margins, we assume that the obtained mechanical and dielectric results at log τ = 0 are equivalent. One of the main achievements in the present study is the identification of α-relaxation of plasticized cellulose acetate. As shown in Figure 83, α-relaxation process is plotted in an isochronal representation and its authentication is based on our experimental DMTA data at frequency 1 Hz: One step in storage modulus (E') of thermo-mechanical analysis as well as a step in real part of permittivity (ε') of dielectric study is considered as a result of α-relaxation. Their corresponding characteristic temperatures are in good agreement with each other.

	Estimated T_0 (K)	T_g DSC (K)	T_g DMTA (K)
DS 2.08 + 10% DEP	398	443	443
DS 2.08 + 30% DEP	375	405	415
DS 2.45 + 15% DEP	367 - 389	391	416
DS 2.45 + 20% DEP	379 - 384	384	402
DS 2.45 + 25% DEP	335 - 361	374	389
DS 2.45 + 35% DEP	330 - 344	348	376
DS 2.45 + 45% DEP	295 - 316	328	346

Table 28: VFT parameters of the α-relaxation of plasticized cellulose acetates.

In Figure 84, we plotted the temperature dependence of the α-relaxation times of plasticized CDA systems. At plasticizer concentrations smaller than the partial miscibility limit, a single α-relaxation is observed. At higher concentrations, one observes two α-relaxation processes associated to the CDA-rich and plasticizer-rich phases, respectively. The temperature dependence of the α-relaxation can be

described by the VFT equation (Equation 22). It is considered that at the ideal glass transition temperature T_0, which is also called "Vogel temperature", the movement of the atoms is totally frozen. According to *Kremer and Schonhals 2002*, this value is found to be 30-70 K below T_g. The corresponding parameters are given in Table 28. We do observe indeed that the plasticizer accelerates the dynamics of cellulose acetate.

α-relaxation of plasticized CDA samples at frequency 1 Hz obtained by mechanical experiments have been added in Figure 83 in order to compare with the dielectric results. A correct match is obtained regarding both techniques. Our results obtained in dielectric spectroscopy do indeed correspond to the final α-relaxation of our cellulose acetate systems.

The mechanical α'-relaxation of plasticized CDAs at frequency 1 Hz have also been plotted in Figure 84. A temperature shift (10 to 15°C, typically) as compared to the dielectric results is observed. However, the relaxation spectrum is very broad and these results may be considered as consistent. In particular, it is possible to explain these differences by the fact that this overlapping peak corresponds to two relaxations (β-relaxation of plasticized cellulose acetate and α'-relaxation of plasticizer-rich phase), the respective amplitudes of which depend on the considered technique.

Plasticized CDA	γ' Secondary Transition of DEP alone	α'' Primary Transition of DEP alone	γ Simple secondary transition of CDA	β Cooperative secondary transition of CDA	α' Primary transition of plasticizer rich phase	α Primary transition of CDA rich phase
DS 1.83 + TA (%TA < 20%)			X	X		X
DS 1.83 + TA (%TA > 20%)			X	X	X	X
DS 1.83 + DEP (%DEP < 25%)	X		X	X		X
DS 1.83 + DEP (%DEP = 30%)	X		X	X	X	X
DS 1.83 + DEP (%DEP > 30%)	X	X	X	X	X	X
DS 2.08 + TA (%TA < 20%)			X	X		X
DS 2.08 + TA (%TA > 20%)			X	X	X	X
DS 2.08 + DEP (%DEP < 25%)	X		X	X		X
DS 2.08 + DEP (%DEP > 25%)	X	X	X	X	X	X
DS 2.45 + TA (%TA < 20%)			X	X		X
DS 2.45 + TA (%TA > 20%)			X	X	X	X
DS 2.45 + DEP (%DEP < 25%)	X		X	X		X
DS 2.45 + DEP (%DEP > 25%)	X		X	X	X	X

Table 29: Summary of secondary and primary transitions of plasticized cellulose acetates with three DS and two plasticizers.

CHAPTER 6

GENERAL INTERPRETATIONS OF PROPERTIES OF PLASTICIZED CELLULOSE ACETATE

In Chapter 6, general interpretations of experimental results of plasticized cellulose acetate are given. Miscibility and dynamic properties of plasticized CDA are reviewed and gathered together for further discussions. Miscibility study of plasticized CDA is first carried out by thermal analysis (MDSC). Glass transition temperatures are successfully identified by MDSC measurement. Phase separation is observed in the plasticized CDA with all three DS: DS 1.83, DS 2.08 and DS 2.45. The miscibility threshold limits are identified at ~20% TA and at ~25% DEP. Furthermore, a third transition is obtained in DS 1.83 and DS 2.08 with high DEP contents. It is supposed to be related to cavities formed during the solvent evaporation step and filled later with plasticizer molecules.

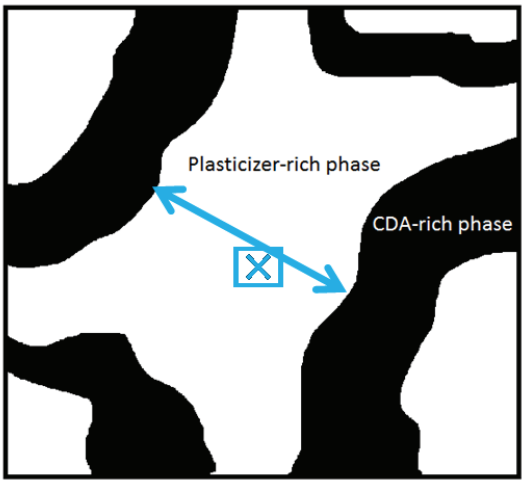

Duplicate of Figure 42 - Phase separation in the plasticized cellulose acetates. ξ: correlation length

Phase separation is considered as a result of partial miscibility between the polymer and the plasticizer. Thus, two phase domains are formed in the plasticized CDA: CDA-rich phase and plasticizer-rich phase (Duplicate of Figure 42). In thermal analysis, phase separation results in the finding of two T_g's, which corresponds to the separated phase domains (Duplicate of Figure 26). In thermo-mechanical and dielectric analysis, primary relaxations (α- and α'-relaxations), which correspond to the CDA-rich phase and the plasticizer-rich phase respectively, are the results due to the phase separation (Duplicate of Figure 36 and 83).

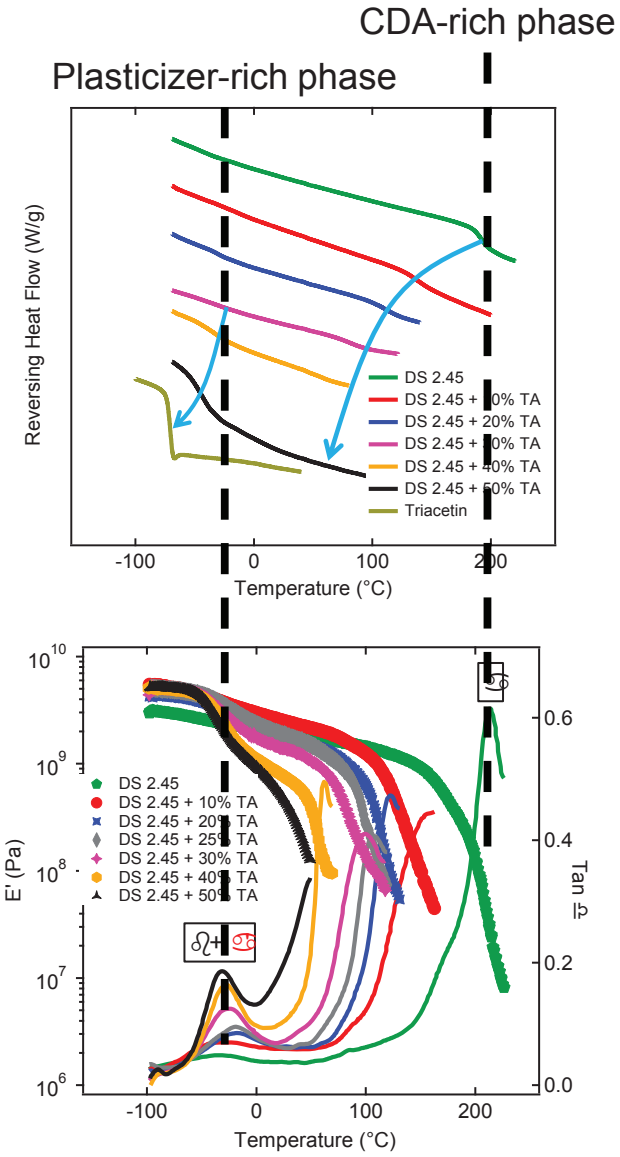

Duplicate of Figure 26 - MDSC thermograms of plasticized DS 2.45 series, arrows indicate glass transition temperatures and Figure 36 - DMTA spectra of plasticized cellulose acetate with DS 2.45 at frequency 1 Hz (only E' and tan δ are represented).

Furthermore, the correlation length (ξ) of separated phase domains is expected to be obtained from the neutron scattering study. Duplicate of Figure 58 presents an example of DS 2.45 + 20% TA, in which the correlation length (ξ) of separated phase domains is estimated ~7.5 nm (plasticizer content at the beginning of the phase separation). The summary of all experimental results due to the phase separation is resumed here and the results are consistent with each other.

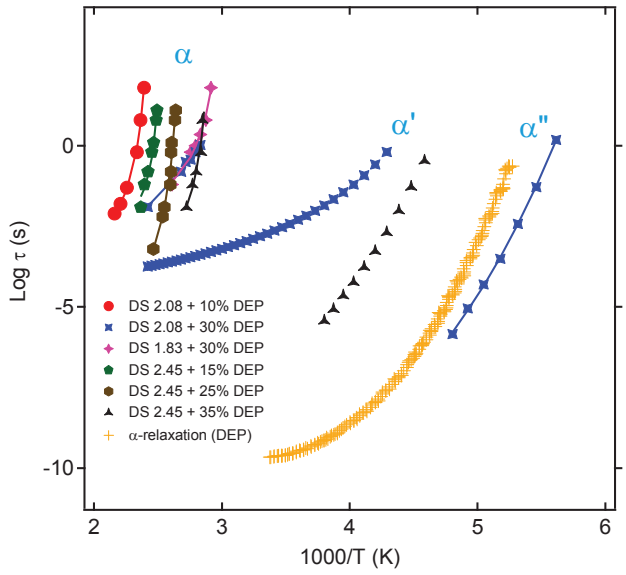

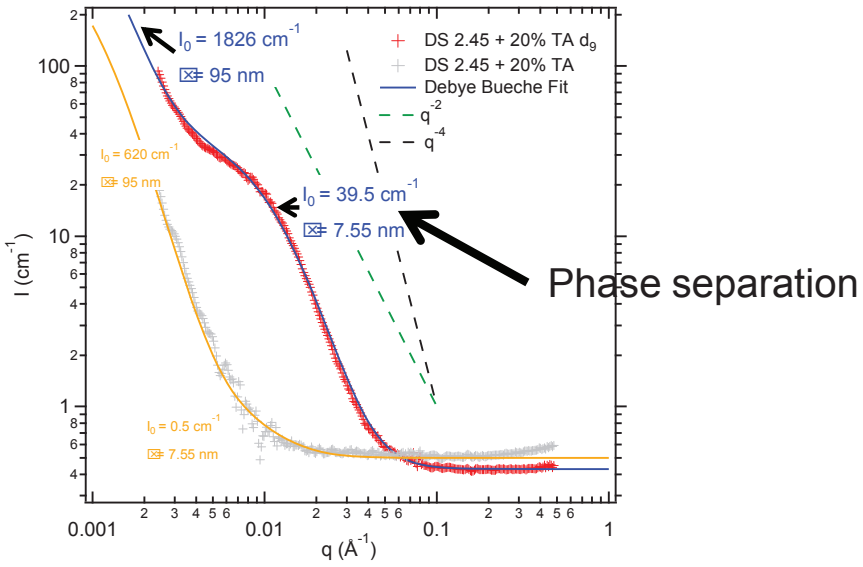

Duplicate of Figure 83 - General feature of the relaxation map of plasticized CDA including three primary transitions and Figure 58 - SANS curve of DS 2.45 + 20% TA d_9, fit by two Debye-Bueche distributions and is compared to its protonated sample.

The second miscibility behavior observed in the present study is the formation of cavities in plasticized DS 1.83 and DS 2.08 with high DEP contents (Duplicate of Figure 45).

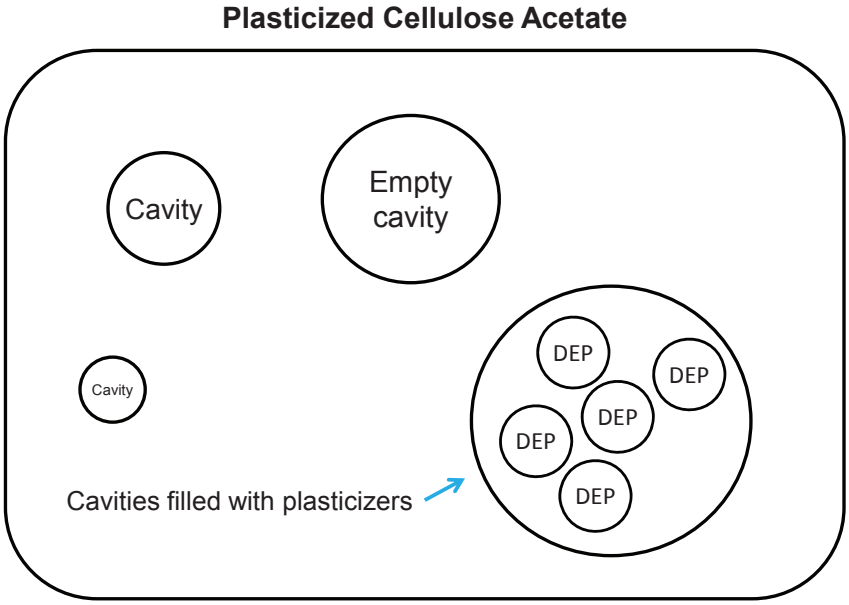

Duplicate of Figure 45 - Empty cavities and cavities partially filled with plasticizer molecules (example of diethyl phthalate) in the plasticized cellulose acetates.

In thermo-mechanical and dielectric measurement, a third primary transition (α"-relaxation) is found and is equivalent to the third T_g in thermal analysis (Duplicate of Figure 39 and 75, figures below).

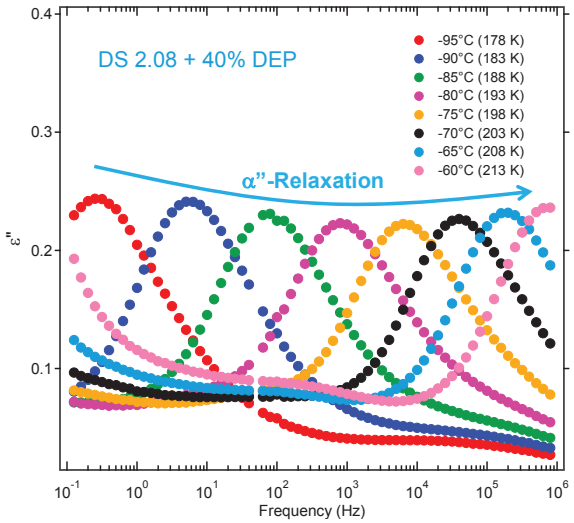

Duplicate of Figure 75 - Frequency dependence of the imaginary part of the complex dielectric permittivity (ε") from 178 to 213 K in steps of 5 K, for α"-relaxation of DS 2.08 + 40% DEP

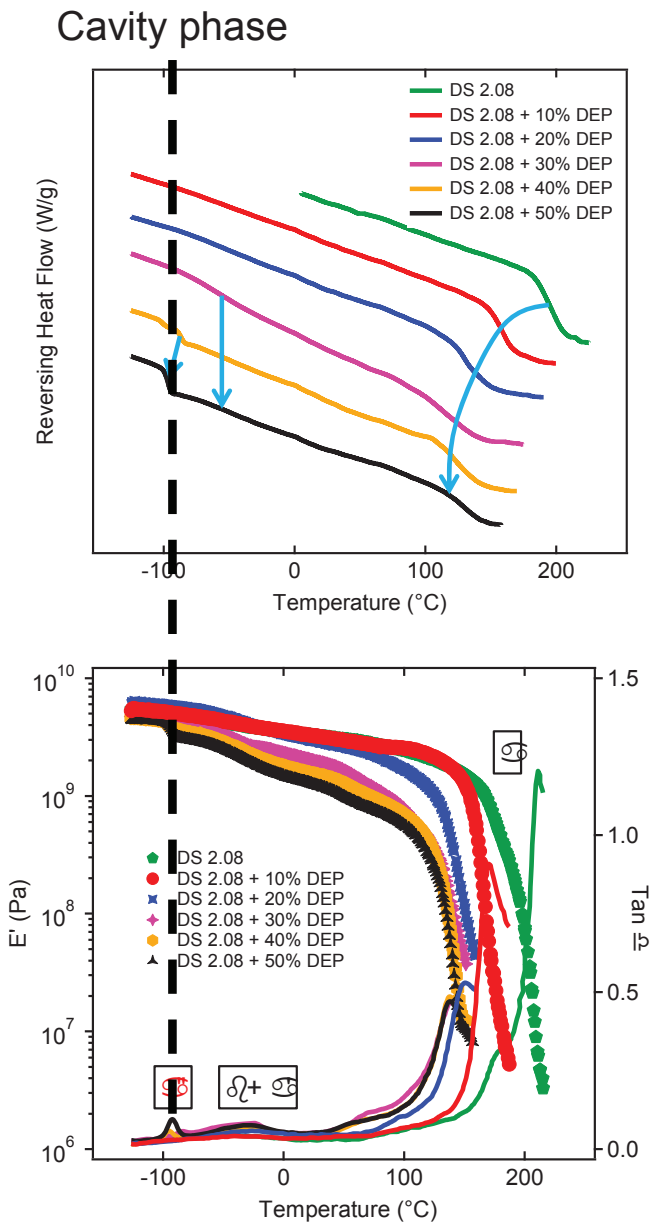

Duplicate of Figure 31 - MDSC thermograms of plasticized DS 2.08 series, arrows indicate glass transition temperatures and of Figure 39 - DMTA spectra of plasticized cellulose acetate with DS 2.08 at frequency 1 Hz (only E' and tan δ are represented). Plasticizer content varies from 0 to 50% in weight fraction.

The behavior of the α"-relaxation is in agreement with the literature result of primary transition of pure DEP liquids (see Chapter 5). The formation of cavities results in the finding of a third T_g in thermal analysis, which is close to the main transition temperature of pure DEP molecules (Duplicate of Figure 31). This can suggest that the cavities are partially filled with plasticizer molecules.

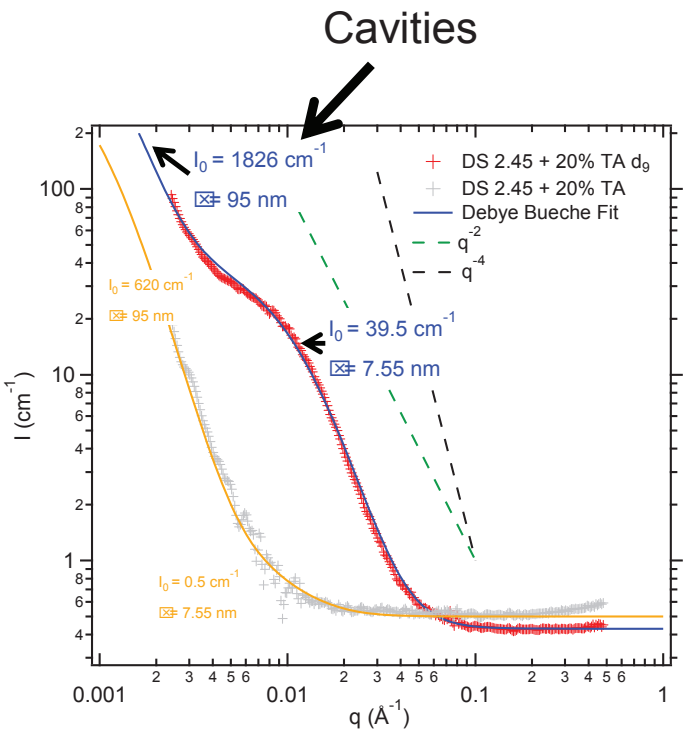

Duplicate of Figure 58 - SANS curve of DS 2.45 + 20% TA d_9, fit by two Debye-Bueche distributions and comparison to its protonated sample.

Most importantly, the cavities partially filled with plasticizer molecules are also observed in neutron scattering study. The characteristic correlation length of the cavity phase is obtained as 50 - 150 nm (Duplicate of Figure 58). Again, a summary of results of cavities is shown above and these results from different characterization techniques are consistent with each other.

The formation of cavities is the most important hypothesis that we made in the present study. Its principle is illustrated in Duplicate of Figure 32: let us consider a CDA film with solvent. Initially, before evaporation takes place, the density may be normalized by 1, corresponding to a dense system. Then, evaporation takes place. The trajectories in the (Φ_p, Φ_s) space are illustrated in the same figure. If the evaporation process is slow enough, the trajectory never enters the unstable domain: the total density remains sufficiently high for the system to be in the stable state (trajectory N°1, green curve). If the evaporation process is fast as compared to the film contraction process, then the trajectory may enters the unstable domain (shaded area in Figure 32, trajectory N°2, yellow trajectory).

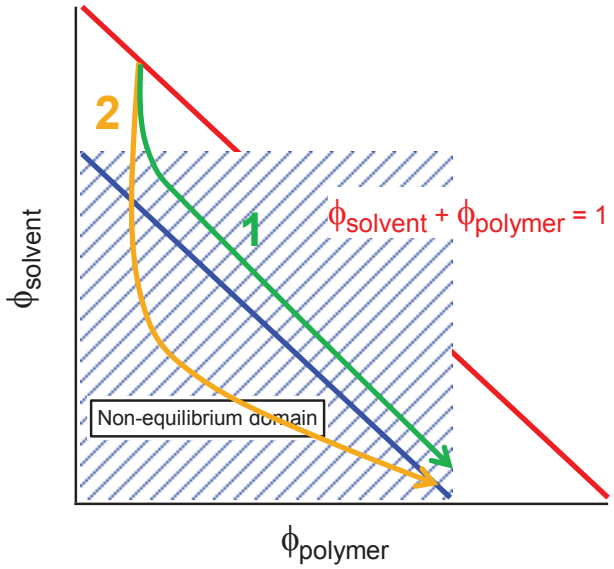

Duplicate of Figure 32: Scheme of proposed cavity theory.

These effects are possible because solvent diffusion and mechanical contraction are two different mechanisms: solvent diffusion is controlled by fast path in the material, whereas film contraction is controlled by the alpha-relaxation process. The latter is controlled by the slowest part of the relaxation spectrum of the material as measured in dielectric spectroscopy or in mechanical spectroscopy (e.g. *Long & Lequeux 2001, Merabia et al. 2004, Julien, PhD thesis, Lyon 2014*).

The formation of cavities is illustrated in Figure 33: in the first step, solvent has diffused out of the sample. Empty regions appear before contraction takes place (Step 2 in Figure 33). If the sample has had time to partially contract, it may still remain in the stable region of the phase space (trajectory N°1, Figure 32). In this case, contraction will continue, without formation of cavities (Step 3 in Figure 33). If the sample has not contracted sufficiently during the solvent evaporation stage, the sample may enter the unstable domain (trajectory N°2). Then, cavities may appear (Step 4 in Figure 33).

Note that the size and volume fraction of the cavities should depend on the glass transition temperature (T_g) of the plasticized CDA. When the T_g is low enough, contraction takes place rapidly, and no cavities may appear. For a higher T_g, contraction may be too slow for preventing cavities. On the other hand, mechanical relaxation may be sufficiently quick for building large cavities in the sample. If the T_g is even higher, the cavity formation process may stop when the cavities are still relatively small.

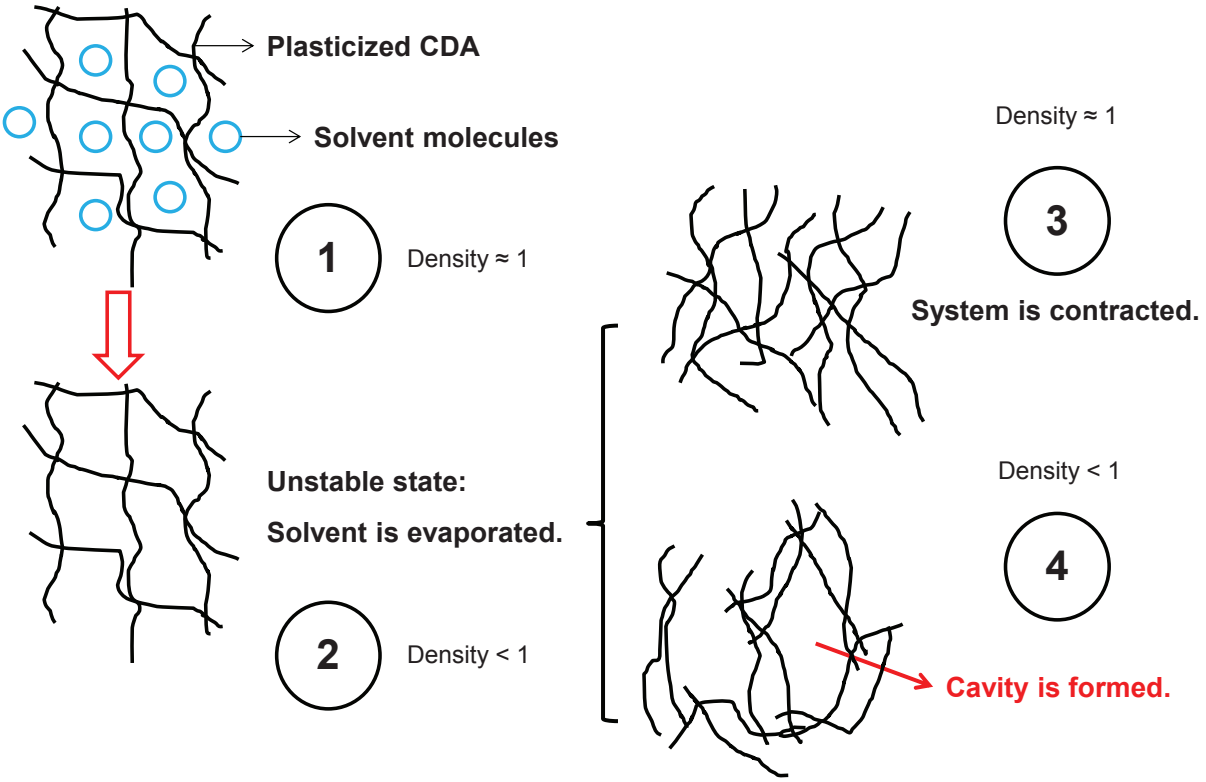

Duplicate of Figure 33: Different steps from solvent evaporation to formation of cavities (Trajectory N°2 in Figure 32).

Dynamic properties of plasticized CDAs are studied by DMTA and BDS techniques. Various primary and secondary transitions are observed and their interpretations are given. Primary α-type relaxations are already discussed in the previous paragraph. Secondary relaxations are also analyzed by these two techniques, but β-relaxation is the only secondary transition detected by both DMTA and BDS measurement. A good agreement is found between the results of β-relaxation obtained from thermo-mechanical and dielectric analysis, as shown in Duplicate of Figure 83. Most importantly, the behavior of the α-relaxation of plasticized CDA is described for the whole series of samples. This is the first time that a thorough study on the α-relaxation of plasticized CDA has ever been reported and the related VFT-like behavior has been described. Vogel temperatures are estimated from the VFT law and are consistent with the experimental values.

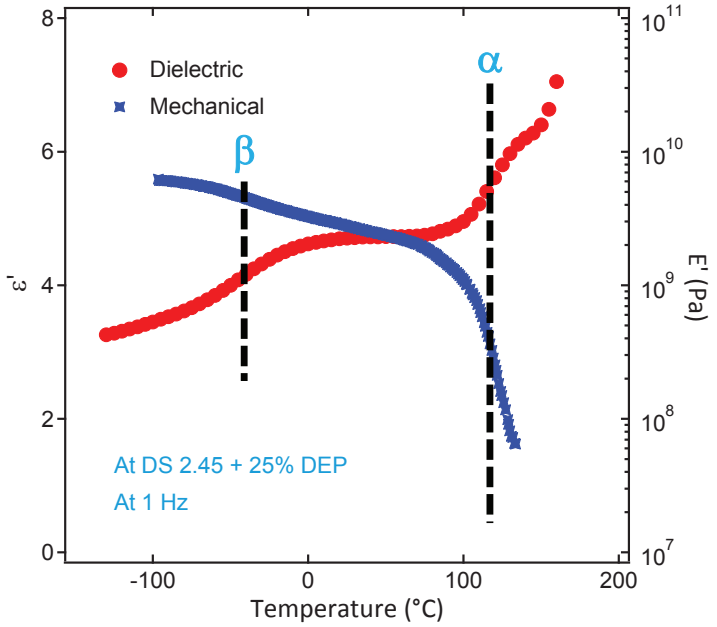

Duplicate of Figure 83: The comparison of the dielectric result with thermo-mechanical result at 1 Hz for DS 2.45 + 25% DEP.

The plasticization power of TA and DEP on cellulose acetate is estimated according to ΔT_g (the decrease of T_g between the unplasticized and plasticized CDAs). Certainly, this is a qualitative study which nevertheless highlights the fact that the mechanism of plasticization of CDA is strongly dependent on the typology of the plasticizer. As previously shown in Chapter 3, TA is a better plasticizer for cellulose acetate than DEP. As both plasticizers have the ability to plasticize CDA through dipolar interactions between ester side groups, the major structural difference probably comes from the aromatic ring of DEP molecules and can vectorize steric effects when interacting with polymer chains. Besides these facts, no clear interpretation concerning the two mechanisms of plasticization can be given at the molecular level.

Another important factor is the degree of substitution of cellulose acetate. In the present study, three different DS are applied: DS 1.83, DS 2.08 and DS 2.45. The lower the DS is, the more the hydroxyl side groups are. These functional groups can form H-bonds with themselves or with acetyl side groups of cellulose acetate. Thus, as the DS of the polymer decreases, the resulting polar interaction network is more and more difficult to be broken and the cellulose acetate becomes less and less plasticized. According to the summary of our results, DS 2.45 is the optimal degree of substitution of cellulose acetate with a good balance of the initial polar interactions. It can be easily plasticized, still remains amorphous and thus has the best viscoelastic behavior suitable for industrial processing. Concerning DS 1.83 and DS 2.08, they have important drawbacks (limited range of plasticization and probably high viscosity value) compared to DS 2.45 which limit their developments and applications in the industrial scale.

CHAPTER 7

CONCLUSION AND PERSPECTIVES

This Ph.D. thesis work is focused on the study of plasticized cellulose acetate and their relaxation behavior as a function of temperature. 3 degrees of substitution (DS) plasticized by triacetin (TA) or diethyl phthalate (DEP) have been analyzed, discussed and compared. TA-plasticized cellulose acetates share similar behaviors. Their phase separation thresholds are found to be close to ~20% TA. DEP-plasticized cellulose acetates are different: some highly-plasticized CDAs display a third transition which we proposed to be related to the formation of cavities, while the phase separation of these systems takes place at the threshold limit of 25% DEP. Results prove that TA is a good plasticizer for all kinds of cellulose acetates while DEP has different plasticizing power on the 3 DS. It also confirms the reason why DS 2.45 is the commercial grade of cellulose acetate: it has the best properties of cellulose acetate for industrial applications.

Miscibility study of plasticized cellulose acetate is also analyzed through small-angle neutron scattering technique. Phase separation, cavities partially filled with plasticizers and concentration fluctuations are found when performing neutron experiments. Dielectric analysis allows us to establish a relaxation map of plasticized cellulose acetate, including three main transitions (α-, α'- and α"-relaxations). This should be the most complete study of α-relaxation of plasticized cellulose acetate. Secondary transitions are also described and compared with literature results. The structural properties of the plasticized CDAs are studied by XRD technique. The influence of plasticizers on the intermolecular organization of the cellulose acetate system is well-observed and a hump is detected and attributed to the cavity phase partially filled with plasticizer molecules.

The present study should be considered as the ultimate reference for further investigations on the various behaviors of the plasticized cellulose acetate system. The first perspective is the further study of the formation of cavities. As explained in the previous chapter, two factors can determine the number and the size of cavities formed in the solvent evaporation step: the affinity between the polymer and the plasticizer and the solvent evaporation rate. Since the latter is a constant rate during the present study, it will be interesting to "play" with this parameter in order to observe its influence on the formation of cavities. This requires multiple experiments by using the solvent casting method. Cavities can also have impact on the optical properties of plasticized CDA because of the important difference of refraction index. The plasticized CDA film should become translucent or turbid with the presence of cavities. Another miscibility behavior of plasticized CDA can also have impact on the optical properties: the large-scale phase separation. Unfortunately, our neutron scattering study attains its experimental limits and the detailed information of phase separation is not revealed. It will be really useful if the light scattering study (LS) can be realized for this purpose. The micrometer-scale phase separation is exactly in the accessible range of LS measurement.

The second perspective is the understanding of the plasticization of cellulose acetate at the molecular level. Molecular dynamics simulation is a good and useful tool for this purpose. 'Amorphous' cells containing polymer chains and plasticizer molecules at increasing amount can be easily built and equilibrated when using these tools. The dynamics of these systems can then be studied at a given temperature through an extremely short time scale (several nanoseconds). A detailed analysis could be expected about the local organizations of plasticizer molecules interacting with the main cellulosic chains. According to the typology of the plasticizer to be studied, it is possible that different associations between the polymer chain and the plasticizer can be predicted which may provide essential information to the interpretation of the plasticization mechanism of cellulose acetate at the molecular level. An experimental approach is also planned by using the Solid-State ^{13}C NMR Spectroscopy. According to the literature and our present study, NMR technique is considered as the most suitable characterization method for the microscopic scale understanding of the plasticization of cellulose acetate. The evolution of each transition under different temperature conditions could also be studied.

The third perspective is the confirmation and the precision of the molecular origins of dynamic transitions. In the present study, assumptions have been made and proposed to certain secondary transitions, such as the γ-relaxation of cellulose acetate. This transition is supposed to correspond to the rotation of acetyl side groups. Experimental results are consistent with this assumption which still needs to be proven. Molecular modeling may once again provide us with this information. With this technique, the rotation of acetyl side groups in the amorphous plasticized CDA cell could be analyzed in terms of an auto-correlation function and then its relaxation time could be calculated.

The theoretical relaxation time at a given temperature can finally be compared to our experimental results in order to find a credible conclusion. Concerning the β-relaxation whose molecular motion is not well identified, emergence of the modeling techniques, such as the "MetaDynamics" could be useful.

The study of dynamic transitions of plasticized CDA is actually the basis of further studies on the mechanical properties of the system. The major drawbacks of the plasticized CDA are the impact resistance performance and limited tensile strength. These two properties are strongly correlated with the positions of different transitions. It is expected that if given additives can modify or displace the transitions of the polymer, then improvements of these properties may be obtained. Certainly, the choice of the plasticizer is also an important factor of this study. By using our methodology for the characterization of the behaviors of plasticized CDA, we may expect to improve mechanical properties of plasticized CDA which will be useful for applicative performance.

REFERENCES

Aminabhavi, T. M., Raikar, S. K., Aralaguppi, M. I., Khinnavar, R. S., Joshi, S. S., & Balundgi, R. H. (1993). Dielectric studies of liquids and liquid mixtures. *INDIAN JOURNAL OF TECHNOLOGY, 31*(10), 739-744.

Aoki, D., Teramoto, Y., & Nishio, Y. (2011). Cellulose acetate/poly(methyl methacrylate) interpenetrating networks: synthesis and estimation of thermal and mechanical properties. *CELLULOSE, 18*, 1441-1454.

Bao, C. Y., Long, D. R., & Vergelati, C. (2015). Miscibility and dynamical properties of cellulose acetate/plasticizer systems. *CARBOHYDRATE POLYMERS, 116*(1), 95-102.

Bocahut, A., Delannoy, J. Y., Vergelati, C., & Mazeau, K. (2014). Conformational analysis of cellulose acetate in the dense amorphous state. *CELLULOSE, 21*(6), 3897-3912.

Boy, R. E., Schulken, R. M., & Tamblyn, J. W. (1967). Crystallinity in secondary cellulose esters. *JOURNAL OF APPLIED POLYMER SCIENCE, 11*, 2453-2465.

Buchanan, C. M., Buchanan, N. L., Debenham, J. S., Gatenholm, P., Jacobsson, M., Shelton, M. C., Watterson, T. L., & Wood, M. D. (2003). Preparation and characterization of arabinoxylan esters and arabinoxylan ester/cellulose ester polymer blends. *CARBOHYDRATE POLYMERS, 52*, 345-357.

Buchanan, C. M., Dorschel, D., Gardner, R. M., Komarek, R. J., Matosky, A. J., White, A. W., & Wood, M. D. (1996). The influence of degree of substitution on blend miscibility and biodegradation of cellulose acetate blends. *JOURNAL OF ENVIRONMENTAL POLYMER DEGRADATION, 4*(3), 179-195.

Buchanan, C. M., Gedon, S. C., Pearcy, B. G., White, A. W., & Wood, M. D. (1993). Cellulose ester - aliphatic polyester blends: the influence of diol length on blend miscibility. *MACROMOLECULES, 26*, 5704-5710.

Buchanan, C. M., Gedon, S. C., White, A. W., & Wood, M. D. (1992). Cellulose acetate butyrate and poly(hydroxybutyrate-co-valerate) copolymer blends. *MACROMOLECULES, 25*, 7373-7381.

Buchanan, C. M., Gedon, S. C., White, A. W., & Wood, M. D. (1993). Cellulose acetate propionate and poly(tetramethylene glutarate) blends. *MACROMOLECULES, 26*, 2963-2967.

Buchanan, C. M., Pearcy, B. G., White, A. W., & Wood, M. D. (1997). The relationship between blend miscibility and biodegradation of cellulose acetate and poly(ethylene succinate) blends. *JOURNAL OF ENVIRONMENTAL POLYMER DEGRADATION, 5*(4), 209-223.

Carrot, C., & Guillet, J. (1999). Viscoélasticité linéaire des polymères fondus. *Technique de l'ingénieur - Plastiques et Composites* (pp. 1-19).

Ceccorulli, G., Pizzoli, M., & Scandola, M. (1986). Influence of water on the secondary relaxations of cellulose acetate. *POLYMER COMMUNICATIONS, 27*(228), 230.

Ceccorulli, G., Pizzoli, M., & Scandola, M. (1993). Effect of a low molecular weight plasticizer on the thermal and viscoelastic properties of miscible blends of bacterial poly(3-hydroxybutyrate) with cellulose acetate butyrate. *MACROMOLECULES, 26*, 6722-6726.

Cerqueira, D. A., Filho, G. R., & Assuncao, R. M. N. (2006). A new value for the heat of fusion of a perfect crystal of cellulose acetate. *POLYMER BULLETIN, 56*, 475-484.

Cerqueira, D. A., Valente, A. J. M., Filho, G. R., & Burrows, H. D. (2009). Synthesis and properties of polyaniline–cellulose acetate blends: The use of sugarcane bagasse waste and the effect of the substitution degree. *CARBOHYDRATE POLYMERS, 78*, 402-408.

Cerveny, S., Colmenero, J., & Alegria, A. (2005). Dielectric investigation of the low-temperature water dynamics in the poly(vinyl methyl ether)/H_2O system. *MACROMOLECULES, 38*, 7056-7063.

Chen, Z. M., Bi, D. Y., & Wang, L. M. (2012). Enthalpy and dielectric relaxations of triacetin in the vicinity of glass transition. *Acta Physico-Chimica Sinica, 28*(9), 2023-2028.

Choi, J. S., Lim, S. T., Choi, H. J., Hong, S. M., Mohanty, A. K., Drzal, L. T., Misra, M., & Wibowo, A. C. (2005). Rheological, thermal, and morphological characteristics of plasticized cellulose acetate composite with natural fibers. *MACROMOL.SYMP, 224*, 297-307.

Cole, K. S., & Cole, R. H. (1941). Dispersion and absorption in dielectrics - I Alternating current characteristics. *JOURNAL OF CHEMICAL PHYSICS, 9*, 341-352.

Cole, K. S., & Cole, R. H. (1942). Dispersion and absorption in dielectrics - II Direct current characteristics. *JOURNAL OF CHEMICAL PHYSICS, 10*, 98-105.

Company, E. C. (1996). For the coatings market -- EASTMAN cellulose acetate for coatings. (pp. 1-16).

Couchman, P. R., & Karasz, F. E. (1978). A classical thermodynamic discussion of the effect of composition on glass-transition temperatures. *MACROMOLECULES, 11*(1), 117-119.

Crofton, D. J., & Pethrick, R. A. (1981). Dielectric studies of proton migration and relaxation in wet cellulose and its derivatives. *POLYMER, 22*, 1048-1053.

Debye, P., Anderson Jr., H. R., & Brumberger, H. (1957). Scattering by an inhomogeneous solid. II. The correlation function and its application. *JOURNAL OF APPLIED PHYSICS, 28*(6), 679.

Debye, P., & Bueche, A. M. (1949). Scattering by an inhomogeneous solid. *JOURNAL OF APPLIED PHYSICS, 20*(6), 518.

Doyle, S. J., & Pethrick, R. A. (1992). Dielectric relaxation studies of heterogeneously substituted cellulose acetate and its plasticization by dibutyl phthalate. *POLYMER INTERNATIONAL, 27*, 321-331.

Dyer, C., Jiang, Z., Bozell, J., Rials, T., Heller, W. T., & Dadmun, M. (2013). Effect of chain structure on the miscibility of cellulose acetate blends: a small-angle neutron scattering study. *SOFT MATTER, ASAP*.

Ehrenfest, P. (1933). Phase changes in the ordinary and extended sense classified according to the corresponding singularities of the thermodynamic potential. *Proceedings Koninklijke Akademie van Wetenschappen, 36*, 153-157.

Einfeldt, J., Meibner, D., & Kwasniewski, A. (2001). Polymer dynamics of cellulose and other polysaccharides in solid state-secondary dielectric relaxation processes. *PROGRESS IN POLYMER SCIENCE, 26*, 1419-1472.

Eyring, H. (1936). Viscosity, plasticity, and diffusion as examples of absolute reaction rates. *JOURNAL OF CHEMICAL PHYSICS, 4*, 283.

Fawcett, T. G., Crowder, C. E., Kabekkodu, S. N., Needham, F., Kaduk, J. A., Blanton, T. N., Petkov, V., Bucher, E., & Shpanchenko, R. (2013). Reference materials for the study of polymorphism and crystallinity in cellulosics. *POWDER DIFFRACTION, 28*(1), 18-31.

Feldmann, K. E., Kade, M. J., Meijer, E. W., Hawker, C. J., & Kramer, E. J. (2009). Model transient networks from strongly hydrogen-bonded polymers. *MACROMOLECULES, 42*, 9072-9081.

Ferrarezi, M. M. F., Rodrigues, G. V., Felisberti, M. I., & Gonçalves, M. C. (2013). Investigation of cellulose acetate viscoelastic properties in different solvents and microstructure. *EUROPEAN POLYMER JOURNAL*.

Fordyce, C. R., & Meyer, L. W. A. (1940). Plasticizers for cellulose acetate and cellulose acetate butyrate. *INDUSTRIAL AND ENGINEERING CHEMISTRY, 32*(8), 1053-1060.

Fox, T. G. (1956). Influence of diluent and of copolymer composition on the glass temperature of a polymer system. *Bulletin of the American Physical Society, 1*, 123.

French, A. D., Bertoniere, N. R., Brown, R. M., Chanzy, H., Gray, D., Hattori, K., & Glasser, W. (2007). Cellulose. In WILEY-VCH (Ed.). *Kirk-Othmer Encyclopedia of Chemical Technology* (Vol. 5, pp. 360-394): Wiley Blackwell.

Fringant, C., Rinaudo, M., Foray, M. F., & Bardet, M. (1998). Preparation of mixed esters of starch or use of an external plasticizer: two different ways to change the properties of starch acetate films. *CARBOHYDRATE POLYMERS, 35*, 97-106.

Fulcher, G. S. (1925). Analysis of recent measurements of the viscosity of glasses *Journal of the American Ceramic Society, 8*(6), 339-355.

Gaibler, D. W., Rochefort, W. E., Wilson, J. B., & Kelley, S. S. (2004). Blends of cellulose ester/phenolic polymers – chemical and thermal properties of blends with polyvinyl phenol. *CELLULOSE, 11*, 225-237.

Gutiérrez, M. C., De Paoli, M.-A., & Felisberti, M. I. (2012). Biocomposites based on cellulose acetate and short curauá fibers: Effect of plasticizers and chemical treatments of the fibers. *COMPOSITES: PART A, 43*(8), 1338-1346.

Havriliak, S., & Negami, S. (1967). A complex plane representation of dielectric and mechanical relaxation processes in some polymers. *POLYMER, 8*, 161-210.

Hensel-Bielowka, S., Sekula, M., Pawlus, S., Psurek, T., & Paluch, M. (2004). Influence of molecular structure on dynamics of secondary relaxation in phthalates. In S. J. Rzoska & V. P. Zhelezny (Eds.). *Nonlinear Dielectric Phenomena in Complex Liquids* (pp. 307-317). Netherlands: Kluwer Academic Publishers.

Higeshiro, T., Teramoto, Y., & Nishio, Y. (2009). Poly(vinyl pyrrolidone-co-vinyl acetate)-graft-polycaprolactone as a compatibilizer for cellulose acetate/polycaprolactone blends. *JOURNAL OF APPLIED POLYMER SCIENCE, 113*, 2945-2954.

Hodge, I. M. (1994). Enthalpy relaxation and recovery in amorphous materials. *JOURNAL OF NON-CRYSTALLINE SOLIDS, 169*(3), 211-266.

Ikada, E., & Watanabe, T. (1974). New asymmetric dielectric relaxations in two liquid triacetates. *THE JOURNAL OF PHYSICAL CHEMISTRY, 78*(11), 1078-1082.

Inoue, T. (2006). On the Relationship between Viscoelastic Segments and Kuhn Segments; Strain-Induced Chain Orientation in Fast Deformation. *MACROMOLECULES, 39*(13), 4615-4618.

Jafarpour, G., Dantras, E., Boudet, A., & Lacabanne, C. (2007). Study of dielectric relaxations in cellulose by combined DDS and TSC. *JOURNAL OF NON-CRYSTALLINE SOLIDS, 353*, 4108-4115.

Julien, G. (2014). Dynamics in polymer blends and polymer-solvent blends close to the glass transition. (Vol. Ph.D.): Université Claude Bernard Lyon 1.

Kadla, J. F., & Dai, Q. Z. (2007). Pulp. In WILEY-VCH (Ed.). *Kirk-Othmer Encyclopedia of Chemical Technology* (Vol. 21, pp. 1-47): Wiley Blackwell.

Kamide, K. (2005). *Cellulose and cellulose derivatives - molecular characterization and its applications*. Elsevier Science.

Kamide, K., & Saito, M. (1985). Thermal analysis of cellulose acetate solids with total degrees of substitution of 0.49, 1.75, 2.46, and 2.92. *POLYMER JOURNAL, 17*(8), 919-928.

Kaminski, K. (2012). Impact of water on molecular dynamics of amorphous cyclodextrins studied by dielectric spectroscopy. *PHYSICAL REVIEW E, 86*, 031506.

Kaminski, K., Kaminska, E., Ngai, K. L., Paluch, M., Wlodarczyk, P., Kasprzycka, A., & Szeja, W. (2009). Identifying the origins of two secondary relaxations in polysaccharides. *THE JOURNAL OF PHYSICAL CHEMISTRY B, 113*, 10088-10096.

Kaminski, K., Kaminska, E., Wlodarczyk, P., Pawlus, S., Kimla, D., Kasprzycka, A., Paluch, M., Ziolo, J., Szeja, W., & Ngai, K. L. (2008). Dielectric studies on mobility of the glucosidic linkage in seven disaccharides. *J.PHYS.CHEM.B, 112*, 12816-12823.

Kawai, K., & Hagura, Y. (2012). Discontinuous and heterogeneous glass transition behavior of carbohydrate polymer-plasticizer systems. *CARBOHYDRATE POLYMERS, 89*, 836-841.

Keely, C. M., Zhang, X., & McBrierty, V. J. (1995). Hydration and plasticization effects in cellulose acetate: a solid-state NMR study. *JOURNAL OF MOLECULAR STRUCTURE, 355*, 33-46.

Kramers, H. A. (1940). Brownien motion in a field of force and the diffusion model of chemical reactions. *Physica, 7*(4), 284-304.

Kremer, F., & Schonhals, A. (2002). *Broadband dielectric spectroscopy*. Germany.

Kulkarni, S., Krause, S., & Wignall, G. D. (1994). Investigation of the pore structure and morphology of cellulose acetate membranes using Small-Angle Neutron Scattering. 2. Ultrafiltration and reverse-osmosis membranes. *MACROMOLECULES, 27*, 6785-6790.

Kulkarni, S., Krause, S., Wignall, G. D., & Hammouda, B. (1994). Investigation of the pore structure and morphology of cellulose acetate membranes using Small-Angle Neutron Scattering. 1. Cellulose acetate active layer membranes. *MACROMOLECULES, 27*, 6777-6784.

Kusumi, R., Inoue, Y., Shirakawa, M., Miyashita, Y., & Nishio, Y. (2008). Cellulose alkyl ester/polycaprolactone blends: characterization of miscibility and crystallization behaviour. *CELLULOSE, 15*, 1-16.

Kusumi, R., Teramoto, Y., & Nishio, Y. (2011). Structural characterization of polycaprolactone-grafted cellulose acetate and butyrate by solid-state 13C NMR, dynamic mechanical, and dielectric relaxation analyses. *POLYMER, 52*, 5912-5921.

Laredo, E., Newman, D., Bello, A., & Muller, A. J. (2009). Primary and secondary dielectric relaxations in semi-crystalline and amorphous starch. *EUROPEAN POLYMER JOURNAL, 45*, 1506-1515.

Laurati, M., Sotta, P., Long, D. R., Fillot, L. A., Arbe, A., Alegria, A., Embs, J. P., Unruh, T., Schneider, G. J., & Colmenero, J. (2012). Dynamics of water absorbed in polyamides. *MACROMOLECULES, 45*, 1676-1687.

Lee, D. H., Lee, J. H., Cho, M. S., Choi, S. H., Lee, Y. K., & Nam, J. D. (2005). Viscoelastic characteristics of plasticized cellulose nanocomposites. *JOURNAL OF POLYMER SCIENCE PART B: POLYMER PHYSICS, 43*, 59-65.

Lodge, T. P., & McLeish, T. C. B. (2000). Self-concentrations and effective glass transition temperatures in polymer blends. *MACROMOLECULES, 33*, 5278-5284.

Long, D. R., & Lequeux, F. (2001). Heterogeneous dynamics at the glass transition in van der Waals liquids, in the bulk and in thin films. *The European Physical Journal E, 4*, 371-387.

Lu, B. L., Xu, A. R., & Wang, J. J. (2014). Cation does matter: how cationic structure affects the dissolution of cellulose in ionic liquids. *GREEN CHEMISTRY, 16*, 1326-1335.

Maeda, A., & Inoue, T. (2011). On the Viscoelastic Segment Size of Cellulose. *NIHON REOROJI GAKKAISHI, 39*(4), 159-163.

Maryott, A. A., & Smith, E. R. (1951). Table of dielectric constants of pure liquids. *National Bureau of Standards Circular 514*. Washington, D. C.: U. S. Government Printing Office.

McBrierty, V. J., Keely, C. M., Coyle, F. M., Xu, H., & Vij, J. K. (1996). Hydration and plasticization effects in cellulose acetate: molecular motion and relaxation. *FARADAY DISCUSS, 103*, 255-268.

Meier, M. M., Kanis, L. A., De Lima, J. C., & Pires, A. T. N. (2004). Poly(caprolactone triol) as plasticizer agent for cellulose acetate films: influence of the preparation procedure and plasticizer content on the physico-chemical properties. *POLYMERS FOR ADVANCED TECHNOLOGIES, 15*, 593-600.

Merabia, S., Sotta, P., & Long, D. R. (2004). Heterogeneous nature of the dynamics and glass transition in thin polymer films. *The European Physical Journal E, 15*, 189-210.

Miyashita, Y., Suzuki, T., & Nishio, Y. (2002). Miscibility of cellulose acetate with vinyl polymers. *CELLULOSE, 9*, 215-223.

Mohanty, A. K., Wibowo, A. C., Misra, M., & Drzal, L. T. (2003). Development of renewable resource-based cellulose acetate bioplastic: effect of process engineering on the performance of cellulosic plastics. *POLYMER ENGINEERING AND SCIENCE, 43*(5), 1151-1161.

Monnerie, L., Halary, J. L., & Kausch, H.-H. (2005). Deformation, Yield and Fracture of Amorphous Polymers: Relation to the Secondary Transitions. *ADVANCES IN POLYMER SCIENCE, 187*, 215-372.

Monnerie, L., Lauprêtre, F., & Halary, J. L. (2005). Investigation of Solid-State Transitions in Linear and Crosslinked Amorphous Polymers. *ADVANCES IN POLYMER SCIENCE, 187*, 35-213.

Montès, H., Mazeau, K., & Cavaillé, J. Y. (1997). Secondary mechanical relaxations in amorphous cellulose. *MACROMOLECULES, 30*, 6977-6984.

Montès, H., Mazeau, K., & Cavaillé, J. Y. (1998). The mechanical β relaxation in amorphous cellulose. *JOURNAL OF NON-CRYSTALLINE SOLIDS, 235-237*, 416-421.

Neal, J. L. (1965). Factors affecting the solution properties of cellulose acetate. *JOURNAL OF APPLIED POLYMER SCIENCE, 9*, 947-961.

Ngai, K. L., & Paluch, M. (2004). Classification of secondary relaxation in glass-formers based on dynamic properties. *JOURNAL OF CHEMICAL PHYSICS, 120*(2), 857-873.

Nielsen, L. E., & Landel, R. F. (1994). *Mechanical properties of polymers and composites*. Marcel Dekker, Inc.

Nilsson, M., Alderborn, G., & Stromme, M. (2003). Water-induced charge transport in tablets of microcrystalline cellulose of varying density: dielectric spectroscopy and transient current measurements. *CHEMICAL PHYSICS, 295*, 159-165.

Nishio, Y., Matsuda, K., Miyashita, Y., Kimura, N., & Suzuki, H. (1997). Blends of polycaprolactone with cellulose alkyl esters: effect of the alkyl side-chain length and degree of substitution on miscibility. *CELLULOSE, 4*, 131-145.

Ohno, T., & Nishio, Y. (2007a). Estimation of miscibility and interaction for cellulose acetate and butyrate blends with N-vinylpyrrolidone copolymers. *MACROMOLECULAR CHEMISTRY AND PHYSICS, 208*, 622-634.

Ohno, T., & Nishio, Y. (2007b). Molecular orientation and optical anisotropy in drawn films of miscible blends composed of cellulose acetate and poly(N-vinylpyrrolidone-co-methyl methacrylate). *MACROMOLECULES, 40*, 3468-3476.

Ohno, T., Yoshizawa, S., Miyashita, Y., & Nishio, Y. (2005). Interaction and scale of mixing in cellulose acetate/poly(N-vinyl pyrrolidone-co-vinyl acetate) blends. *CELLULOSE, 12*, 281-291.

Ornstein, L. S., & Zernike, F. (1914). Accidental deviations of density and opalescence at the critical point of a single substance. *Proceedings Koninklijke Akademie van Wetenschappen, 17*, 793-806.

Pang, Y. X., Jia, D. M., Hu, H. J., Hourston, D. J., & Song, M. (1999). A quantitative estimation of the extent of compatibilization in heterogeneous polymer blends using their heat capacity increment at the glass transition. *JOURNAL OF APPLIED POLYMER SCIENCE, 74*(12), 2868-2876.

Park, H.-M., Misra, M., Drzal, L. T., & Mohanty, A. K. (2004). “Green” nanocomposites from cellulose acetate bioplastic and clay: effect of eco-friendly triethyl citrate plasticizer. *BIOMACROMOLECULES, 5*, 2281-2288.

Pawlus, S., Paluch, M., Sekula, M., Ngai, K. L., Rzoska, S. J., & Ziolo, J. (2003). Changes in dynamic crossover with temperature and pressure in glass-forming diethyl phthalate. *PHYSICAL REVIEW E, 68*, 021503.

Quintana, R., Persenaire, O., Lemmouchi, Y., Sampson, J., Martin, S., Bonnaud, L., & Dubois, P. (2013). Enhancement of cellulose acetate degradation under accelerated weathering by plasticization with eco-friendly plasticizers. *POLYMER DEGRADATION AND STABILITY, 98*(9), 1556-1562.

Roche, E., Chanzy, H., Boudeulle, M., Marchessault, R. H., & Sundararajan, P. (1978). Three-dimensional crystalline structure of cellulose triacetate II. *MACROMOLECULES, 11*(1), 86-94.

Roig, F., Dantras, E., Dandurand, J., & Lacabanne, C. (2011). Influence of hydrogen bonds on glass transition and dielectric relaxations of cellulose. *JOURNAL OF PHYSICS D: APPLIED PHYSICS, 44*, 045403.

Russell, J., & Van Kerpel, R. G. (1957). Transitions in plasticized and unplasticized cellulose acetates. *JOURNAL OF POLYMER SCIENCE, 25*, 77-96.

Rustemeyer, P. (2004). *Cellulose acetates: properties and applications*. WILEY-VCH.

Saad, G. R., Botros, M. G., & Nessim, R. I. (1992). Dielectric study of acetylated cotton cellulose and saponified cellulose acetate. *DIE ANGEWANDTE MAKROMOLEKULARE CHEMIE, 197*, 23-39.

Scandola, M., & Ceccorulli, G. (1985a). Viscoelastic properties of cellulose derivatives: 1. Cellulose acetate. *POLYMER, 26*, 1953-1957.

Scandola, M., & Ceccorulli, G. (1985b). Viscoelastic properties of cellulose derivatives: 2. Effect of diethylphthalate on the dynamic mechanical relaxations of cellulose acetate. *POLYMER, 26*, 1958-1962.

Sears, V. F. (1992). Neutron scattering lengths and cross sections. *NEUTRON NEWS, 3*(3), 26-37.

Seymour, R. W., Weinhold, S., & Haynes, S. K. (1979). Mechanical and dielectric relaxation in cellulose esters. *JOURNAL OF MACROMOLECULAR SCIENCE PART B: PHYSICS, B16*(3), 337-353.

Shaikh, H. M., Pandare, K. V., Nair, G., & Varma, A. J. (2009). Utilization of sugarcane bagasse cellulose for producing cellulose acetates: novel use of residual hemicellulose as plasticizer. *CARBOHYDRATE POLYMERS, 76*(1), 23-29.

Shashidhara, G. M., Guruprasad, K. H., & Varadarajulu, A. (2002). Miscibility studies on blends of cellulose acetate and nylon 6. *EUROPEAN POLYMER JOURNAL, 38*, 611-614.

Songsurang, K., Miyagawa, A., Manaf, M. E. A., Phulkerd, P., Nobukawa, S., & Yamaguchi, M. (2013). Optical anisotropy in solution-cast film of cellulose triacetate. *CELLULOSE, 20*(1), 83-96.

Sousa, M., Bras, A. R., Veiga, H. I. M., & Ferreira, F. C. (2010). Dynamical characterization of a cellulose acetate polysaccharide. *J.PHYS.CHEM.B, 114*, 10939-10953.

Starkweather, H. W. (1988). Noncooperative relaxations. *MACROMOLECULES, 21*(6), 1798-1802.

Suvorova, A. I., Demchik, L. Y., & Peshekhonova, A. L. (1995). Plasticization of cellulose diacetate with a mixture of triacetin and esters of butylcellosolve and aliphatic dicarboxylic acids. *CELLULOSE, 2*(1), 23-29.

Tammann, G., & Hesse, W. (1926). Die Abhängigkeit der Viscosität von der Temperatur bie unterkühlten Flüssigkeiten. *Zeitschrift für anorganische und allgemeine Chemie, 156*(1), 245-257.

Townend, D. J., & Warren, R. C. (1985). Relaxations in double base propellants. *POLYMER, 26*, 79-83.

Unohara, T., Teramoto, Y., & Nishio, Y. (2011). Molecular orientation and optical anisotropy in drawn films of cellulose diacetate-graft-PLLA: comparative investigation with poly(vinyl acetate-co-vinyl alcohol)-graft-PLLA. *CELLULOSE, 18*, 539-553.

Vogel, H. (1921). The law of the relationship between viscosity of liquids and the temperature. *Physikalische Zeitschrift, 22*, 645-646.

Wakelyn, P. J. (2007). Cotton. In WILEY-VCH (Ed.). *Kirk-Othmer Encyclopedia of Chemical Technology* (Vol. 8, pp. 1-40): Wiley Blackwell.

Warren, R. C. (1988). Transitions and relaxations in plasticised nitrocellulose. *POLYMER, 29*, 919-923.

Warth, H., Mulhaupt, R., & Schatzle, J. (1996). Thermoplastic cellulose acetate and cellulose acetate compounds prepared by reactive processing. *JOURNAL OF APPLIED POLYMER SCIENCE, 64*(2), 231-242.

Wood, L. A. (1958). Glass transition temperatures of copolymers. *JOURNAL OF POLYMER SCIENCE, 28*(117), 319-330.

Yamaguchi, M., & Masuzawa, K. (2008). Transparent polymer blends composed of cellulose acetate propionate and poly(epichlorohydrin). *CELLULOSE, 15*(1), 17-22.

Yoshitake, S., Suzuki, T., Miyashita, Y., Aoki, D., Teramoto, Y., & Nishio, Y. (2013). Nanoincorporation of layered double hydroxides into a miscible blend system of cellulose acetate with poly(acryloyl morpholine). *CARBOHYDRATE POLYMERS, 93*, 331-338.

Zhou, Q., Zhang, L., Zhang, M., Wang, B., & Wang, S. J. (2003). Miscibility, free volume behavior and properties of blends from cellulose acetate and castor oil-based polyurethane. *POLYMER, 44*, 1733-1739.

Zugenmaier, P. (2004). Characterization and physical properties of cellulose acetates. In WILEY-VCH (Ed.). *Cellulose acetates: properties and applications* (pp. 81-166).

APPENDIX I - D11 INSTRUMENT CHARACTERISTICS & DESCRIPTION

D11	
Monochromator	
velocity selector	
Eleanore/ Felicia (ASTRIUM standard selectors)	$\Delta\lambda/\lambda$ = 9% (FWHM)
incident wavelength	variable, 4.5 ≤ λ [Å] ≤ 40
max. wavelength at max. detector dist. (39 m)	λ = 22 Å
selector rotation normal to n-beam possible minimum wavelength at rotation -7 deg	-7 deg to + 7 deg λ = 3.2 Å
Collimation	
11 guide sections (computer controlled) uncoated glass guides (SwissNeutronics) diverging "trumpet" + straight guide + focusing guide near sample position	 cross section (height x width) : 50 x 30 mm^2 -> 50 x 45 mm^2 over 6.5 m straight guide 50 x 45 mm^2 over 28 m 50 x 45 mm^2 -> 35 x 31.5 mm^2 over 4 m
guide-to-sample distances	1.5, 2.5, 4, 5.5, 8, 10.5, 13.5, 16.5, 20.5, 28, 34, 40.5 m (12 discrete distances)
Attenuators	
choice between 3 cadmium sheets of different transmission (computer controlled) T_a=3.461 10^{-3} (att 1), T_a=1.089 10^{-3} (att 2), T_a=3.524 10^{-4} (att 3)	
Sample area	
flux at specimen at lowest resolution	$1 \cdot 10^8$ $ncm^{-2}s^{-1}$
typical sample size	10 x 10 mm^2
Detector	
sample-to-detector distances L	variable between 1.2 m and 39 m
momentum transfer range	$3\ 10^{-4} \leq Q\ [Å^{-1}] \leq 1$
detector type	^{3}He gas detector (CERCA)
area	96 x 96 cm^2
pixel size	7.5 x 7.5 mm^2
background	1 Hz on whole multi-detector
detector dead time	420 ns

APPENDIX II - SUPPLEMENTARY INFORMATION OF THE PAPER

Miscibility and Dynamical Properties of Cellulose Acetate / Plasticizer Systems

Supplementary Information

Congyu BAO*[(1)], Didier R. LONG[(1)], Caroll VERGELATI[(2)]

(1) Laboratoire Polymères & Matériaux Avancés, UMR 5268, CNRS - Solvay Laboratory

(2) Advanced Polymer Material Department, Solvay Research & Innovation, Saint-Fons, France

* Electronic mail: Congyu.BAO-EXTERIEUR@solvay.com

Sample drying procedure

We applied a drying procedure for preparing our samples in order to reduce the water content as much as possible, still by controlling the possible loss of plasticizer molecules (DEP). We describe this procedure in Table 1. The drying temperature of plasticized samples was lower as compared to the unplasticized ones.

	MDSC	DMTA	BDS
CDA (DS 2.45)	Dried at 70°C 20 min	Dried at 70°C 15 min	Heated gradually up to 100°C 100°C for 10 min Total time = 90 min
CDA + 10% DEP	Dried at 70°C 15 min	Dried at 70°C 15 min	Heated gradually up to 100°C 100°C for 10 min Total time = 90 min
CDA + 20% DEP	Dried at 70°C 15 min	Dried at 70°C 15 min	Heated gradually up to 70°C 70°C for 10 min Total time = 60 min
CDA + 30% DEP	Dried at 50°C 15 min	Dried at 50°C 15 min	Heated gradually up to 50°C 50°C for 10 min Total time = 40 min
CDA + 40% DEP	Dried at 30°C 15 min	Dried at 25°C 15 min	Heated gradually up to 30°C 30°C for 10 min Total time = 30 min
CDA + 50% DEP	Dried at 30°C 15 min	Dried at 25°C 15 min	Heated gradually up to 25°C 25°C for 10 min Total time = 30 min

Table 1: Sample drying procedure for each CDA film and for each characterization technique

Karl Fischer titration

The remaining water amount is quantified by using the Karl Fischer (KF) titration method. Samples are dried at 160°C so that water is evaporated and then captured for quantification.

Water Content measured by Karl Fischer titration

	Before Drying %	After Drying %	After DMTA Analysis %
CDA (DS 2.45)	2.44	0.56	0.26
CDA + 10% DEP	1.86	0.57	0.61
CDA + 20% DEP	1.17	0.39	0.14
CDA + 30% DEP	0.87	0.56	0.13
CDA + 40% DEP	0.74	0.63	0.09
CDA + 50% DEP	0.50	0.54	0.13

Table 2: Remaining water trace in CDA films measured by Karl Fischer titration at 160°C
After Drying: after the sample drying procedure (Table 1)
After DMTA Analysis: after DMTA measurement at 1 Hz (Table 4)

The potential influence of water on the dielectric properties of CDA film is calculated with its dielectric constant. 0.5 wt.% is the most significant amount of water that we could find in all dielectric samples. The dielectric constant of water at ambient temperature is about 80. 0.5 wt.% * 80 = 0.4, this should be the biggest water contribution to the real part of complex permittivity. This contribution is negligible compared to the contribution of cellulose acetate whose dielectric constant is about 4 to 5.5 in the high frequency conditions.

Plasticizer Loss

Plasticizer Loss during Different Steps

	After Drying %	After DMTA Analysis %
CDA (DS 2.45)	≈ 0	≈ 0
CDA + 10% DEP	≈ 0	1.63
CDA + 20% DEP	0.29	1.34
CDA + 30% DEP	0.32	2.54
CDA + 40% DEP	0.33	5.33
CDA + 50% DEP	0.27	5.99

Table 3: Plasticizer loss (%) of plasticized CDA films during different steps

Plasticizer loss (%) = initial DEP content in sample (%) – final DEP content in sample (%)

% in weight

After Drying: after the sample drying procedure (Table 1)

After DMTA Analysis: after DMTA measurement at 1 Hz (Table 4)

It is important to make sure that the sample drying procedure is a reasonable compromise between efficient water removal and limited plasticizer loss. As illustrated in Table 3, the plasticizer loss after drying is 0.3% which is more likely in the error margin of balance. Thus we consider that plasticizer loss during the sample drying procedure is totally negligible. Plasticizer loss took place at high temperatures during mechanical analysis. The departure of DEP from each sample is smaller than 12% of the nominal amount.

	Max T (°C) During DMTA Analysis
CDA (DS 2.45)	230°C
CDA + 10% DEP	208°C
CDA + 20% DEP	150°C
CDA + 30% DEP	130°C
CDA + 40% DEP	150°C
CDA + 50% DEP	115°C

Table 4: Final temperatures for DMTA measurement for each sample at 1 Hz

Supplementary Dielectric Results

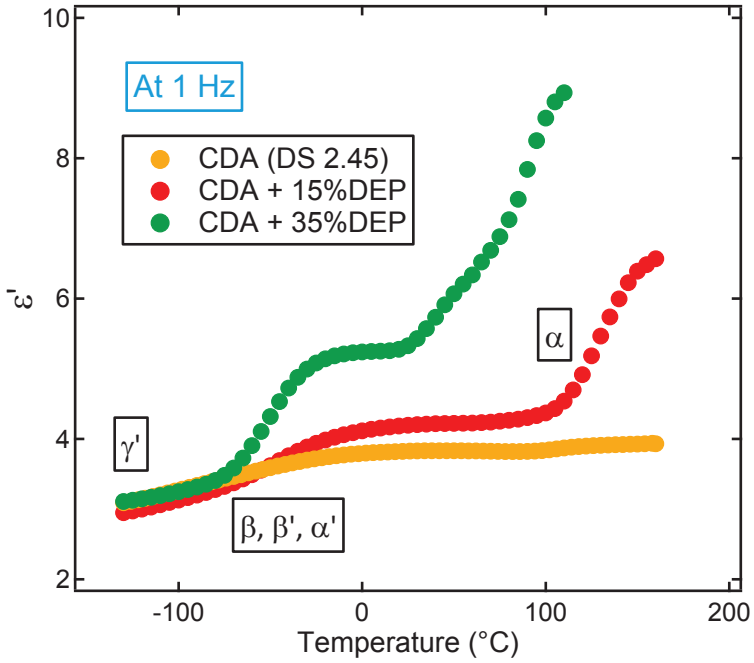

Figure 1: Temperature dependence of the real part of the complex permittivity (ε') at frequency 1 Hz for the unplasticized cellulose acetate (orange plots), CDA + 15% DEP (red plots) and CDA + 35% DEP (green plots) systems.

The dielectric α-relaxation results are consistent with those obtained by mechanical experiments.

APPENDIX III - A LOSS PEAK IN THE NON-REVERSIBLE HEATING FLOW

Page 78

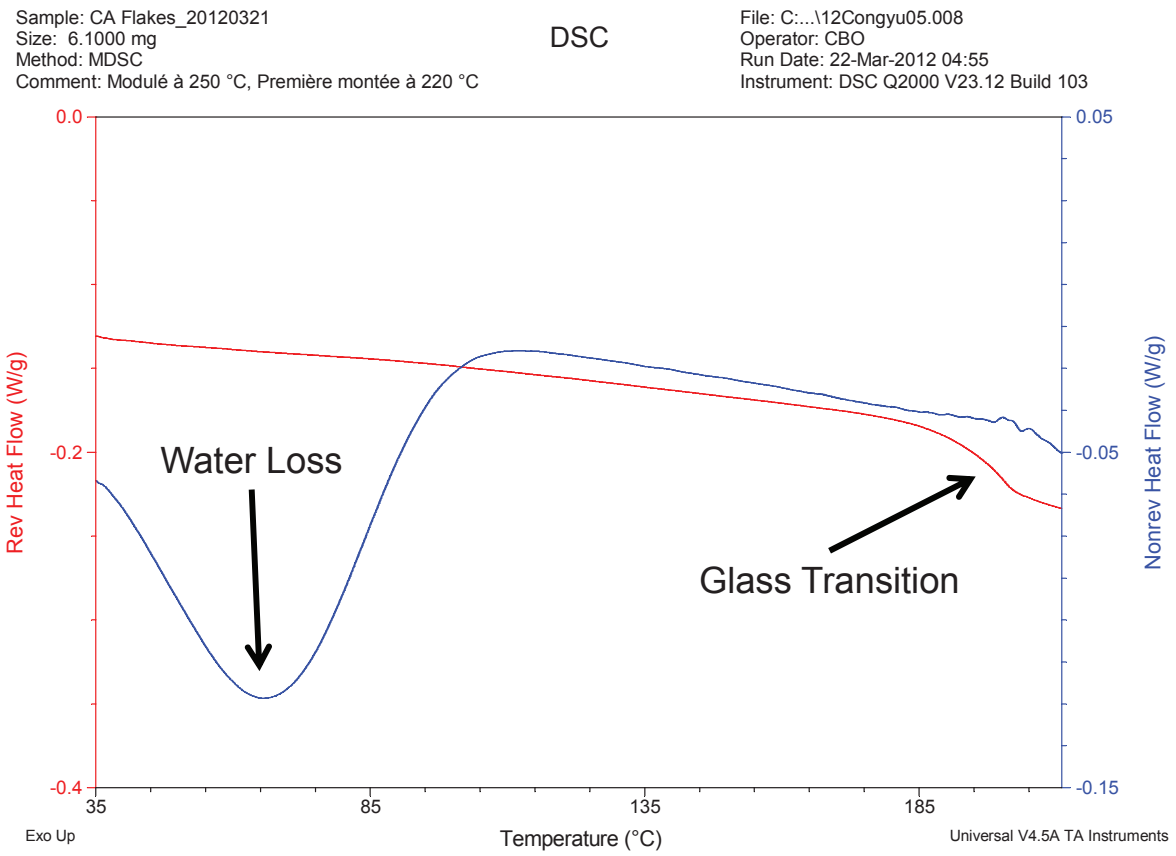

Figure 1: General feature of the first heating run of cellulose acetate in MDSC thermogram. The loss of water trace is indicated.

APPENDIX IV - CONVERSION OF UNITS

Page 126

Conversion of units for the activation energy of β-relaxation of DEP in *Hensel-Bielowka et al. 2004*

Hensel-Bielowka et al. 2004 determined the mean activation energy of β-relaxation of DEP as **3395 K**, which is equal to 28.20 kJ.mol^{-1}. The conversion is displayed as follows:

$$[kJ.mol^{-1}] = \frac{[K]k_B}{1000} \times N_A$$

Where

- [J] = kg.m^2.s^{-2}
- k_B = 1.38 x 10^{-23} kg.m^2.s^{-2}.K^{-1}
- N_A = 6.02 x 10^{23} mol^{-1}

APPENDIX V - JOHARI-GOLDSTEIN β–RELAXATION (JG RELAXATION)

Page 131

Johari-Goldstein β–relaxation (JG relaxation) has been named several times in the literature in order to precise the nature of secondary β–relaxation of cellulose acetate. It is generally related to the primary α–relaxation and is considered as a precursor of α–relaxation. However, in the current literature, there is a tendency to refer any observed β–relaxation as JG relaxation. *Ngai and Paluch 2004* thus made clear the definition of JG relaxation. Several criterions are mentioned:

- The molecular motion of JG relaxation must involve all parts of the basic structural unit (a repeat unit in the case of polymer).

- The JG relaxation time τ_{JG} has qualitatively similar though quantitatively different behaviors as the α–relaxation time τ_α in dependences on temperature, pressure and aging.

- Relaxation strength of JG relaxation senses the glass transition in having different temperature dependence above and below T_g.

- A change of the dynamics of the α–relaxation invariably changes the relation between τ_{JG} and τ_α.

τ_{JG} of genuine JG relaxation is approximately the same at all temperatures and pressures as the primitive relaxation time of the coupling model (τ_0), which is calculated by using solely the parameters of the α–relaxation.

APPENDIX VI - TABLE OF CALCULATED VOGEL TEMPERATURES

	Estimated T_0 (K)	T_g DSC (K)	T_g DMTA (K)
DS 1.83 + 10% TA	~401	420	435
DS 1.83 + 20% TA	~375	389	402
DS 1.83 + 30% TA	~330	362	375
DS 1.83 + 40% TA	~300	346	N/A
DS 2.08 + 10% TA	~406	429	441
DS 2.08 + 20% TA	~384	398	414
DS 2.08 + 30% TA	~359	374	395
DS 2.08 + 40% TA	~298	347	N/A
DS 2.45 + 10% TA	390 - 395	413	433
DS 2.45 + 15% TA	~336	393	412
DS 2.45 + 20% TA	323 - 333	382	392
DS 2.45 + 30% TA	~330	366	378
DS 2.45 + 40% TA	~213	330	335

DS 1.83 + 10% DEP	~411	428	440
DS 1.83 + 20% DEP	~351	398	413
DS 1.83 + 30% DEP	~333	381	397
DS 1.83 + 40% DEP	~342	373	394
DS 2.08 + 10% DEP	~398	443	443
DS 2.08 + 20% DEP	~381	407	426
DS 2.08 + 30% DEP	~375	405	415
DS 2.08 + 40% DEP	~373	404	411
DS 2.08 + 50% DEP	N/A	407	411
DS 2.45 + 15% DEP	367 - 389	391	416
DS 2.45 + 20% DEP	379 - 384	384	402
DS 2.45 + 25% DEP	335 - 361	374	389
DS 2.45 + 35% DEP	330 - 344	348	376
DS 2.45 + 45% DEP	295 - 316	328	346

Complete table of Table 28 (page 137)

RESUME DE THESE EN FRANÇAIS

I. Contexte générale

Les polysaccharides sont l'une des principales options à retenir pour progresser dans l'utilisation ou la conception de polymères renouvelables. Depuis les années cinquante, le développement industriel de ce type de polymères s'était considérablement réduit du fait de l'avènement des polymères synthétiques. Cependant, cet intérêt a cru considérablement ces dernières années en raison de la sensibilisation du public sur la limite des ressources fossiles. Ces biopolymères sont donc devenus un sujet d'importance, tant sur le plan industriel que sur celui de la recherche fondamentale. Toutefois, les systèmes à base de polysaccharides sont le plus souvent transformés via l'utilisation d'importantes quantités de solvants (y compris l'eau), ce qui globalement pénalise le procédé associé en l'affligeant d'une charge environnementale supplémentaire. Par la voie 'fondue', le développement de polymères thermoplastiques à base de dérivés de la cellulose est un véritable défi, qui concerne autant le mode de transformation de ces systèmes que le niveau des propriétés du matériau final. Pour exemple, la température de dégradation de l'acétate de cellulose (CA) (dont le degré de substitution 2,5 est développé par le Groupe Solvay) est si proche de sa température de fusion que son procédé de mise en œuvre ne peut être envisagé qu'avec l'ajout d'une quantité importante de plastifiants externes (entre 20 et 30% en poids selon le type d'additif). Le comportement d'un mélange CA-plastifiant est principalement régi par un «réseau» de très fortes interactions polaires, dont la force et la densité dépendent de 3 paramètres spécifiques: le degré de substitution de CA, la typologie de plastifiant et la quantité de plastifiant. Pour expliquer les différents mécanismes de plastification, il est donc important pour nous d'étudier et de comprendre les propriétés dynamiques (en ce qui concerne les phénomènes de relaxation) de ce type de systèmes et comment les trois leviers que nous avons identifiés peuvent influencer ou moduler les différentes interactions échangées dans les mélanges.

II. Matériaux d'étude et problématique scientifique

Nous avons préparé des films d'acétate de cellulose via la méthode « Solvent Casting » avec le phtalate de diéthyle (DEP) et de la triacétine (TA) comme plastifiants. Le solvant ou le mélange de solvant contient principalement de l'acétone. Trois degrés de substitutions (DS) de CA ont été testés: DS 1,83, DS 2,08 et DS 2,45. Les structures chimiques de polymère (DS 2,45) et des deux plastifiants sont présentées dans les Figures 1 et 2.

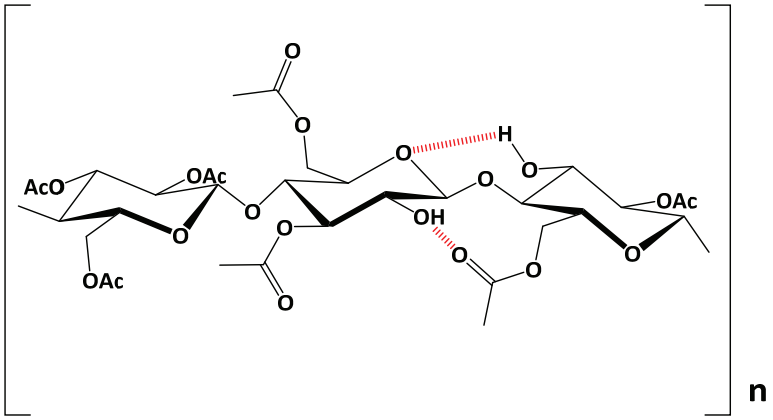

Figure 1: La structure chimique de l'acétate de cellulose (DS 2,45, grade commerciale) avec des possibilités de liaison hydrogène

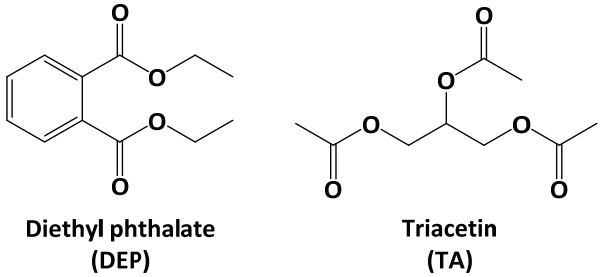

Figure 2: Les structures chimiques des plastifiants - le phtalate de diéthyle et la triacétine

Le DS 2,45 est le grade commercial d'acétate de cellulose et est considéré comme notre système de référence. TA est décrit comme un plastifiant efficace des dérivés de cellulose (*Fordyce et Meyer 1940; Suvorova et al. 1995, Fringant et al. 1998*). DEP est l'un des plastifiants les plus utilisés de CA. Les groupes esters de TA et de DEP sont censés interagir avec l'acétate de cellulose via des interactions dipolaires et/ou des liaisons hydrogènes. L'influence de ces interactions polaires sur la transition vitreuse du système reste inconnue. La différence structurale de deux plastifiants (c.à.d. le cycle aromatique du DEP) peut jouer un rôle déterminant dans ces comportements. Une autre variable en jeu est le degré de substitution de CA : quand le DS est plus petit, le nombre des groupements hydroxyles dans le polymère est plus important et donc la possibilité de former des liaisons hydrogènes (intra- et inter-moléculaire) est plus grande.

La prédiction de la T_g dans un mélange binaire est généralement décrite par plusieurs équations empiriques, telles que l'équation de Couchman-Karasz ou l'équation de Fox (*Fox 1956, Couchman et Karasz 1978*). Ces modèles empiriques sont basées sur l'hypothèse d'un système binaire idéal dans lequel les deux constituants n'interagissent pas les uns avec les autres. En conséquence, des écarts entre résultats expérimentaux et résultats obtenus à partir du modèle empirique sont attendus pour notre série d'acétates de cellulose plastifiés.

La prédiction de T_g mesurée expérimentalement par l'analyse thermique sera basée sur l'équation de Couchman-Karasz, telle qu'utilisée dans le cadre d'autres études (*Fringant et al. 1998*). La transition vitreuse peut être identifiée soit par un saut du « flux de chaleur» ou par un pic de la dérivée de «capacité calorifique». La réponse de la transition vitreuse de l'acétate de cellulose est large et peu intense en raison de la répartition hétérogène des 8 motifs d'anhydroglucose présents dans le polymère.

III. Méthodes de caractérisation

L'étude de la miscibilité entre le polymère et le plastifiant a été réalisée par calorimétrie (MDSC) et analyse thermomécanique (DMTA). Les propriétés dynamiques des CA plastifiés ont été analysées par DMTA et spectroscopie diélectrique (BDS). Transitions primaires et secondaires ont ainsi été étudiées avec les équations modèles VFT (ou WLF) et Arrhenius. Les informations microstructurales ont été obtenues par la diffraction des rayons X (XRD) et la diffusion de neutrons aux petits angles (SANS). Cette dernière technique a également été utilisée pour l'identification de la morphologie, de la séparation de phase et de la cavitation dans les systèmes de CA plastifiés.

IV. Analyse thermique

L'étude de la miscibilité a été réalisée par calorimétrie (MDSC) et analyse thermomécanique (DMTA). Dans notre système de référence - CA (DS 2,45) + TA, la séparation de phase se produit à partir de 20% et pour le système plastifié par le DEP, la séparation de phase se produit à partir de 25% (Figure 3). Une phase riche en CA et une phase riche en plastifiant sont formées au-dessus du seuil de miscibilité. Les écarts entre les T_g expérimentales et les prédictions de l'équation de Couchman-Karasz (*Couchman & Karasz, 1978*) sont observés comme prévu. Cela est attribué à la présence des interactions dipolaires et des liaisons H créées entre le polymère et le plastifiant. L'équation de Couchman-Karasz ne tient pas compte des interactions intermoléculaires.

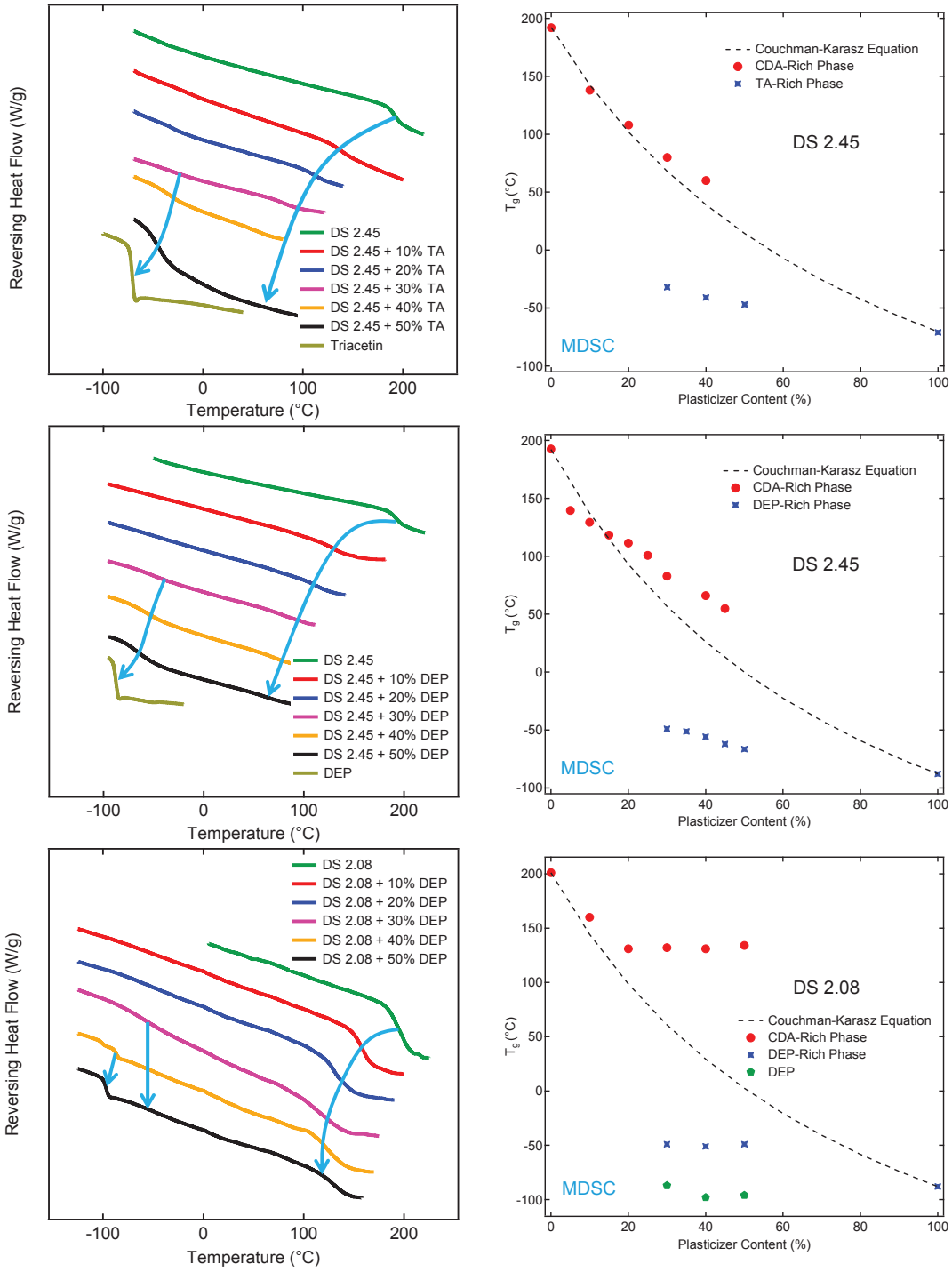

Figure 3: Gauche– MDSC Thermogrammes de DS 2,45 plastifié par TA et DEP et de DS 2,08 plastifié par DEP, les flèches indiquent les températures de transition vitreuse. Droite - Diagrammes de miscibilité de DS 2,45 et de DS 2,08 plastifiés, l'équation de Couchman-Karasz est utilisée pour la prédiction théorique de Tg.

Il est à noter que dans les cas des DS 1,83 et DS 2,08 plastifiés par DEP, une troisième transition vitreuse (proche de la température de la transition du DEP pur) est observée dans les compositions à haute fraction volumique en DEP (Figure 3, où l'exemple de DS 2,08 + DEP est représenté). Pour expliquer ce phénomène, nous avons proposé que des cavités se forment lors de la préparation des échantillons, pendant l'étape d'évaporation du solvant. Nous supposons que ces cavités se remplissent ensuite de DEP (Figure 4).

V. Hypothèse de la cavitation

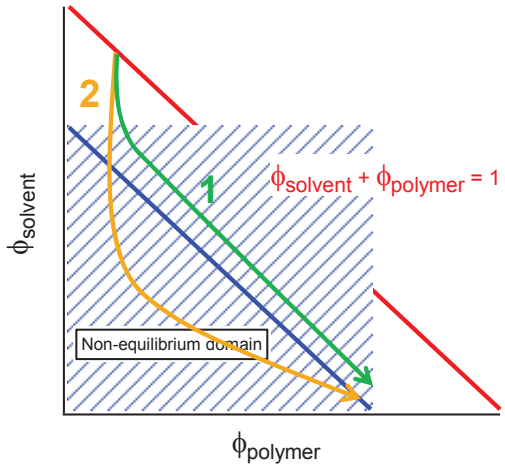

Figure 4: Schéma de la formation de cavités (trajectoire N°2, courbe jaune). Pas de cavités formées au travers de la trajectoire N°1 (courbe verte).

Prenons un film d'acétate de cellulose avec du solvant. Initialement, avant que l'évaporation ait lieu, la densité du système peut être normalisée à 1, correspondant à un système dense. Ensuite, l'évaporation a lieu. Les trajectoires dans l'espace (Φp, Φs) sont illustrées dans la même figure. Si le processus d'évaporation est assez lent, la trajectoire n'entre jamais dans le domaine instable: la densité du système reste suffisamment élevée pour que le système soit dans l'état stable (trajectoire N°1, courbe verte). Si le processus d'évaporation est rapide par rapport au processus de contraction du film, alors la trajectoire peut entrer dans le domaine instable (zone ombrée dans la figure 4, trajectoire N°2, courbe jaune).

La formation des cavités est illustrée sur la Figure 5: dans la première étape, l'évaporation du solvant a lieu. Des vides apparaissent dans le système avant que la contraction ait lieu (étape 2 de Figure 5). Si l'échantillon a eu le temps de se contracter, il peut encore rester dans le domaine stable de l'espace des phases (trajectoire N°1, Figure 4). Dans ce cas, la contraction se poursuivra sans formation de cavités (étape 3 de Figure 5). Si l'échantillon ne s'est pas suffisamment contracté lors de l'étape d'évaporation du solvant, l'échantillon peut entrer dans le domaine instable (trajectoire N°2). Puis, des cavités peuvent apparaître (étape 4 de Figure 5).

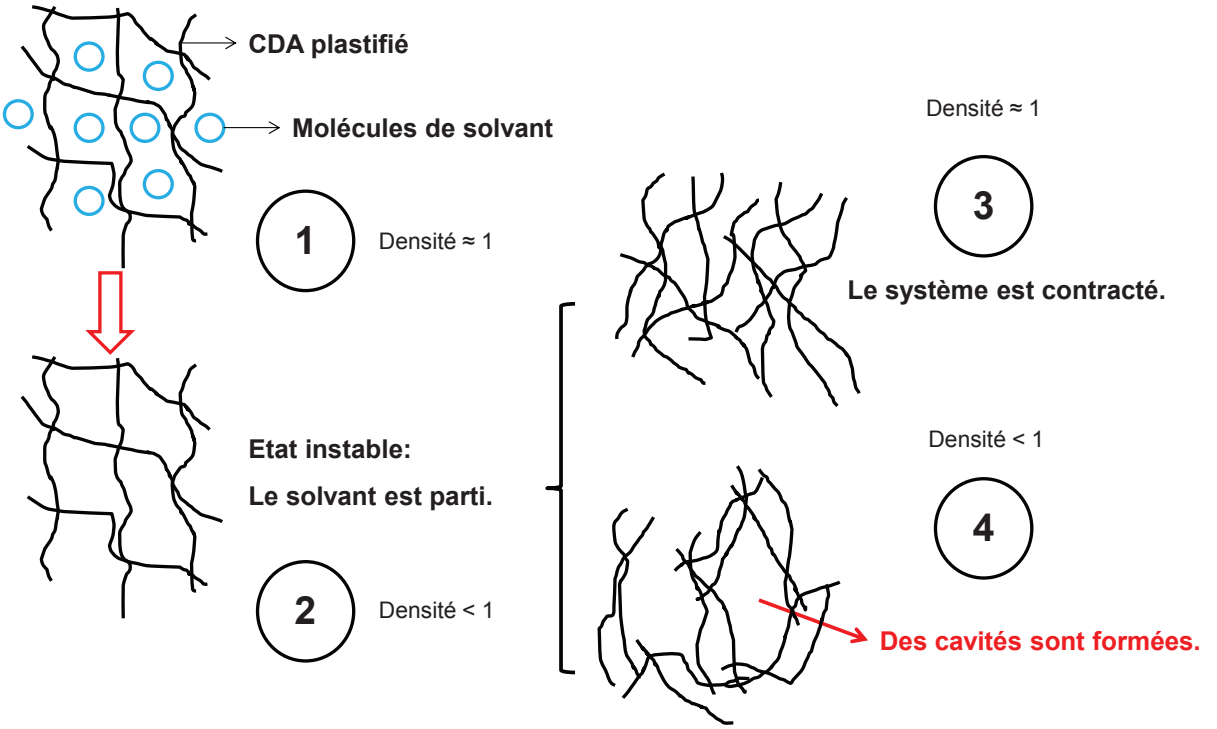

Figure 5: Les différentes étapes de l'évaporation du solvant à la formation de cavités (Trajectoire N°2 sur la figure 4).

A noter que la taille et le volume des cavités doit dépendre de la température de transition vitreuse (T_g) de l'acétate de cellulose plastifié. Lorsque la T_g est suffisamment basse, la contraction peut avoir lieu rapidement, et les cavités ne peuvent apparaître. Pour une T_g plus élevée, la contraction peut être trop lente pour éviter la formation de cavités. D'autre part, la relaxation mécanique peut être suffisamment rapide pour la construction de cavités de grandes tailles dans l'échantillon. Si la T_g est très élevée, le processus de formation de cavités peut s'arrêter lorsque les cavités sont encore relativement petites.

Selon les caractérisations de MDSC et de DMTA, la plastification de la triacétine est efficace pour les trois degrés de substitution de l'acétate de cellulose. En revanche, l'effet de plastification de DEP est différent d'un DS à l'autre. La 3ème transition observée dans DS 1,83 et DS 2,08 entraîne donc un système de CA à trois phases: la phase riche en CA, la phase riche en DEP et la phase de cavités remplies de molécules de DEP. Parmi les trois DS, le degré de substitution de référence - DS 2,45 présente le meilleur comportement de la miscibilité avec les deux plastifiants. La plastification par le DEP devient moins efficace pour DS 1,83 et DS 2,08. L'influence de la structure moléculaire de l'acétate de cellulose et des plastifiants sur les comportements en termes de miscibilité et de formation de cavités est donc de première importance.

Le 'pouvoir' plastifiant de TA et de DEP sur l'acétate de cellulose est estimé selon ΔT_g (la diminution de T_g entre l'acétate de cellulose non plastifié et plastifié) dans notre analyse thermique MDSC. Certes, c'est une étude qualitative mais elle met néanmoins en lumière le fait que le mécanisme de plastification du système est fortement dépendant de la typologie du plastifiant. Comme les deux plastifiants ont tous la capacité de plastifier CA par des interactions dipolaires entre des groupes acétates, la principale différence structurale vient probablement du cycle aromatique présent sur la molécule de DEP et peut contribuer à des effets stériques lors de l'interaction avec des chaînes de polymère. Outre ces faits, il n'y a pas encore d'interprétations claires concernant les deux mécanismes de plastification à l'échelle moléculaire.

Plus le DS est faible, plus les groupes hydroxyles sont nombreux dans l'acétate de cellulose. Ces groupes fonctionnels peuvent former des liaisons H avec eux-mêmes ou avec des groupes acétates latéraux. Donc comme le DS du polymère diminue, le réseau d'interaction polaire résultant est de plus en plus difficile à rompre et l'acétate de cellulose devient de moins en moins plastifié. Selon le résumé de nos résultats, DS 2,45 est le degré optimal de substitution de l'acétate de cellulose avec un bon compromis des interactions polaires susceptibles d'être établies avec le polymère. Il peut être facilement plastifié, conserve un caractère amorphe et dispose d'un comportement viscoélastique approprié pour la mise en œuvre à l'échelle industrielle. Concernant DS 1,83 et DS 2,08, des inconvénients importants sont évoqués (une gamme de plastification limitée et probablement une valeur de viscosité élevée comparée à celle du DS 2,45) qui limitent leurs développements et applications à l'échelle industrielle.

VI. Analyse structurale

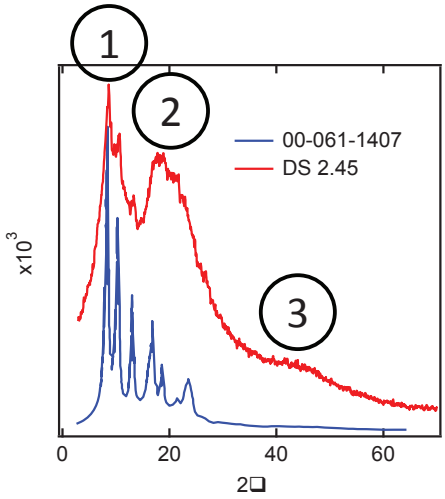

Figure 6: Diffractogramme XRD d'acétate de cellulose (DS 2,45) comparé à la référence: ICDD Powder Diffraction File N°00-061-1407 triacétate de cellulose (polymorphe CTA II).

Les informations microstructurales ont été obtenues par la diffraction des rayons X (XRD) et les techniques de diffusion de neutrons. De petites quantités de micro-cristallites du triacétate de cellulose (type CTA II) ont été observées dans le DS 2,45 (Figure 6). À plus grande échelle, le comportement de la miscibilité du système d'acétate de cellulose plastifié a été étudié par la diffusion de neutrons à très petits angles (USANS). Nous avons obtenu un ensemble complet et cohérent concernant la structure, la morphologie et la dynamique des systèmes d'acétate de cellulose plastifiés (Figure 7 et Tableau 1). En particulier, nous avons montré que selon les méthodes de préparations et les plastifiants utilisés, des cavités peuvent apparaître dans certains échantillons.

VII. Morphologie, séparation de phase et cavitation : étude par la diffusion de neutron aux petites angles

L'étude USANS a été menée dans la gamme de q de 2.10^{-3} à 0,5 $Å^{-1}$. Nous nous intéressons particulièrement aux propriétés de miscibilité entre le polymère et le plastifiant. Les fluctuations de concentration du système, des cavités remplies de molécules de plastifiant et la séparation de phase ont été observées comme représenté sur la Figure 7 :

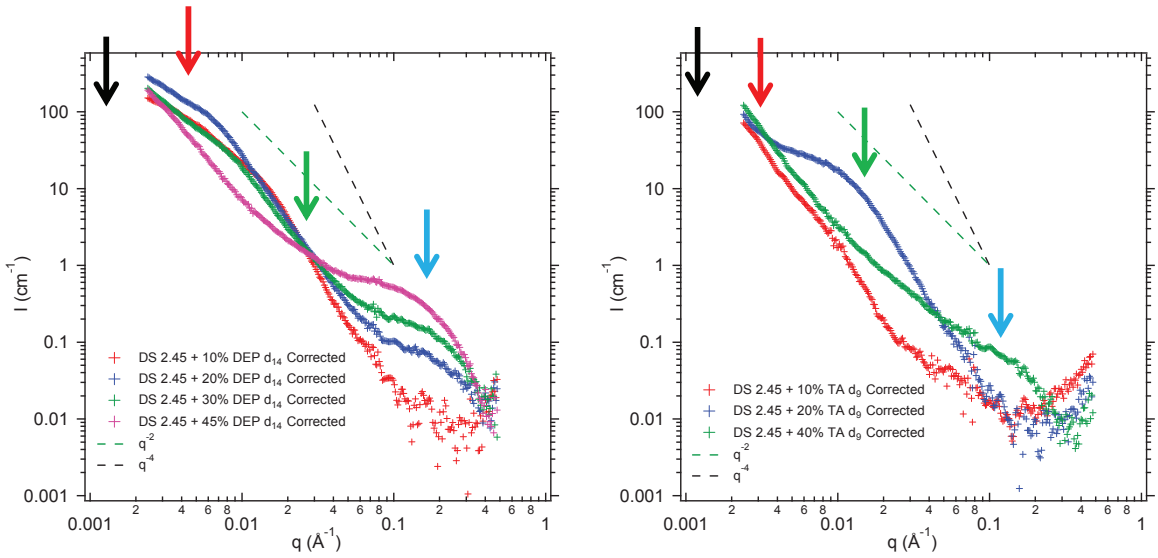

Figure 7: Résultats SANS des acétates de cellulose plastifiés par la triacétine et le phtalate de diéthyle deutérés. Ici, la diffusion incohérente a été soustraite.

- Flèche noire : indique une contribution correspondant à une grande longueur de corrélation ($\xi \approx$ µm), qui se trouve hors de la gamme expérimentale. Nous proposons que cette contribution soit liée à la séparation de phase. Par conséquent, ce phénomène a été partiellement exploité, une analyse complète pouvant être espérée via l'utilisation de la diffusion de lumière.

- Flèche rouge : indique une 2ème contribution correspondant à une grande longueur de corrélation ($\xi \approx$ 50 à 150 nm), qui se trouve dans l'intervalle expérimental. La présence de cavités est attribuée à cette contribution.

- Flèche verte : indique une 3ème contribution correspondant à une longueur de corrélation intermédiaire ($\xi \approx$ 8 à 12 nm), qui est proposée suite aux fluctuations de concentration crées par les chaînes d'acétate de cellulose. Sa longueur de corrélation est équivalente à la longueur de persistance de l'acétate de cellulose.

- Flèche bleue : indique une 4ème et dernière contribution correspondant à une petite longueur de corrélation ($\xi \approx$ 0.5 nm). Nous proposons que cette contribution corresponde aux fluctuations de concentration des molécules de plastifiant.

VIII. Relaxations diélectriques

Les propriétés dynamiques des CA plastifiés ont été analysées par analyse thermomécanique (DMTA) et spectroscopie diélectrique (BDS). Deux types de relaxations secondaires (γ et β) ont été identifiés et attribués aux mouvements locaux d'acétate de cellulose. La relaxation γ est attribuée à la rotation des groupements acétates portés par le squelette cellulosique de CA (Figure 9). Nous proposons que la relaxation β soit liée à un mouvement local et coopératif de la chaîne d'acétate de cellulose. Les deux transitions secondaires obéissent à la loi d'Arrhenius. Il est difficile d'analyser la relaxation β dans l'acétate de cellulose plastifié parce qu'elle se superpose avec la relaxation α' de la phase riche en plastifiant après le seuil de séparation de phase. La séparation de deux transitions est possible lorsque la 3ème transition primaire (la relaxation α") apparait. Une autre relaxation secondaire (γ') qui a été observée exclusivement dans des systèmes plastifiés par DEP est considérée comme la relaxation secondaire des molécules de DEP (Figure 8). Les relaxations γ' et α" ont été directement comparées avec des données de la littérature.

Trois relaxations primaires ont été également identifiées: la relaxation α du DEP pur, désignée comme α", qui n'est observée que dans les DS 1,83 et DS 2,08 à des teneurs de DEP élevées; la relaxation α de la phase riche en plastifiant (notée α') et la relaxation α de la phase riche en CA.

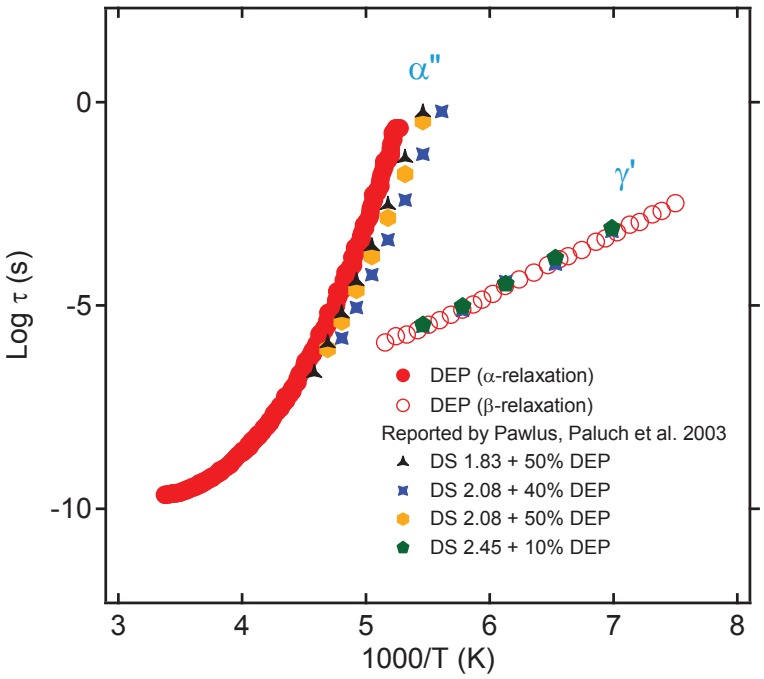

Figure 8: Evolution des relaxations α" et γ' avec l'augmentation de la teneur en DEP dans l'acétate de cellulose plastifié. Comparaison avec les résultats de la littérature de DEP pur (Pawlus et al. 2003).

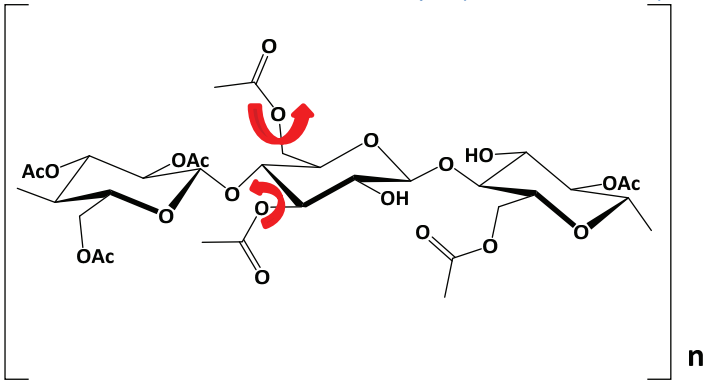

Figure 9: La rotation des groupes acétates de CA, l'une des propositions les plus courantes concernant les mouvements moléculaires liés à la relaxation γ.

Nous avons également étudié le régime dit de Williams-Landel-Ferry (WLF) ou de Vogel-Fulcher-Tammann (VFT) des relaxations primaires en utilisant à la fois la spectroscopie diélectrique et les mesures thermomécaniques dans la gamme de fréquence de 0,06 Hz à 10^6 Hz (Figure 10 et 11). À notre connaissance, c'est la première fois que le régime WLF est réellement et clairement démontré pour le comportement des systèmes d'acétate de cellulose plastifié. Nos résultats sont très cohérents et la température de Vogel calculée selon la loi VFT est aussi en bon accord avec les résultats expérimentaux obtenus à partir des trois techniques de caractérisation (MDSC, DMTA et BDS).

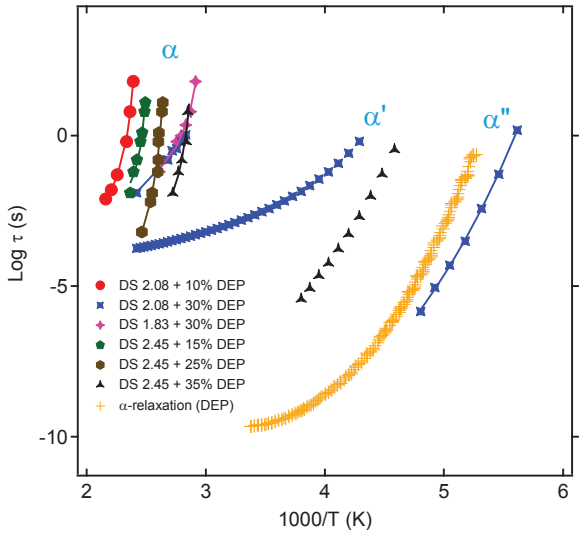

Figure 10: Caractéristique générale de la carte des relaxations d'acétate de cellulose plastifiée dont les trois transitions primaires.

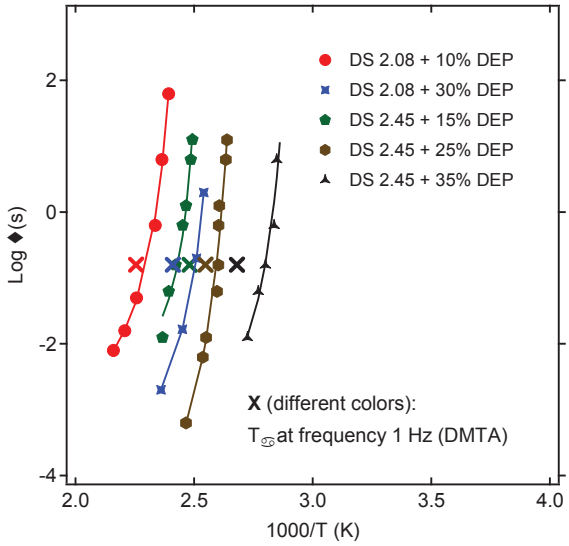

Figure 11: Relaxation α dans les séries d'acétate de cellulose plastifié par DEP (données DMTA à la fréquence 1 Hz et des données BDS).

Notre travail ouvre la voie à de nouvelles études concernant les mécanismes microscopiques responsables des différentes modes de relaxation que nous avons identifiés. Ces types d'études pourraient être effectués par spectrométrie RMN solide, de concert avec d'autres études expérimentales telles que la diffusion de la lumière, ainsi que des travaux théoriques impliquant les simulations par dynamique moléculaire. D'autre part, les mécanismes de séparation de phase seront prochainement étudiés dans les détails afin de compléter les données et analyses manquantes en USANS.

RESUME IN ENGLISH

Cellulose Acetate/Plasticizer Systems: Structure, Morphology and Dynamics

Cong Yu BAO

Polysaccharides are one of the main options to the on-going move towards the use of renewable polymers. The industrial interest in this type of polymers drastically shrunk by the advent of synthetic polymers in the fifties, but is currently reviving due to the public awareness on the limit of fossil resources. These biopolymers are nowadays offering a challenging and industrially profitable playground for researchers. However, current polysaccharides based materials are mostly processed with extensive use of solvents (including water) making the total process an environmental burden despite the advantage of the starting material. Development of thermoplastic cellulose-based materials is very challenging regarding both final material properties and polymer processing. The degradation temperature of Cellulose Acetate (CA) (degree of substitution 2.5) is so close to its melting temperature that it can only be processed with a significant amount of external plasticizers (between 20 et 30 wt.% depending on the type of the additive). Behavior of a CA-plasticizer blend is mainly governed by a 'network' of high polar interactions, the strength and the density of which clearly depend of 3 specific parameters: the CA's degree of substitution, the typology of the plasticizer, the amount of plasticizer. In an attempt to explain the different plasticization mechanisms, it is thus of utmost importance for us to study and understand the dynamic properties (regarding the relaxation phenomena) of this kind of systems and how the three levers that we identified can influence or modulate the different interactions exchanged within the blends.

At the first stage of this research work, we prepared CA films via solvent casting method with diethyl phthalate (DEP) and triacetin (TA) as plasticizers. Three different cellulose acetates were tested: DS 1.83, DS 2.08 and DS 2.45. Miscibility study was carried out via calorimetry MDSC and thermo-mechanical DMTA analysis.

In our reference system – CA (DS 2.45) + TA, the phase separation occurs starting from 20 wt.% TA and from 25 wt.% for the DEP-based system. Two phase domains: CA-rich phase and plasticizer-rich phase were formed above phase separation threshold. The miscibility study of the CA (DS 1.83 and DS 2.08) + TA systems followed well that of the reference system. However, a third glass transition temperature (close to the T_g of DEP) was found in the systems CA (DS 1.83 and DS 2.08) at high DEP contents. For explaining this observation, we proposed the hypothesis that cavities were formed during the solvent evaporation step.

Dynamical properties were analyzed by DMTA and broadband dielectric spectroscopy (BDS). Two kinds of secondary relaxations (γ and β/β') were identified and attributed to the 'local' motions of cellulose acetate. Another secondary relaxation which was found exclusively in the systems CA + DEP was considered as the β-relaxation of DEP molecules. Three kinds of primary relaxations were also identified: the α-relaxation of DEP, which we denoted by α", occurred only in the systems CA (DS 1.83 and DS 2.08) at high DEP contents; the α-relaxation of plasticizer-rich phase (denoted by α') and the α-relaxation of CA or CA-rich phase. These two specific transitions were identified as strictly following the so-called Williams-Landel-Ferry (WLF) or Vogel-Fulcher-Tammann (VFT) relaxation regime using both dielectric spectroscopy and mechanical measurement in a frequency range from 0.06 Hz to 10^6 Hz.

For the whole range of our systems, micro-structural information was obtained by X-ray diffraction (XRD) and neutron scattering techniques. Small quantities of cellulose triacetate micro-crystallites were found in the CA (DS 2.45) film. At a larger scale, miscibility behavior between CA and the two different plasticizers has been studied by ultra-small-angle neutron scattering (USANS).

We obtained a complete and consistent picture regarding the structure, morphology and dynamics of plasticized cellulose acetate systems. In particular, we have shown that depending on the solvent casting preparation and the typology of the plasticizer, cavities may appear in the samples.

Our work opens the way to further studies regarding the microscopic mechanisms responsible for the different relaxation modes that we identified. These kinds of studies may be performed e.g. by solid-state NMR spectrometry, in conjunction with other experimental studies such as light scattering and theoretical works involving molecular dynamics simulations.

RESUME EN FRANÇAIS

Systèmes d'acétate de cellulose plastifiés : structure, morphologie et dynamique

Cong Yu BAO

Les polysaccharides sont l'une des principales options à retenir pour progresser dans l'utilisation ou la conception de polymères renouvelables. Depuis les années cinquante, le développement industriel de ce type de polymères s'était considérablement réduit du fait de l'avènement des polymères synthétiques. Cependant, cet intérêt a cru considérablement ces dernières années en raison de la sensibilisation du public sur la limite des ressources fossiles. Ces biopolymères sont donc devenus un sujet d'importance, tant sur le plan industriel que sur celui de la recherche fondamentale. Toutefois, les systèmes à base de polysaccharides sont le plus souvent transformés via l'utilisation d'importantes quantités de solvants (y compris l'eau), ce qui globalement pénalise le procédé associé en l'affligeant d'une charge environnementale supplémentaire. Par la voie 'fondue', le développement de polymères thermoplastiques à base de dérivés de la cellulose est un véritable défi, qui concerne autant le mode de transformation de ces systèmes que le niveau des propriétés du matériau final. Pour exemple, la température de dégradation de l'acétate de cellulose (CA) (dont le degré de substitution 2,5 est développé par le Groupe Solvay) est si proche de sa température de fusion que son procédé de mise en œuvre ne peut être envisagé qu'avec l'ajout d'une quantité importante de plastifiants externes (entre 20 et 30 en poids selon le type d'additif). Le comportement d'un mélange CA-plastifiant est principalement régi par un «réseau» de très fortes interactions polaires, dont la force et la densité dépendent de 3 paramètres spécifiques: le degré de substitution de CA, la typologie de plastifiant et la quantité de plastifiant. Pour expliquer les différents mécanismes de plastification, il est donc important pour nous d'étudier et de comprendre les propriétés dynamiques (en ce qui concerne les phénomènes de relaxation) de ce type de systèmes et comment les trois leviers que nous avons identifiés peuvent influencer ou moduler les différentes interactions échangées dans les mélanges.

Dans la première partie de la recherche, nous avons préparé des films d'acétate de cellulose via la méthode « Solvent Casting » avec le phtalate de diéthyle (DEP) et de la triacétine (TA) comme plastifiants. Trois degrés de substitutions (DS) de CA ont été testés: DS 1,83, DS 2,08 et DS 2,45. L'étude de la miscibilité a été réalisée par calorimétrie (MDSC) et analyse thermomécanique (DMTA). Dans notre système de référence - CA (DS 2,45) + TA, la séparation de phase se produit à partir de 20% TA et pour le système plastifié par le DEP, la séparation de phase se produit à partir de 25% DEP. Une phase riche en CA et une phase riche en plastifiant sont formées au-dessus du seuil de miscibilité. Nous avons également étudié la miscibilité de deux autres DS plastifiés par TA et DEP. Il est à noter que dans les cas des DS 1,83 et DS 2,08 plastifiés par DEP, une troisième transition vitreuse (proche de la T_g du DEP pur) est observée dans les cas à haute fraction volumique en DEP. Pour expliquer ce phénomène, nous avons proposé que des cavités se forment lors de la préparation des échantillons, pendant l'étape d'évaporation du solvant. Nous supposons que ces cavités se remplissent ensuite de DEP.

Les propriétés dynamiques des CA plastifiés ont été analysées par analyse thermomécanique (DMTA) et spectroscopie diélectrique (BDS). Deux types de relaxations secondaires (γ et β) ont été identifiés et attribués aux mouvements locaux d'acétate de cellulose. Une autre relaxation secondaire (γ') qui a été observée exclusivement dans des systèmes plastifiés par DEP est considérée comme la relaxation secondaire des molécules de DEP. Trois relaxations primaires ont été également identifiées: la relaxation α du DEP pur, désignée comme α", qui n'est observée que dans les DS 1,83 et DS 2,08 à des teneurs de DEP élevées; la relaxation α de la phase riche en plastifiant (notée α') et la relaxation α de la phase riche en CA. Nous avons également étudié le régime dit Williams-Landel-Ferry (WLF) ou Vogel-Fulcher-Tammann (VFT) des relaxations primaires en utilisant à la fois la spectroscopie diélectrique et la mesure thermomécanique dans la gamme de fréquence de 0,06 Hz à 10^6 Hz. A notre connaissance, c'est la première fois que le régime WLF d'acétate de celluloses plastifiées est étudié.

Les informations microstructurales ont été obtenues par la diffraction des rayons X (XRD) et les techniques de diffusion de neutrons. De petites quantités de micro-cristallites du triacétate de cellulose ont été observées dans le DS 2,45. À plus grande échelle, le comportement de la miscibilité a été étudié par la diffusion de neutrons à très petits angles (USANS). Nous avons obtenu un ensemble complet et cohérent concernant la structure, la morphologie et la dynamique des systèmes d'acétate de cellulose plastifiés. En particulier, nous avons montré que selon les méthodes de préparations et les plastifiants utilisés, des cavités peuvent apparaître dans les échantillons. Notre travail ouvre la voie à d'autres études concernant les mécanismes microscopiques responsables des différentes modes de relaxation que nous avons identifiés. Ces types d'études pourraient être effectués par spectrométrie RMN solide, de concert avec d'autres études expérimentales telles que la diffusion de lumière, ainsi que des travaux théoriques impliquant les simulations par dynamique moléculaire.